Republic of Iraq
Ministry of Higher Education and Scientific Research
University of Babylon
College of Science / Department of Physics

Non-linear Optical Properties of Organic Laser Dyes Doped by (Ag, Al_2O_3) Nanoparticles and its Optical Applications

AThesis
Submitted to the council of College of Science, University of Babylon in Partial Fulfillment of the Requirements Of the Doctorate of Philosophy in Physics.

By
Ban Raheem Saleh Kzar
B.Sc.in Physics / 2014
M.Sc. in Physics / 2017

Supervised By
Prof. Dr.
Ban Ali Naser Ghalib

2023 A.D. **1445A.H.**

جمهورية العراق
وزارة التعليم العالي والبحث العلمي
جامعة بابل / كلية العلوم ـ قسم الفيزياء

الخصائص البصرية اللاخطية لصبغة عضوية ليزرية مطعمة بجسيمات (Ag , Al_2O_3) النانوية وتطبيقاتها البصرية

أطروحة

مقدمة إلى مجلس كلية العلوم ـ جامعة بابل
وهي جزء من متطلبات نيل درجة الدكتوراه فلسفة في العلوم/ الفيزياء

من قبل
بان رحيم صالح كزار
بكالوريوس علوم فيزياء/ ٢٠١٤
ماجستير علوم فيزياء /٢٠١٧

بأشراف
الاستاذ الدكتور
بان علي ناصر غالب

٢٠٢٣ م **١٤٤٥هـ**

﴿ اللَّهُ نُورُ السَّمَاوَاتِ وَالْأَرْضِ مَثَلُ نُورِهِ كَمِشْكَاةٍ فِيهَا مِصْبَاحٌ الْمِصْبَاحُ فِي
زُجَاجَةٍ الزُّجَاجَةُ كَأَنَّهَا كَوْكَبٌ دُرِّيٌّ يُوقَدُ مِن شَجَرَةٍ مُّبَارَكَةٍ
زَيْتُونِةٍ لَّا شَرْقِيَّةٍ وَلَا غَرْبِيَّةٍ يَكَادُ زَيْتُهَا يُضِيءُ وَلَوْ لَمْ تَمْسَسْهُ نَارٌ نُّورٌ
عَلَى نُورٍ يَهْدِي اللَّهُ لِنُورِهِ مَن يَشَاءُ وَيَضْرِبُ اللَّهُ الْأَمْثَالَ لِلنَّاسِ
وَاللَّهُ بِكُلِّ شَيْءٍ عَلِيمٌ ﴾

صدق الله العلي العظيم

سورة النور: الآية (٣٥)

Supervisor Certification

I certify that this thesis is titled (**Non-linear Optical Properties of an Organic Laser Dye Doped Nanoparticles and its Optical Applications)** was prepared by **(Ban Raheem Saleh Kzar)** under my supervision at Department of Physics, College of Science, University of Babylon, as a partial fulfillment of the requirements for the degree of doctor of philosophy science in physics.

Signature:

Supervisor: Dr. Ban Ali Naser Ghalib

Title: Professor

Address: Department of Physics,

College of Science, University of Babylon.

Date: / / 2023

Certification of the Head of the Department

In view of the available recommendation, I forward this thesis for debate by the examination committee.

Signature :

Name: Dr. Samira A. Mahdi

Title: Assist. Prof

Address: Head of Physics Department,

College of Science, University of Babylon.

Date: / /2023

Supervisor Certification

I certify that this thesis is titled (**Non-linear Optical Properties of Organic Laser Dye Doped by (Ag, Al_2O_3) Nanoparticles and its Optical Applications)** was prepared by **(Ban Raheem Saleh Kzar)** under my supervision at Department of Physics, College of Science, University of Babylon, as a partial fulfillment of the requirements for the degree of doctor of philosophy science in physics.

Signature:

Supervisor: Dr. Ban Ali Naser Ghalib

Title: Professor

Address: Department of Physics,

College of Science, University of Babylon.

Date: / / 2023

Certification of the Head of the Department

In view of the available recommendation, I forward this thesis for debate by the examination committee.

Signature :

Name: Dr. Samira A. Mahdi

Title: Asst. Prof

Address: Head of Physics Department,

College of Science, University of Babylon.

Date: / /2023

الخلاصة

يتضمن البحث الحالي دراسة الخصائص التركيبية والبصرية الخطية واللاخطية لصبغتين عضويتين ليزريتين : الكومارين (334) والفلورسين المطعمة ببوليمر بولي فينيل الكحول ((PVA وجسيمات الفضة النانوية وجسيمات الألومينا النانوية وذلك للإستفادة منهما في مجال البصريات اللاخطية. ان العديد من خصائص الصبغات الليزرية العضوية يمكن تحسينها و تطويرها بالتطعيم ببوليمرات ومواد نانوية، بحيث تكون مناسبة للعديد من التطبيقات العملية . اذ تعد الصبغات الليزرية العضوية (النقية والمطعمة) من المواد الجيدة في مجال البصريات اللاخطية وتطبيقاتها وذلك لاستجابتها اللاخطية العالية التي تعمل عند مدى طيفي واسع.

تم تحضير خليط للصبغتين الليزريتين المذابتين في مذيب الايثانول بنسب خلط مختلفة (1:1, 2:1 ,3:1 ،4:1) وتراكيز مختلفة (3×10-5, 5×10-5, 7×10-5) M).

وتحضير اغشية رقيقة من محاليل هذه الصبغات بنسبة خلط (4:1). تم تشخيص هذه الصبغات العضوية باستخدام مطياف الاشعة تحت الحمراء FT-IR)). تم دراسة الخصائص البصرية الخطية لجميع النماذج المحضرة، اذ تم دراسة طيفي الامتصاصية والنفاذية باستخدام مطياف الاشعة المرئية - الفوق البنفسجية لتراكيز مختلفة مذابة في الايثانول المطلق. تبين من خلال النتائج انه كلما زاد التركيز ازدادت الامتصاصية لنفس الطول الموجي بينما يحدث العكس بالنسبة لطيف النفاذية. تم دراسة الخصائص البصرية الطيفية لجميع النماذج المحضرة باستخدام مطياف الفلورة.

تضمنت الفحوصات اللاخطية استخدام تقنية Z-Scan في حالتي الفتحة المفتوحة و الفتحة المغلقة للحصول على معامل الامتصاص اللاخطي (β) ومعامل الانكسار اللاخطي (n_2) على التوالي. تم اجراء القياسات باستخدام ليزر الحالة الصلبة ذو الطول الموجي (457) نانومتر وقدرة mW) 84) .

أظهرت النتائج ان زيادة التركيز تؤدي الى زيادة معامل الانكسار اللاخطي ((n_2، و انخفاض معامل الامتصاص اللاخطي (β)لكل نماذج الصبغات الليزرية العضوية المحضرة، وان خليط الصبغات المطعمة يمتلك خصائص بصرية طيفية وخطية ولا خطية كبيرة بالمقارنة مع الصبغات النقية المنفردة. تمتلك الاغشية الرقيقة خصائص بصرية طيفية خطية ولا خطية أفضل بالمقارنة مع المحاليل. وان النماذج المحضرة من خليط الصبغات المطعمة ببوليمرات ومواد نانوية تمتلك خصائص بصرية لا خطية أفضل مقارنة مع النماذج المحضرة من الصبغات النقية. اظهرت النتائج ان عتبة محدد القدرة البصرية تتناسب عكسيا مع تركيز المحلول لكل النماذج.

ان الاغشية المحضرة من خليط من الصبغات الليزرية بنسبة (4:1) والمطعمة ببوليمر , وجسيمات الفضة النانوية اعطت معاملات بصرية, طيفية خطية ولا خطية اعلى مقارنة بنسب الخلط الاخرى. حيث تم الحصول على اعلى قيمة للكفاءة الكمية (96%) واعلى قيمة لكل من معامل الانكسار اللاخطي (15.12×10^{-7} cm^2/mW) ومعامل الامتصاص اللاخطي (7.52 cm/mW) على التوالي.

بينت النتائج امكانية استخدام جميع نماذج الصبغات المطعمة والنقية وخليطها (المحاليل والاغشية) كأوساط جهد لمختلف التطبيقات الكهروبصرية كمحددات للقدرة البصرية وكأوساط ليزرية فعالة في الليزرات السائلة.

Summery

The present research includes studying the structural, linear and nonlinear optical properties of two organic laser dyes: Coumarin (334) , Fluorescein with poly vinyl alcohol (PVA) polymer doped (Ag, Al_2O_3) nanoparticles to be used in the nonlinear application. Many properties of organic laser dyes can be improved and enhanced by doping with polymer and nanoparticles materials, which are favorable for practical applications. Organic laser dyes (pure and doped) are good materials for the field of nonlinear optics (NLO) and its applications because of their large response nonlinearity which works extended spectral transparency.

In this work, preparation mixture of two organic laser dyes Coumarin (334) and Fluorescein dissolved in ethanol solvent, at different mixing ratios (1:1, 2:1, 3:1 and 4:1) with different concentrations (3×10^{-5}, 5×10^{-5} and 7×10^{-5}) M at room temperature, and preparing thin films from solutions of these dyes for each mixing ratio. "These organic laser dyes have been characterized using Fourier Transform Infrared (FT-IR)".

The linear optical properties for all prepared samples studied by using UV-VIS spectrometer in the wavelength ranges (190-390) nm and (390-1100) nm, respectively for different concentrations for each dye dissolved in absolute ethanol solvent, then study of absorption and transmission spectra for all samples. The spectral optical properties of all the prepared samples have been studied using fluorescence spectroscopy.

The results showed that the concentrations increased the when absorbance also increased for the same wavelength. The opposite relationship was observed for transmittance.

The nonlinear optical properties have been calculate by using (Z - Scan) technique in two cases (Close aperture) and (Open aperture) for the purpose of determining the nonlinear refractive index (n_2) and nonlinear absorption

coefficient (β). The experiments were carried out with a diode pump solid state laser operating at a wavelength (457 nm) and power of (84 mW).

The results showed an increase of the nonlinear refractive index coefficient while decreasing of nonlinear absorption coefficient when increasing concentrations for all samples of organic laser dyes. Doped dyes mixture have large linear and nonlinear optical properties as compared with pure dyes. "Thin films have better linear and non-linear spectral optical properties as compared to solutions". All prepared samples from mixture dyes doped with polymer and nanoparticles have better nonlinear optical properties compared to samples prepared from pure dyes.

The results indicate that the optical power limiting threshold is inversely related to the solution concentration for all samples. The prepared thin films of mixture laser dyes with ratio (4:1) doped with PVA polymer and Ag nanoparticles give spectral, linear and nonlinear optical parameters high compared with thin films doped with PVA polymer and Al_2O_3. Where the highest value of the quantum efficiency (96%) and the highest value of the nonlinear refractive index and the nonlinear absorption coefficient (15.12×10^{-7} cm^2/mW) and (7.52 cm/mW) were obtained respectively.

The results indicate that all samples of pure and doped dyes and its mixture (solutions and thin films) could be employed as a suitable medium for variety of optoelectronic applications, including optical power limiting and active laser medium in liquid lasers.

1.1 Introduction

Nonlinear optical properties have been the subject of numerous investigations theoretically and experimentally during recent years due to their applications to many branches. The nonlinear optical properties are important parameters in characterizing and determining the applicability of any material to nonlinear optical device. There are several techniques for measuring these parameters like degenerate four waves mixing, third harmonic generation and Z-Scan technique [1].

Organic compounds have been the subject of intense theoretical and experimental study due to their promising applications in different life science fields. The organic compounds are defined as hydrocarbons and their derivatives [2].They can be subdivided into saturated and unsaturated compounds. Organic dyes are fluorescent molecules with large molecular weights, characterized by a strong absorption band in the visible region of the electromagnetic spectrum. Such a property is found only in organic compounds which contain an extended system of conjugated bonds alternating single and double bonds [3]. In a dye laser, these molecules are dissolved in an organic solvent or incorporated in to a solid matrix. Although dyes have been demonstrated to laser in the solid, liquid, or gas phase, it is in the liquid and solid phases that dyes have made a significant impact as laser media [4].

Organic dyes are one of the materials which play an important role in the nonlinear optics field, because of the large variety of these compounds at high intensities, fast response, large nonlinear properties, and easy to process integrated into optical devices. "The organic materials such as organic dyes have compatibility with other materials mainly related to the need of employing large volumes of organic solutions of dyes that are both toxic and expensive" [5]. So that the dye has to be changed for different wavelength regions, so attempts were made to overcome the problems posed by dye solutions by incorporating

dye molecules into solid matrices. This has resulted in significant advances towards the development of practical tunable solid-state lasers [6].

Dye doped polymers find applications in similar fields of modern photonic technology, optical amplifiers, fiber optics, and optical limiting which is used for protecting the human eye and the sensors by handling the laser output [7]. Polyvinyl Alcohol (PVA) is synthetic polymer utilized from the early 1930 in a wide range of industrial, commercial, medical and food applications, and has numerous properties like being effectively fabricated, with relatively a minimal cost, and dielectric material [8].

Nanotechnology represents one of the major break throughs of modern science, enabling materials of distinctive size, structure and composition to be formed. For the smaller particles the percentage of surface atoms increases, leading to changes in physical and chemical properties of the materials [9]. PVA composite thin films are modulated and improved by addition of (Ag and Al_2O_3) nanoparticles and those properties can be applied in the fields of optics and electronics .The nonlinear properties of dyes solutions, dyes doped polymer thin films and nanoparticles composite can be studied by using a simple technique called Z_ scan [10]. It is a sensitive and popular experimental method to measure intensity dependent of nonlinear optical (NLO) properties of materials which can rapidly measure both nonlinear absorption (NLA) and nonlinear refraction (NLR) in solids, liquids and then studying the optical limiting behavior [11].

1.2 Literature Survey

Several researches on using Z-scan for study nonlinear properties of organic dyes.

In (2013) **B. Anand *et al*** . [12] studied the spectral dispersion of ultrafast optical limiting in the laser dye Coumarin-120 in the wavelength region (630 to 900) nm, measured in a single Z-scan, using the white-light continuum as the excitation source. Optical limiting is found to arise from two-photon absorption, and its spectrum agrees very well in shape with the linear absorption spectrum.

In (2014) **A .Hassan *et al*** . [13] studied the spectral properties (absorption and fluorescence) for Fluorescein Sodium dye by solving it in Ethanol ,at different concentrations at room temperature. The intensity of absorption increased and fluorescence decreased while concentration increases with agreement of Beer - Lambert Law. The fluorescence spectrum followed and entirely the same as absorption spectrum. The quantum efficiency of the dissolved Fluorescein Sodium dye in Ethanol were (88%, 85% and 70%) respectively. In addition to the radiative life time was (0.55,0.91 and 1.3) ns and the fluorescence life time (0.49,0.77 and 0.9) ns respectively.

In (2015) **R. Nader**. [14] studied the nonlinear optical properties of fluorescein Sodium dye in water at different concentrations in a constant thickness of (1 mm) , by using Z-Scan method to evaluate the nonlinear refractive index (n_2) and the absorption nonlinear coefficient (β).It found that the nonlinear coefficients changes with increasing the concentrations of the dye.

In (2016) **N. Habeeb *et al* .** [15] studied the spectral properties of mixed Coumarin (334) and Rhodamine (590) in ethanol solvent at different concentration had been studied. The absorption intensity of these dyes increases as the concentrations increase in addition to that the spectrum was shifted towards the longer wavelength (red shift). The energy transfer process has been investigated after achievement this condition. The fluorescence peak intensity of donor molecule was decrease and its bandwidth will increases on the contrary of

the acceptor molecule its intensity increase gradually and its bandwidth decreases as the acceptor concentration increase.

In (2017) **T.Ali Naser** [16] studied effect of polarity of solvent on the phenomenon of the fluorescence energy transfer between the laser dyes, and the preparation of two samples, one of the mixing of the acridine orange dye as a donor with the Orcein dye as a acceptor and the other mixing of acridine orange dye as a donor with Rhodamine B as a acceptor. When the absorption and fluorescence spectra of both models are achieved, the large overlap between them is achieved, and this confirms the achievement of the (acceptor-donor) sample. The results of the study showed a significant increase in the intensity of the fluorescence spectra of the mixing samples compared to the dyes individually for all the prepared samples. This increase was increased with the polarity of the solvent and the highest fluorescence intensity was in the first mixing sample of these.

In (2017) **M.Jassim *et al.*** [17] studied linear and non-linear optical property for PMMA thin films doped with the Rhodamine B laser dye and (Ag) nano particles are used in medicine. Four different mixtures of (10^{-3}) M Rhodamine B laser dye had been prepared using chloroform solvent .Four different thin films had been made from these mixtures using drop casting method. The absorption spectra of these thin films had been taken. The absorption spectra properties had been measured depending on the absorption spectra for thin films. The non- linear optical properties were calculated according to normalized transmittance data obtained from Z-scan setup with closed and open aperture. The main conclusion is that the (Ag) nano particles causes a shift of the absorption wavelengths to longer wavelengths (red shift).

In (2018) **A. Lafta *et al.*** [18] studied optical limiting performances in Fluorescein with different concentrations of (2, 4, 6 and 8) mM are investigated by using (473 nm) continuous wave (CW) laser. The optical limiting behavior is investigated transmission measurement through the sample at different

concentrations. The investigation shows that the optical limiting capability is concentration dependent. The results showed that the sample has obvious optical limiting effect. (8 mM) concentration has the best limiting effect among the four concentrations chosen. It is also found that the threshold value of optical limiting is affected by sample absorption coefficient. The Fluorescein exhibits good optical limiting properties in solution.

In (2018) **K. Jamel and F. Tawil** [19] studied fluorescein sodium dye doped in polymer poly polyvinyl alcohol (PVA) at various thicknesses, the optical properties of the dye at various thicknesses. The Z-scan method was utilized at (532nm), and the UV-Visible and fluorescence spectrometers were used to examine the spectrum features in order to compute optical characteristics that are nonlinear in two cases: closed aperture and open aperture. The results were compared between the two cases. Open-aperture empirical data indicated that the fluorescein sodium dye film models exhibited saturation absorption or two-photon absorption as well as a positive or negative effect in closed-aperture experiments.

In (2019) **N. Al-Huda *et at*** [20] studied Spectral and linear optical properties for a mixture of Rhodamine B (RB) and Fluorescein Sodium (Na Fl) organic laser dyes were determined at different concentrations (10^{-3} and 10^{-4}) M in ethanol solvent at room temperature. The intensity of absorption range is towards longer wavelengths (red shift). The quantum efficiency diminished while the radiative and fluorescence life time increased when increment concentration, organic laser dyes have a spectrum within the range (540-500) nm. Results demonstrate that a mixture of laser dyes are effective optical materials when contrasted with individual laser dyes. It can be utilized as resonator in cavity lasers.

In (2020) **S. Haider** [21] studied the effect of fluorescence energy transfer between laser organic dyes. It included preparing a mixture model consisting of Aniline blue dye as (donor) with a Malachite green dye as

(accepter) . And when measuring the absorption and fluorescence spectra of both dyes, the big overlap between them is achieved, and this confirms that the accepter + donor model has occurred. Initially the absorption and emission (fluorescence) spectra of the two dyes were studied at four different concentrations that is dissolved with ethanol solvent. The results show that the decrease in concentration leads to a decrease in the intensity of absorption and emission (fluorescence) for all the prepared samples.

In (2021) **A. Afrah and A. Ban** [22] studied the spectral linear, and nonlinear optical properties of (Acriflavine) organic laser dye at concentrations (10^{-5}M), as well as thin films of this dye doped with (PVA) polymer and (Ag) nanomaterial for use in nonlinear optics. Nonlinear calculations were performed using the (Z-Scan) technique . The measurements were made with a diode pump solid state laser operating at a wavelength of (457nm). The results indicated that higher powers increased the nonlinear refractive index but decreased the nonlinear absorption coefficient for all prepared samples.

In (2022) **H**. **Fadhel and A .Ban** [23] studied optical nonlinearities and optical limiting behaviors for mixture of two organic laser dyes: Rhodamine B (RB) and Methyl violet (10B) dissolved in ethanol solvent at concentration (10^{-6}) M , have been measured utilizing Z-Scan setup. The measurement was completed using continuous wave(CW) diode pump solid state laser at wavelength (457 nm) and power (84mW).The closed-case Z-scans of all samples give self-defocousing phenomena. The consequences of the open-case of all samples give two photon absorbtion. Non-linear optical properties of mixture dye is larger than those for single dyes. The results revealed that all samples can be a good candidate for optoelectronic and photonic applications.

In (2022) **M. Afrah *et al***. [24] studied non-linear optical properties of azure A organic laser dye, dissolved in ethanol solvent with concentration (10^{-4} M). The nonlinear optical properties measured using a highly sensitive method known as Z-Scan technique in two cases (close) aperture and (open) aperture

for obtain two important optical phenomena: nonlinear refractive index and nonlinear absorption coefficient. The result indicates that the sample of this dye show a negative nonlinear refractive index and two photon absorption (2PA). The results indicate (Azure A) is a promising material to be used in photonic and nonlinear optical devices. It can be used as a potential medium for various optoelectronic applications including that in optical power limiting.

In (2023) **M. Sarah *et al***. [25] studied the non-linear optical characteristics of organic laser dyes (Acriflavine, Orcein, and Azur-B) dissolved in Ethanol solvent with concentration (10^{-5}M) were investigated in this study. It was determined the nonlinear optical characteristics by using the Z-Scan method, which represents a very sensitive approach for obtaining two essential optical phenomena: nonlinear refractive index and nonlinear absorption coefficient, in two different situations (close aperture) and (open aperture). The results indicate these dyes are a promising material to be used in photonic and nonlinear optical devices. An optical power limiter uses this promising medium for a range of optoelectronic applications.

In (2023) **S. Hemalatha *et al*.** [26] studied the fabrication, characterization and the third-order nonlinear optical (NLO) properties of basic blue 7 (BB 7) dye -doped polyvinyl alcohol (PVA) polymer thin films. The absorption spectra of BB 7 dye-PVA films were measured by UV-visible absorption studies. The functional groups of BB 7-PVA films have been identified by FT-IR spectroscopic analysis.

The nonlinear absorption and refraction of BB 7-PVA films were respectively explored by open aperture and closed aperture Z-scan technique using a (50 mW) semiconductor diode laser of (635 nm) wavelengths. The BB 7-PVA films exhibit the reverse saturable absorption (RSA) and self-defocusing effect .The present experimental results show that BB 7- PVA films may have potential applications in future photonic and NLO devices.

1.3 Aims of the Work

The main aims of this work are:

1. Study the spectral, linear and non-linear optical properties for all samples of two organic laser dyes Coumarin (334) and Fluorescein dissolved in ethanol solvent at different concentrations .
2. Study the spectral, linear and non-linear optical properties for thin films of Coumarin (334), Fluorescein dyes and their mixture with Polyvinyl alcohol polymer (PVA) doped (Ag, Al_2O_3) nanoparticles using drop casting method .
3. Possibility of using all samples of organic laser dyes and their mixture as optical limiting and active laser medium .

1.1 Introduction

Nonlinear optical properties have been the subject of numerous investigations theoretically and experimentally during recent years due to their applications to many branches. The nonlinear optical properties are important parameters in characterizing and determining the applicability of any material to nonlinear optical device. There are several techniques for measuring these parameters like degenerate four waves mixing, third harmonic generation and Z-Scan technique[1].

Organic compounds have been the subject of intense theoretical and experimental study due to their promising applications in different life science fields. The organic compounds are defined as hydrocarbons and their derivatives[2].They can be subdivided into saturated and unsaturated compounds. Organic dyes are fluorescent molecules with large molecular weights, characterized by a strong absorption band in the visible region of the electromagnetic spectrum .Such a property is found only in organic compounds which contain an extended system of conjugated bonds alternating single and double bonds [3]. In a dye laser, these molecules are dissolved in an organic solvent or incorporated in to a solid matrix. Although dyes have been demonstrated to laser in the solid, liquid, or gas phase ,it is in the liquid and solid phases that dyes have made a significant impact as laser media [4].

Organic dyes are one of the materials which play an important role in the nonlinear optics field, because of the large variety of these compounds at high intensities, fast response, large nonlinear properties, and easy to process integrated into optical devices. The organic materials such as organic dyes have compatibility with other materials mainly related to the need of employing large volumes of organic solutions of dyes that are both toxic and expensive[5]. So that the dye has to be changed for different wavelength regions, so attempts were made to overcome the problems posed by dye solutions by incorporating

dye molecules into solid matrices .This has resulted in significant advances towards the development of practical tunable solid-state lasers[6].

Dye doped polymers find applications in similar fields of modern photonic technology, optical amplifiers, fiber optics, and optical limiting which is used for protecting the human eye and the sensors by handling the laser output [7].Polyvinyl Alcohol (PVA) is synthetic polymer utilized from the early 1930 in a wide range of industrial, commercial, medical and food applications, and has numerous properties like being effectively fabricated, with relatively a minimal cost, and dielectric material [8].

Nanotechnology represents one of the major break throughs of modern science, enabling materials of distinctive size, structure and composition to be formed. For the smaller particles the percentage of surface atoms increases, leading to changes in physical and chemical properties of the materials [9].PVA composite thin films are modulated and improved by addition of (Ag and Al_2O_3) nanoparticles and those properties can be applied in the fields of optics and electronics .The nonlinear properties of dyes solutions, dyes doped polymer thin films and nanoparticles composite can be studied by using a simple technique called Z - scan[10]. It is a sensitive and popular experimental method to measure intensity dependent of nonlinear optical (NLO) properties of materials which can rapidly measure both nonlinear absorption (NLA) and nonlinear refraction (NLR) in solids, liquids and then studying the optical limiting behavior [11].

1.2 Literature Survey

Several researches on using Z-scan for study nonlinear properties of organic dyes.

In (2013) **B. Anand *et al*** . [12] studied the spectral dispersion of ultrafast optical limiting in the laser dye Coumarin-120 in the wavelength region (630 to 900) nm, measured in a single Z-scan, using the white-light continuum as the excitation source. Optical limiting is found to arise from two-photon absorption, and its spectrum agrees very well in shape with the linear absorption spectrum.

In (2014) **A .Hassan *et al*** . [13] studied the spectral properties (absorption and fluorescence) for Fluorescein Sodium dye by solving it in Ethanol ,at different concentrations at room temperature .The intensity of absorption increased and fluorescence decreased while concentration increases with agreement of Beer - Lambert Law. The fluorescence spectrum followed and entirely the same as absorption spectrum. The quantum efficiency of the dissolved Fluorescein Sodium dye in Ethanol were (88%, 85% and 70%) respectively. In addition to the radiative life time was (0.55,0.91 and 1.3) ns and the fluorescence life time (0.49,0.77 and 0.9) ns respectively.

In (2015) **R. Nader**. [14] studied the nonlinear optical properties of fluorescein Sodium dye in water at different concentrations in a constant thickness of (1 mm) , by using Z-Scan method to evaluate the nonlinear refractive index (n_2) and the absorption nonlinear coefficient (β).It found that the nonlinear coefficients changes with increasing the concentrations of the dye.

In (2016) **N. Habeeb *et al* .** [15] studied the spectral properties of mixed Coumarin (334) and Rhodamine (590) in ethanol solvent at different concentration had been studied. The absorption intensity of these dyes increases as the concentrations increase in addition to that the spectrum was shifted towards the longer wavelength (red shift). The energy transfer process has been investigated after achievement this condition. The fluorescence peak intensity of donor molecule was decrease and its bandwidth will increases on the contrary of

the acceptor molecule its intensity increase gradually and its bandwidth decreases as the acceptor concentration increase.

In (2017) **T.Ali Naser** [16] studied effect of polarity of solvent on the phenomenon of the fluorescence energy transfer between the laser dyes, and the preparation of two samples, one of the mixing of the acridine orange dye as a donor with the Orcein dye as a acceptor and the other mixing of acridine orange dye as a donor with Rhodamine B as a acceptor. When the absorption and fluorescence spectra of both models are achieved, the large overlap between them is achieved, and this confirms the achievement of the (acceptor-donor) sample. The results of the study showed a significant increase in the intensity of the fluorescence spectra of the mixing samples compared to the dyes individually for all the prepared samples. This increase was increased with the polarity of the solvent and the highest fluorescence intensity was in the first mixing sample of these.

In (2017) **M.Jassim *et al.*** [17] studied linear and non-linear optical property for PMMA thin films doped with the Rhodamine B laser dye and (Ag) nano particles are used in medicine .Four different mixtures of (10^{-3}) M Rhodamine B laser dye had been prepared using chloroform solvent .Four different thin films had been made from these mixtures using drop casting method .The absorption spectrums of these thin films had been taken . The absorption spectra properties had been measured depending on the absorption spectra for thin films. The non- linear optical properties were calculated according to normalized transmittance data obtained from Z-scan setup with closed and open aperture .The main conclusion is that the (Ag) nano particles causes a shift of the absorption wavelengths to longer wavelengths (red shift).

In (2018) **A. Lafta *et al.*** [18] studied optical limiting performances in Fluorescein with different concentrations of (2, 4, 6 and 8) mM are investigated by using (473 nm) continuous wave (CW) laser. The optical limiting behavior is investigated via transmission measurement through the sample at different

concentrations. The investigation shows that the optical limiting capability is concentration dependent. The results showed that the sample has obvious optical limiting effect. (8 mM) concentration has the best limiting effect among the four concentrations chosen. It is also found that the threshold value of optical limiting is affected by sample absorption coefficient. The Fluorescein exhibits good optical limiting properties in solution.

In (2018) **K. Jamel and F. Tawil** [19] studied fluorescein sodium dye doped in polymer poly polyvinyl alcohol (PVA) at various thicknesses, the optical properties of the dye at various thicknesses. The Z-scan method was utilized at (532nm), and the UV-Visible and fluorescence spectrometers were used to examine the spectrum features in order to compute optical characteristics that are nonlinear in two cases: closed aperture and open aperture. The results were compared between the two cases. Open-aperture empirical data indicated that the fluorescein sodium dye film models exhibited saturation absorption or two-photon absorption as well as a positive or negative effect in closed-aperture experiments.

In (2019) **N. Al-Huda et at .** [20] studied Spectral and linear optical properties for a mixture of Rhodamine B (RB) and Fluorescein Sodium (Na Fl) organic laser dyes were determined at different concentrations (10^{-3} and 10^{-4}) M in ethanol solvent at room temperature. The intensity of absorption range is towards longer wavelengths (red shift). The quantum efficiency diminished while the radiative and fluorescence life time increased when increment concentration, organic laser dyes have a spectrum within the range (540-500) nm. Results demonstrate that a mixture of laser dyes are effective optical materials when contrasted with individual laser dyes. It can be utilized as resonator in cavity lasers.

In (2020) **S. Haider** [21] studied the effect of fluorescence energy transfer between laser organic dyes. It included preparing a mixture model consisting of Aniline blue dye as (donor) with a Malachite green dye as

(accepter) . And when measuring the absorption and fluorescence spectra of both dyes, the big overlap between them is achieved, and this confirms that the accepter + donor model has occurred. Initially the absorption and emission (fluorescence) spectra of the two dyes were studied at four different concentrations that is dissolved with ethanol solvent. The results show that the decrease in concentration leads to a decrease in the intensity of absorption and emission (fluorescence) for all the prepared samples.

In (2021) **A. Afrah and A. Ban** [22] studied the spectral linear, and nonlinear optical properties of (Acriflavine) organic laser dye at concentrations (10^{-5}M), as well as thin films of this dye doped with (PVA) polymer and (Ag) nanomaterial for use in nonlinear optics. Nonlinear calculations were performed using the (Z-Scan) technique . The measurements were made with a diode pump solid state laser operating at a wavelength of (457nm). The results indicated that higher powers increased the nonlinear refractive index but decreased the nonlinear absorption coefficient for all prepared samples.

In (2022) **H**. **Fadhel and A .Ban** [23] studied optical nonlinearities and optical limiting behaviors for mixture of two organic laser dyes: Rhodamine B (RB) and Methyl violet (10B) dissolved in ethanol solvent at concentration (10^{-6}) M , have been measured utilizing Z-Scan setup. The measurement was completed using continuous wave(CW) diode pump solid state laser at wavelength (457 nm) and power (84mW).The closed-case Z-scans of all samples give self-defocousing phenomena. The consequences of the open-case of all samples give two photon absorbtion. Non-linear optical properties of mixture dye is larger than those for single dyes. The results revealed that all samples can be a good candidate for optoelectronic and photonic applications.

In (2022) **M. Afrah *et al***. [24] studied non-linear optical properties of azure A organic laser dye, dissolved in ethanol solvent with concentration (10^{-4} M). The nonlinear optical properties measured using a highly sensitive method known as Z-Scan technique in two cases (close) aperture and (open) aperture

for obtain two important optical phenomena: nonlinear refractive index and nonlinear absorption coefficient. The result indicates that the sample of this dye show a negative nonlinear refractive index and two photon absorption (2PA) . The results indicate (Azure A) is a promising material to be used in photonic and nonlinear optical devices. It can be used as a potential medium for various optoelectronic applications including that in optical power limiting.

In (2023) **M .Sarah *et al***. [25] studied the non-linear optical characteristics of organic laser dyes (Acriflavine, Orcein, and Azur-B) dissolved in Ethanol solvent with concentration (10^{-5}M) were investigated in this study. It was determined the nonlinear optical characteristics by using the Z-Scan method, which represents a very sensitive approach for obtaining two essential optical phenomena: nonlinear refractive index and nonlinear absorption coefficient, in two different situations (close aperture) and (open aperture). The results indicate these dyes are a promising material to be used in photonic and nonlinear optical devices. An optical power limiter uses this promising medium for a range of optoelectronic applications.

In (2023) **S. Hemalatha *et al*.** [26] studied the fabrication, characterization and the third-order nonlinear optical (NLO) properties of basic blue 7 (BB 7) dye -doped polyvinyl alcohol (PVA) polymer thin films. The absorption spectra of BB 7 dye-PVA films were measured by UV-visible absorption studies. The functional groups of BB 7-PVA films have been identified by FT-IR spectroscopic analysis.

The nonlinear absorption and refraction of BB 7-PVA films were respectively explored by open aperture and closed aperture Z-scan technique using a (50 mW) semiconductor diode laser of (635 nm) wavelengths. The BB 7-PVA films exhibit the reverse saturable absorption (RSA) and self-defocusing effect .The present experimental results show that BB 7- PVA films may have potential applications in future photonic and NLO devices.

1.3 Aims of the Work

The main aims of this work are:

1. Study the spectral, linear and non-linear optical properties for all samples of two organic laser dyes Coumarin (334) and Fluorescein dissolved in ethanol solvent at different concentrations .
2. Preparing mixing of these two dyes in different ratios and different concentrations dissolved in ethanol solvent.
3. Preparing thin films of Coumarin (334) , Fluorescein dyes and their mixture with Polyvinyl alcohol polymer (PVA) doped (Ag , Al_2O_3) nanoparticles using drop casting method .
4. Study spectral, linear and non-linear optical properties for all samples of mixture of two organic laser dyes and as solutions and thin films .
5. Possibility of using all samples of organic laser dyes and their mixture as optical limiting and active laser medium .

2.1 Introduction

This chapter defines laser dyes , parameters effecting on properties of laser dye, concentration effect, solvent effect, photo physical process of laser dyes, Fluorescence spectra characteristics, fluorescence quantum efficiency ,applications of organic laser dye, transfer of energy between laser dyes, organic hosts (Polymers), polymer and nanoparticles, laser light interaction with matter , optical properties, linear and nonlinear optical properties, Z-scan technique and optical limiting.

2.2 Laser Dyes

Laser dyes are large organic molecules with molecular weights of few hundred mu. When one of these organic molecules is dissolved in a suitable liquid solvent (such as ethanol, methanol, or an ethanol-water mixture) it can be used as laser medium in a dye laser. Generally, laser dyes are complex molecules containing a number of ring structures, which lead to complex absorption and emission spectra. The laser dyes can be classified into different classes by virtue of their structures that are chemically similar. Common examples are the coumarins, xanthenes and pyrromethenes as in Figure (2.1)[27].

Laser dyes that can be used to extent continuously the emission spectrum from the near ultraviolet to the near infrared . Laser dyes, either as solutions or solid, are the active medium in pulsed and CW dye lasers as well as ultrafast shutters for Q-switching and passive mode-locking. Thus a variety of dyes is necessary to cover the entire spectral range[27].Dye molecules are used mostly to generate tunable laser. The basic absorption processes in laser dyes could be divided into linear absorption, saturation of absorption (SA) and reverse saturable absorption (RSA). Saturation of absorption is vital for use of the dyes in mode locking. The most important application of optical limiting devices that protect sensitive optical components, including human eye from laser induced

damage. Laser dyes are promising compounds for nonlinear optical applications because they exhibit strong nonlinear optical behavior . For effective performance, laser dyes molecules should have the following characteristics [28]:

1. Strong absorption at excitation wavelength and minimal absorption at lasing wavelength.
2. High quantum yield (0.5-1.0) .
3. Good photochemical stability.
4. A short fluorescence lifetime (5-10) ns.
5. Low probability of intersystem crossing to the triplet state.
6. Laser dyes have to be very pure since impurities frequently quench the laser output.

By appropriate dye selection it is possible to produce coherent light of any wavelength from (320 to 1200) nm. The approximate working ranges of various laser dyes are shown schematically as in Figure(2.1).

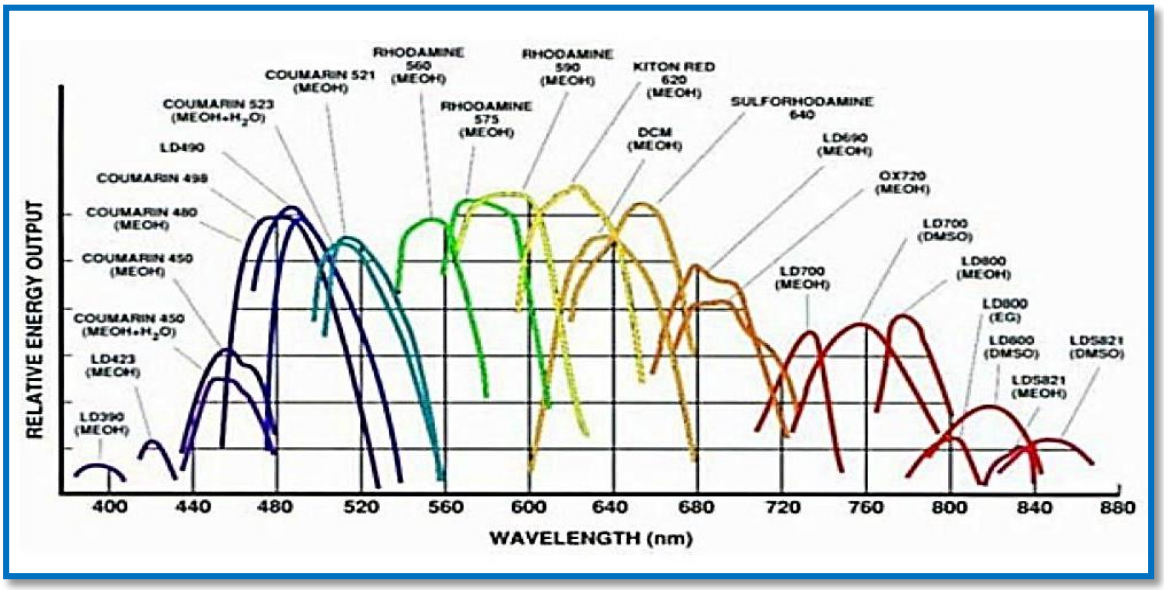

Figure (2.1) : Laser Dyes [29].

2.3 Types of Laser dyes

Laser dyes are classified into four groups based on the wavelength they emit [30]:

1- Polymethine Dyes: such as Cyanines dye, emit in the red and near-infrared region of the spectrum between (700-1000) nm.

2- Xanthine Dye: such as Rhodamine dye, emits light in the visible region of the spectrum between (500-700) nm.

3- Coumarin Dye: such as Coumarin, emit light in the green and blue area between (400-500) nm.

4- Scintillator dyes: such as Y11 dye, emit in the UV area between (320-400) nm.

2.4 Parameters Effecting on Properties of Laser Dye

There are many factors that affect the laser properties of the dyes. The solid laser active medium, the liquid and the gas are generally affected by the design conditions of the laser system. In liquid laser active medium, special factors are affected by the concentration of the solution, the type of solvent, the viscosity of the solution and its acid, and all the influencing factors affect the electronic structure i.e the distribution of the electrons of the effective medium at its energy levels, the molecular electronic energy transitions, molecular oscillatory energy, which changes the wavelength ranges of the emission spectra in the active medium, especially the laser dyes, and this has led to the possibility of synthesis (change wavelength) of the dyes. These include [31]:

2.4.1 Concentration Effect

The concentration is one of the most important parameters that has influence on the organic dyes, where in very dilute samples, dye dissolves completely into monomers. In such kind of dye solutions, the intrinsic absorption of the dye molecules is affected by dye-solvent interaction. Dye- dye interaction is negligible because of the large average distance between the dye

molecules in dilute solution. By increasing dye concentration, dimer or higher aggregates are formed [32]. Increasing the dye concentration leads to red shifts, that may be caused by changes in the environment of dye molecules, such as changes in polarity or polarizability. This leads to interactions between neighboring molecules, which lowers their excited state energy and produces a red shift in the spectra. At high concentrations, the dye-dye interaction gains importance since the mean distance between dye molecules becomes small and this leads to deviation from the Beer-Lambert law[33].

2.4.2 Solvent Effect

Two features distinguish gas phase spectra from those obtained in the condensed phase, broadening due to solute-solvent interaction and stokes shift i.e. non-coincidence at the maxima of (0-0) bands due to solvation effect. Solvation refers to reorientation of solvent molecule around a solute molecule, an effect which does not take place in rigid medium[34].

Solvents can also cause displacement of the absorption and fluorescence spectra. Displacement of both absorption and fluorescence spectra imply an interaction of the solvent of both the ground state and the excited state of the molecule on the other hand, when the fluorescence emission spectrum alone is changed ,the implication is an interaction of the solvent with the excited state of the molecule but not with the ground state. Since the solvent reorientation process is a direct of the polarization of the excited of the solute, it is not surprising that solvent effects on the Franck-Condon shift have been related to the dielectric constant of the solvent, as in Figure (2.2). The solvents also affect the fluorescence lifetime. In the case of large molecules, the spectra are shifted toward longer wavelengths but fluorescence lifetime are less affected[35].

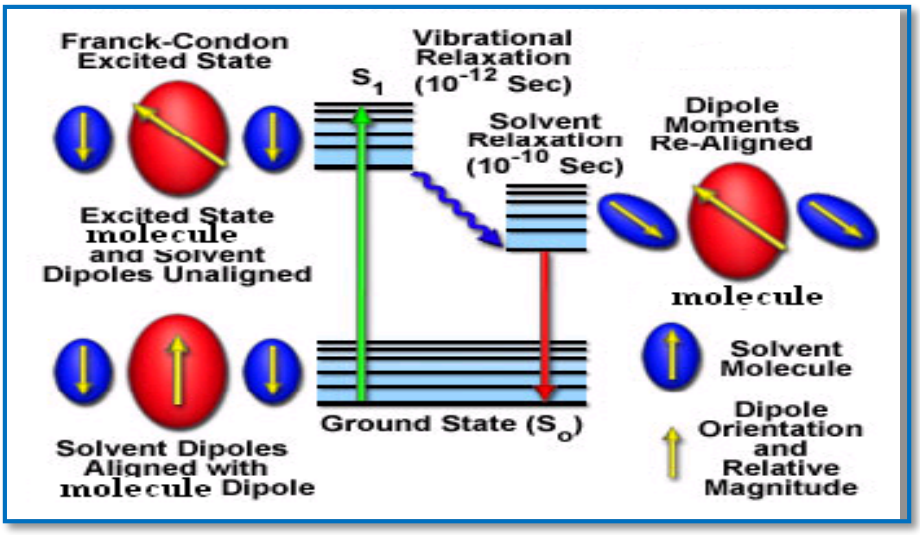

Figure (2.2): Solvent effect[36].

2.4.3 Radiation Effect

Radiation normally affects organic compounds in two basic manners, both resulting from excitation or ionization of atoms. The two mechanisms are chain scission, a random rupturing of bonds, which reduces the molecular weight (i.e. strength) of organic compounds, and cross-linking of organic molecules, which results in the formation of large three-dimensional molecular networks. Most often, both of these mechanisms occur as organic materials are subjected to ionizing radiation, but frequently one mechanism predominates with in a specific organic compound. As a result of chain scission, very-low-molecular-weight fragments, gas evolution, and unsaturated bonds may appear. Cross-linking generally results in an initial increase in tensile strength, while impact strength decreases and the organic materials become more brittle with increased dose[37].

When organic materials are subjected to irradiation by ionizing radiation such as gamma rays, X-rays, various effects can be expected from the ionizations. The ratio of resultant recombination, cross-linking and chain scission will vary from organic materials to organic materials and to some degree from part to part based on the chemical composition of the organic

compounds, the total radiation dose absorbed, and the rate at which the dose was deposited. The ratio is also significantly affected by the residual stress processed into the part, the environment present during irradiation (especially the presence or absence of oxygen), and storage environment (temperature and oxygen)[38].

2.5 Photophysical Process of Laser Dyes

Jablonski diagram is a very important diagram used to describe the most important processes as shown in Figure (2.3). Absorbed light excites dye molecules from the lowest levels of the ground state (S00)to higher vibrational levels of the (S1n)state, thermal redistribution of the populations among the continuum of sublevels takes place within a very short time (~ 10 -11 sec).A Boltzmann distribution in the continuum is achieved, with most of the excited molecules decaying nonradiatively to level (S10). Excitation of the (S1)state can also be affected by direct absorption from the ground state to the second excited singlet state (S2n). For most organic dye solutions, the decay from (S2 to S1) state is non-radiative and very rapid(~ 10-10 to 10-11 sec) [38].

A molecule in (S10)can return to (S00)by emitting a photon of light whose energy is less than the absorbed light. This spontaneous radiative process (fluorescence) is thus shifted to longer wavelengths from the absorption. The intersystem crossing from singlet to triplet manifold is comparatively slow considering the small energy gap between (S1 and T1). Frequently the highest energy fluorescence band is of lower energy than the lowest energy absorption band. The difference in wavelength observed between these two bands is called the Stokes shift. A Stokes shift is the most easily observed as the difference between the wavelength of maximum absorption and the wavelength of maximum fluorescence[39].

Phosphorescence is the emission of a photon involving a change of multiplicity, because the change in multiplicity is formally forbidden. The phosphorescence lifetimes are significantly longer than the fluorescence lifetimes. Phosphorescence is commonly observed from (T1 to So). Because the

lifetime of phosphorescence is so long, molecules in (T1)may lose their energy by other transitions that are more efficient or by chemical reaction [39].

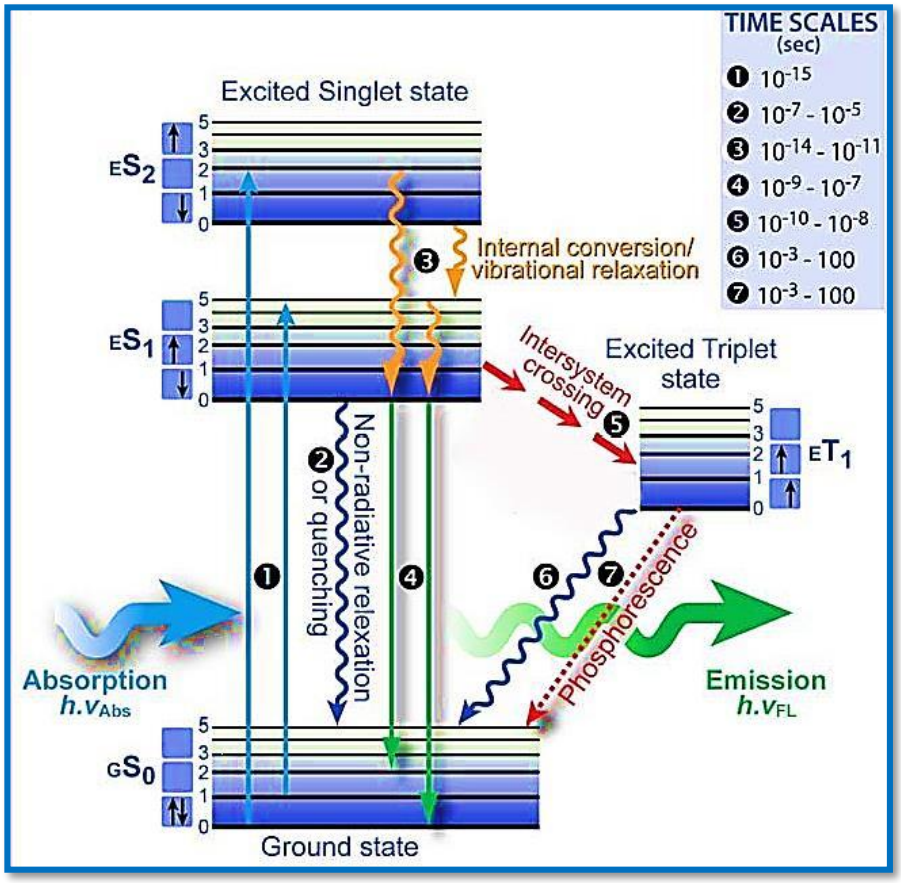

Figure (2.3) : Jablonski Diagram [39].

2.5.1 Radiative Process

The amount of light absorbed by a molecule is determined by the electromagnetic radiation field's interaction with the molecule. If the photon's energy is equivalent to the energy of the material's gap between its ground and excited states, a photon can be absorbed from an electromagnetic field and an electron stimulated to a higher energy level. Then absorption is referred to as a resonant process, as the absorbed photon's energy must equal the energy difference between two levels. This indicates that only photons with a specific frequency (wavelength) are absorbed [40].

2.6 Fluorescence Spectra Characteristics

These transitions are accompanied by an energy emission during their acquisition. The molecule that is raised after reaching the lowest vibrational level (S1) and the loss of the amount of energy in the vibration relaxation process is caused by the molecule or atom absorbing a photon and entering the irritating level. The only way to relax is by emitting the electrons, which causes an energy loss (So) of the fluorescence process, which causes a direct radiation transmission between (10-8-10-9) sec [41].

This time period differs from one sample to another and is known as the life time of the fluorescence sample and the wavelength longer than the wavelength that produced the excitation (energy loss), i.e, the stokes phenomenon. Stokes displacement can be defined as the difference in wavelength or frequency units in the position of the absorption and emission (fluorescence) spectra of the same electronic transitions. Stokes displacement happen due to the vibration relaxation in excited states. Figure (2.4) shows the Stokes shift between the absorption and emission (fluorescence) spectra[42].

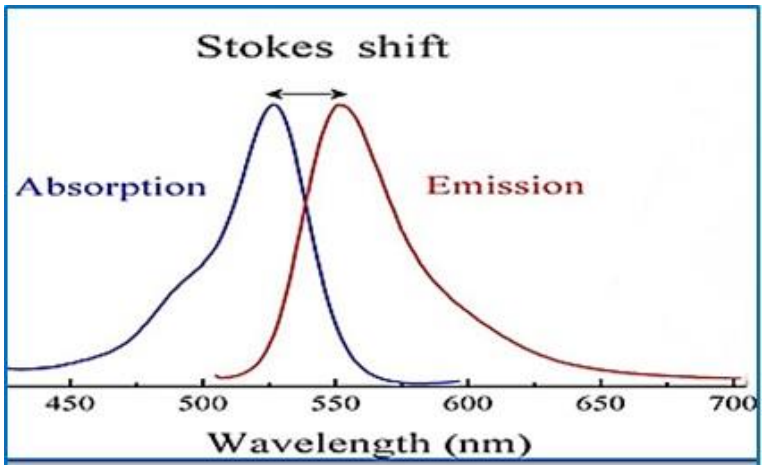

Figure (2.4): Stokes displacement between the absorption and the emission spectra[43].

2.6.1 Phosphorescence

A radiative transition between states of different multiplicity is described as phosphorescence. It occurs when the molecules goes from (T1)to various

vibration levels of the ground state (S0) and emits photons, at life time is about (10-3 to 10-2) (Sec), and is larger than the life time of the fluorescence process. Since the energy of triplet state (T10) is less than that of singlet state (S10) (The state of fluorescence emission), thus, the energy of phosphorescence photons is less than that of fluorescence photons, as shown in Figure (2.3) [43].

2.6.2 Non-radiative Processes

Sometimes the electron can be relaxed without emission photon, where the photon energy can convert to kinetic energy. In the case of a solid, such as crystal and an ionic, the excited ion given energy them to lattice material, therefore the non-radiative processes do not emit the photons[44].

2.6.3 Intersystem Crossing

Intersystem crossing is a non-radiative transition, which occurs when singlet state S1 can be changed to the triplet (T1)without emission radiation and the decay time of this translation about (5×10-8) sec. This process involves a change in the spin multiplicity of the molecule. Intersystem crossing occurs faster than the fluorescence, example, the benzophenone molecule, (S1) undergoes intersystem crossing to (T1) with life time (10-10) Sec and the fluorescence life time is (10-6) Sec, so, Intersystem crossing at a rate that is (104) times faster than fluorescence. And because the excited triple state is lower in energy from the excited single state, the molecule cannot return to the excited single state, but, it can easily return to the ground state by phosphorescence processes[45].

2.6.4 Internal Conversion

If no spin-change occurs, the non-radiative process called internal conversion. This is the means by which higher excited singlet states decay rapidly to the lowest excited singlet before further photo physical change occurs. Similarly, higher triplet states decay rapidly to the lowest triplet state by this

process, internal conversion can also occur from the lowest singlet state to the ground state [46].

2.7 Fluorescence Quantum Efficiency

The time of the radiative transition from the lower vibrational level to the excited electronic state then to a ground vibrational level and back to its first state after this period of time is called radiative life time (τFM), which is defined as the inverted rate of fluorescence emission (KFM) in unit (S-1) [47]:

$$\tau_{FM} = \frac{1}{K_{FM}} \qquad (2.1)$$

Where : (KFM) represents the probability of radiation transition. Because of the presence of non-radiative processes competing with the possibility of radiation transition (KFM), it will reduce the number of particles qualified for fluorescence emission, so the total probability of transition (KF) will be the sum of the radiated and nonradiative transition [48]:

$$\tau_F = \frac{1}{K_{FM} + \sum K_d} = \frac{1}{K_F} \qquad (2.2)$$

Where : (Σ Kd) is the sum of constants (rate constants) for non-radioactive processes for the lowest vibratory state. The time of the fluorescence life time (τF) is the actual time of the fluorescence, which is equal to the inverted total constants of all non-radiative and radioactive processes that cause energy loss[49]:

$$\tau_F = \frac{1}{K_{FM} + K_{IC} + K_{ISC}} \qquad (2.3)$$

Where (KIC)is the rate of inter conversion (sec-1) and (KISC)is the rate of intersystem crossing (sec-1). The life time of the fluorescence (τF) can be the main life time of the excited state. There is a relation between fluorescence intensity and fluorescence life time (τF)[50]:

$$I = I_{\circ} \exp(-t / \tau_F) \qquad (2.4)$$

Where: (I) is the fluorescence intensity at time (t), (Io) represents the highest fluorescence intensity and (t) time immediately after the stopping of excitation.

The life time of fluorescence (τF) can be calculated from a standard compound known as its chronological age, as well as the area under curve, as in the following relationship[51]:

$$\tau_F = \frac{a \times \tau_{fRB}}{a_{RB}} \qquad (2.5)$$

Where :(τfRB) is the time-span of the standard compound, the Rhodamine B (3.230 ns) at concentration (10-4) M and (aRB) is the area under the fluorescence curve of rhodamine B and its value (117.6 cm-1), a is the area under the curve of the compound required in this research.The quantum efficiency (ØF) represents the quantum yield of fluorescence, which is the ratio between the probability of radiation transition (KFM) and the average of processes for the singles state (KFM+KIC+KISC).This value is a physical constant of each type of excited particles, or the ratio of total energy emitted to the amount of absorbed energy[52]:

$$\phi_F = \frac{K_{FM}}{K_{FM} + K_{IC} + K_{ISC}} = \frac{K_{FM}}{K_{FM} + \sum K_d} \qquad (2.6)$$

$$\phi_F = K_{FM}\tau_F = \frac{\tau_F}{\tau_{FM}} \qquad (2.7)$$

It is also possible to calculate the quantum yield of fluorescence (ØF) by calculating the ratio between the area of the fluorescence spectrum and the area of the absorbance spectrum, as shown in the following equation [53]:

$$\phi_F = \frac{\int F(\nu')d\nu'}{\int \varepsilon(\nu')d\nu'} \qquad (2.8)$$

It has been observed that the quantum yield of fluorescence for several compounds depends on the wavelength used in the excitation and the temperature. So the quantum yield of fluorescence increases when non-radiative

processes decrease and when the temperature is reduced, the relation between them is reversed. The values of fluorescence production are between (0-1), therefore, the life time of the fluorescence is far less than the radiation life time due to the non-radiactive processes competing for the fluorescence process. Since values of the quantum efficiency are less than or equal to one, then ($\tau FM > \tau F$) [54].

2.8 Transfer of Energy Between Laser Dyes

Energy transfer happened when the energy transferred from donor to accepter, an energy transfer from one system to another is said to occur when an amount of energy crosses the boundary between them, thus increasing the energy content of one system while decreasing the energy content of the other system by the same amount[55]. The condition for this mechanism is when there is an overlap between fluorescence of the donor and absorption of the accepter as in Figure (2.5). The aim of energy transfer was to improve the efficiency and broadband the tunable spectral range of dye lasers. The main mechanisms that have been proposed for energy transfer are [56]:

1. Radiative energy transfer, i.e., the absorption of donor emission by an acceptor molecule. This process can by represented by [56]:

$$D^* \longrightarrow D + h\nu$$

$$A + h\nu \longrightarrow A^*$$

Where the star indicates an electronically excited state. In a radiative energy transfer process, the fluorescence life time of both the donor and the acceptor dye

molecules are kept unchanged.

2. Non-radiative energy transfer: either you get by long-range resonance energy transfer, or as a result of collision of molecules the donor and the acceptor. The process of fluorescence quenching of the donor (D) due to the interaction with the acceptor (A) can be represented by [56]:

$$D^* + A \xrightarrow{KET} D + A^*$$

Where: KET is the energy transfer rate constant.

Energy transfer reduces the emission intensity from (D*) and sensitizes emission from (A*). Another important application of energy transfer is in dye lasers. Dye lasers have some limitations as the dye solution used as an active medium absorbs energy from the excitation source in a very limited spectral range and so the emission band also has these limitations. If a dye laser has to be used as an ideal source, its spectral range needs to be extended. In order to extend the spectral range of operation, mixtures of different dye solutions dye molecules embedded in solid matrices are being used [57].

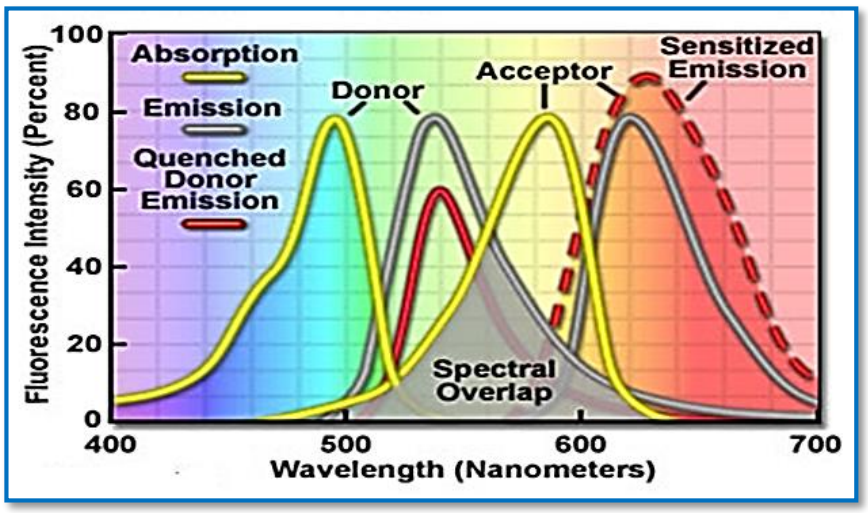

Figure(2.5): Energy Transfer between Laser Dyes [57].

2.9 Applications of Laser Dyes

There are many applications for laser dyes, including [58] :

1- Industrial applications of laser dyes include separation of isotopes of important radioactive elements such as Uranium. Uranium is used as fuel in the nuclear power reactors to generate electricity.

2- Medical applications of laser dyes include skin treatments, including tattoo removal, diagnostic measurements, lithotripsy and activation of photosensitive drugs for photodynamic therapy, etc.

3- Optical communications.

4- Image processing .

5- Switching.

6- 3D data storage and optical limiting.

2.10 Coumarin (334) Organic Laser Dye and its Applications

Coumarin is one of the most essential class of laser dyes. Coumarin laser dyes have a strong electron donating substituent [either an amino (-NR2) or hydroxyl (-OH)] in the 7-position. The first Coumarin derivative was coumarin by Sorokin and Lankard [59]. From that point, about 100 Coumarin laser dyes have come to be known [60] . Based on chelation-enhanced fluorescence (CHEF), Coumarins are scantily utilize as chemical sensors for metal ions. Thus a wide tunable range of (420 to 580 nm) can be covered with Coumarin dyes. Coumarin is a dye and is used in some of the most successful laser sources . This dye is known as laser dye and is found in natural products. It can be made synthetically and is well suited for many applications such as dye doped lasers due to its excellent fluorescent properties . It is also useful in other applications including environment friendly fluorescent probes, dopant for photonic crystals, to enhance fluorescence for application in biochemical sensing etc [60].

2.11 Fluorescein Organic Laser Dye and its Applications

This dye has a place with the family of xanthine class dyes where this family is characterized by high chemical stability of the type of solvent (polarity), efficient manufacturing. Fluorescein has an orange- red to dark crystalline powder that dissolved in water and alcohol (except chloroform) . Fluorescein has been widely used as a fluorescent tracer in technical chemistry, microscopy, serology and forensics [61]. Fluorescein has been employed for diagnostic purposes in other branches of medicine [62]. surgery for brain tumors, angiography and ophthalmology and used as sterile, it is on the list of essential medicines of the world health organization.

2.12 Organic Hosts (Polymers)

The name polymer is derived from the Greek word, in which the first word "Poly" means multiple and the second one "mer" means part. The polymer has a synonym word "macromolecule". The building block unit of the polymer is the monomer. Polymers are macromolecules composed of repeated units (monomer), and sometimes these units are repeated linearly and the chain is formed by connecting these units or the chains to form branches or they are interconnected [63]. The polymer chain length is determined by the number of the repeated unites (monomer) in the chain and it is called the degree of polymerization. Its molecular weight is equal to the product of the molecular weight of the monomer by the degree of polymerization [64]. One of the important characteristics of polymers is their high molecular weight . Atoms are bonded together in the polymer chain by strong covalent bonds, and are attracted by very weak internal forces. The polymer is called "homopolymer" if the repeated units are the same whereas the polymer formed of different units is called "copolymer" or "mixed polymer" . The polymer is said to be "ordered" if its monomers repetition is constant. However if any reduction occurs to the arrangement of the monomers, the polymer becomes "Amorphous"[65].

2.12.1 The Classification of Polymer

Polymers can be classified according to molecular structure to four types as shown in Figure (2.6) [66]:

a- Linear polymers. c- Network polymers

b- Branched polymers. d- Cross linked polymers.

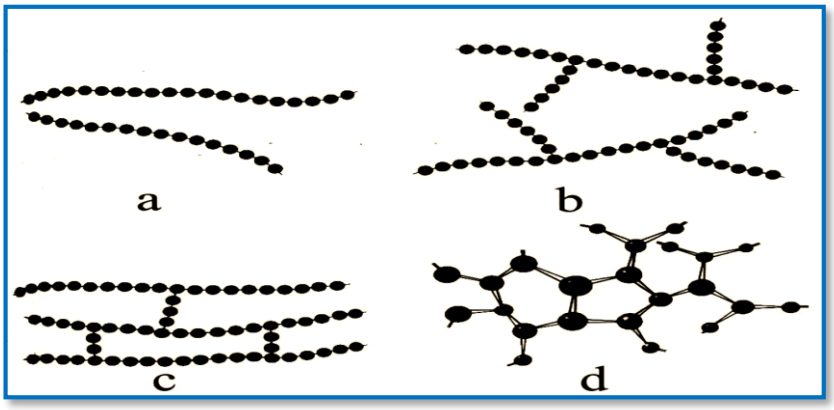

Figure (2.6) Types of polymers : (a) Linear (b) Branched (c) Network (d) Cross linked [66].

2.13 Polyvinyl alcohols (PVA)

Polyvinyl Alcohols (PVA) have been utilized in a variety of industrial, commercial, medical, and food applications since the early 1930, including resins, lacquers, surgical threads, and food-contact applications. It has the ability to dissolve in water which is resistant to solvents, oils, and has an exceptional ability to adhesive materials cellulosic so it's extensive uses included in the paper industry and in textile industries in membranes of industry resistance to oxygen in the coating photographic film as well as in high-voltage applications to possess high tensile strength in a high storage capacity, electrical and optical properties depending on the type of additives and impurities [67].

2.14 Nanoparticles

Nanoparticle has a size range between (1 to 100) nm. Unexpected physical and chemical behavior of matter occurs at the nanometer scale, paving the way for a number of scientific exploitations, making nanoparticles a great area of scientific research. The transition from microparticles to nanoparticles yields dramatic changes in all properties. Nanoscale materials have a large surface area for a given volume. Many important chemical and physical

interactions are governed by surfaces and surface properties. Nanostructures material can have substantially different properties from a larger-dimensional material of the same composition [68].In nanomaterial, the surface area per unit volume is inversely proportional to the material's diameter, thus, the smaller the diameter, the greater the surface area per unit volume, change in particle diameter, layer thickness, or fibrous material diameter from the micrometer to nanometer range, will affect the surface area to volume ratio by three orders of magnitude generally, there are different approaches for a classification of nano materials, the main classes of nanoscale structures can be classified by dimensions, some of which are summarized in Table(2.1) Also can be shown in Figure (2.7) [69].

Table (2.1) Classification of Nanomaterials by Dimension [69].

Dimension	Example
0 dimension ⩽100 nm	Particles , quantum dots
1 dimension ⩽100 nm	Nanotubes,Nanowire,Nanorods
2 dimension ⩽100 nm	Thin films,Coatings, Multilayers
3 dimension ⩽100 nm	Nanometar-sized cluster

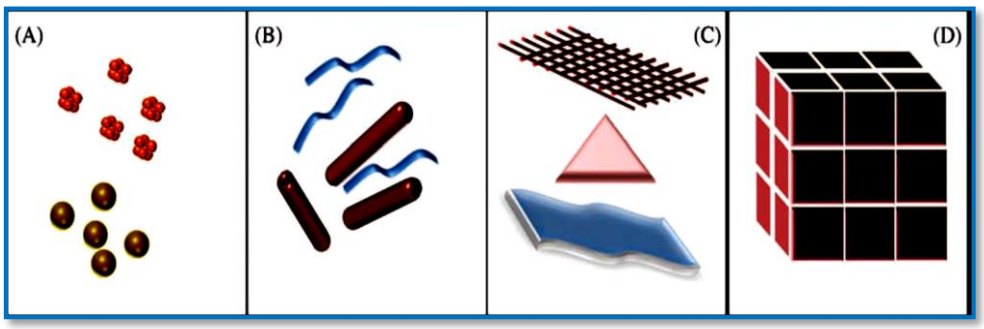

Figure (2.7) : Various Kinds of Nanomaterials. (A) 0D spheres and clusters.(B) 1D nanofibers, wires, and rods. (C) 2D films, plates, an networks. (D) 3D nanomaterials [69].

2.14.1 Silver Nanoparticle (Ag NPS) and its Applications

Silver nanoparticles are nanoparticles of silver of between (1 -100) nm in size. While frequently described as being 'silver' some are composed of a large percentage of silver oxide due to their large ratio of surface-to-bulk silver atoms. Different shapes of nanoparticles can be constructed depending on the application of the study [70].

Silver nanoparticles are being used in numerous technologies and incorporated into a wide array of consumer products that take advantage of their desirable optical, conductive, and antibacterial properties [71]:

1. Optical Applications: Silver nanoparticles are used to efficiently harvest light and for enhanced optical spectroscopies.
2. Conductive Applications: Silver nanoparticles are used in conductive inks and integrated into composites to enhance thermal and electrical conductivity.
3. Antibacterial Applications: Silver nanoparticles are incorporated in apparel, footwear, paints, wound dressings, appliances, cosmetics, and plastics.

2.14.3 Alumina Nanoparticles (Al_2O_3) and its Applications

Metal oxide nanoparticles have been extensively developed in the past decades. They have been widely used in many applications such as catalysts, sensors, semiconductors, medical science, capacitors, and batteries. Alumina generally refers to corundum. It is a white oxide. Alumina has several phases such as gamma, delta, theta, and alpha. However, the alpha alumina phase is the most thermodynamically stable phase[72]. In general, Alumina has many interesting properties, for example high hardness, high stability, high insulation, and transparency.

Al_2O_3 Nanoparticles can be synthesized by many techniques including ball milling, solgel, pyrolysis, sputtering, hydrothermal, and laser ablation Among them, the laser ablation is a widely used technique for the synthesis of nanoparticles since it can be synthesized in gas or liquid. This technique offers several advantages such as rapid and high purity process compared with other methods[72]. Alumina (Al_2O_3) in particular possesses a variety of commercial and industrial uses and has become one of the most important commercial ceramic materials [73]. Aluminum oxide (Al_2O_3) has good physical properties like abrasion resistance, corrosion resistance, thermal stability, electrical insulation and high mechanical strength, etc. Therefore, in order to increase Tg and enhance mechanical properties of the (PVA), Al_2O_3 nanoparticles were added into the (PVA) [74,75].

2.15 Interaction of Laser Light with Matter

When laser radiation strikes a material surface, part of it is absorbed and part is reflected. The energy that is absorbed begins to heat the surface. There are several regimes of parameters that should be considered, depending on the time scale and on the flounce. When laser beam acts on the material, laser energy is first absorbed by free electrons. The absorbed energy then propagates through the electron subsystem and then transferred to lattice therefore laser energy is transferred to material [76].

This process has a resonant feature because materials show different absorptions to lasers with different wavelengths, this dependence of absorption on wavelength is decided by the microstructure and electromagnetic properties of the material. The intensity of laser light produces a wide range of interaction. The interaction of matter can be classified as linear interaction and nonlinear interaction. The advent of the laser as a coherent light with high intensity source gives birth of nonlinear optics. It plays an important role in many areas of science and technology now [77] The NLO effects are associated with light-induced changes in the optical constants of the material, either the absorption

coefficient, the refractive index, or both. They are best treated by considering the interaction of the light beam with the atoms of the material as driving force acting on an ensemble of oscillator with natural resonance frequency[78].

2.16 Nonlinear Optical Properties

Nonlinear optics is the study of phenomena that occur as consequence of the modification of the optical properties of materials on interaction with intense light. Nonlinear phenomena has been studied extensively. The particles of the medium are displaced from their equilibrium positions, so that positive charged particles move in the direction of the electric field, while the negative charged particles move in the direction opposite to the direction of the applied electric fields. Dipole moments are created because of the displacement between positive and negative charged particles, and the dipole moment per unit volume describes the induced polarization of the medium [79].

When the applied electric fields are sufficiently small, the electric polarization is approximately linearly proportional with the applied electric field E [80]:

$$P = \varepsilon_o \chi.E \qquad (2.9)$$

Where (ε_o) is the permittivity of free space, (χ) is the electric susceptibility tensor. This is the case of linear optics. However, when the applied electric fields are high enough, the induced polarization has a nonlinear dependence on these electric fields and can be expressed as a power series with respect to the electric field [80]:

$$P = \varepsilon_o (\chi^{(1)}.E + \chi^{(2)}. EE + \chi^{(3)}.EEE+\ldots \qquad (2.10)$$

$$P = P^{(1)} + P^{(2)} + P^{(3)}+\ldots. \qquad (2.11)$$

Where $\chi^{(1)}$ is the linear susceptibility, $\chi^{(2)}$ is the second order nonlinear susceptibility, and $\chi^{(3)}$ is the third order nonlinear susceptibility. The term $\chi^{(1)}$ is responsible for linear absorption and refraction, and is the only term that reflects the linearity between the induced polarization and the incident electric field. The

term $\chi^{(2)}$ is present only in non-centrosymmetric materials, i.e. materials that do not have inversion symmetry. The third order nonlinear optical interactions, which are described by the term $\chi^{(3)}$ [81].The field of nonlinear optics (NLO) has been developing for a few decades as a promising field with important applications in the domain of photo electronics and photonics. Organic materials are considered as one of the important classes of third order NLO materials because they exhibit large and fast nonlinearities[82].

Various types of organic compounds have been studied to obtain materials with large third order nonlinearity. On the other hand, a wide range of techniques has been used to measure third order nonlinearity e.g. degenerate four waves mixing, third harmonic generation and Z-Scan technique. Among all these techniques Z-Scan is a simple for the measurement of the nonlinear refractive index and nonlinear absorption coefficient[83]. It provides not only the magnitudes of the real and imaginary parts of the nonlinear susceptibility but also the sign of the real part. Both nonlinear refraction and nonlinear absorption in solid and liquid samples can be rapidly measured by the Z-Scan technique, which utilizes self-focusing or self-defocusing phenomena in optical nonlinear materials. There are two methods of Z-Scan, the closed -aperture and open -aperture system[84]:

2.16.1 Closed-aperture Z-Scan

A closed aperture Z-Scan measures the change in intensity of a beam, focused by lens (L) in Figure (2.8), as the sample passes through the focal plane. Photo detector (PD) collects the light that passes through an axially centered aperture (A) in the far field. The change on axis intensity is caused by self-focusing or self-defocusing by the sample (S) as it will create a change in index of refraction forming a lens in a nonlinear sample as shown in Figure (2.8) [85].

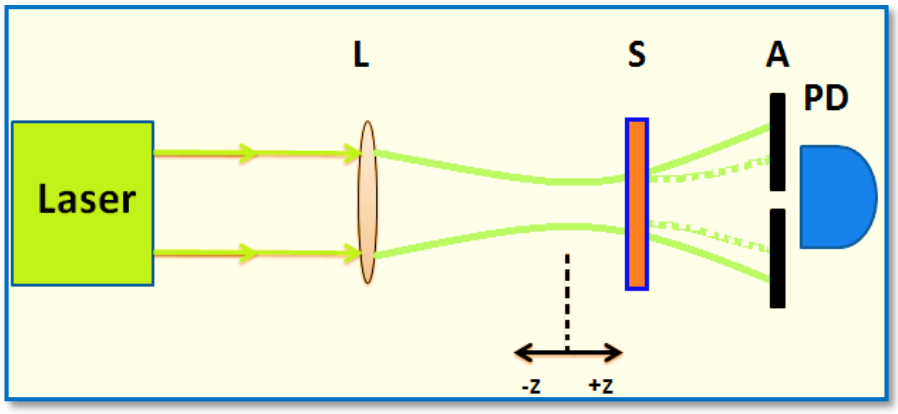

Figure (2.8): Closed aperture Z-Scan[85].

To show how the Z-Scan transmittance as a function of (Z) is related to the nonlinear refraction of the sample, if a medium with a negative nonlinear refraction index and a thickness smaller than the diffraction length of the focused beam. This can be considered as a thin lens of variable focal length. Beginning far from the focus (Z<0), the beam irradiance is low and nonlinear refraction is negligible. In this condition, the measured transmittance remains constant (i.e., Z-independent). As the sample approaches the beam focus, irradiance increases, leading to self-lensing in the sample. A negative self-lens before the focal plane will tend to collimate the beam on the aperture in the far field, increasing the transmittance measured at the iris position[86].

After the focal plane, the same self-defocusing increases the beam divergence, leading to a widening of the beam at the aperture and thus reducing the measured transmittance. Far from focus (Z >0), again the nonlinear refraction is low resulting in a transmittance Z-independent. A transmittance maximum (peak), followed by a transmittance minimum (valley) is a Z-Scan signature of a negative nonlinearity. An inverse Z-Scan curve (i.e., a valley followed by a peak) characterizes a positive nonlinearity. Figure (2.9) depicts these two situations [86].

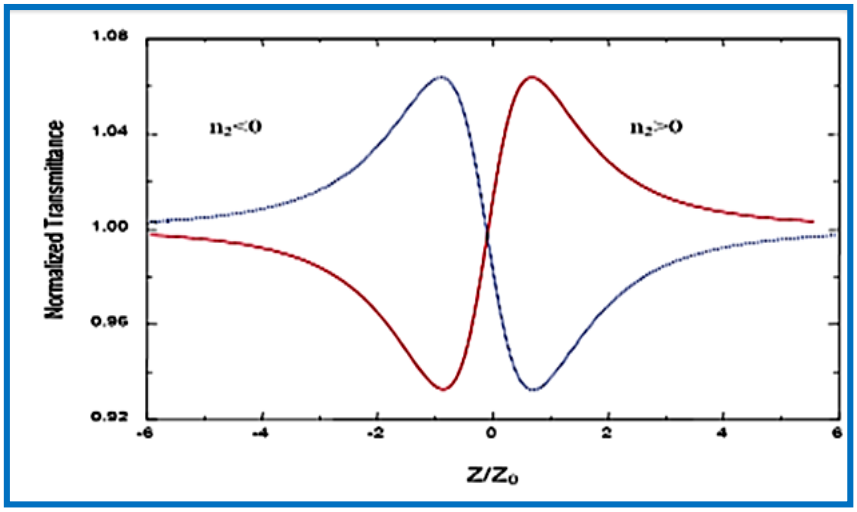

Figure (2.9): Calculated Z-Scan transmittance curves for nonlinearity[86].

The nonlinear refractive coefficient is calculated from the peak to valley difference of the normalized transmittance by the following formula [87]:

$$n_2 = \frac{\Delta\Phi_o}{I_o L_{eff} k} \qquad (2.12)$$

Where, $k = 2\pi/\lambda$, (k) is wave number, (I_o) is the intensity at the focal spot and $(\Delta\Phi_o)$is the nonlinear phase shift[87]:

$$\Delta T_{p-v} = 0.406|\Delta\Phi_o| \qquad (2.13)$$

(ΔT_{p-v}) the difference between the normalized peak and valley transmittances, $(L_{eff})$is the effective length of the sample, determined from[88]:

$$L_{eff} = \frac{(1-exp^{-\alpha_o L})}{\alpha_o} \qquad (2.14)$$

Where (L) is the sample length and$(\alpha_o)$is linear absorption coefficient which is given as[88]:

$$\alpha_o = \frac{\ln(\frac{1}{T})}{t} \qquad (2.15)$$

Where (T) is the transmittance, (t) is the cuvette thickness. The linear refractive index(n_o) obtained from equation[88]:

$$n_o = \frac{1}{T} + \left[\left(\frac{1}{T^2} - 1\right)\right]^{1/2} \qquad (2.16)$$

The intensity at the focal spot is given by[89]:

$$I_o = \frac{2P_{peak}}{\pi \omega_o{}^2} \qquad (2.17)$$

Is defined as the peak intensity within the sample at the focus, Where(ω_o)is the beam radius at the focal point.

2.16.2 Open-aperture Z-Scan

An open-aperture Z-Scan analyzes the change in intensity of a beam in the far field at photo detector PD, which captures the full beam, as focused by lens (L)in Figure (2.10), in the far field at photo detector (PD), which captures the entire beam. The change in intensity is caused by two photon absorption in the sample S as it travels through the beam waist[90].

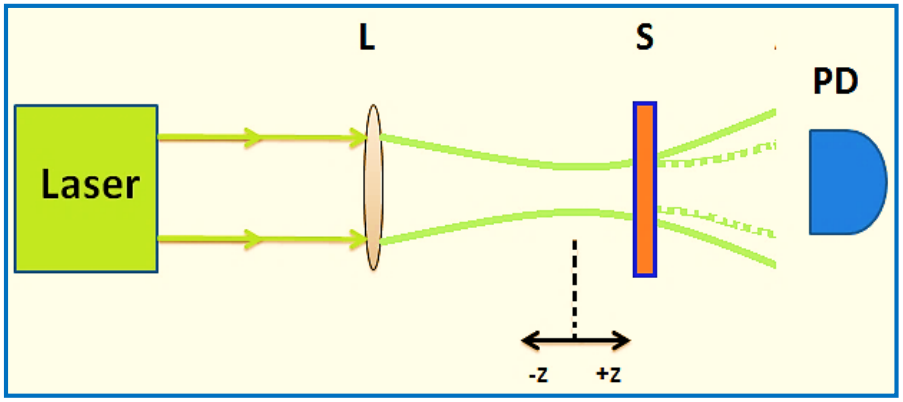

Figure (2.10): Open-aperture Z-Scan[90].

Clearly, even with nonlinear absorption, a Z-Scan with a fully open aperture is insensitive to nonlinear refraction (thin sample approximation). The Z-Scan traces with no aperture are expected to be symmetric with respect to the focus (Z = 0) where they have a minimum transmittance (e.g., two photon absorption)or maximum transmittance (e.g., saturation of absorption). In fact, the coefficients of nonlinear absorption can be easily calculated from such transmittance curves. Nonlinear absorption coefficient (β),can be easily calculated by using following equation [91]:

$$\beta = \frac{2\sqrt{2}\,T(z)}{I_o L_{eff}} \qquad (2.18)$$

Where T(z):The minimum value of normalized transmittance at the focal point, at (Z=0). It should be clear that the transmittance versus sample position graph of such an open aperture Z-Scan should be symmetric around the focus as shown in Figure (2.11).

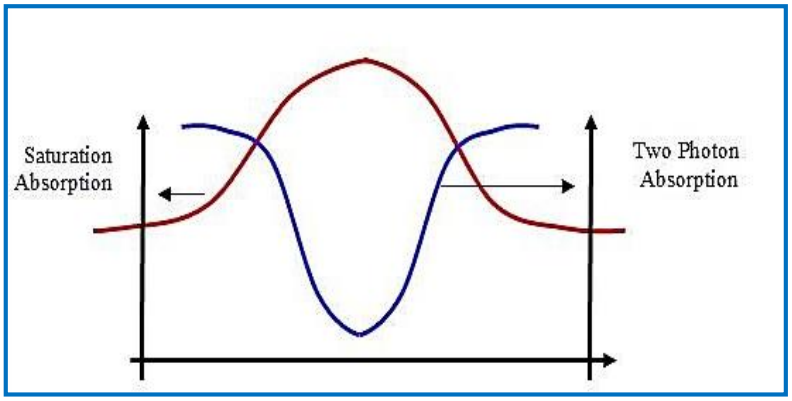

Figure (2.11): Open aperture Z-Scan curve [91].

2.16.3 Nonlinear Absorption and Nonlinear Refraction

The basic optical properties involved in the light matter interaction are absorption, which is defined by the absorption coefficient (α), and refraction, which is defined by the index of refraction (n). When the material is irradiated, the energy of the absorbed photons makes it possible for the transition from the ground state to the excited state. There is also a change in the refractive index when a material is placed in a strong electric field. In fact, the index of refraction becomes dependent on the intensity of the electric field. At high intensity, the refractive index is given by[92]:

$$n = n_o + n_2 I \qquad (2.19)$$

Where (n_2)is the nonlinear refractive coefficient related to the intensity.

The absorption of the material is also intensity dependent given by[92]:

$$\alpha = \alpha_o + \beta I \qquad (2.20)$$

Where, (α_o) is the linear absorption coefficient and (β) is the nonlinear absorption coefficient related to the intensity. The coefficients (n), and (α) are related to the intensity of laser.

2.16.4 Saturable Absorption

A nonlinear process that can be associated with real (rather than virtual) energy levels and population changes in those levels is that of saturable absorption. This process occurred when the nonlinear absorption coefficient ($\beta < 0$), which can be appeared when a strong light absorption between two levels causes saturation (bleaching) of the corresponding electronic transition. The two levels involved surface resonance ground and excited state. On the other hand, this is a process in which a material can be highly absorbing at a specific wavelength when a low-intensity beam is incident upon the material, yet an extremely intense beam (at that same wavelength) will pass through the medium with little change in intensity [93].

2.16.5 Two Photon Absorption (TPA)

Two-photon absorption (TPA) is the simultaneous absorption of two photons of identical or different frequencies in order to excite a molecule from one state (usually the ground state) to a higher energy electronic state. The energy difference between the involved lower and upper states of the molecule is equal to the sum of the energies of the two photons, as in the case of a saturable absorber, is the process of two-photon absorption. This process occurred when the nonlinear absorption coefficient $\beta > 0$. This effect is shown in Figure (2.12). The two-photon transition rate can be significantly enhanced if an intermediate level (2) is located near the virtual level shown by the dashed line in Figure (2.12) [94].

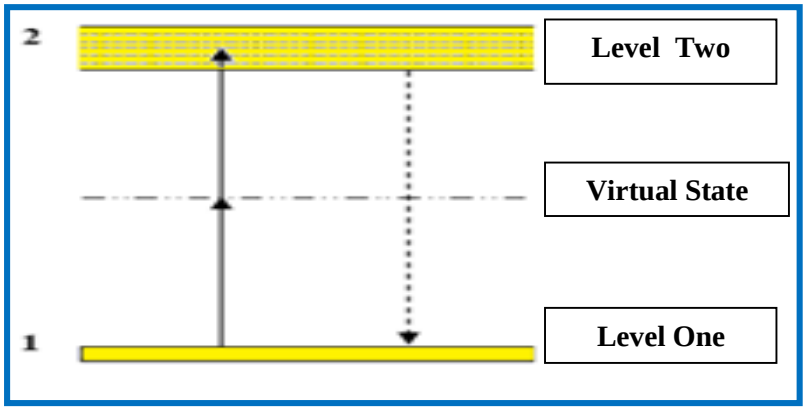

Figure (2.12): Energy levels for two-photon absorption process[94].

2.16.6 Kerr Effect

A nonlinear interaction of light in a medium related to the nonlinear electronic polarization, which can be described as modifying the refractive index. For high-intensity laser beams, the Kerr effect can create a local change in the refractive index that causes the laser material to act as a lens. This can result in self-focusing of laser beams[95].

2.16.7 Self-Focusing

A nonlinear process that causes a spatial variation of the laser intensity, in which an intense beam of light modifies the optical properties of a material medium in such a manner that the beam is caused to come to a focus within the material. The material acts as a positive lens, because the laser beam induces a refractive index variation within the material with a larger refractive index at the center of the beam than at its periphery. Self-focusing can be obtained when the nonlinear refractive index is positive in sign[96].

2.17 Optical Limiting

Following the invention of the laser, it was recognized that intense laser beams can easily damage delicate optical instruments, and especially the human eye. Nowadays, lasers have become common in daily life and they are even being incorporated into toys. Thus, protection from lasers is not only a scientific subject but also a potential public safety issue. Over the last few decades, many scientists have sought so called optical limiting materials that exhibit ‘nonlinear

extinction', i.e. strongly attenuate intense, potentially dangerous laser beams, while readily transmitting low intensity ambient light[97].

Protection of eyes and sensors from intense laser pulses. Candidates for optical limiting materials should have low transmittance for strong incident light, and instantaneous response over a broad spectral range. An optical limiter is a device designed to keep the power, irradiance, or energy by an optical system. The most important application of such a device is the protection of sensitive optical sensors and components from laser damage[98]. A common geometry is illustrated in Figure (2.13). Laser beam is focused into a material and then collected through a finite aperture in the far field. At high irradiance the far field beam distortion arising from the self-focusing of the laser beam inside the medium will result in the limiting of the transmitted light through the aperture. Where (Z) is the distance between the focal plane in free space and the center of the sample, and (d) is the distance from this plane to the aperture plane. [98].

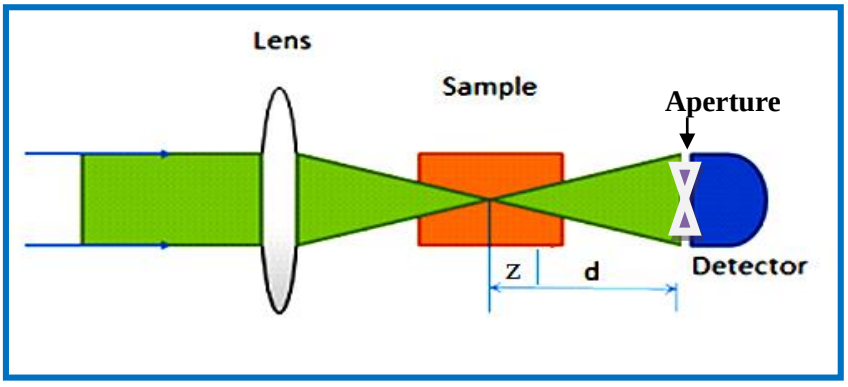

Figure (2.13) : Schematic of the limiting geometry[98].

2.1 Introduction

This chapter defines laser dyes ,parameters effecting on properties of laser dye, concentration effect, solvent effect, photo physical process of laser dyes, Fluorescence spectra characteristics, fluorescence quantum efficiency, applications of organic laser dye, transfer of energy between laser dyes, organic hosts (Polymers), polymer and nanoparticles, laser light interaction with matter, optical properties, linear and nonlinear optical properties, Z-scan technique and optical limiting.

2.2 Laser Dyes

Laser dyes are large organic molecules with molecular weights of few hundred mu. When one of these organic molecules is dissolved in a suitable liquid solvent (such as ethanol, methanol, or an ethanol-water mixture) it can be used as laser medium in a dye laser. Generally,laser dyes are complex molecules containing a number of ring structures,which lead to complex absorption and emission spectra. The laser dyes can be classified into different classes by virtue of their structures that are chemically similar. Common examples are the coumarins, xanthenes and pyrromethenes as in Figure (2.1) [27].

Laser dyes that can be used to extent continuously the emission spectrum from the near ultraviolet to the near infrared . Laser dyes, either as solutions or solid, are the active medium in pulsed and CW dye lasers as well as ultrafast shutters for Q-switching and passive mode-locking. Thus a variety of dyes is necessary to cover the entire spectral range [27]. Dye molecules are used mostly to generate tunable laser. The basic absorption processes in laser dyes could be divided into linear absorption, saturation of absorption (SA) and reverse saturable absorption (RSA). Saturation of absorption is vital for use of the dyes in mode locking. The most important application of optical limiting devices that protect sensitive optical components, including human eye from laser induced damage. Laser dyes are promising compounds for nonlinear optical applications

because they exhibit strong nonlinear optical behavior. For effective performance, laser dyes molecules should have the following characteristics [28]:

1. Strong absorption at excitation wavelength and minimal absorption at lasing wavelength.
2. High quantum yield (0.5-1.0) .
3. Good photochemical stability.
4. A short fluorescence lifetime (5-10) ns.
5. Low probability of intersystem crossing to the triplet state.
6. Laser dyes have to be very pure since impurities frequently quench the laser output.

By appropriate dye selection it is possible to produce coherent light of any wavelength from (320 to 1200) nm. The approximate working ranges of various laser dyes are shown schematically as in Figure (2.1).

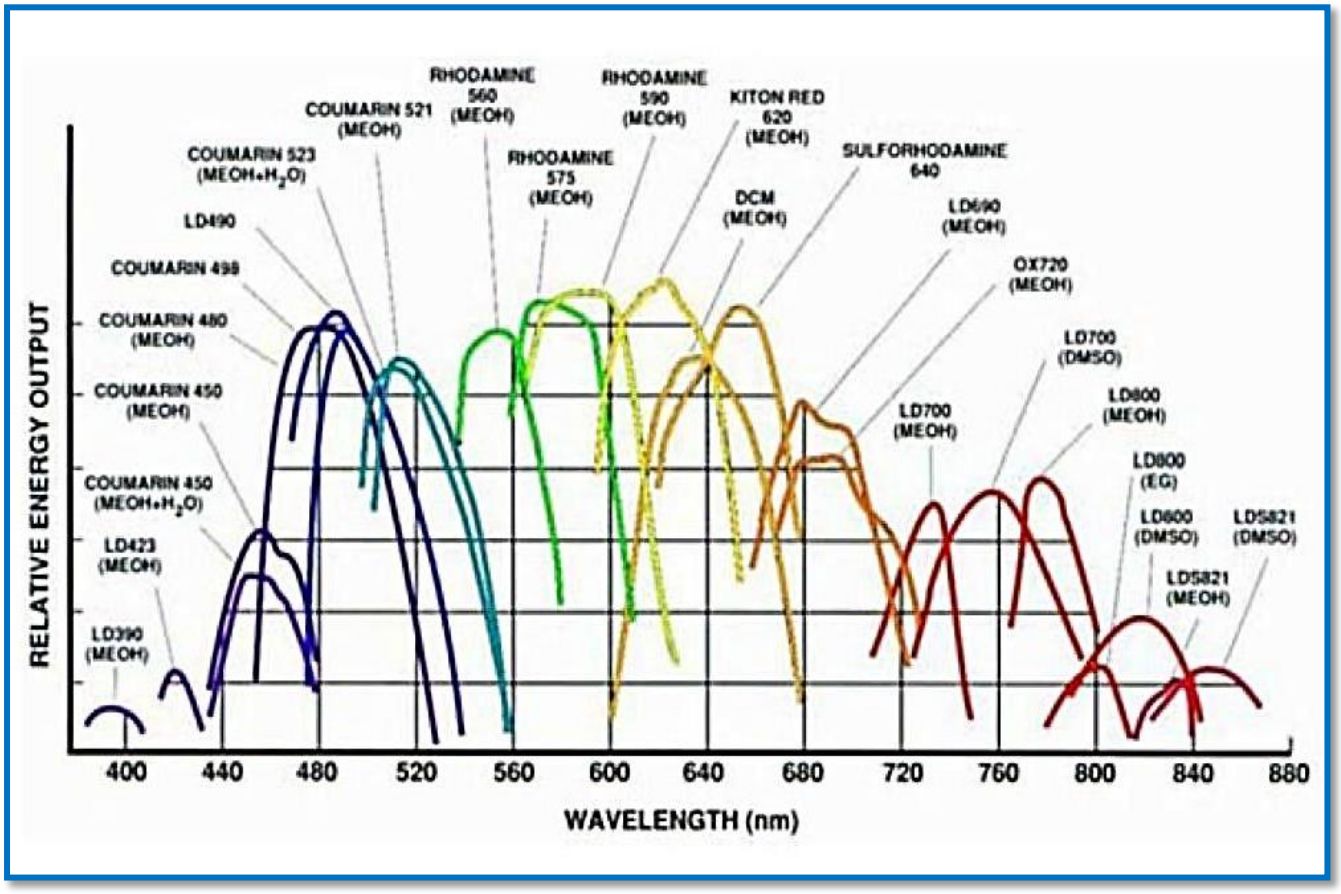

Figure (2.1): Laser Dyes [29].

2.3 Types of Laser dyes

Laser dyes are classified into four groups based on the wavelength which emit [30]:

1- Polymethine Dyes: such as Cyanines dye, emits in the red and near-infrared region of the spectrum between (700-1000) nm.

2- Xanthine Dye: such as Rhodamine dye, emits light in the visible region of the spectrum between (500-700) nm.

3- Coumarin Dye: such as Coumarin, emits light in the green and blue region between (400-500) nm.

4- Scintillator dyes: such as Y11 dye, emits in the UV region between (320-400) nm.

2.4 Effect Parameters on Properties of Laser Dye

There are many factors that affect the laser properties of the dyes. The solid laser active medium, the liquid and the gas are generally affected by the design conditions of the laser system. In liquid laser active medium, special factors are affected by the concentration of the solution, the type of solvent, the viscosity of the solution and its acid, and all the influencing factors affect the electronic structure i.e the distribution of the electrons of the effective medium at its energy levels, the molecular electronic energy transitions, molecular oscillatory energy, which changes the wavelength ranges of the emission spectra in the active medium, especially the laser dyes, and this has led to the possibility of synthesis (change wavelength) of the dyes. These include [31]:

2.4.1 Concentration Effect on Properties of Laser Dye

The concentration is one of the most important parameters that has influence on the organic dyes, where in very dilute samples, dye dissolves completely into monomers. In such kind of dye solutions, the intrinsic absorption of the dye molecules is affected by dye-solvent interaction. Dye- dye interaction is negligible because of the large average distance between the dye

molecules in dilute solution. By increasing dye concentration, dimer or higher aggregates are formed [32]. Increasing the dye concentration leads to red shifts, that may be caused by changes in the environment of dye molecules, such as changes in polarity or polarizability. This leads to interactions between neighboring molecules, which lowers their excited state energy and produces a red shift in the spectra. At high concentrations, the dye-dye interaction gains importance since the mean distance between dye molecules becomes small and this leads to deviation from the Beer-Lambert law [33].

2.4.2 Solvent Effect on Properties of Laser Dye

Two features distinguish gas phase spectra from those obtained in the condensed phase, broadening due to solute-solvent interaction and stokes shift i.e. non-coincidence at the maxima of (0-0) bands due to solvation effect. Solvation refers to reorientation of solvent molecule around a solute molecule, an effect which does not take place in rigid medium [34].

Solvents can also cause displacement of the absorption and fluorescence spectra. Displacement of both absorption and fluorescence spectra imply an interaction of the solvent of both the ground state and the excited state of the molecule on the other hand, when the fluorescence emission spectrum alone is changed ,the implication is an interaction of the solvent with the excited state of the molecule but not with the ground state. Since the solvent reorientation process is a direct of the polarization of the excited of the solute, it is not surprising that solvent effects on the Franck-Condon shift have been related to the dielectric constant of the solvent, as in Figure (2.2). The solvents also affect the fluorescence lifetime. In the case of large molecules, the spectra are shifted toward longer wavelengths but fluorescence lifetime are less affected [35].

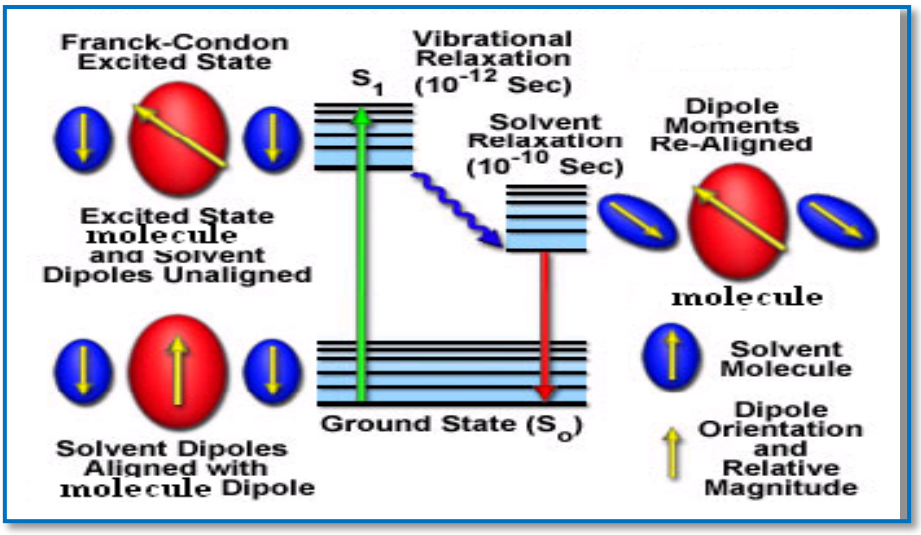

Figure (2.2): Solvent effect on Properties of Laser Dye [36].

2.4.3 Radiation Effect on Properties of Laser Dye

Radiation normally affects organic compounds in two basic manners, both resulting from excitation or ionization of atoms. The two mechanisms are chain scission, a random rupturing of bonds, which reduces the molecular weight (i.e. strength) of organic compounds, and cross-linking of organic molecules, which results in the formation of large three-dimensional molecular networks. Most often, both of these mechanisms occur as organic materials are subjected to ionizing radiation, but frequently one mechanism predominates with in a specific organic compound. As a result of chain scission, very-low-molecular-weight fragments, gas evolution, and unsaturated bonds may appear. Cross-linking generally results in an initial increase in tensile strength, while impact strength decreases and the organic materials become more brittle with increased dose [37].

When organic materials are subjected to irradiation by ionizing radiation such as gamma rays, X-rays, various effects can be expected from the ionizations. The ratio of resultant recombination, cross-linking and chain scission will vary from organic materials to organic materials and to some degree from part to part based on the chemical composition of the organic

compounds, the total radiation dose absorbed, and the rate at which the dose was deposited. The ratio is also significantly affected by the residual stress processed into the part, the environment present during irradiation (especially the presence or absence of oxygen), and storage environment (temperature and oxygen) [38].

2.5 Photophysical Process of Laser Dyes

Jablonski diagram is a very important diagram used to describe the most important processes as shown in Figure (2.3). Absorbed light excites dye molecules from the lowest levels of the ground state (S_{00})to higher vibrational levels of the (S_{1n})state, thermal redistribution of the populations among the continuum of sublevels takes place within a very short time (~ 10^{-11} sec).A Boltzmann distribution in the continuum is achieved, with most of the excited molecules decaying nonradiatively to level (S_{10}). Excitation of the (S_1)state can also be affected by direct absorption from the ground state to the second excited singlet state (S_{2n}). For most organic dye solutions, the decay from (S_2 to S_1) state is non-radiative and very rapid (~ 10^{-10} - 10^{-11} sec) [38].

A molecule in (S_{10}) can return to (S_{00}) by emitting a photon of light whose energy is less than the absorbed light. This spontaneous radiative process (fluorescence) is thus shifted to longer wavelengths from the absorption. The intersystem crossing from singlet to triplet manifold is comparatively slow considering the small energy gap between (S_1 and T_1). Frequently the highest energy fluorescence band is of lower energy than the lowest energy absorption band. The difference in wavelength observed between these two bands is called the Stokes shift. A Stokes shift is the most easily observed as the difference between the wavelength of maximum absorption and the wavelength of maximum fluorescence [39].

Phosphorescence is the emission of a photon involving a change of multiplicity, because the change in multiplicity is formally forbidden. The phosphorescence lifetimes are significantly longer than the fluorescence lifetimes. Phosphorescence is commonly observed from (T_1 to S_o). Because the

lifetime of phosphorescence is so long, molecules in (T_1)may lose their energy by other transitions that are more efficient or by chemical reaction [39].

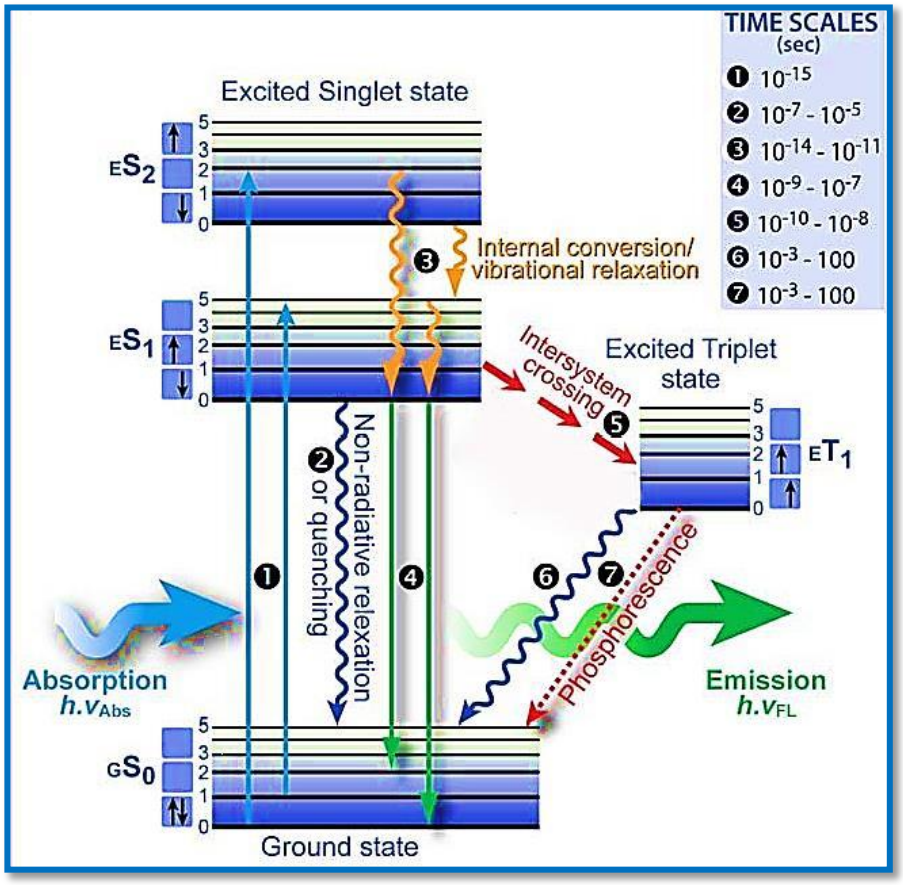

Figure (2.3) : Jablonski Diagram [39].

2.5.1 Radiative Process

The amount of light absorbed by a molecule is determined by the electromagnetic radiation field's interaction with the molecule. If the photon's energy is equivalent to the energy of the material's gap between its ground and excited states, a photon can be absorbed from an electromagnetic field and an electron stimulated to a higher energy level. Then absorption is referred to as a resonant process, as the absorbed photon's energy must equal the energy difference between two levels. This indicates that only photons with a specific frequency (wavelength) are absorbed [40].

2.6 Fluorescence Spectra Characteristics

These transitions are accompanied by an energy emission during their acquisition. The molecule that is raised after reaching the lowest vibrational level (S_1) and the loss of the amount of energy in the vibration relaxation process is caused by the molecule or atom absorbing a photon and entering the irritating level. The only way to relax is by emitting the electrons, which causes an energy loss (S_o) of the fluorescence process, which causes a direct radiation transmission between (10^{-8}-10^{-9}) sec [41].

This time period differs from one sample to another and is known as the life time of the fluorescence sample and the wavelength longer than the wavelength that produced the excitation (energy loss), i.e, the stokes phenomenon. Stokes displacement can be defined as the difference in wavelength or frequency units in the position of the absorption and emission (fluorescence) spectra of the same electronic transitions. Stokes displacement happen due to the vibration relaxation in excited states. Figure (2.4) shows the Stokes shift between the absorption and emission (fluorescence) spectra [42].

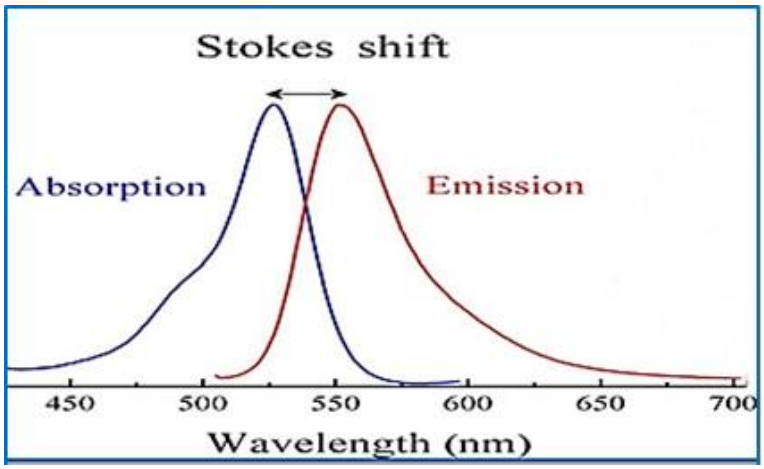

Figure (2.4): Stokes displacement between the absorption and the emission spectra [43].

2.6.1 Phosphorescence

A radiative transition between states of different multiplicity is described as phosphorescence. It occurs when the molecules goes from (T_1) to various

vibration levels of the ground state (S_0) and emits photons, at life time is about (10^{-3} to 10^{-2}) (Sec), and is larger than the life time of the fluorescence process. Since the energy of triplet state (T_{10}) is less than that of singlet state (S_{10}) (The state of fluorescence emission), thus, the energy of phosphorescence photons is less than that of fluorescence photons, as shown in Figure (2.3) [43].

2.6.2 Non-radiative Processes

Sometimes the electron can be relaxed without emission photon, where the photon energy can convert to kinetic energy. In the case of a solid, such as crystal and an ionic, the excited ion given energy them to lattice material, therefore the non-radiative processes do not emit the photons [44].

2.6.3 Intersystem Crossing

Intersystem crossing is a non-radiative transition, which occurs when singlet state S1 can be changed to the triplet (T_1)without emission radiation and the decay time of this translation about (5×10^{-8}) sec. This process involves a change in the spin multiplicity of the molecule. Intersystem crossing occurs faster than the fluorescence, example, the benzophenone molecule, (S_1) undergoes intersystem crossing to (T_1) with life time (10^{-10}) Sec and the fluorescence life time is (10^{-6}) Sec, so, Intersystem crossing at a rate that is (10^4) times faster than fluorescence. And because the excited triple state is lower in energy from the excited single state, the molecule cannot return to the excited single state, but, it can easily return to the ground state by phosphorescence processes [45].

2.6.4 Internal Conversion

If no spin-change occurs, the non-radiative process called internal conversion. This is the means by which higher excited singlet states decay rapidly to the lowest excited singlet before further photo physical change occurs. Similarly, higher triplet states decay rapidly to the lowest triplet state by this

process, internal conversion can also occur from the lowest singlet state to the ground state [46].

2.7 Fluorescence Quantum Efficiency

The time of the radiative transition from the lower vibrational level to the excited electronic state then to a ground vibrational level and back to its first state after this period of time is called radiative life time (τ_{FM}), which is defined as the inverted rate of fluorescence emission (K_{FM}) in unit (S^{-1}) [47]:

$$\tau_{FM} = \frac{1}{K_{FM}} \qquad (2.1)$$

Where K_{FM} represents the probability of radiation transition. Because of the presence of non-radiative processes competing with the possibility of radiation transition (K_{FM}), it will reduce the number of particles qualified for fluorescence emission, so the total probability of transition (K_F) will be the sum of the radiated and nonradiative transition [48]:

$$\tau_F = \frac{1}{K_{FM} + \sum K_d} = \frac{1}{K_F} \qquad (2.2)$$

Where : (Σ K_d) is the sum of constants (rate constants) for non-radioactive processes for the lowest vibratory state. The time of the fluorescence life time (τ_F) is the actual time of the fluorescence, which is equal to the inverted total constants of all non-radiative and radioactive processes that cause energy loss [49]:

$$\tau_F = \frac{1}{K_{FM} + K_{IC} + K_{ISC}} \qquad (2.3)$$

Where (K_{IC})is the rate of inter conversion (sec^{-1}) and (K_{ISC})is the rate of intersystem crossing (sec^{-1}). The life time of the fluorescence (τ_F) can be the main life time of the excited state. There is a relation between fluorescence intensity and fluorescence life time (τ_F) [50]:

$$I = I_{\circ} \exp(-t / \tau_F) \qquad (2.4)$$

Where: (I) is the fluorescence intensity at time (t), (I_o) represents the highest fluorescence intensity and (t) time immediately after the stopping of excitation.

The life time of fluorescence (τ_F) can be calculated from a standard compound known as its chronological age, as well as the area under curve, as in the following relationship [51]:

$$\tau_F = \frac{a \times \tau_{fRB}}{a_{RB}} \qquad (2.5)$$

Where: (τ_{fRB}) is the time-span of the standard compound, the Rhodamine B (3.230 ns) at concentration (10^{-4}) M and (a_{RB}) is the area under the fluorescence curve of rhodamine B and its value (117.6 cm^{-1}), a is the area under the curve of the compound required in this research.The quantum efficiency ($\emptyset_F$) represents the quantum yield of fluorescence, which is the ratio between the probability of radiation transition (K_{FM}) and the average of processes for the singles state ($K_{FM}+K_{IC}+K_{ISC}$). This value is a physical constant of each type of excited particles, or the ratio of total energy emitted to the amount of absorbed energy [52]:

$$\phi_F = \frac{K_{FM}}{K_{FM} + K_{IC} + K_{ISC}} = \frac{K_{FM}}{K_{FM} + \sum K_d} \qquad (2.6)$$

$$\phi_F = K_{FM}\,\tau_F = \frac{\tau_F}{\tau_{FM}} \qquad (2.7)$$

It is also possible to calculate the quantum yield of fluorescence ($\emptyset_F$) by calculating the ratio between the area of the fluorescence spectrum and the area of the absorbance spectrum, as shown in the following equation [53]:

$$\emptyset_F = \frac{\int F(V")\,dv}{\int \varepsilon(v")\,dv} \qquad (2.8)$$

It has been observed that the quantum yield of fluorescence for several compounds depends on the wavelength used in the excitation and the temperature. So the quantum yield of fluorescence increases when non-radiative

processes decrease and when the temperature is reduced, the relation between them is reversed. The values of fluorescence production are between (0-1), therefore, the life time of the fluorescence is far less than the radiation life time due to the non-radiactive processes competing for the fluorescence process. Since values of the quantum efficiency are less than or equal to one, then ($\tau_{FM}>\tau_F$) [54].

2.8 Transfer of Energy Between Laser Dyes

Energy transfer happened when the energy transferred from donor to accepter, an energy transfer from one system to another is said to occur when an amount of energy crosses the boundary between them, thus increasing the energy content of one system while decreasing the energy content of the other system by the same amount [55]. The condition for this mechanism is when there is an overlap between fluorescence of the donor and absorption of the accepter as in Figure (2.5). The aim of energy transfer was to improve the efficiency and broadband the tunable spectral range of dye lasers. The main mechanisms that have been proposed for energy transfer are [56]:

1. Radiative energy transfer, i.e., the absorption of donor emission by an acceptor molecule. This process can by represented by [56]:

$$D^* \longrightarrow D + h\nu$$

$$A + h\nu \longrightarrow A^*$$

Where the star indicates an electronically excited state. In a radiative energy transfer process, the fluorescence life time of both the donor and the acceptor dye molecules are kept unchanged.

2. Non-radiative energy transfer: either you get by long-range resonance energy transfer, or as a result of collision of molecules the donor and the acceptor.

   The process of fluorescence quenching of the donor (D) due to the interaction with the acceptor (A) can be represented by [56]:

$$D^* + A \xrightarrow{KET} D + A^*$$

Where: KET is the energy transfer rate constant.

Energy transfer reduces the emission intensity from (D*) and sensitizes emission from (A*). Another important application of energy transfer is in dye lasers. Dye lasers have some limitations as the dye solution used as an active medium absorbs energy from the excitation source in a very limited spectral range and so the emission band also has these limitations. If a dye laser has to be used as an ideal source, its spectral range needs to be extended. In order to extend the spectral range of operation, mixtures of different dye solutions dye molecules embedded in solid matrices are being used [57].

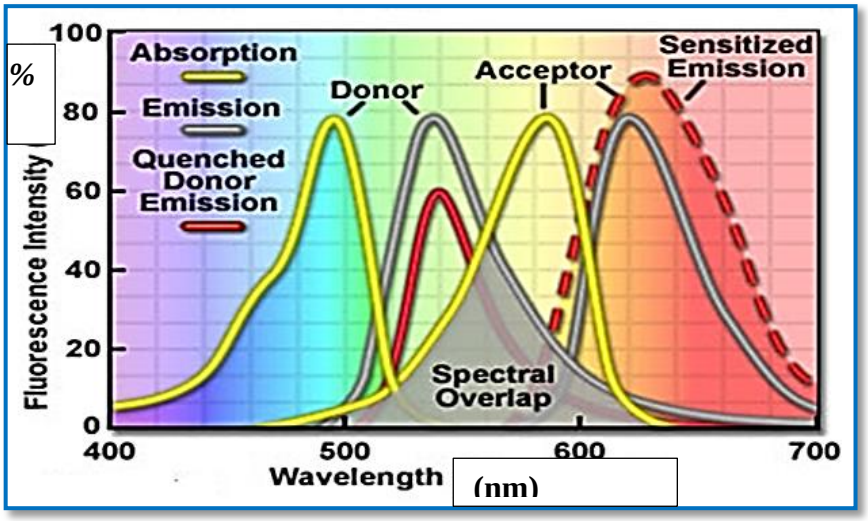

Figure (2.5): Energy Transfer between Laser Dyes [57].

2.9 Applications of Laser Dyes

There are many applications for laser dyes, including [58] :

1- optical limiting and 3D data storage

2- Medical applications of laser dyes include skin treatments, including tattoo removal, diagnostic measurements, lithotripsy and activation of photosensitive drugs for photodynamic therapy, etc.

3- Optical communications.

4- Image processing .

5- Switching.

6- Industrial applications of laser dyes include separation of isotopes of important radioactive elements such as Uranium. Uranium is used as fuel in the nuclear power reactors to generate electricity.

2.10 Coumarin (334) Organic Laser Dye and its Applications

Coumarin is one of the most essential class of laser dyes. Coumarin laser dyes have a strong electron donating substituent [either an amino ($-NR_2$) or hydroxyl (-OH)] in the 7-position. The first Coumarin derivative was coumarin by Sorokin and Lankard [59]. From that point, about 100 Coumarin laser dyes have come to be known [60]. Based on chelation-enhanced fluorescence (CHEF), Coumarins are scantily utilize as chemical sensors for metal ions. Thus a wide tunable range of (420 to 580) nm can be covered with Coumarin dyes. Coumarin is a dye and is used in some of the most successful laser sources . this dye is known as laser dye and is found in natural products. It can be made synthetically and is well suited for many applications such as dye doped lasers due to its excellent fluorescent properties. It is also useful in other applications including environment friendly fluorescent probes, dopant for photonic crystals, to enhance fluorescence for application in biochemical sensing etc [60].

2.11 Fluorescein Organic Laser Dye and its Applications

This dye has a place with the family of xanthine class dyes where this family is characterized by high chemical stability of the type of solvent (polarity), efficient manufacturing. Fluorescein has an orange- red to dark crystalline powder that dissolved in water and alcohol (except chloroform). Fluorescein has been widely used as a fluorescent tracer in technical chemistry, microscopy, serology and forensics [61]. Fluorescein has been employed for diagnostic purposes in other branches of medicine [62]. Surgery for brain tumors, angiography and ophthalmology and used as sterile, it is on the list of essential medicines of the world health organization.

2.12 Organic Hosts (Polymers)

The name polymer is derived from the Greek word, in which the first word "Poly" means multiple and the second one "mer" means part. The polymer has a synonym word "macromolecule". The building block unit of the polymer is the monomer. Polymers are macromolecules composed of repeated units (monomer), and sometimes these units are repeated linearly and the chain is formed by connecting these units or the chains to form branches or they are interconnected [63]. The polymer chain length is determined by the number of the repeated unites (monomer) in the chain and it is called the degree of polymerization. Its molecular weight is equal to the product of the molecular weight of the monomer by the degree of polymerization [64]. One of the important characteristics of polymers is their high molecular weight . Atoms are bonded together in the polymer chain by strong covalent bonds, and are attracted by very weak internal forces. The polymer is called "homopolymer" if the repeated units are the same whereas the polymer formed of different units is called "copolymer" or "mixed polymer". The polymer is said to be "ordered" if its monomers repetition is constant. However if any reduction occurs to the arrangement of the monomers, the polymer becomes "Amorphous" [65].

2.12.1 The Classification of Polymer

Polymers can be classified according to molecular structure to four types as shown in Figure (2.6) [66]:

a- Linear polymers. c- Network polymers

b- Branched polymers. d- Cross linked polymers.

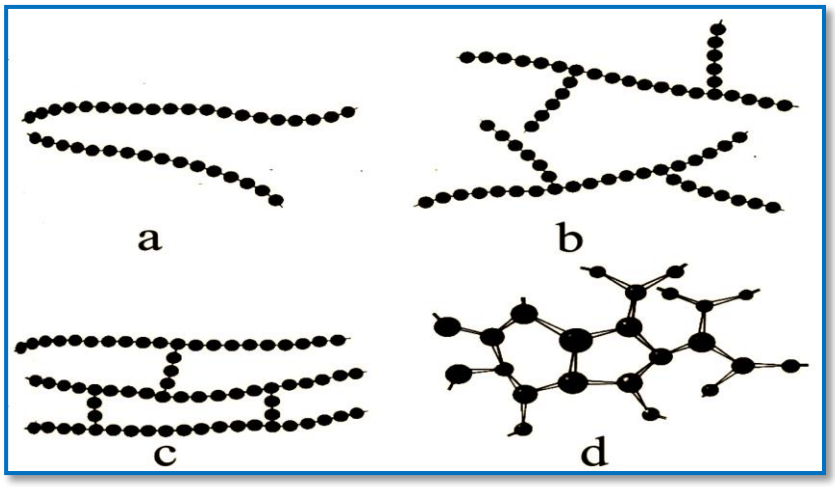

Figure (2.6)Types of polymers : (a) Linear (b) Branched (c) Network (d) Cross linked [66].

2.13 Polyvinyl alcohols (PVA)

Polyvinyl Alcohols (PVA) have been utilized in a variety of industrial, commercial, medical, and food applications since the early 1930, including resins, lacquers, surgical threads, and food-contact applications. It has the ability to dissolve in water which is resistant to solvents, oils, and has an exceptional ability to adhesive materials cellulosic so it's extensive uses included in the paper industry and in textile industries in membranes of industry resistance to oxygen in the coating photographic film as well as in high-voltage applications to possess high tensile strength in a high storage capacity, electrical and optical properties depending on the type of additives and impurities [67].

2.14 Nanoparticles

Nanoparticle has a size range between (1 to 100) nm. Unexpected physical and chemical behavior of matter occurs at the nanometer scale, paving the way for a number of scientific exploitations, making nanoparticles a great area of scientific research. The transition from microparticles to nanoparticles yields dramatic changes in all properties. Nanoscale materials have a large surface area for a given volume. Many important chemical and physical interactions are governed by surfaces and surface properties. Nanostructures

material can have substantially different properties from a larger-dimensional material of the same composition [68]. In nanomaterial, the surface area per unit volume is inversely proportional to the material's diameter, thus, the smaller the diameter, the greater the surface area per unit volume, change in particle diameter, layer thickness, or fibrous material diameter from the micrometer to nanometer range, will affect the surface area to volume ratio by three orders of magnitude generally, there are different approaches for a classification of nano materials, the main classes of nanoscale structures can be classified by dimensions, some of which are summarized in Table (2.1) also can be shown in Figure (2.7) [69].

Table (2.1) Classification of Nanomaterials by Dimension [69].

Dimension	Example
0 dimension $\leq$100 nm	Particles , quantum dots
1 dimension $\leq$100 nm	Nanotubes,Nanowire,Nanorods
2 dimension $\leq$100 nm	Thin films,Coatings, Multilayers
3 dimension $\leq$100 nm	Nanometar-sized cluster

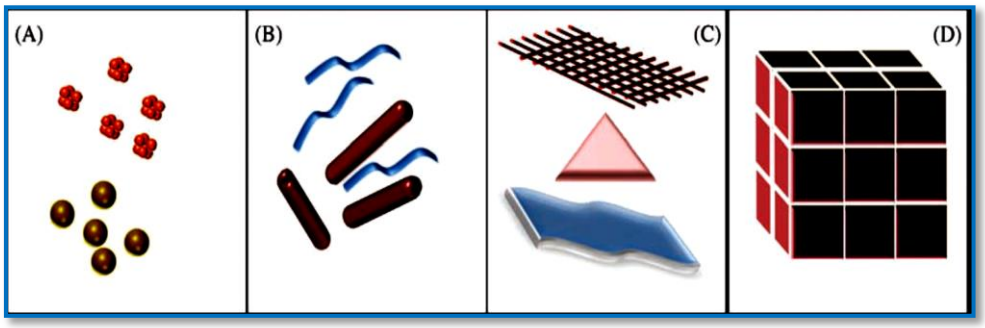

Figure (2.7) : Various Kinds of Nanomaterials. (A) 0D spheres and clusters. (B) 1D nanofibers, wires, and rods. (C) 2D films, plates, an networks. (D) 3D nanomaterials [69].

2.14.1 Silver Nanoparticle (Ag NPS) and its Applications

Silver nanoparticles are nanoparticles of silver of between (1-100) nm in size. While frequently described as being 'silver' some are composed of a large percentage of silver oxide due to their large ratio of surface-to-bulk silver atoms. Different shapes of nanoparticles can be constructed depending on the application of the study [70].

Silver nanoparticles are being used in numerous technologies and incorporated into a wide array of consumer products that take advantage of their desirable optical, conductive, and antibacterial properties [71]: The applications of Silver Nanoparticle (Ag NPS)

1. Optical Applications: Silver nanoparticles are used to efficiently harvest light and for enhanced optical spectroscopies.
2. Conductive Applications: Silver nanoparticles are used in conductive inks and integrated in to composites to enhance thermal and electrical conductivity.
3. Antibacterial Applications: Silver nanoparticles are incorporated in apparel, footwear, paints, wound dressings, appliances, cosmetics, and plastics.

2.14.2 Alumina Nanoparticles (Al_2O_3) and its Applications

Metal oxide nanoparticles have been extensively developed in the past decades. They have been widely used in many applications such as catalysts, sensors, semiconductors, medical science, capacitors, and batteries. Alumina generally refers to corundum. It is a white oxide. Alumina has several phases such as gamma, delta, theta, and alpha. However, the alpha alumina phase is the most thermodynamically stable phase [72]. In general, Alumina has many interesting properties, for example high hardness, high stability, high insulation, and transparency.

Al_2O_3 Nanoparticles can be synthesized by many techniques including ball milling, solgel, pyrolysis, sputtering, hydrothermal, and laser ablation Among them, the laser ablation is a widely used technique for the synthesis of

nanoparticles since it can be synthesized in gas or liquid. This technique offers several advantages such as rapid and high purity process compared with other methods [72]. Alumina (Al_2O_3) in particular possesses a variety of commercial and industrial uses and has become one of the most important commercial ceramic materials [73]. Aluminum oxide (Al_2O_3) has good physical properties like abrasion resistance, thermal stability, electrical insulation and high mechanical strength, etc. Therefore, in order to increase Tg and enhance mechanical properties of the (PVA), Al_2O_3 nanoparticles were added in to the (PVA) [74,75].

2.15 Interaction of Laser Light with Matter

When laser radiation strikes a material surface, part of it is absorbed and part is reflected. The energy that is absorbed begins to heat the surface. There are several regimes of parameters that should be considered, depending on the time scale and on the flounce. When laser beam acts on the material, laser energy is first absorbed by free electrons. The absorbed energy then propagates through the electron subsystem and then transferred to lattice therefore laser energy is transferred to material [76].

This process has a resonant feature because materials show different absorptions to lasers with different wavelengths, this dependence of absorption on wavelength is decided by the microstructure and electromagnetic properties of the material. The intensity of laser light produces a wide range of interaction. The interaction of matter can be classified as linear interaction and nonlinear interaction. The advent of the laser as a coherent light with high intensity source gives birth of nonlinear optics. It plays an important role in many areas of science and technology now [77] The NLO effects are associated with light-induced changes in the optical constants of the material, either the absorption coefficient, the refractive index, or both. They are best treated by considering the interaction of the light beam with the atoms of the material as driving force acting on an ensemble of oscillator with natural resonance frequency [78].

2.16 Nonlinear Optical Properties

Nonlinear optics is the study of phenomena that occur as consequence of the modification of the optical properties of materials on interaction with intense light. Nonlinear phenomena has been studied extensively. The particles of the medium are displaced from their equilibrium positions, so that positive charged particles move in the direction of the electric field, while the negative charged particles move in the direction opposite to the direction of the applied electric fields. Dipole moments are created because of the displacement between positive and negative charged particles, and the dipole moment per unit volume describes the induced polarization of the medium [79].

When the applied electric fields are sufficiently small, the electric polarization is approximately linearly proportional with the applied electric field E [80]:

$$P = \varepsilon_o \chi.E \qquad (2.9)$$

Where (ε_o) is the permittivity of free space, (χ) is the electric susceptibility tensor. This is the case of linear optics. However, when the applied electric fields are high enough, the induced polarization has a nonlinear dependence on these electric fields and can be expressed as a power series with respect to the electric field [80]:

$$P = \varepsilon_o (\chi^{(1)}.E + \chi^{(2)}. EE + \chi^{(3)}.EEE+\dots) \qquad (2.10)$$

$$P = P^{(1)} + P^{(2)} +P^{(3)}+\dots. \qquad (2.11)$$

Where $\chi^{(1)}$ is the linear susceptibility, $\chi^{(2)}$ is the second order nonlinear susceptibility, and $\chi^{(3)}$ is the third order nonlinear susceptibility. The term $\chi^{(1)}$ is responsible for linear absorption and refraction, and is the only term that reflects the linearity between the induced polarization and the incident electric field. The term $\chi^{(2)}$ is present only in non-centrosymmetric materials, i.e. materials that do not have inversion symmetry. The third order nonlinear optical interactions, which are described by the term $\chi^{(3)}$ [81]. The field of nonlinear optics (NLO)

has been developing for a few decades as a promising field with important applications in the domain of photo electronics and photonics. Organic materials are considered as one of the important classes of third order NLO materials because they exhibit large and fast nonlinearities [82].

Various types of organic compounds have been studied to obtain materials with large third order nonlinearity. On the other hand, a wide range of techniques has been used to measure third order nonlinearity e.g. degenerate four waves mixing, third harmonic generation and Z-Scan technique. Among all these techniques Z-Scan is a simple for the measurement of the nonlinear refractive index and nonlinear absorption coefficient [83]. It provides not only the magnitudes of the real and imaginary parts of the nonlinear susceptibility but also the sign of the real part. Both nonlinear refraction and nonlinear absorption in solid and liquid samples can be rapidly measured by the Z-Scan technique, which utilizes self-focusing or self-defocusing phenomena in optical nonlinear materials. There are two methods of Z-Scan, the closed -aperture and open -aperture system [84]:

2.16.1 Closed-aperture Z-Scan

A closed aperture Z-Scan measures the change in intensity of a beam, focused by lens (L) in Figure (2.8), as the sample passes through the focal plane. Photo detector (PD) collects the light that passes through an axially centered aperture (A) in the far field. The change on axis intensity is caused by self-focusing or self-defocusing by the sample (S) as it will create a change in index of refraction forming a lens in a nonlinear sample as shown in Figure (2.8) [85].

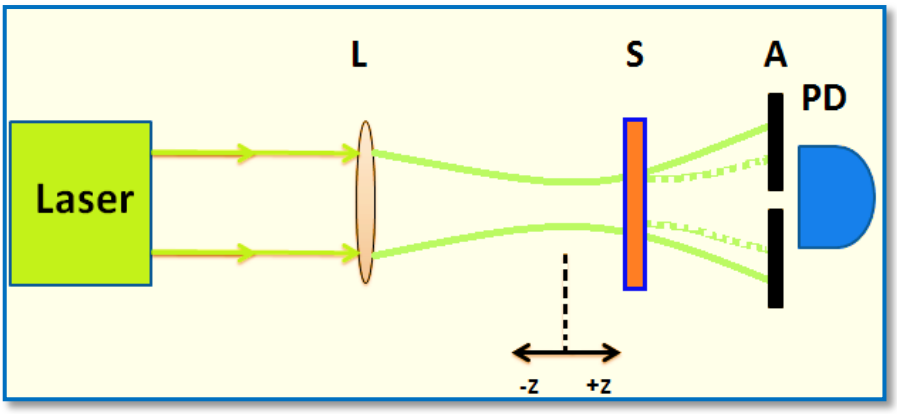

Figure (2.8): Closed aperture Z-Scan [85].

To show how the Z-Scan transmittance as a function of (Z) is related to the nonlinear refraction of the sample, if a medium with a negative nonlinear refraction index and a thickness smaller than the diffraction length of the focused beam. This can be considered as a thin lens of variable focal length. Beginning far from the focus (Z<0), the beam irradiance is low and nonlinear refraction is negligible. In this condition, the measured transmittance remains constant (i.e., Z-independent). (As the sample approaches the beam focus, irradiance increases, leading to self-lensing in the sample) . A negative self-lens before the focal plane will tend to collimate the beam on the aperture in the far field, increasing the transmittance measured at the iris position [86].

After the focal plane, the same self-defocusing increases the beam divergence, leading to a widening of the beam at the aperture and thus reducing the measured transmittance. Far from focus (Z >0), again the nonlinear refraction is low resulting in a transmittance Z-independent. A transmittance maximum (peak), followed by a transmittance minimum (valley) is a Z-Scan signature of a negative nonlinearity. An inverse Z-Scan curve (i.e., a valley followed by a peak) characterizes a positive nonlinearity. Figure (2.9) depicts these two situations [86].

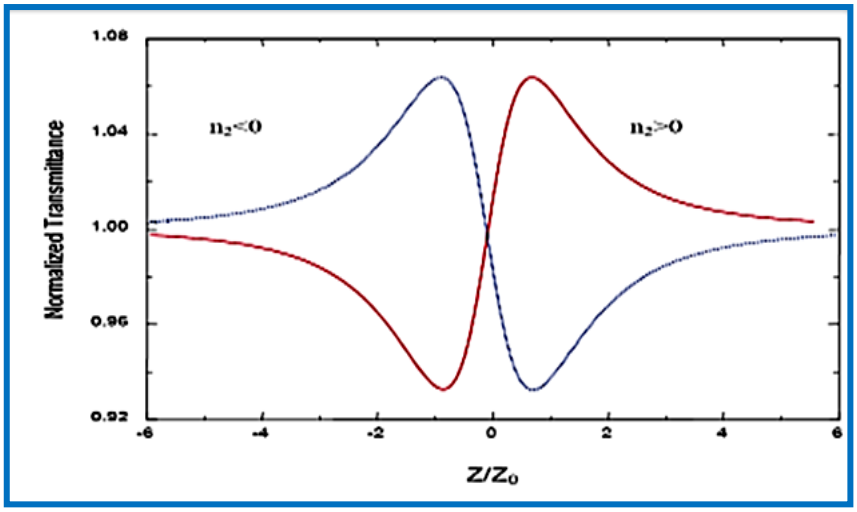

Figure (2.9): Calculated Z-Scan transmittance curves for nonlinearity[86].

The nonlinear refractive coefficient is calculated from the peak to valley difference of the normalized transmittance by the following formula [87]:

$$n_2 = \frac{\Delta\Phi_o}{I_o L_{eff} k} \qquad (2.12)$$

Where, $k = 2\pi/\lambda$, (k) is wave number, (I_o) is the intensity at the focal spot and $(\Delta\Phi_o)$is the nonlinear phase shift [87]:

$$\Delta T_{p-v} = 0.406|\Delta\Phi_o| \qquad (2.13)$$

(ΔT_{p-v}) the difference between the normalized peak and valley transmittances, $(L_{eff})$is the effective length of the sample, determined from [88]:

$$L_{eff} = \frac{(1-exp^{-\alpha_o L})}{\alpha_o} \qquad (2.14)$$

Where (L) is the sample length and$(\alpha_o)$is linear absorption coefficient which is given as [88]:

$$\alpha_o = \frac{\ln(\frac{1}{T})}{t} \qquad (2.15)$$

Where (T) is the transmittance, (t) is the cuvette thickness. The linear refractive index(n_o) obtained from equation[88]:

$$n_o = \frac{1}{T} + \left[\left(\frac{1}{T^2} - 1\right)\right]^{1/2} \qquad (2.16)$$

The intensity at the focal spot is given by [89]:

$$I_o = \frac{2P_{peak}}{\pi \omega_o{}^2} \qquad (2.17)$$

Is defined as the peak intensity within the sample at the focus, Where(ω_o) is the beam radius at the focal point.

2.16.2 Open-aperture Z-Scan

An open-aperture Z-Scan analyzes the change in intensity of a beam in the far field at photo detector PD, which captures the full beam, as focused by lens (L) in Figure (2.10), in the far field at photo detector (PD), which captures the entire beam. The change in intensity is caused by two photon absorption in the sample S as it travels through the beam waist [90].

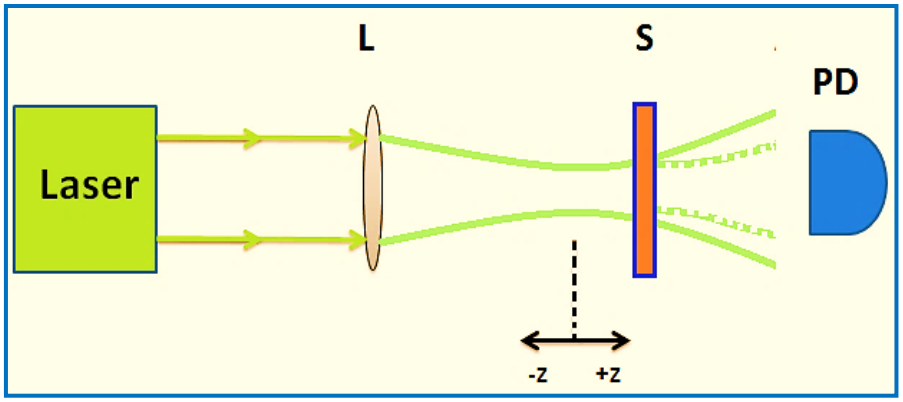

Figure (2.10): Open-aperture Z-Scan[90].

Clearly, even with nonlinear absorption, a Z-Scan with a fully open aperture is insensitive to nonlinear refraction (thin sample approximation). The Z-Scan traces with no aperture are expected to be symmetric with respect to the focus (Z = 0) where they have a minimum transmittance (e.g., two photon absorption)or maximum transmittance (e.g., saturation of absorption). In fact, the coefficients of nonlinear absorption can be easily calculated from such transmittance curves. Nonlinear absorption coefficient (β), can be easily calculated by using following equation [91]:

$$\beta = \frac{2\sqrt{2}\,T(z)}{I_o L_{eff}} \qquad (2.18)$$

Where T(z):The minimum value of normalized transmittance at the focal point, at (Z=0). It should be clear that the transmittance versus sample position graph of such an open aperture Z-Scan should be symmetric around the focus as shown in Figure (2.11).

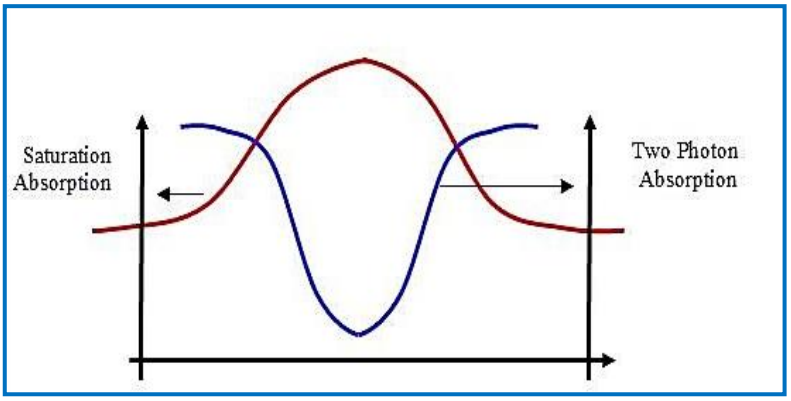

Figure (2.11): Open aperture Z-Scan curve [91].

2.16.3 Nonlinear Absorption and Nonlinear Refraction

The basic optical properties involved in the light matter interaction are absorption, which is defined by the absorption coefficient (α), and refraction, which is defined by the index of refraction (n). When the material is irradiated, the energy of the absorbed photons makes it possible for the transition from the ground state to the excited state. There is also a change in the refractive index when a material is placed in a strong electric field. In fact, the index of refraction becomes dependent on the intensity of the electric field. At high intensity, the refractive index is given by [92]:

$$n = n_o + n_2 I \qquad (2.19)$$

Where (n_2)is the nonlinear refractive coefficient related to the intensity.

The absorption of the material is also intensity dependent given by [92]:

$$\alpha = \alpha_o + \beta I \qquad (2.20)$$

Where, (α_o) is the linear absorption coefficient and (β) is the nonlinear absorption coefficient related to the intensity. The coefficients (n), and (α) are related to the intensity of laser.

2.16.4 Saturable Absorption

A nonlinear process that can be associated with real (rather than virtual) energy levels and population changes in those levels is that of saturable absorption. This process occurred when the nonlinear absorption coefficient ($\beta < 0$), which can be appeared when a strong light absorption between two levels causes saturation (bleaching) of the corresponding electronic transition. The two levels involved surface resonance ground and excited state. On the other hand, this is a process in which a material can be highly absorbing at a specific wavelength when a low-intensity beam is incident upon the material, yet an extremely intense beam (at that same wavelength) will pass through the medium with little change in intensity [93].

2.16.5 Two Photon Absorption (TPA)

Two-photon absorption (TPA) is the simultaneous absorption of two photons of identical or different frequencies in order to excite a molecule from one state (usually the ground state) to a higher energy electronic state. The energy difference between the involved lower and upper states of the molecule is equal to the sum of the energies of the two photons, as in the case of a saturable absorber, is the process of two-photon absorption. This process occurred when the nonlinear absorption coefficient $\beta > 0$. This effect is shown in Figure (2.12). The two-photon transition rate can be significantly enhanced if an intermediate level (2) is located near the virtual level shown by the dashed line in Figure (2.12) [94].

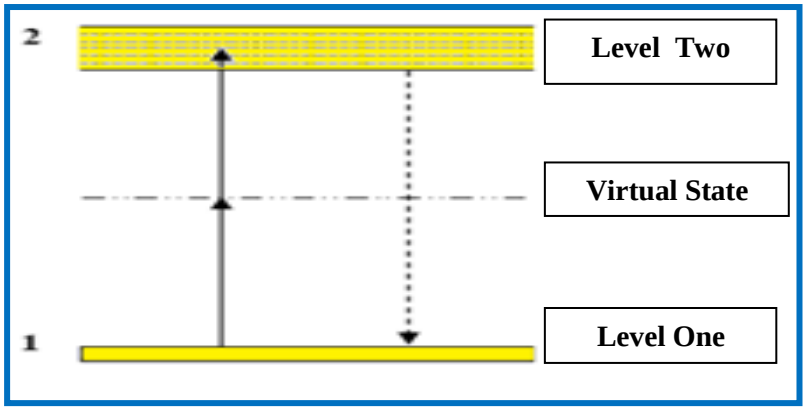

Figure (2.12): Energy levels for two-photon absorption process [94].

2.16.6 Kerr Effect

A nonlinear interaction of light in a medium related to the nonlinear electronic polarization, which can be described as modifying the refractive index. For high-intensity laser beams, the Kerr effect can create a local change in the refractive index that causes the laser material to act as a lens. This can result in self-focusing of laser beams [95].

2.16.7 Self-Focusing

A nonlinear process that causes a spatial variation of the laser intensity, in which an intense beam of light modifies the optical properties of a material medium in such a manner that the beam is caused to come to a focus within the material. The material acts as a positive lens, because the laser beam induces a refractive index variation within the material with a larger refractive index at the center of the beam than at its periphery. Self-focusing can be obtained when the nonlinear refractive index is positive in sign [96].

2.17 Optical Limiting

Following the invention of the laser, it was recognized that intense laser beams can easily damage delicate optical instruments, and especially the human eye. Nowadays, lasers have become common in daily life and they are even being incorporated into toys. Thus, protection from lasers is not only a scientific subject but also a potential public safety issue. Over the last few decades, many scientists have sought so called optical limiting materials that exhibit ‘nonlinear

extinction', i.e. strongly attenuate intense, potentially dangerous laser beams, while readily transmitting low intensity ambient light [97].

Protection of eyes and sensors from intense laser pulses. Candidates for optical limiting materials should have low transmittance for strong incident light, and instantaneous response over a broad spectral range. The most important application of such a device is the protection of sensitive optical sensors and components from laser damage [98]. A common geometry is illustrated in Figure (2.13). Laser beam is focused into a material and then collected through a finite aperture in the far field. At high irradiance the far field beam distortion arising from the self-focusing of the laser beam inside the medium will result in the limiting of the transmitted light through the aperture. Where (Z) is the distance between the focal plane in free space and the center of the sample, and (d) is the distance from this plane to the aperture plane. [98].

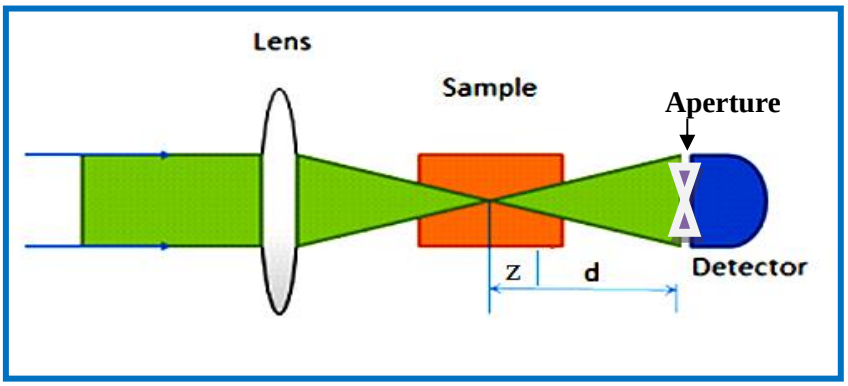

Figure (2.13) : Schematic of the limiting geometry[98].

3.1 Introduction

This chapter describes preparation solutions and thin films of the two organic laser dyes and their mixture, and the instruments that used for characterization of these dyes. The Z-Scan system was presented and a measurement was done using diode pump solid state laser (DPSS) at wavelength (457) nm and power 84 mW, and the procedure of these measurements with their photographic pictures.

3.2 The Used Materials

The main materials that are used in this work:

3.2.1 Coumarin (334) Organic Laser Dye

Coumarin and their derivatives represent a class of well-known laser dyes in the blue-green spectral region, characterized by high-emission quantum yields and find many practical applications in the various fields of science and technology. Since they exhibit fluorescence in the UV- VIS region, they are used as colorants, dye lasers, and non-linear optical devices [99–101]. Dye molecular structure is shown in Figure (3.1). The principle characteristics of Coumarin (334) dye are shown in Table (3.1). Coumarin emits light in the green and blue area between (420 - 580) nm.

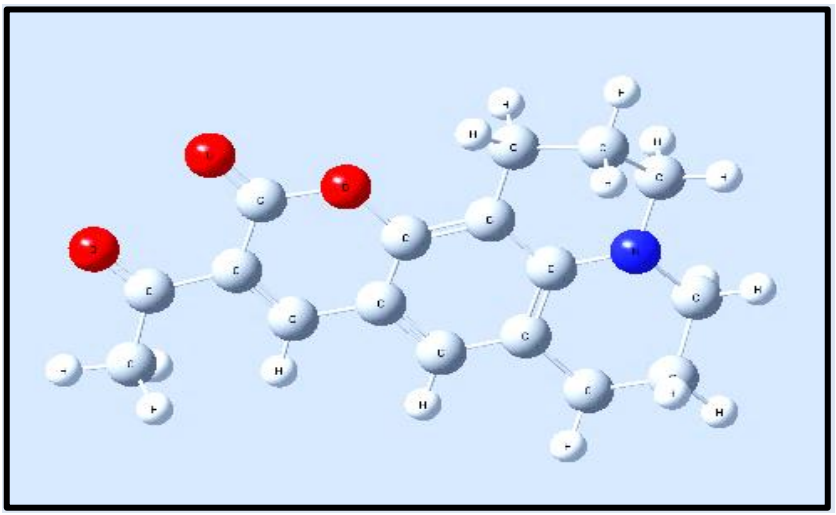

Figure (3.1): Molecular structure of Coumarin (334) dye molecule.

Table (3.1): The principle characteristics of Coumarin (334) dye [102].

Properties	Coumarin (334)
Molecular formula	$C_{17}H_{17}NO_3$
Molecular weight	283.32 g/mole
Appearance	Orange crystalline powder
Other names	acetyl-3, oxa-13,azatetracyclo7,heptadeca

3.2.2 Fluorescein Organic Laser Dye

This dye has a place with the family of xanthine class dyes where this family is characterized by high chemical stability of the type of solvent (polarity), efficient manufacturing. Fluorescein has an orange- red to dark crystalline powder that dissolved in water and alcohol (except chloroform). Fluorescein has been widely used as a fluorescent tracer in technical chemistry, microscopy, serology and forensics. Fluorescein has been employed for diagnostic purposes in other branches of medicine surgery for brain tumors, angiography and ophthalmology and used as sterile, it is on the list of essential medicines of the world health organization. Dye molecular structure is shown in Figure (3.2).The principle characteristics of Fluorescein dye are shown in Table (3.2) [103].

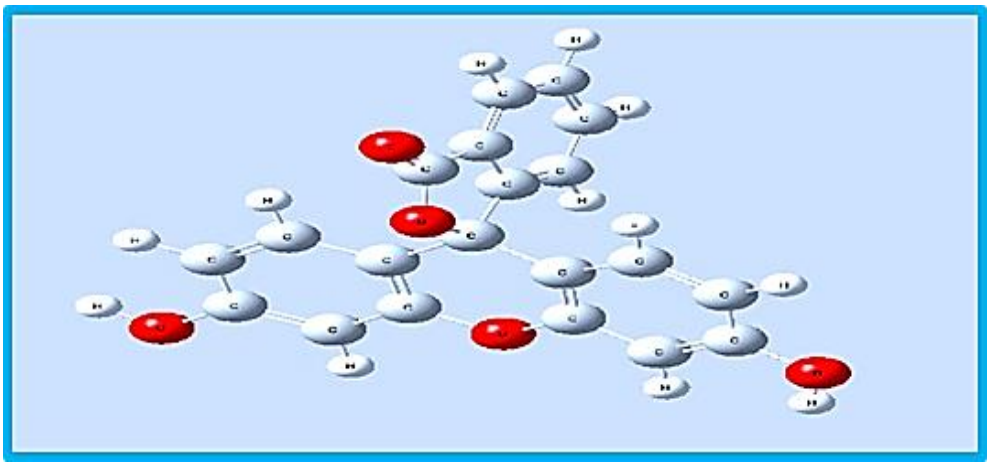

Figure (3.2): Molecular structure of Fluorescein dye molecule.

Table (3.2) : The principle characteristics of Fluorescein dye [103].

Properties	Fluorescein
Molecular formula	$C_{20}H_{12}O_5$
Molecular weight	332.31 g/mole
Appearance	Orange - crystalline powder
Density	1.602 g/mL

3.3 Ethanol Absolute Solvent

Ethanol also called (ethyl alcohol) is a pure alcohol, colorless liquid. Ethanol can cause alcohol intoxication when consumed. It burns with blue flame. The physical properties of ethanol stem primarily from the presence of its hydroxyl group and the shortness of its carbon chain [104]. Figure (3.3) shows the chemical structure of the ethanol. Table (3.3) shows the principle characteristics of ethanol solvent.

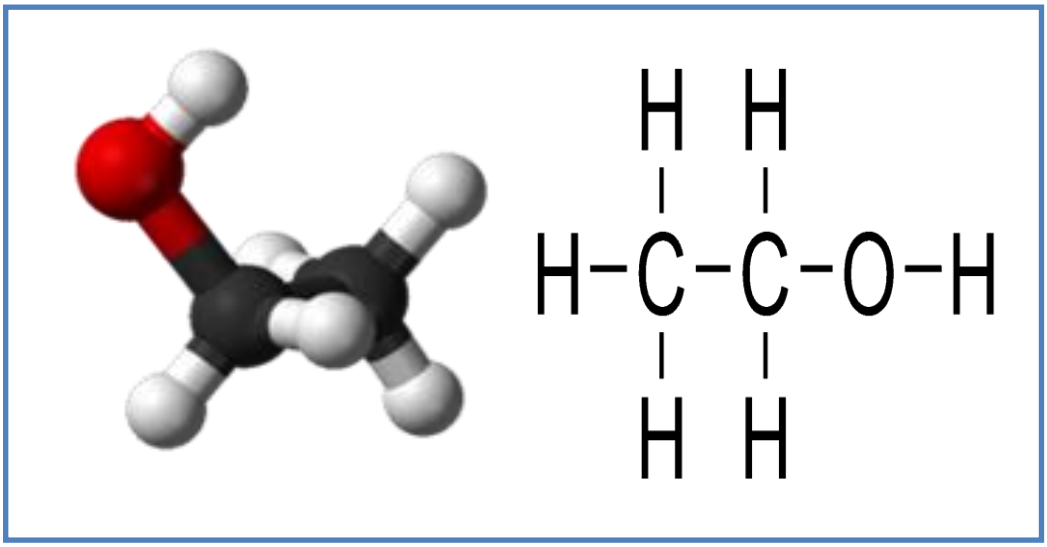

Figure (3.3): The structure of Ethanol molecule [104].

Table (3.3): The principle characteristics of Ethanol solvent [104].

Properties	Ethanol Solvent
Molecular formula	C_2H_6O
Molar mass	46.07 $g.mol^{-1}$
Density	0.789 gm/cm3
Boiling point	78.4 C°
Freezing point	-114.3 C°
Purity	99.9%

3.4 PVA Polymer

Polyvinyl alcohol (PVA), which is derived primarily from polyvinyl acetate by hydrolysis, is easily degradable by biological organisms and is a crystalline structure polymer that is soluble in water. PVA is a synthetic polymer that was widely utilized in the first part of the twentieth century. It has been utilized in the industrial, commercial, medical, and food sectors to manufacture a variety of end products, including lacquers, resins, surgical threads, and food packaging materials that come into contact with food often [105]. Figure (3.4) demonstrate the structure of polyvinyl Alcohol. Table (3.4) shows the principle characteristics of PVA polymer.

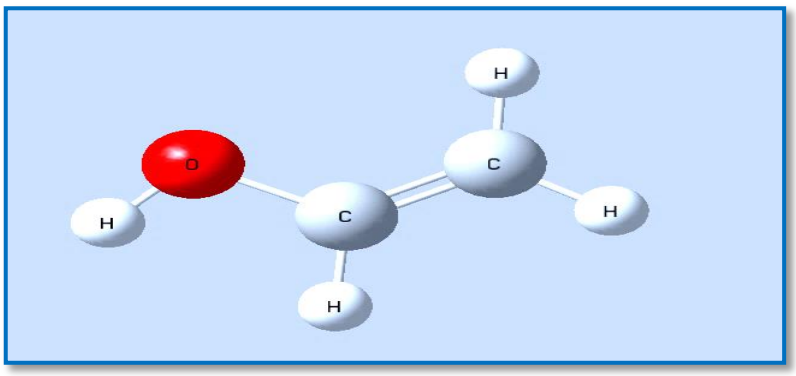

Figure (3.4): The structure of polyvinyl alcohol (PVA) [105].

Table (3.4): The principle characteristics of PVA polymer [105].

Properties	PVA polymer
Molecular formula	$(C_2H_4O)_x$
Molecular weight	44.05 g/mol
Melting Temperature (T_m)	200 C°
Density	g /cm^3 1.31 -1.19

3.5 Silver Nanoparticles (Ag NPS)

Silver nanoparticles are between (1-100) nm in size. While frequently described as being 'silver' some are composed of a large percentage of silver oxide due to their large ratio of surface-to-bulk silver atoms. Numerous shapes of nanoparticles can be constructed depending on the application of the study it have main characteristics are shown in Table (3.5) [106].

Table (3.5): The principle characteristics of (Ag) nanoparticles [106].

Ag Nanoparticle	Description
Productive company	SIGMA-ALDRICH, Germany
Form	Nano powder
Surface area	> 40 m^2/g
Particle size	(1-100) nm

3.6 Alumina Nanoparticles (Al_2O_3)

Metal oxide nanoparticles have been extensively developed in the past decades. They have been widely used in many applications such as catalysts, sensors, semiconductors, medical science, capacitors, and batteries. Alumina generally refers to corundum. It is a white oxide. Alumina has several phases

such as gamma, delta, theta, and alpha. However, the alpha alumina phase is the most thermodynamically stable phase. In general, Alumina has many interesting properties, for example high hardness, high stability, high insulation, and transparency .Alumina (Al_2O_3) in particular possesses a variety of commercial and industrial uses and has become one of the most important commercial ceramic materials. Aluminum oxide (Al_2O_3) has good physical properties like abrasion resistance, corrosion resistance, thermal stability, electrical insulation and high mechanical strength. Table (3.6) shows the properties of Al_2O_3 nanoparticles [107].

Table (3.6): The principle characteristics of (Al_2O_3) nanoparticles [107].

Al_2O_3 Nanoparticle	Description
Molecular weight	101.96 g
Appearance	white solid
Density	3.95– 4.1 g/cm^3
Melting point	2072 °C
Boiling point	2977 °C

3.7 Work Scheme

Figure (3.5) shows the experimental procedure as a block diagram of the main steps that were followed in this work:

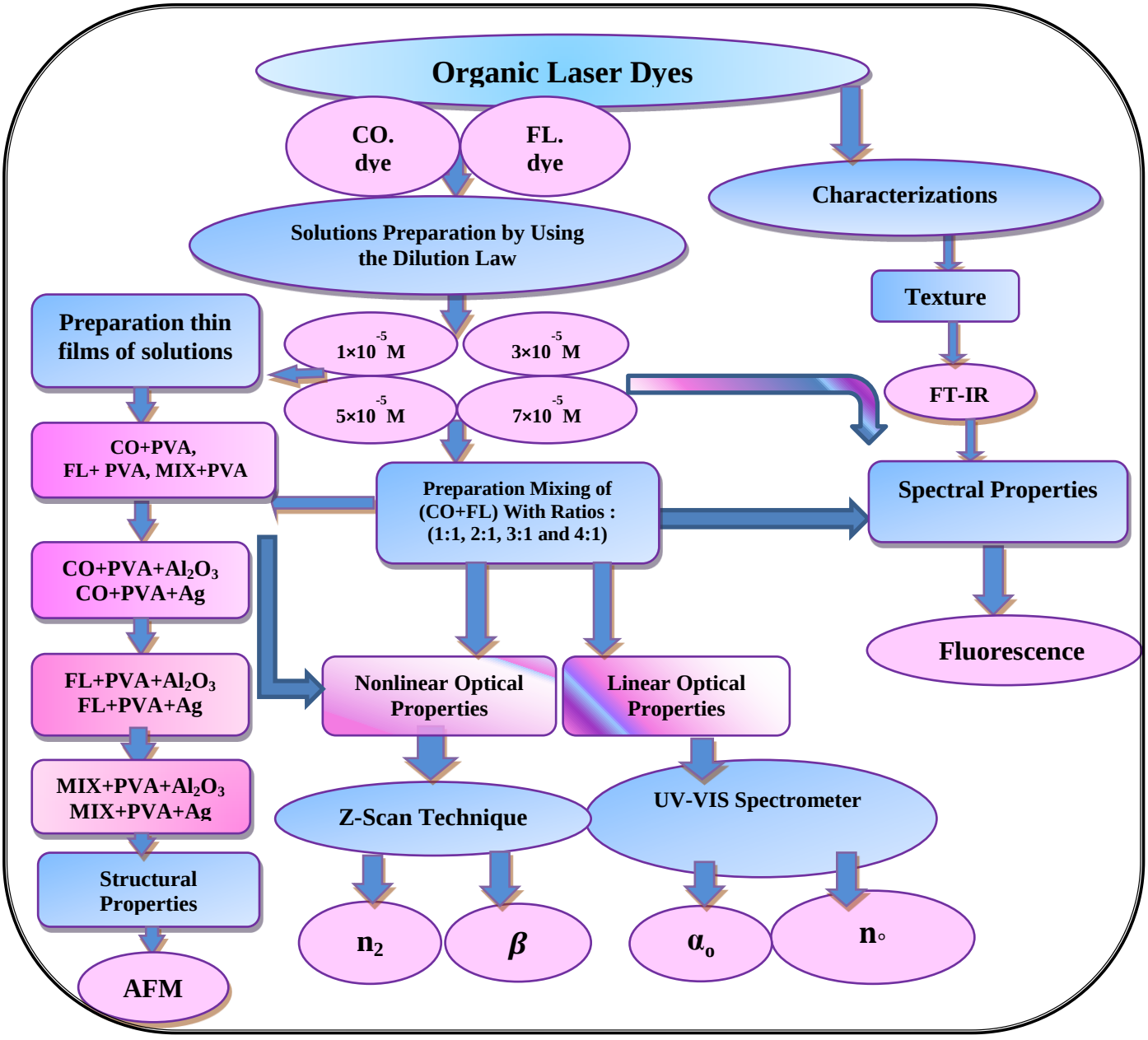

Figure (3.5): Main steps of the experimental work.

3.8 Solutions Preparation

Solutions of concentrations (10^{-3}) M of each organic laser dye in ethanol solvent were prepared. The powder was weighted using an electronic balance type (BL 210 S, Germany) having a sensitivity of four digits. Different concentrations were prepared according to the following equation [108]:

$$W = \frac{M_W \times V \times C}{1000} \quad (3.1)$$

Where, W: Weight of the dissolved in material (g), M_w: Molecular weight of the material (g /mol),V: Volume of the solvent (mL) and C: The concentration (M).The prepared solutions were diluted according to the following equation [108].

$$C_1V_1 = C_2V_2 \quad (3.2)$$

Where: C_1: Primary concentration , C_2: New concentration .V_1: The volume before dilution and V_2: The volume after dilution.

In this work four concentrations (1×10^{-5}, 3×10^{-5}, 5×10^{-5}, and 7×10^{-5}) M of each of Coumarin (334) dye and Fluorescein dye are used to prepare mixing of these two dyes (1 ml) from Coumarin (334) with (1 ml) from Fluorescein to to obtain (1:1), ratio and (4 ml ,6 ml and 8ml) of Fluorescein dye adding to (2 ml) of Coumarin (334) dye to prepare other ratios (2:1, 3:1 and 4:1) at different concentrations (3×10^{-5}, 5×10^{-5}, and 7×10^{-5}) M. As shown in Figures (3.6), (3.7) and (3.8) respectively.

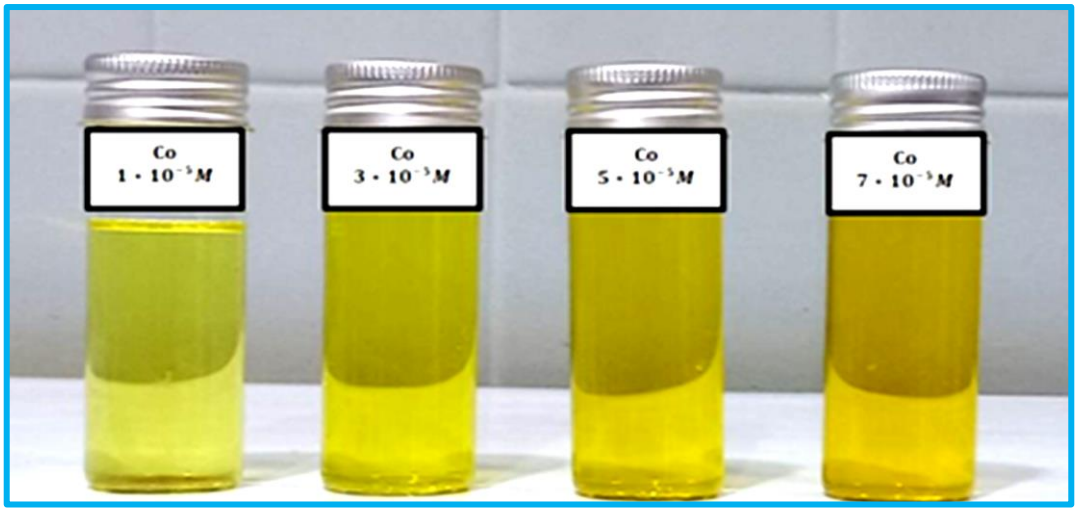

Figure (3.6): Solutions of Coumarin (334) dye at different concentrations.

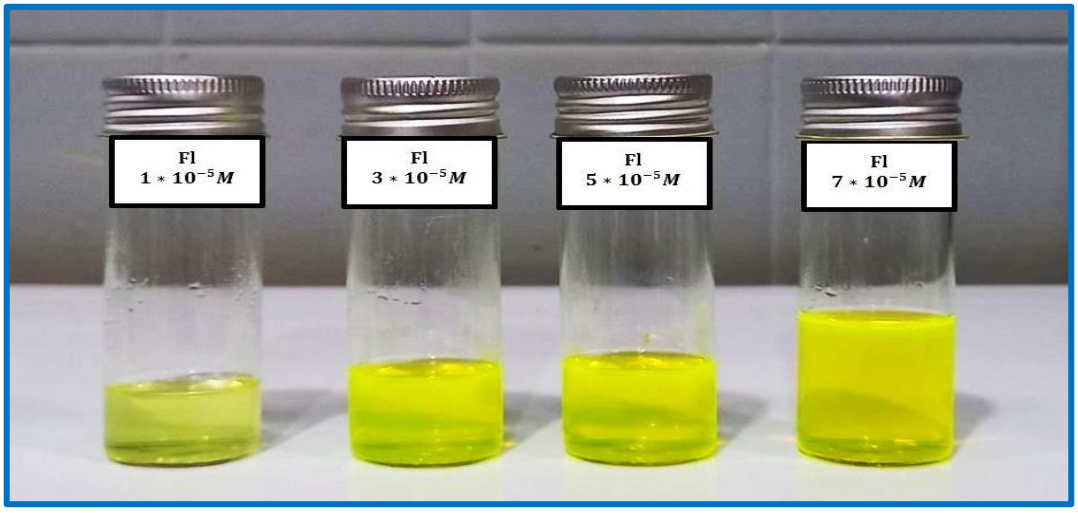

Figure (3.7): Solutions of Fluorescein dye at different concentrations.

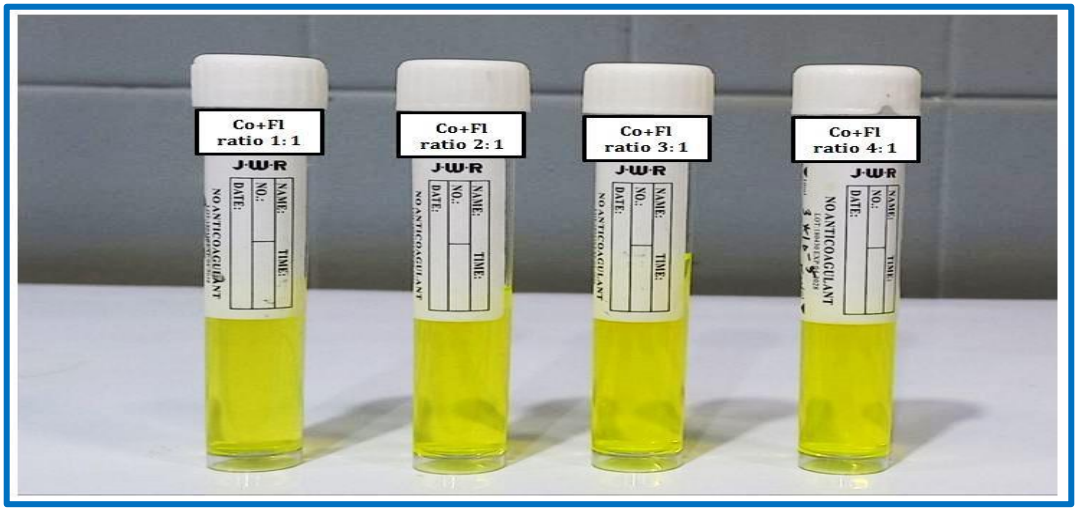

Figure (3.8): Solutions of Mixture of Coumarin (334) and Fluorescein dyes at different mixing ratios.

3.9 Thin Films Preparation

Thin films of Coumarin (334), Fluorescein organic laser dyes and mixture of them with (PVA polymer doped Ag and Al_2O_3) nanoparticles were prepared on a clean glass slide using the drop casting method, with a solution at concentration (10^{-3} M) for each of them, and dried at room temperature (25-30) C° for (2) days. The thickness of these thin films is approximately (110-210) nm.

The thickness of the thin films was measured by optical method which is done by optical thin film measurement model (LIMF -10). Polymer solution is prepared by dissolving the desired amount of polymer in water (2 g in 30 ml of water solvent). A desired amount of dye solution was added to the polymer solution and mixed at room temperature (25-30) C° using a magnetic stirrer to obtain a homogenous mixture.

(0.06 g) weight of (Ag and Al_2O_3) nanoparticles powder were added and mixed with a magnetic stirrer to obtain a homogenous mixture. Thin films of Coumarin (334) dye and Fluorescein organic laser dyes and mixture of them doped with PVA polymer, doped (Ag and Al_2O_3) nano particles were formed by leaving the mixture to dry at room temperature (25-30) C° on a slide. This procedure was carried out for each dye as shown in Figure (3.9).

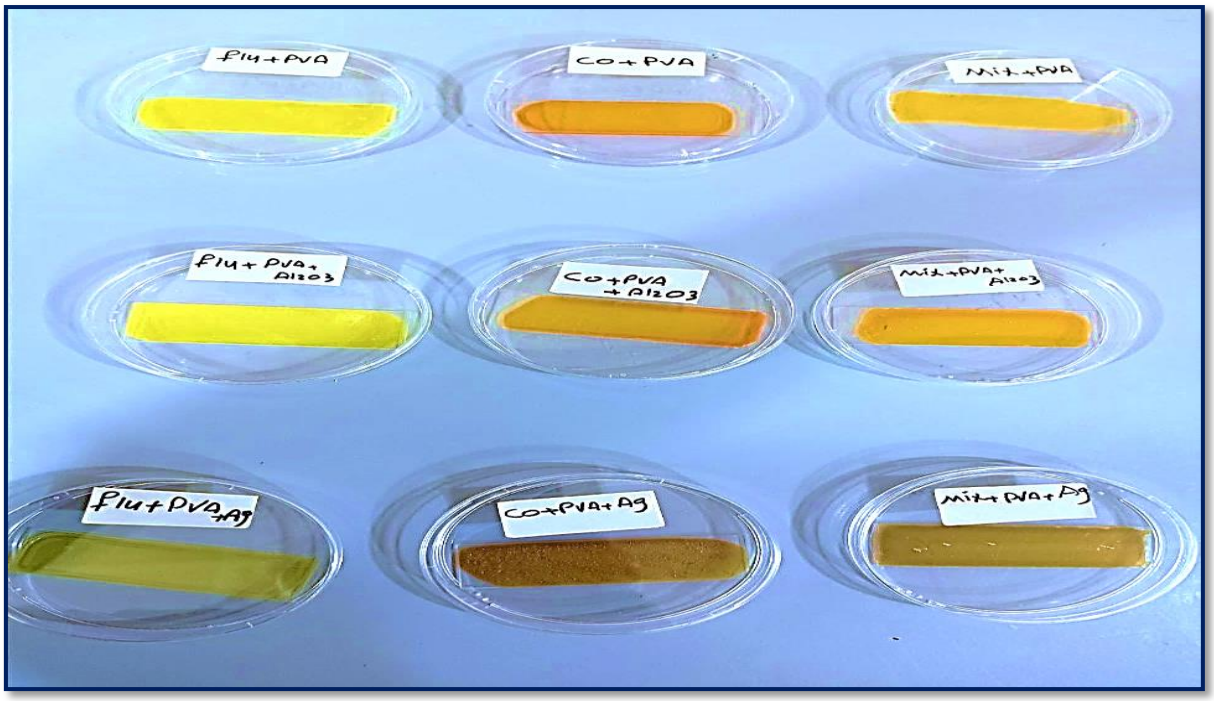

Figure (3.9) : Thin films of Coumarin (334) , Fluorescein dyes and their mixture with PVA polymer doped (Al_2O_3 and Ag) NPs at ratio (4:1).

3.10 Measurement of thickness

Thickness is one of the most important thin film's parameters since it largely determines the properties of thin films. The thickness of thin films is usually measured by monitoring the rate of the deposition during the coating process. However there are several methods used for measuring thickness of thin films, such as weight, optical, electrical and other methods. In our work the thickness of the thin films was measured by optical method done by optical thin film measurement model (LIMF -10, Lambda Scientific Pty Lt). This measured is done in Electro- Optics Laboratory in Babylon University - Science College - Physics department. Figure (3.10) with following specifications.

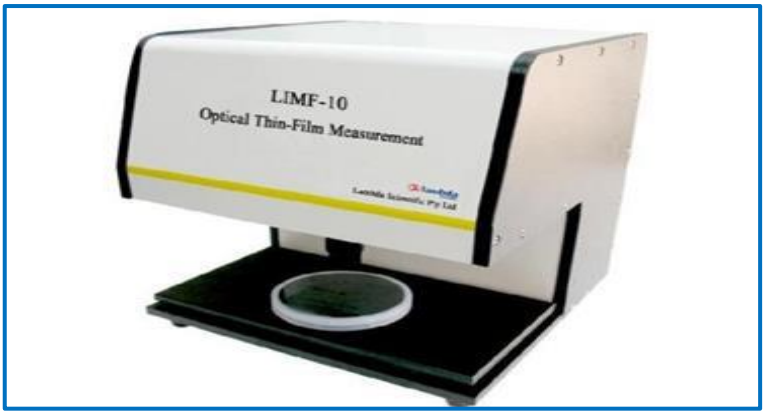

Figure (3.10): optical thin film thickness measurement.

3.11 Structural Properties Measurements (FT-IR)

The structural testing included FT-IR . The infrared spectra of the produced compounds were taken using FT-IR spectroscopy at the laboratories of the department of chemistry, college of science, university of Kufa. The FT-IR spectrometer is illustrated in Figure (3.11).

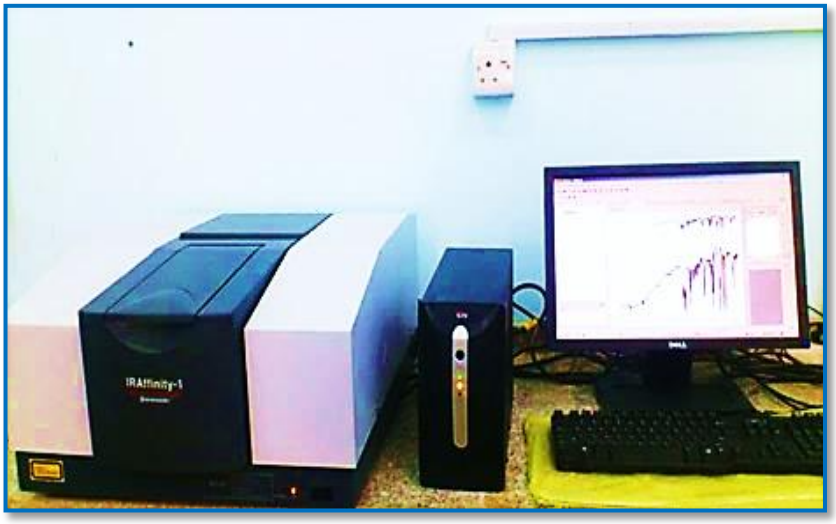

Figure (3.11): FT-IR spectroscopy.

3.12 Optical Properties Measurements

Optical properties measurements of Coumarin (334) and Fluorescein organic laser dyes and mixture of them were measured with different ratios (1:1, 2:1, 3:1 and 4:1) as solution at different concentrations (1×10^{-5}, 3×10^{-5},

5×10^{-5}, and 7×10^{-5}) M as solution and thin films with PVA polymer doped (Ag, Al_2O_3) nanoparticles .

3.12.1 UV-Visible spectroscopy

The linear optical properties including transmittance, absorption coefficient, and refractive index for all prepared samples have been determined by utilizing a UV-Visible Shimadzu 1800 Spectroscopy. This Spectroscopy is equipped with two light sources: a deuterium lamp and a tungsten lamp that operate in the wavelength ranges (190-390) nm and (390-1100) nm, respectively. The wavelength, transmittance, and absorbance output data are employed in a computer program to calculate the optical constants. The detector is a silicon photodiode as shown in Figure (3.12). This device is located in the physics department's laboratory at the college of education for pure science in the university of Babylon.

Figure (3.12) : UV-Visible spectroscopy.

3.12.2 Fluorescence Measurement

Fluorescence spectra was measured for all the prepared samples using spectrometer type (FluoroMate FS-2). The samples were mounted in cuvette cell of quartz dimensions (1×1×5) cm^3 perpendicularly with incident beam. Table (3.7) shows the specifications of this device. All samples were examined in the

laboratory of thin film at University of Babylon College of Education for Pure Science Department of Physics as shown in Figure (3.13).

Table (3.7): Specifications of spectrometer.

Wavelength range	(200 - 900) nm
Wavelength scan rate	200/400/600 nm / min
Light source	150 W (Xenon arc lamp)
Detector	PMT
Power requirements	(220-240) V (AC)
Resolution	0.5 nm
Wavelength Accuracy	1.0 nm

Figure (3.13): Fluorescence spectroscopy.

3.12.3 Atomic Force Microscopy Measurement (AFM)

In order to observe the surface roughness and topography of deposited thin films, AFM micrographs were obtained using digital instruments. Nano scope and III Dimension 3100. AFM images data include root mean square (r.m.s) roughness and grain size. It has three main modes of mapping topography: contact (which is used in our morphology investigation), non-contact and intermittent contact or tapping. The most important part of an AFM is the tip with its nanoscale radius of

curvature. The tip is attached to a micron scale which reacts to the Van der Waals interaction and other forces between the tip and sample. (Model :CSPM AA3000) It was measured in the laboratory of the ministry of science and technology as shown in the Figure (3.14).

Figure (3.14) : Atomic force microscope.

3.12.4 Nonlinear Optical Properties

The equipment used to determine the nonlinear optical properties of all prepared samples will be explained in details in the following section:

3.12.5 Z-Scan Technique

Z-Scan measurements were made in two parts: closed aperture and open aperture. Each component was fabricated utilizing a continuous wave (CW) diode pumped solid state blue laser operating at a wavelength (457 nm) and a power (84 mW). The nonlinear refractive index was determined using a closed-aperture Z-Scan, whereas the nonlinear absorption coefficient was determined using an open-aperture Z-Scan. The beam was focused using a convex lens (f = 15 cm), A convex lens was used to focus the laser beam on the sample and the beam waist was determined to be (0.025) cm at the focus. The focus point laser intensity is (20.408×10^{3}) mW/cm^{2}, and the sample was moved along the Z-axis.

The transmittance of the sample as a function of sample position is measured. Figure (3.15) shows the open-aperture and closed-aperture Z-Scan setup.

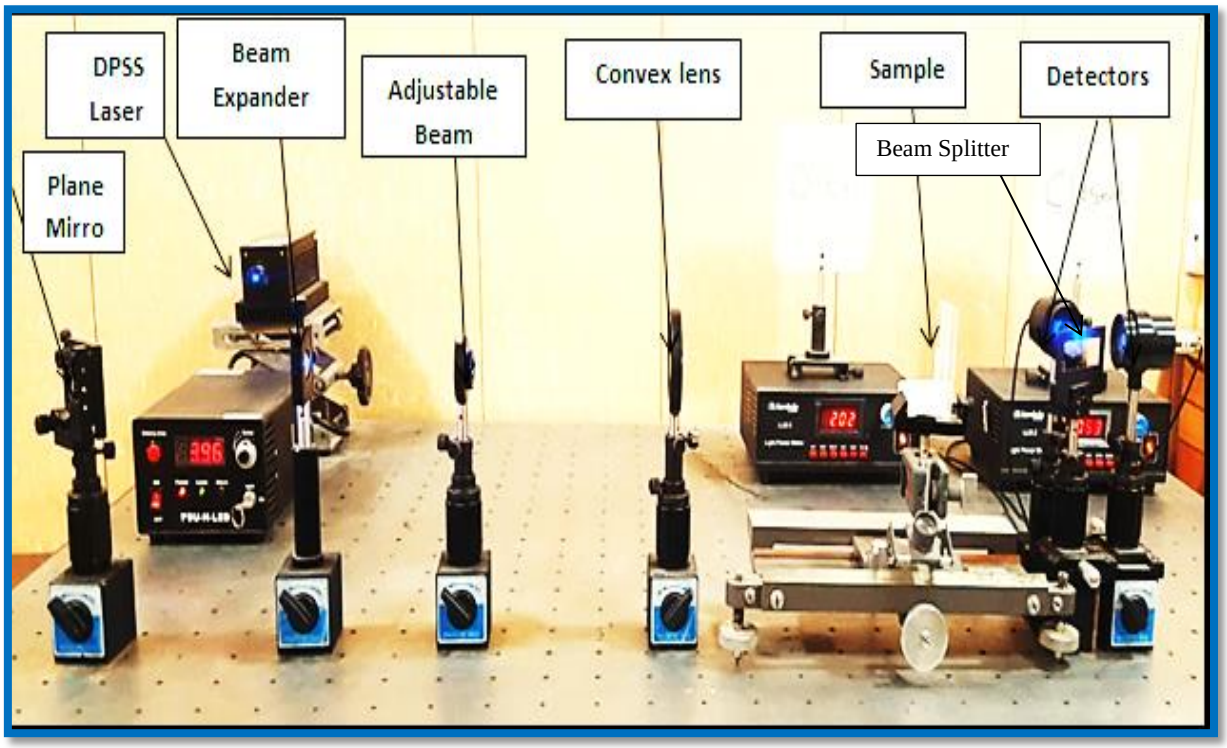

Figure (3.15) : Z-Scan set-up.

3.12.5.1 Diode Pumped Solid State Laser (DPSS)

Continuous wavelength 457 nm DPSS laser is used. Table (3.8) shows the characteristics of the laser, which were used in this work.

Table (3.8): Characterization of (457) nm DPSS laser.

Model	MBL-457 nm
Wavelength (nm)	457 nm
Output power (mW)	142.5 mW
Transverse mode	TEM_{00}
Operating mode	CW
Power stability (rms, over 4 hours)	5.71%
Beam divergence, full angle (mrad)	1. 8
Beam diameter at $1/e^2$ (mm)	X:1.883 nm Y:1.285 nm
Power supply	(100-240)Volt

3.12.5.2 Detector

The third optical element in the Z-Scan is the optical power meter detector type (LLM-2), which is used to measure the output power of the laser. The detector was placed at the far field of a Gaussian laser beam.

3.12.5.3 Aperture

The aperture is an important parameter in Z-Scan system to measure non-linear refractive index (n_2) in the closed-aperture technique, and its diameter was (1mm). Aperture aligned with the lens in the same axis.

3.12.5.4 The Sample

All solutions was filled into the glass cuvette (1) mm thickness. The cuvette was hand made in the laboratory, which consists from five slides of glass as shown in Figure (3.16). The geometry of sample cuvette can be shown in Figure (3.17), which is represented engineering drawing of sample cuvette.

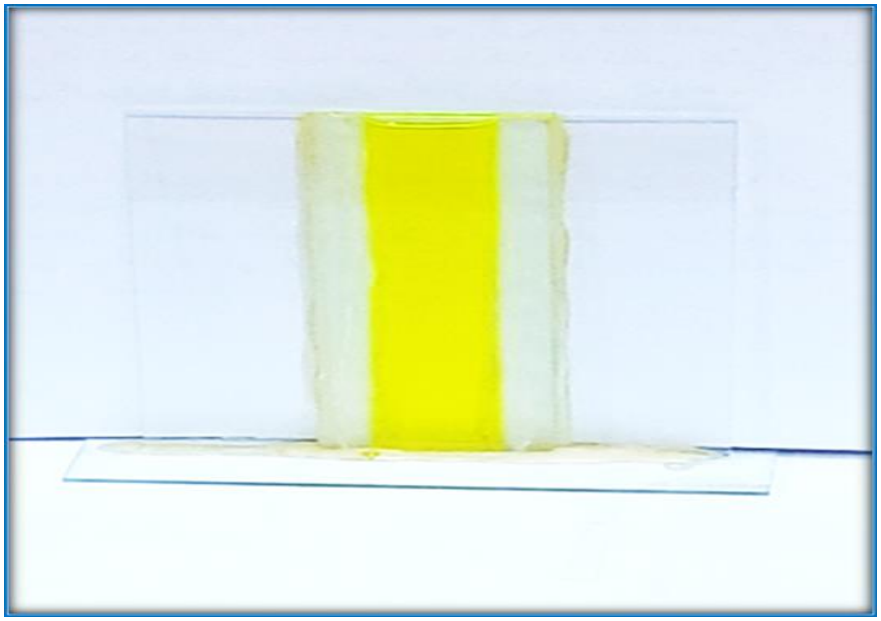

Figure (3.16): Photograph of sample.

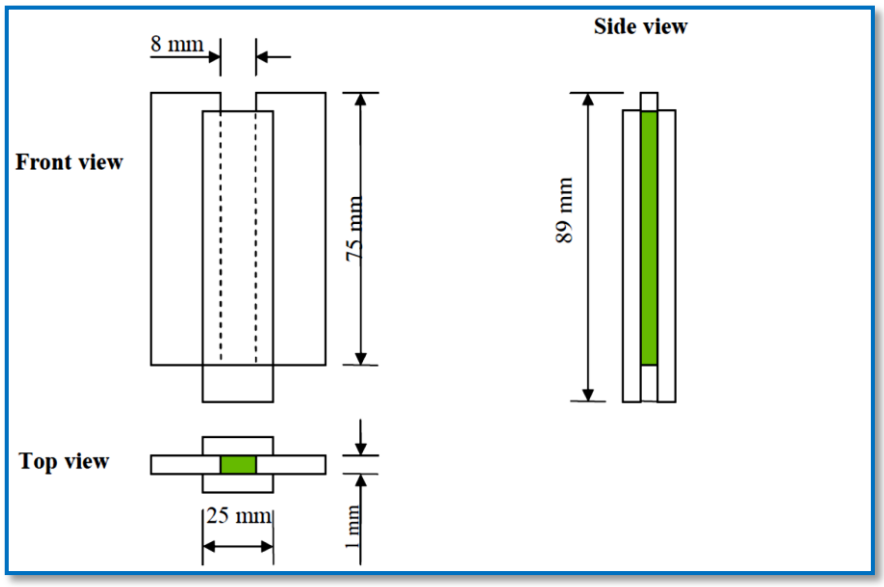

Figure (3.17): Geometry of sample cuvette [20].

3.12.5.5 Reference Beam Measurements

In order to measure the reference power of a CW laser, the detector was placed directly in front of the 457 nm DPSS laser. The normalized transmission as a function of sample position is given by [109]:

$$T(z) = \frac{P(I)}{P(I)_{ref}} \tag{3.3}$$

Where, P(I) is the power of the transmitted laser beam, when the cuvette is filled by dye solution, and $P(I)_{ref}$ is power of the reference laser beam.

3.13 Optical Limiting Behavior

Optical limiting occurs when the optical transmission of a material saturates with increasing laser intensity, a property that is desirable for the protection of sensors and human eyes from the intense laser radiation. The optical power limiting property of pure and doped dyes and their thin films, is measured with the same laser used in Z-Scan technique. Set up the optical limiting as shown in the previous Figure (3.15).

3.1 Introductio

This chapter describes preparation solutions and thin films of the two organic laser dyes and their mixture, and the instruments used for characterization of these dyes. The Z-Scan system was presented and a measurement was done using diode pump solid state laser (DPSS) at wavelength (457) nm and power (84) mw, and the procedure of these measurements with their photographic pictures.

3.2 The Used Materials

The main materials that are used in this work:

3.2.1 Coumarin (334) Organic Laser Dye

Coumarin and their derivatives represent a class of well-known laser dyes in the blue-green spectral region, characterized by high-emission quantum yields and find many practical applications in the various fields of science and technology. Since they exhibit fluorescence in the UV- region, they are used as colorants, dye lasers, and non-linear optical fluorophores [99–101].Dye molecular structure is shown in Figure (3.1). The principle characteristics of Coumarin (334) dye are shown in Table (3.1). Coumarin emit light in the green and blue area between (420 to 580) nm.

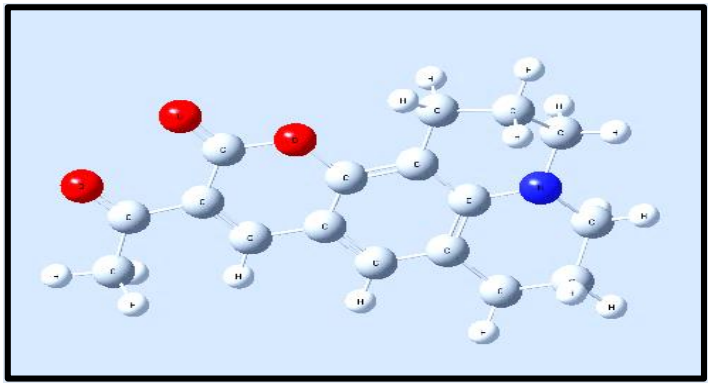

Figure (3.1): Molecular structure of Coumarin (334) dye molecule.

Table (3.1): The principle characteristics of Coumarin (334) dye [102].

Properties	Coumarin (334)
Molecular formula	$C_{17}H_{17}NO_3$
Molecular weight	283.32 g/mole
Appearance	Orange -red to dark red crystalline powder
Other names	acetyl-3, oxa-13,azatetracyclo7,heptadeca

3.2.2 Fluorescein Organic Laser Dye

This dye has a place with the family of xanthine class dyes where this family is characterized by high chemical stability of the type of solvent (polarity), efficient manufacturing. Fluorescein has an orange- red to dark crystalline powder that dissolved in water and alcohol (except chloroform) . Fluorescein has been widely used as a fluorescent tracer in technical chemistry, microscopy, serology and forensics. Fluorescein has been employed for diagnostic purposes in other branches of medicine surgery for brain tumors, angiography and ophthalmology and used as sterile, it is on the list of essential medicines of the world health organization .Dye molecular structure is shown in Figure (3.2).The principle characteristics of Fluorescein dye are shown in Table (3.2) [103].

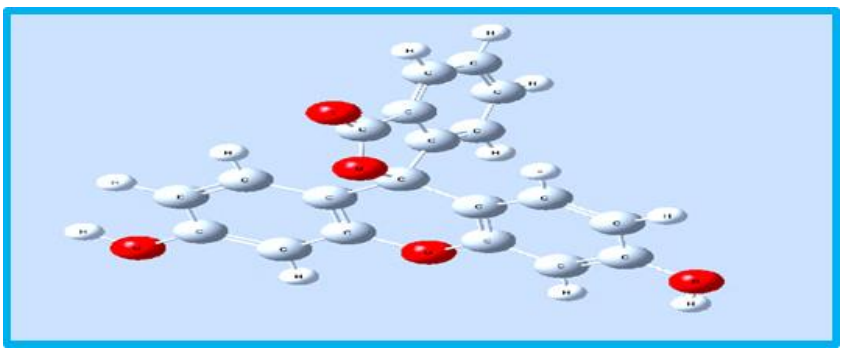

Figure (3.2): Molecular structure of Fluorescein dye molecule.

Table (3.2) : The principle characteristics of Fluorescein dye[103].

Properties	Fluorescein
Molecular formula	$C_{20}H_{12}O_5$
Molecular weight	332.31 g/mole
Appearance	Orange - crystalline powder
Density	1.602 g/mL

3.3 Ethanol Absolute Solvent

Ethanol also called (ethyl alcohol) is a pure alcohol, colorless liquid. Ethanol can cause alcohol intoxication when consumed. It burns with blue flame. The physical properties of ethanol stem primarily from the presence of its hydroxyl group and the shortness of its carbon chain [104]. Figure (3.3) shows the chemical structure of the ethanol. Table (3.3) shows the principle characteristics of ethanol solvent.

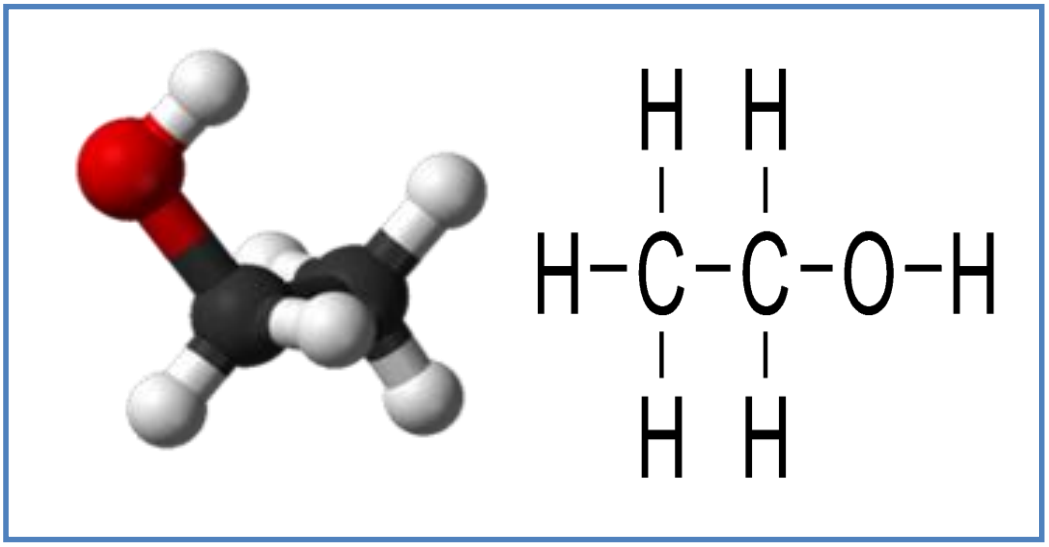

Figure (3.3): The structure of Ethanol molecule [104].

Table (3.3): The principle characteristics of Ethanol solvent [104].

Properties	Ethanol Solvent
Molecular formula	C_2H_6O
Molar mass	46.07 $g.mol^{-1}$
Density	0.789 gm/cm3
Boiling point	78.4 C°
Freezing point	-114.3 C°
Purity	99.9%

3.4 PVA Polymer

Polyvinyl alcohol (PVA), which is derived primarily from polyvinyl acetate by hydrolysis, is easily degradable by biological organisms and is a crystalline structure polymer that is soluble in water. PVA is a synthetic polymer that was widely utilized in the first part of the twentieth century. It has been utilized in the industrial, commercial, medical, and food sectors to manufacture a variety of end products, including lacquers, resins, surgical threads, and food packaging materials that come into contact with food often [105]. Figure (3.4) demonstrate the structure of polyvinyl Alcohol. Table (3.4) shows the principle characteristics of PVA polymer.

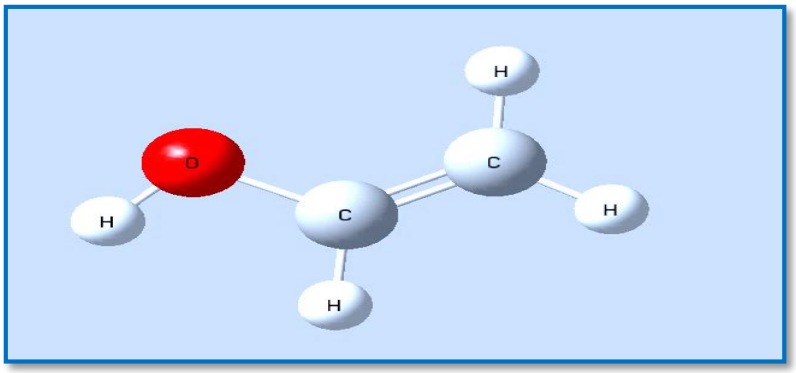

Figure (3.4): The structure of polyvinyl alcohol (PVA) [105].

Table (3.4): The principle characteristics of PVA polymer [105].

Properties	PVA polymer
Molecular formula	$(C_2H_4O)_x$
Molecular weight	44.05 g/mol
Melting Temperature (T_m)	200 C°
Density	g /cm^3 1.31 -1.19

3.5 Silver Nanoparticles (Ag NPS)

Silver nanoparticles were supplied by laboratory Reagent LTD, Silver nanoparticles are nanoparticles of silver of between (1 -100) nm in size. While frequently described as being 'silver' some are composed of a large percentage of silver oxide due to their large ratio of surface-to-bulk silver atoms. Numerous shapes of nanoparticles can be constructed depending on the application of the study it have main characteristics are shown in Table(3.5) [106].

Table (3.5): The principle characteristics of (Ag) nanoparticles [106].

Ag Nanoparticle	Description
Productive company	SIGMA-ALDRICH, Germany
Form	Nano powder
Surface area	> 40 m^2/g
Particle size	(1-100) nm

3.6 Alumina Nanoparticles (Al2O3)

Metal oxide nanoparticles have been extensively developed in the past decades. They have been widely used in many applications such as catalysts, sensors, semiconductors, medical science, capacitors, and batteries. Alumina

generally refers to corundum. It is a white oxide. Alumina has several phases such as gamma, delta, theta, and alpha. However, the alpha alumina phase is the most thermodynamically stable phase. In general, Alumina has many interesting properties, for example high hardness, high stability, high insulation, and transparency .Alumina (Al_2O_3) in particular possesses a variety of commercial and industrial uses and has become one of the most important commercial ceramic materials. Aluminum oxide (Al_2O_3) has good physical properties like abrasion resistance, corrosion resistance, thermal stability, electrical insulation and high mechanical strength. Table (3.6) shows the properties of Al_2O_3 nanoparticles [107].

Table (3.6): The principle characteristics of (Al_2O_3) nanoparticles [107].

Al_2O_3 Nanoparticle	Description
Molecular weight	101.96 g mol^{-1}
Appearance	white solid
Density	3.95– 4.1 g/cm^3
Melting point	2072 °C
Boiling point	2977 °C

3.7 Work Scheme

Figure (3.7) shows the experimental procedure as a block diagram of the main steps that are followed in this work:

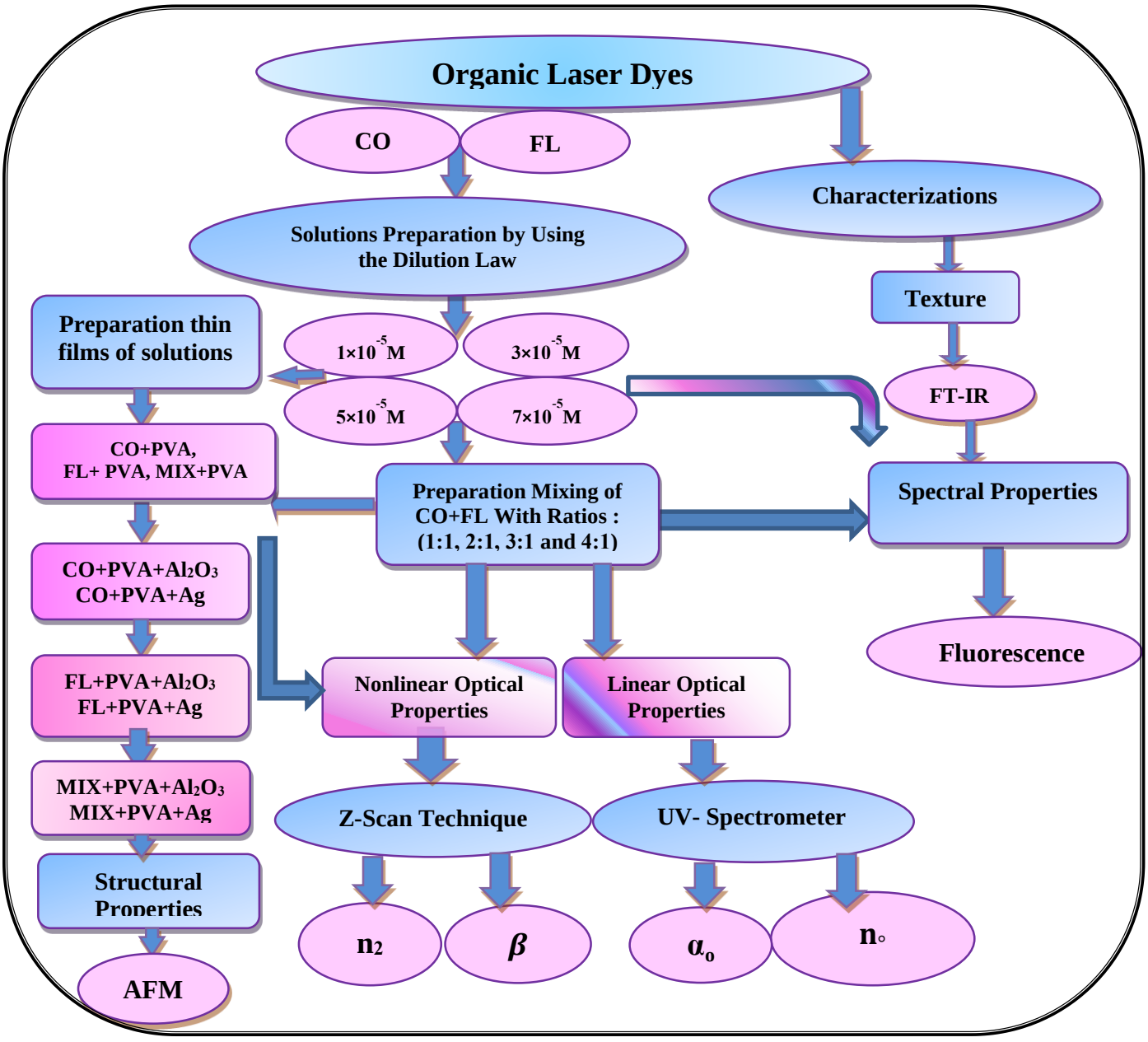

Figure (3.7): Main steps of the experimental work.

3.8 Solutions Preparation

Solutions of concentrations (10^{-3}) M of each organic laser dye in (ethanol) solvent were prepared. The powder was weighted using an electronic balance type (BL 210 S), Germany, having a sensitivity of four digits. Different concentrations were prepared according to the following equation [108]:

$$W = \frac{M_W \times V \times C}{1000} \quad (3.1)$$

Where, W: Weight of the dissolved in material (g), M_w: Molecular weight of the material (g /mol),V: Volume of the solvent (mL) and C: The concentration (M).The prepared solutions were diluted according to the following equation [108].

$$C_1V_1 = C_2V_2 \quad (3.2)$$

Where: C_1: Primary concentration , C_2: New concentration .V_1: The volume before dilution and V_2: The volume after dilution.

In this work four concentrations (1×10^{-5}, 3×10^{-5}, 5×10^{-5}, and 7×10^{-5}) M of each of Coumarin (334) dye and Fluorescein dye to prepare mixing of these two dyes (1 ml) from Coumarin (334) mixing with (1 ml) from Fluorescein to prepare mixing at ratio (1:1), and (4,6ml and 8ml) of Fluorescein dye adding to (2 ml) of Coumarin (334) dye to prepare other ratios (2:1, 3:1 and 4:1) at different concentrations (3×10^{-5}, 5×10^{-5}, and 7×10^{-5}) M. As shown in Figures (3.8), (3.9) and (3.10) respectively.

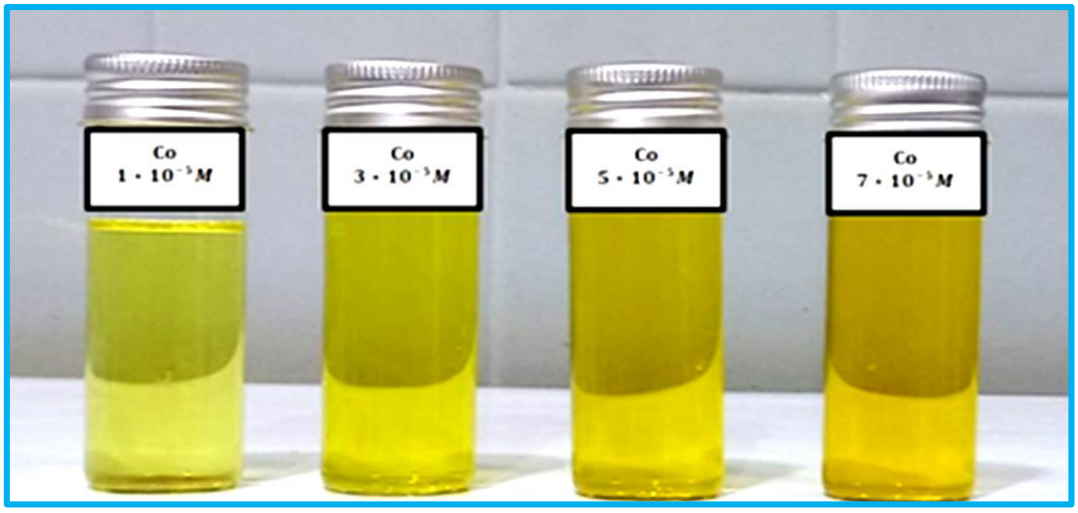

Figure (3.8): Solutions of Coumarin (334) dye at different concentrations.

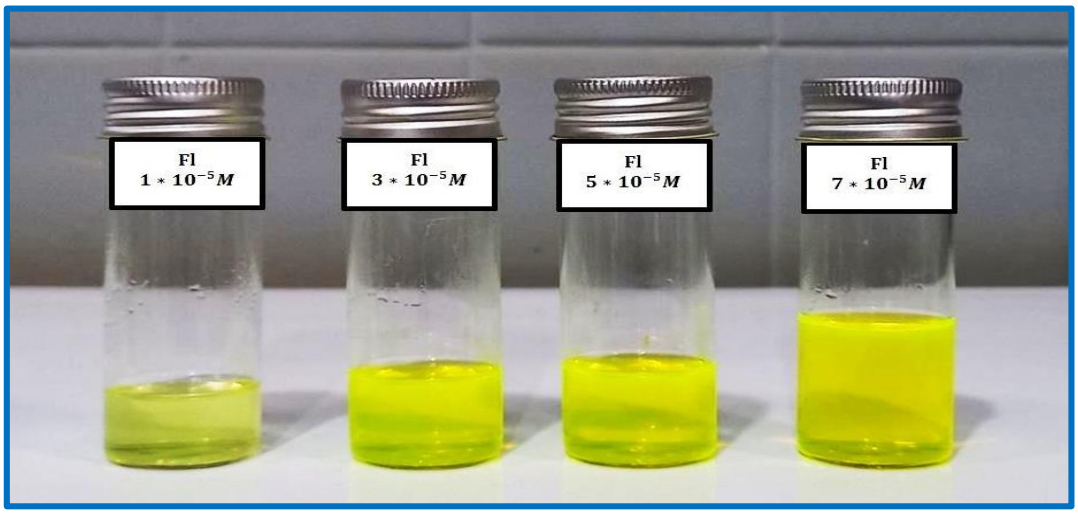

Figure (3.9): Solutions of Fluorescein dye at different concentrations.

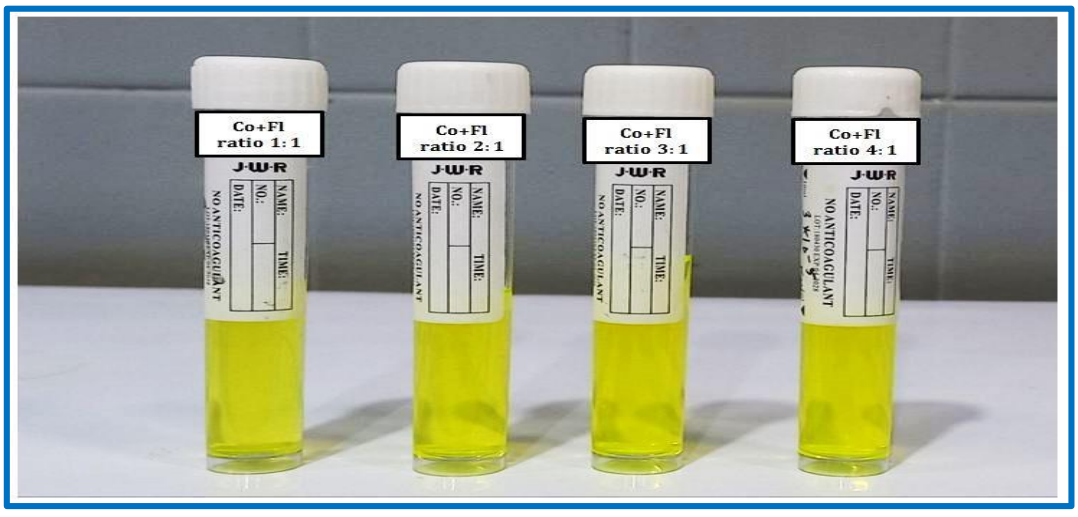

Figure (3.10): Solutions of Mixture of Coumarin (334) and Fluorescein dyes at different mixing ratios .

3.9 Thin Films Preparation

Thin films of Coumarin (334) , Fluorescein organic laser dyes and mixture of them with (PVA polymer doped Ag and Al_2O_3) nanoparticles were prepared on a clean glass slide using the drop casting method, with a solution at concentration (10^{-3} M) for each of them, and dried at room temperature (25-30) C° for (2) days. The thickness of these thin films is approximately (1 10-210) nm.

Thickness of thin films was determined using an optical thin film measurement (Ellipsometry) model (HOLMARC). Polymer solution is created by dissolving the desired amount of polymer in water (2 g in 30 ml of water solvent). A desired amount of dye solution was added to the polymer solution and round at room temperature (25-30)C° using a magnetic stirrer to obtain a homogenous mixture.

(0.06 g) Weight of (Ag and Al_2O_3) nanoparticles powder were added and mixed with a magnetic stirrer to obtain a homogenous mixture. Thin films of Coumarin (334) dye and Fluorescein organic laser dyes and mixture of them doped with PVA polymer , doped Ag and Al_2O_3 nano particles were formed by leaving the mixture to dry at room temperature (25-30)C° on a slide. This procedure was carried out for each dye as shown in Figure (3.11) .

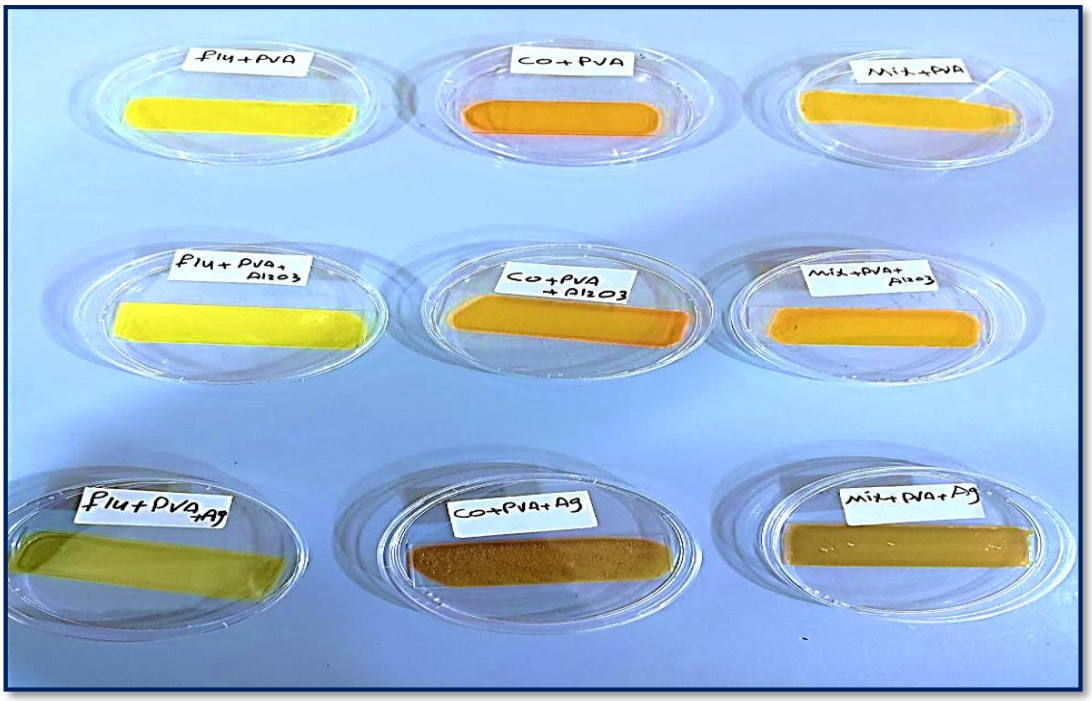

Figure (3.11) : Thin films of Coumarin (334) , Fluorescein dyes and their mixture with PVA polymer doped Al_2O_3 and Ag NPs at ratio (4:1).

3.10 Measurement of thickness

Thickness is one of the most important thin film parameters since it largely determines the properties of thin films. The thickness of thin films is usually measured by monitoring the rate of the deposition during the coating process. However there are several methods used for measuring thickness of thin films, such as weight, optical, electrical and other methods. In our work the thickness of the thin films was measured by optical method it's done by optical thin-film measurement model (LIMF -10, Lambda Scientific Pty Lt). This measured is done in Electro- Optics Laboratory in Babylon University - Science College - Physics department. Figure (3.12) with following specifications .

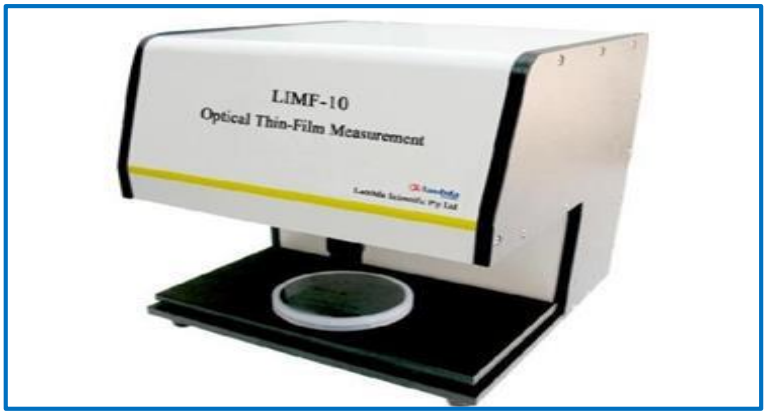

Figure (3.12): Image and specifications for optical thin film thickness measurement.

3.11 Structural Properties Measurements (FT-IR)

The structural testing included FT-IR absorption. The infrared spectra of the produced compounds were taken using FT-IR spectroscopy at the laboratories of the department of chemistry, college of science, university of Kufa. The FT-IR spectrometer is illustrated in Figure (3.13).

Figure (3.13) : FT-IR spectroscopy.

3.12 Optical Properties Measurements

Optical properties measurements of Coumarin (334) , Fluorescein (CO334 and FL) organic laser dyes and mixture of them with different ratios (1:1, 2:1, 3:1 and 4:1) as solution at different concentrations (1×10^{-5}, 3×10^{-5}, 5×10^{-5}, and

7×10^{-5}) M as solution and thin films with PVA polymer doped (Ag, Al_2O_3) nanoparticles will be explain in details in the following paragraph:

3.12.1 UV-Visible spectroscopy

The linear optical properties including transmittance, absorption coefficient, and refractive index for all prepared samples have been determined by utilizing a UV-Visible Shimadzu 1800 Spectroscopy. This Spectroscopy is equipped with two light sources: a deuterium lamp and a tungsten lamp that operate in the wavelength ranges (190-390) nm and (390-1100) nm, respectively. The wavelength, transmittance, and absorbance output data are employed in a computer program to calculate the optical constants. The detector is a silicon photodiode as shown in Figure (3.14). This device is located in the physics department's laboratory at the college of education for pure science in the university of Babylon.

Figure (3.14) : UV-Visible spectroscopy.

3.12.2 Fluorescence Measurement

Fluorescence spectra was measured for all the prepared samples using spectrometer type (FluoroMate FS-2). The samples were mounted in cubic cell of quartz dimensions (1×1×5) cm^3 perpendicularly with incident beam. As showing in Table (3.8) the specifications of this device. All samples were

examined in the laboratory of thin film at University of Babylon College of Education for Pure Science Department of Physics as shown in Figure (3.15).

Table (3.8) : Specifications of spectrometer.

Wavelength range	(200 - 900) nm
Wavelength scan rate	200/400/600 nm / min
Light source	150 W (Xenon arc lamp)
Detector	PMT
Power requirements	(220-240) V (AC)
Resolution	0.5 nm
Wavelength Accuracy	1.0 nm

Figure (3.15): Fluorescence spectroscopy.

3.12.3 Atomic Force Microscopy (AFM)

In order to observe the surface roughness and topography of deposited thin films, AFM micrographs were obtained using digital instruments. Nano scope and III Dimension 3100. AFM images data include root mean square (r.m.s) roughness and grain size. It has three main modes of mapping topography: contact (which is used in our morphology investigation), non-contact and intermittent contact or tapping. The most important part of an AFM is the tip with its nanoscale radius of

curvature. The tip is attached to a micron scale which reacts to the Van der Waals interaction and other forces between the tip and sample. (Model :CSPM AA3000) It was measured in the laboratory of the ministry of science and technology as shown in the Figure (3.16).

Figure (3.16) : Atomic force microscope.

3.12.4 Nonlinear Optical Properties

The equipment used to determine the nonlinear optical properties of all prepared samples will be explained in details in the following paragraph:

3.12.5 Z-Scan Technique

Z-Scan measurements were made in two parts: closed aperture and open aperture. Each component was fabricated utilizing a continuous wave (CW) diode pump solid state blue laser operating at a wavelength (457 nm) and a power (84 mW). The nonlinear refractive index was determined using a closed-aperture Z-Scan, whereas the nonlinear absorption coefficient was determined using an open-aperture Z-Scan. The beam was focused using a convex lens (f = 15 cm), A convex lens was used to focus the laser beam on the sample and the beam waist was determined to be (0.025)cm at the focus. The focus point laser intensity is (20.408×10^{3})mW/cm^{2}, and the sample was moved along the Z-axis.

The transmittance of the sample as a function of sample position is measured. Figure (3.17)shows the open-aperture and closed-aperture Z-Scan setup.

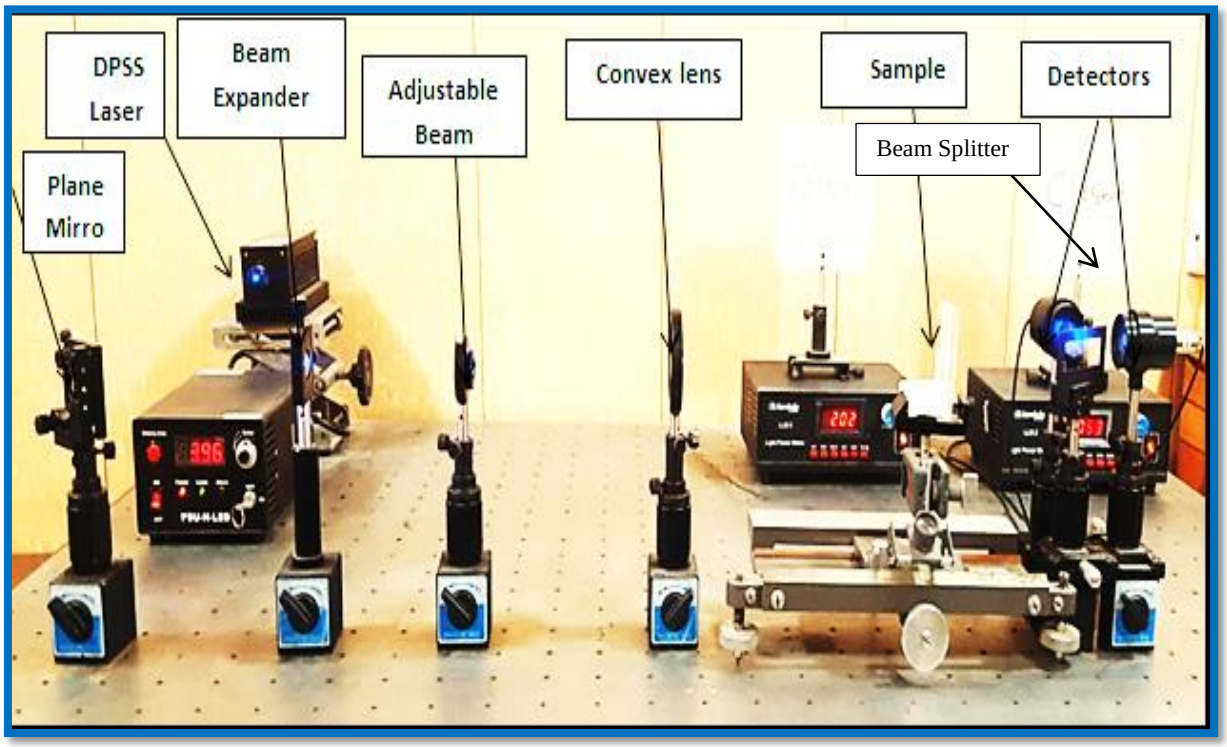

Figure (3.17) : Z-Scan set-up.

3.12.5.1 Diode Pump Solid State Laser (DPSS)

Continuous wavelength (457) nm DPSS laser is used. Table (3.8) shows the characteristics of the laser, which were used in this work.

Table (3.8): Characterization of (457) nm DPSS laser.

Model	**MBL-III-473**
Wavelength (nm)	473±1
Output power (mW)	>1, 5, 10, … , 100
Transverse mode	TEM_{00}
Operating mode	CW
Power stability (rms, over 4 hours)	<3%, <5%, <10%
Beam divergence, full angle (mrad)	<1. 5
Beam diameter at $1/e^2$ (mm)	~1.2
Operating temperature (℃)	10~35
Expected lifetime (hours)	10000

3.12.5.2 Detector

The third optical element in the Z-Scan is the optical power meter detector type (LLM-2), which is used to measure the output power of the laser. The detector was placed at the far field of a Gaussian laser beam.

3.12.5.3 Aperture

The aperture is an important parameter in Z-Scan system to measure non-linear refractive index (n_2) in the closed-aperture technique, and its diameter was (1mm). Aperture aligned with the lens in the same axis.

3.12.5.4 The Sample

All solutions was filled into the glass cuvette (1) mm thickness. The cuvette was hand made in the laboratory, which consists from five slides of glass as shown in Figure (3.18). The geometry of sample cuvette can be shown in Figure (3.19), which is represented engineering drawing of sample cuvette.

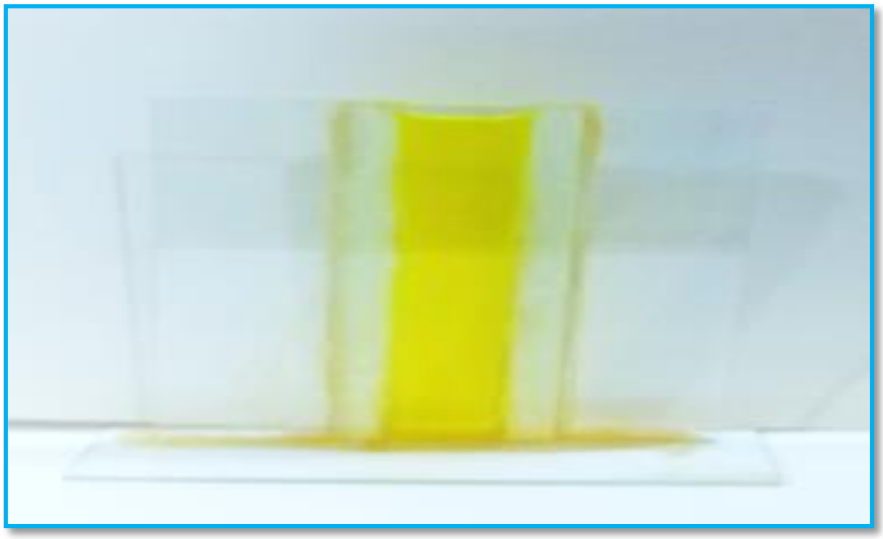

Figure (3.18): Photograph of sample.

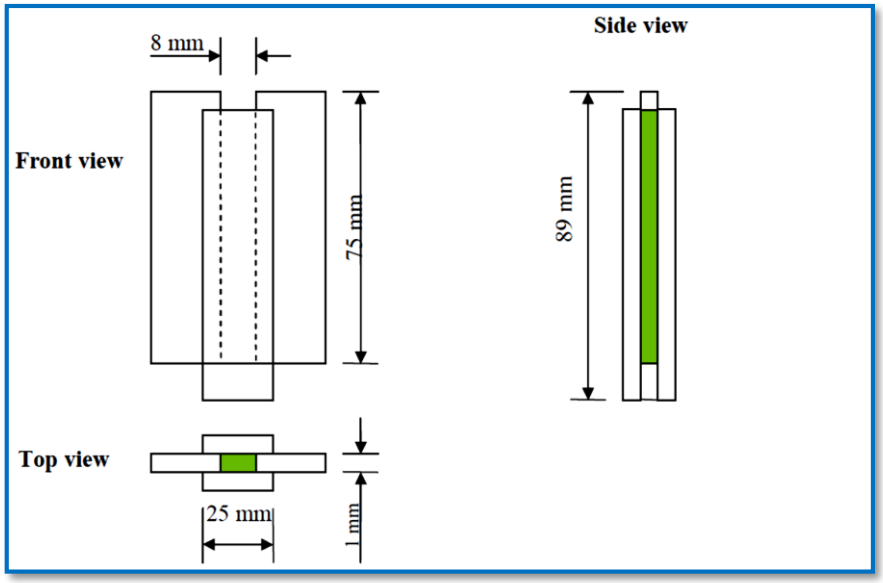

Figure (3.19): Geometry of sample cuvette [20].

3.12.5.5 Reference Beam Measurements

In order to measure the reference power of a CW laser, the detector was placed directly in front of the (457 nm) DPSS laser. The normalized transmission as a function of sample position is given by [109]:

$$T(z) = \frac{P(I)}{P(I)_{ref}} \qquad (3.3)$$

Where, P(I) is the power of the transmitted laser beam, when the cuvette is filled by dye solution, and $P(I)_{ref}$ is power of the reference laser beam.

3.13 Optical Limiting Behavior

Optical limiting occurs when the optical transmission of a material saturates with increasing laser intensity, a property that is desirable for the protection of sensors and human eyes from the intense laser radiation. The optical power limiting property of pure and doped dyes and their thin films, is measured with the same laser used in Z-Scan technique. Set up the optical limiting as shown in the previous Figure (3.17).

4.1 Introduction

In this chapter, the results of all prepared samples were presented, the structural properties which including atomic force microscopy (AFM) , also Fourrier transform infrared (FT-IR).The spectral, linear and non-linear optical properties for all prepared samples were measured . Also using Z-Scan for two cases, closed and open aperture utilized a continuous wave diode pump solid state laser operating at a wavelength 457 nm and power 84 mW. The optical limiting behavior of all samples are also discussed.

4.2 Structure Measurements (FT-IR)

Charts of infrared (FT-IR) spectra of Coumarin (334) , Fluorescein . FT-IR spectra for Coumarin (334) , Fluorescein as Powder was measured at room temperature (25-30) C^{o} as shown in Figures (4.1) and (4.2) respectively. Figure (4.1) shows there were more than one peak obtained in region of the C–H bending vibrations out phase bend (943-688) cm^{-1} can support the presence of an aromatic structure. In region (1176-1031) cm^{-1}, there is a peak at (1109) cm^{-1} refers to C–H bending vibrations in of plane. That acts the C=C stretching (1450-1641) cm^{-1}, and a peak at (3402) cm^{-1} for C–H stretching (3851-3740) cm^{-1} which agree with reference [110].

The FT-IR spectrum for Fluorescein powder shows the bond of stretching represented by the peak at (2118) cm^{-1} indicate carbon-hydrogen bond (C-H), the peak at (1321) cm^{-1} indicate (O-H) , the peak at (1562) cm^{-1} indicate (C=C) carbon–carbon bond is a covalent bond between two carbon atoms. The peak at (1163) cm^{-1} indicate (C-O), the range (839-759) cm^{-1} which indicate the (C-C) group which agree with reference [111]. As shown in Figure (4.2).

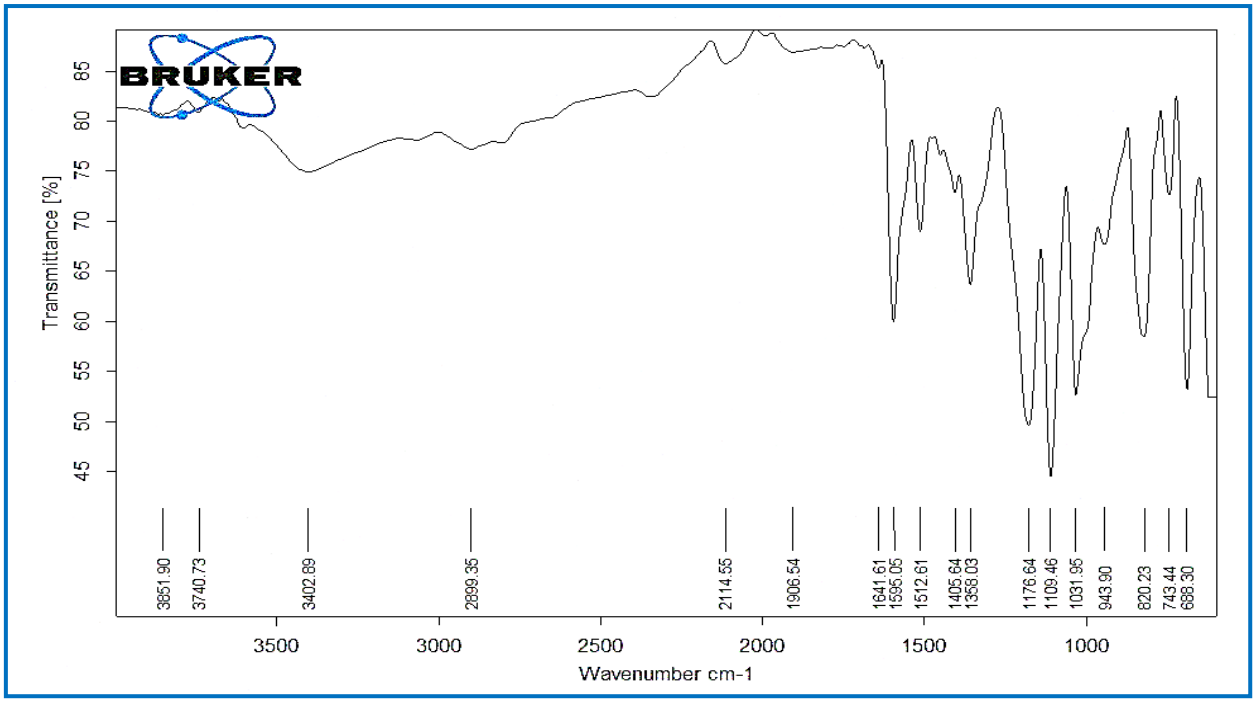

Figure(4.1): FT-IR spectrum for Coumarin (334) dye as powder.

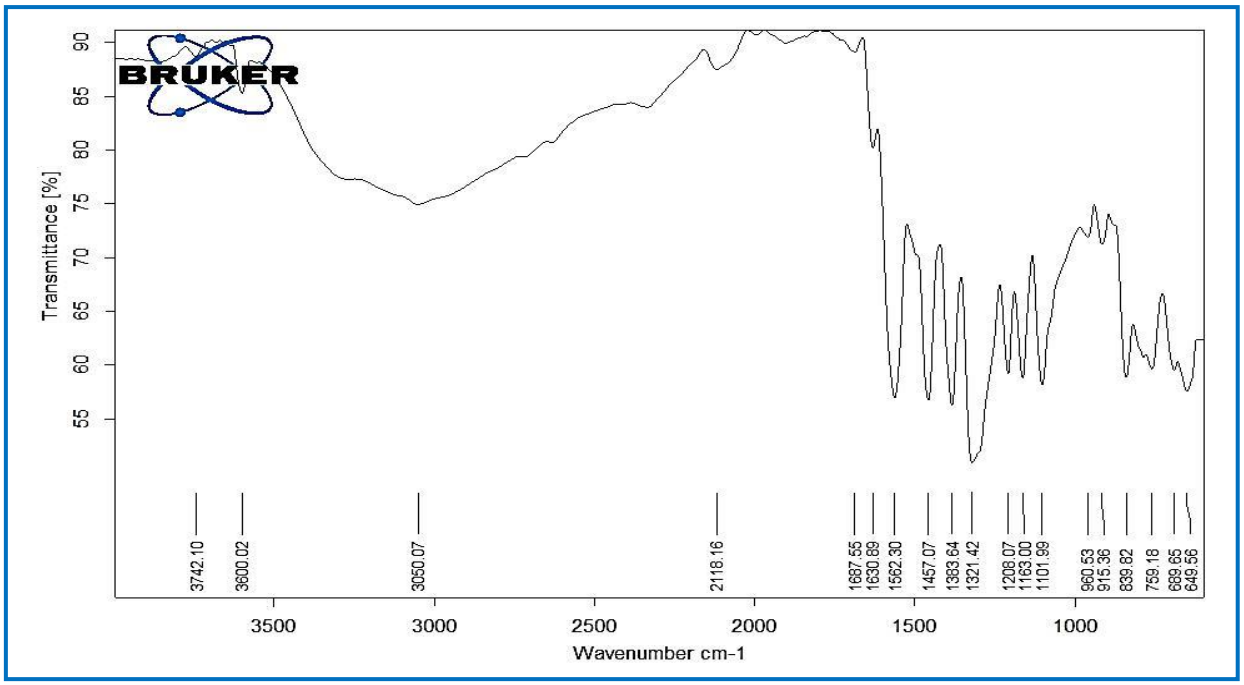

Figure (4.2): FT-IR spectrum for Fluorescein dye as powder.

4.3 Atomic Force Microscope Measurements (AFM)

The 3-D AFM images and granularity accumulation distribution charts for thin films of Coumarin (334), Fluorescein and their mixture with ratio (4:1) that deposited on glass substrate are able to depict and analysis of the surfaces and give the statistical values with high accuracy about surface roughness values depending on the root mean square (r.m.s) of the average roughnes.

The study of microscopic analysis (AFM) of the thickness, concentration, temperature and method of preparation , etc.), effect on the properties of the deposited film material to the fact that the study of the surfaces of film materials

Is important to recognize how the distribution and arrangement of atoms on surfaces, and to identify the differences or homogeneity properties or attributes relating to each atom separately and illustrative image about the distribution rate of the crystalline size on to surfaces.

Figures (4.3 - 4.11) show 2-D and 3-D images respectively of AFM for thin films of Coumarin (334) , Fluorescein and their mixtures with PVA polymer doped (Ag, Al_2O_3) nanoparticles at (10^{-3}) M with ratio (4:1), a diagram of distribution of growth granular groups on the surfaces of the deposited films Table (4.1) shows that the average diameters (grain size) of thin films .It is found that the grain size and the (r.m.s) of surface roughness increases when thickness increases for all preapared samples, it agree with reference [112].

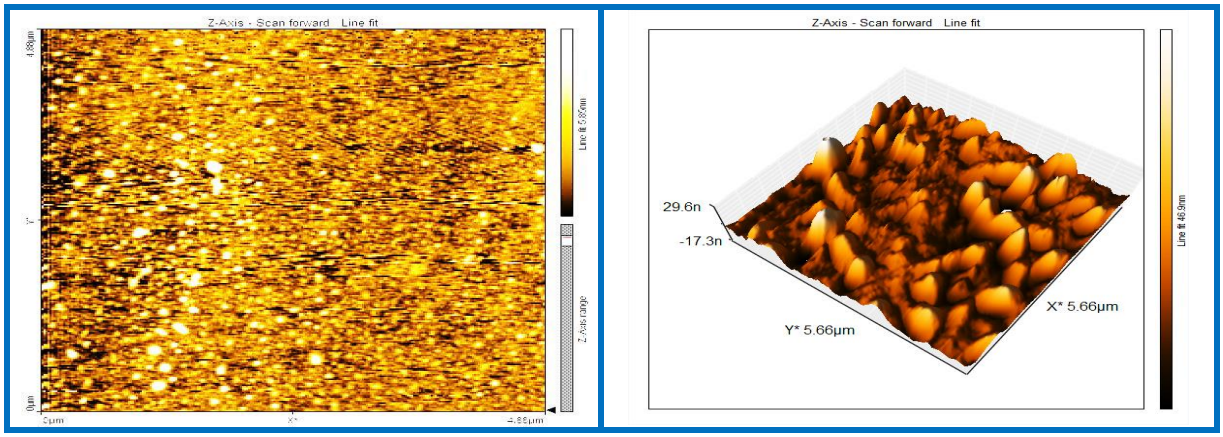

Figure (4.3): 2-D and 3-D AFM images for thin films of Coumarin (334) with PVA polymer.

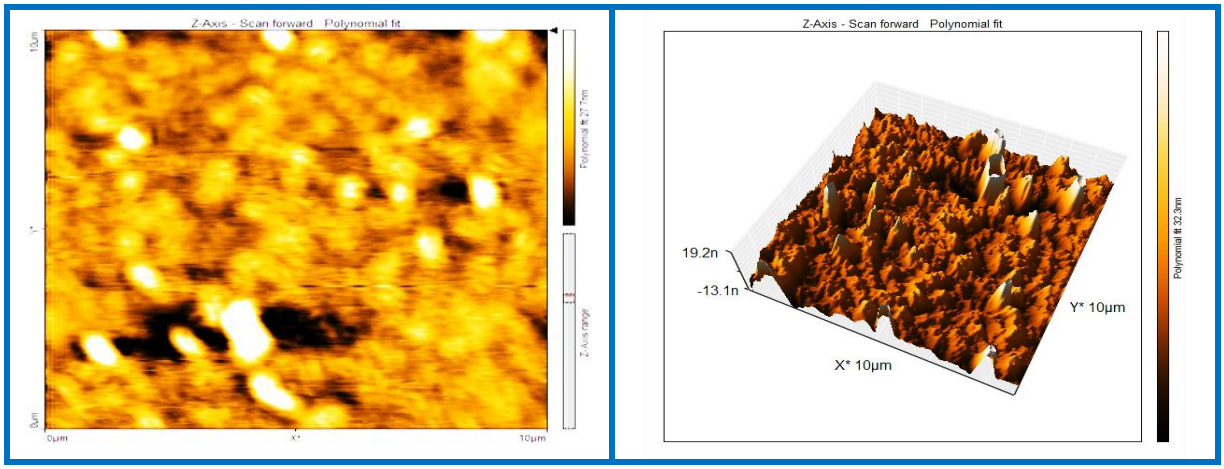

Figure (4.4): 2-D and 3-D AFM images for thin films of Coumarin (334) with PVA polymer doped Al_2O_3 NPs.

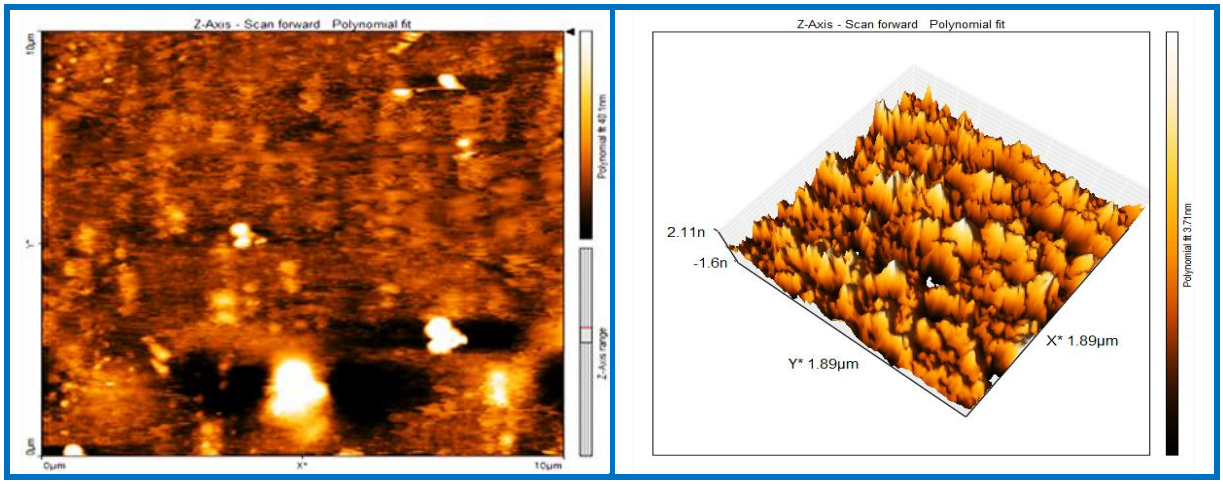

Figure (4.5): 2-D and 3-D AFM images for thin films of Coumarin (334) doped PVA polymer doped Ag NPs.

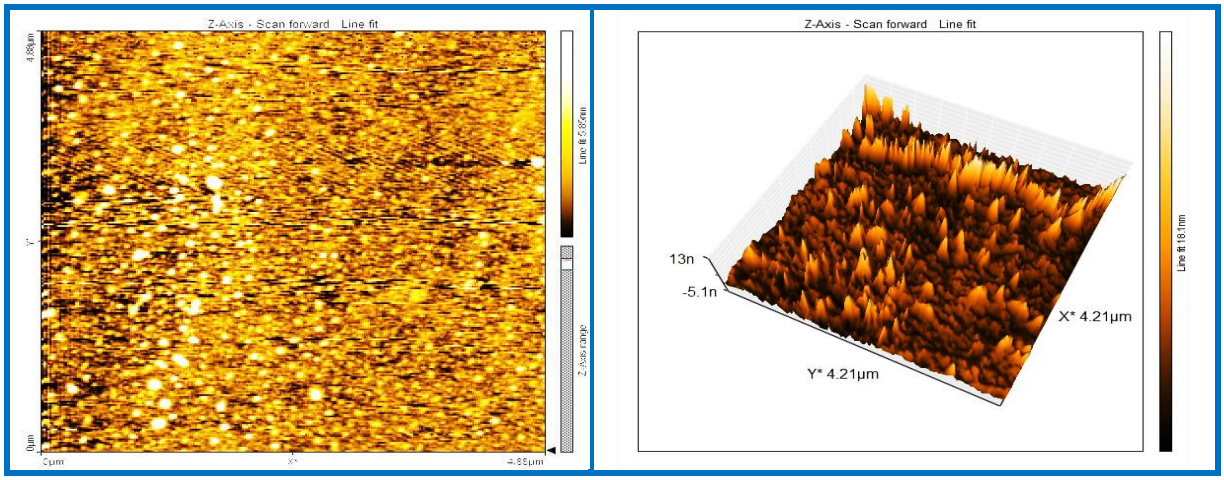

Figure (4.6): 2-D and 3-D AFM images for thin films of Fluorescein with PVA polymer.

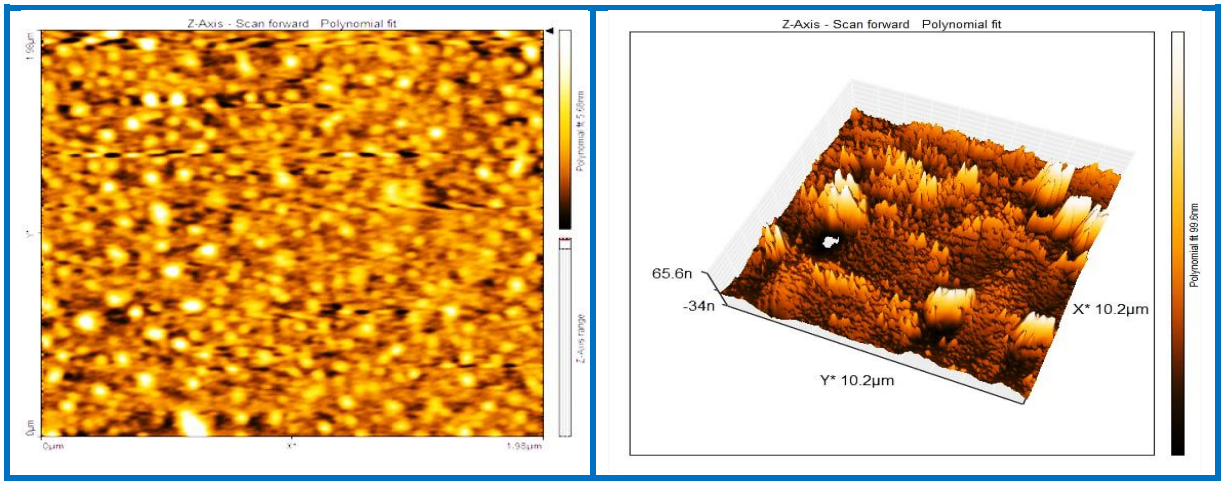

Figure (4.7): 2-D and 3-D AFM images for thin films of Fluorescein with PVA polymer doped Al_2O_3 NPs.

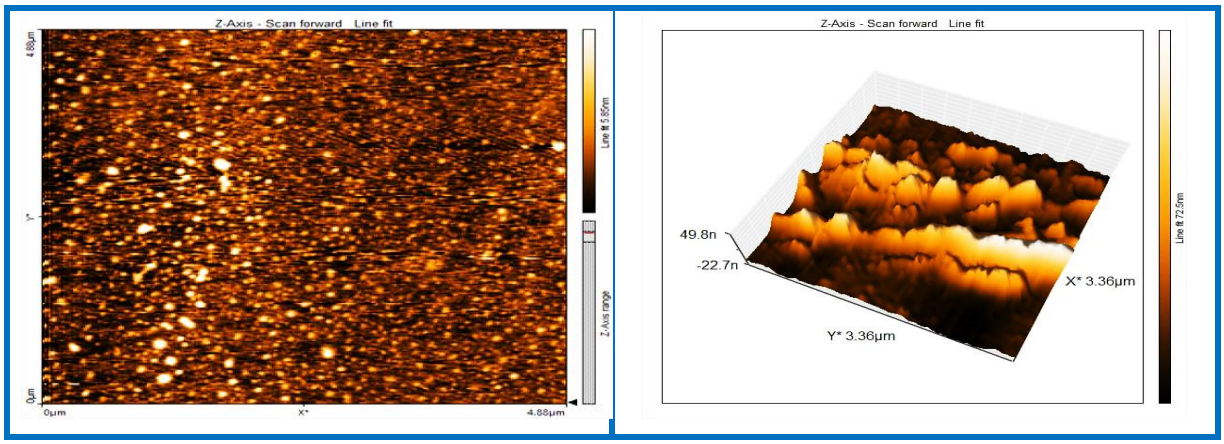

Figure (4.8): 2-D and 3-D AFM images for thin films of Fluorescein with PVA polymer doped Ag NPs.

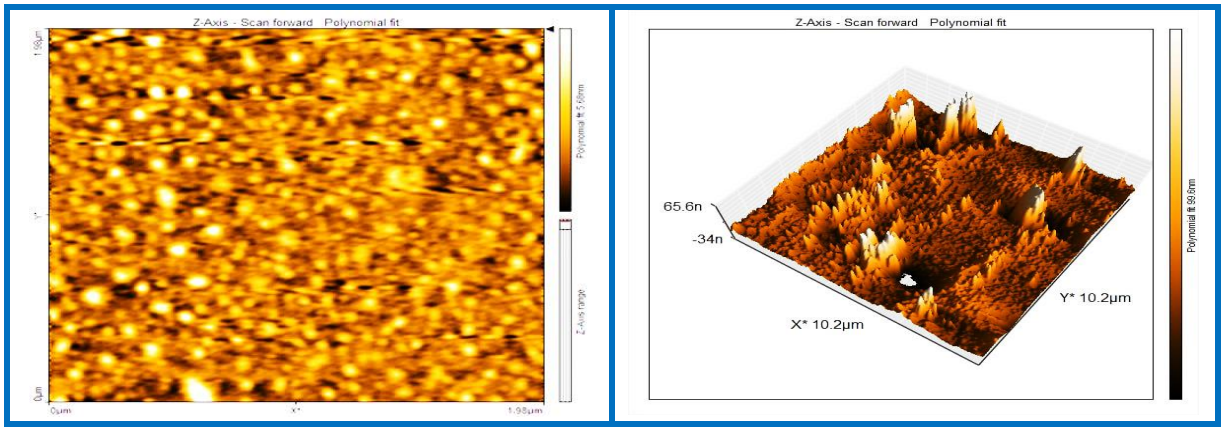

Figure (4.9): 2-D and 3-D AFM images for thin films of (CO+FL) with PVA polymer at mixing ratio (4:1).

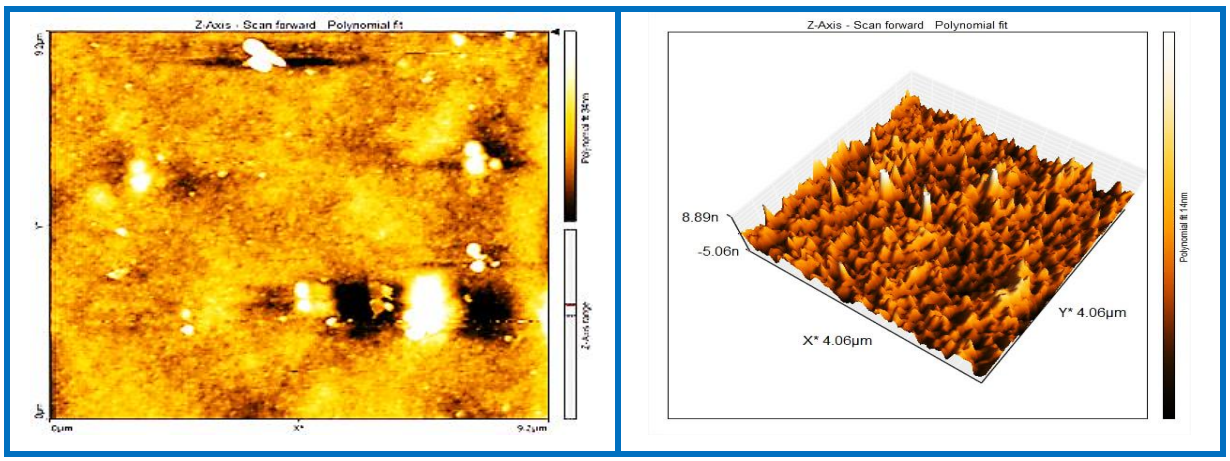

Figure (4.10): 2-D and 3-D AFM images for thin films of (CO+FL) with PVA polymer doped Al_2O_3 NPs at mixing ratio (4:1).

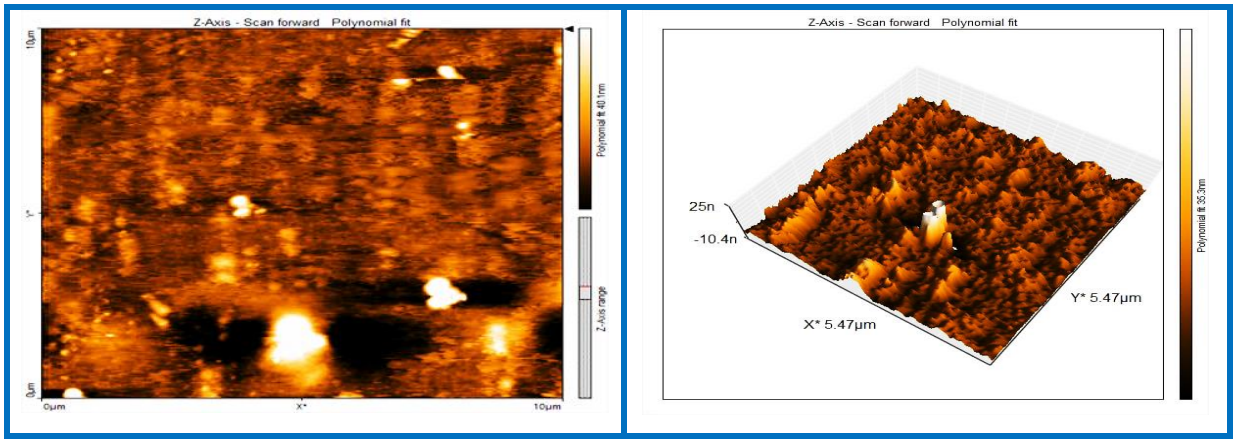

Figure (4.11): 2-D and 3-D AFM images for thin films of (CO+FL) with PVA polymer doped Ag NPs at mixing ratio (4:1).

Table (4.1) : AFM parameters of thin films of Coumarin (334) , Fluorescein and their mixture with PVA polymer doped (Al_2O_3 and Ag) NPs.

Material	r.m.s (nm)	Roughness (nm)	Average Grain Size (nm)	Thickness (nm)
CO+PVA polymer	0.324	0.277	69.89	110
CO+PVA polymer +Al_2O_3 NPs	0.538	0.467	70.10	114
CO+PVA polymer +Ag NPs	0.630	0.694	73.12	120
FL+PVA polymer	0.491	0.341	75.31	115
FL+PVA polymer +Al_2O_3 NPs	0.772	0.778	77.23	118
FL+PVA polymer +Ag NPs	0.941	0.833	78.69	125
CO+FL+PVA polymer (4:1)	0.664	0.517	82.18	175
CO+FL+PVApolymer+Al_2O_3 NPs (4:1)	0.950	0.834	84.24	200
CO+FL+PVA polymer +Ag NPs (4:1)	1.476	1.170	89.95	210

4.4 Optical Testing Results

The optical testing included the linear and nonlinear optical properties of Coumarin (334) , Fluorescein organic laser dyes and mixture of them with different mixing ratios (1:1,2:1,3:1 and 4:1) as solution at different concentrations (1×10^{-5}, 3×10^{-5}, 5×10^{-5}, and 7×10^{-5}) M and thin films with PVA polymer doped (Ag , Al_2O_3 nanoparticles) at concentrations (10^{-3}) M.

4.4.1 Linear Optical Properties Measurements

The linear optical properties consisted of absorption and transmission spectra, as well as measurement of linear refractive index and linear coefficient.

4.4.1.1 Absorbance Spectra of Coumarin (334) and Fluorescein Organic Laser Dyes and their mixture (as solutions)

The linear absorption spectra of all samples, recorded for wavelengths (190 - 1100) nm were tested using UV-VIS spectrophotometer model (Aquarius 7000, Optima, Japan) at room temperature, as shown in Figures (4.12 - 4.16) respectively.

The absorption spectra for Coumarin (334) dye are shown in Figure (4.12).The present results show that the absorption peaks were shifted toward the longer wavelengths (red shift) with increasing concentrations. This shift is due to increasing number of molecules per volume unit at high concentrations, the absorption increasing with increases concentration according to Beer-Lambert law. This behavior agrees with [15].The Figure show that the four spectra have two clear bands, in UV region which is called B-band at the range about (225-340) nm, that resulted from an electronic transitions for ($\pi \rightarrow \pi^*$). The second band at visible region which is called Q-band at the range about (350-550) nm with highest wavelengths belongs to transition of ($n \rightarrow \pi^*$) This behavior agrees with [15].

The absorbance spectra for Fluorescein dye at different concentrations, are shown in Figure (4.13). The intensity increase of absorption with the increased concentration is due to the increased number of molecules which in turn to increases the probability of absorption with the concentrations used, this agrees with Beer-Lambert law. The peaks of absorption spectra shifted toward the longer wavelengths (Red shift) when the concentration increased because of the dipole moment of the excited state is higher than the ground state.

The Figure show that the four spectra have two clear bands, in UV region which is called B-band at the range about (200-300) nm, that resulted from an electronic transitions for ($\pi \rightarrow \pi^*$). The second band at visible region which is called Q-band at the range about (400-540) nm with highest wavelengths belongs to transition of ($n \rightarrow \pi^*$). The absorbance for Q-bands increases strongly with concentration increases, it agree with reference [18].

The absorbance spectra for mixing of (CO 334 and FL) organic laser dyes at concentrations (3×10^{-5}, 5×10^{-5}, and 7×10^{-5}) M as solutions at different mixing ratios (1:1, 2:1, 3:1 and 4:1) are shown in Figures (4.14 - 4.16). The Figure show that the four spectra have two clear bands, in UV region which is called B-band at the range about (200-350) nm, that resulted from an electronic transitions for ($\pi \rightarrow \pi^*$).The second band at visible region which is called Q-band at the range about (350-550) nm with highest wavelengths belongs to transition of ($n \rightarrow \pi^*$)**.** It has also increased the absorbance due to the increase in mixing ratios which produces an increase in number of molecules in volumetric unit which effect in the energy state it agree with reference [15].

This is accompanied by the emission of a photon (radiative relaxation) or by a transfer of energy to another particle. The released energy is equal to the difference in energy between the electron energy states, this behavior is attributed to the increasing in the energy of atoms that leads to the increasing of the number of collision between atoms. Increasing absorption within the material. When an excited electron falls back to a state of lower energy, it undergoes electron relaxation. It is a good agreement with Beer-Lambert law [15].The results showed that the absorbance of Fluorescein dye is higher than that of Coumarin (334) dye, as well as that the absorbance of mixture (CO 334 and FL) organic laser dyes at concentration (7×10^{-5}) M with mixing ratio (4:1) is higher than that of other concentrations and other ratios due to the occurrence of energy transfer between the donor and the acceptor.

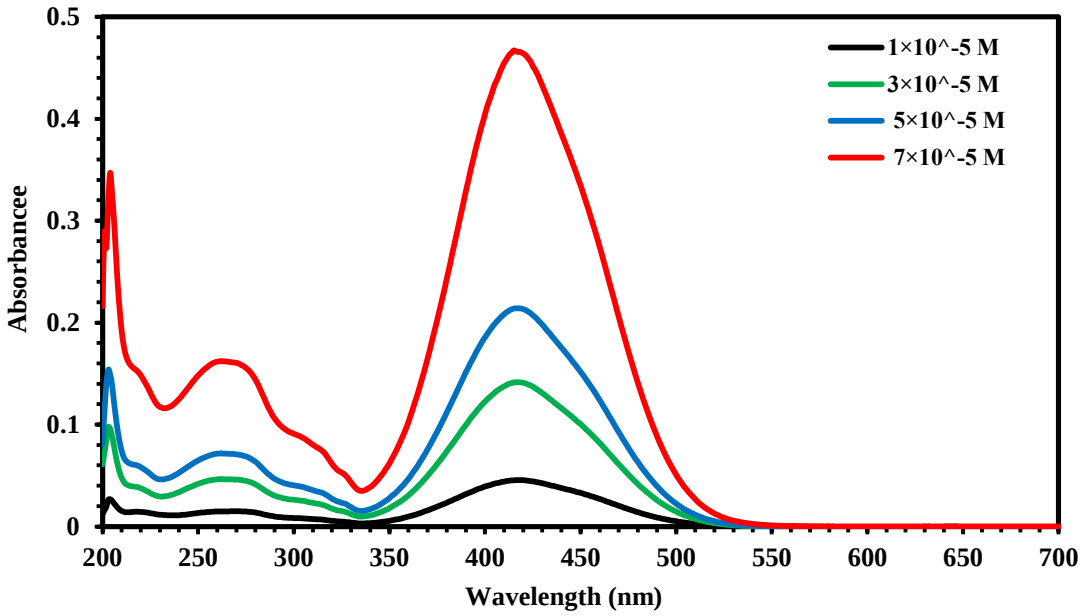

Figure (4.12):The absorbance spectra For Coumarin (334) organic Laser Dye at different Concentrations.

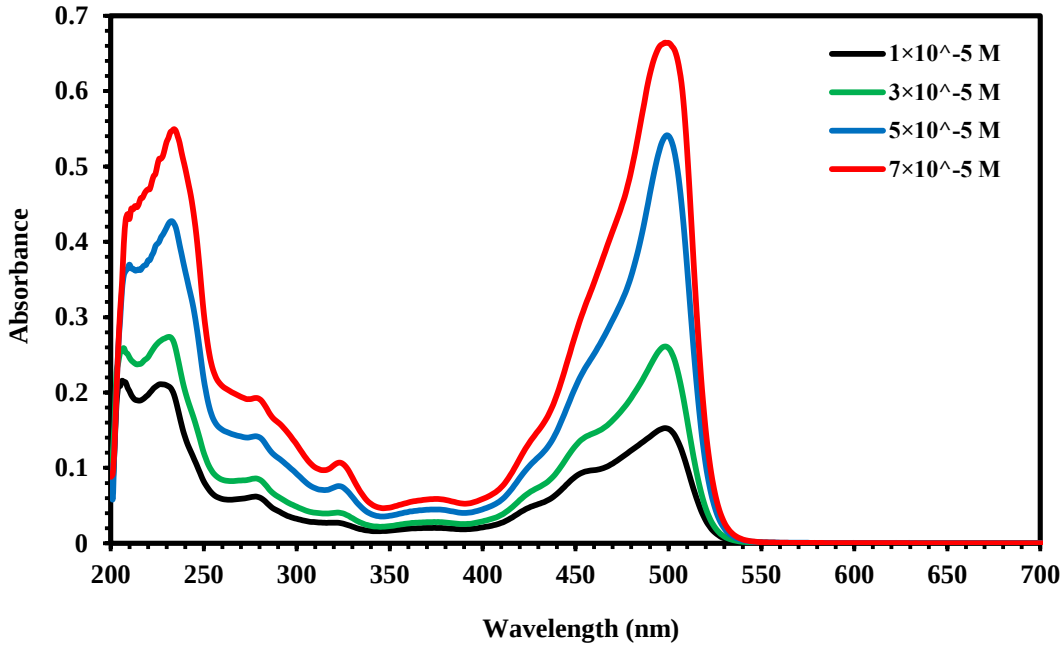

Figure (4.13):The absorbance spectra for Fluorescein organic laser dye at different concentrations.

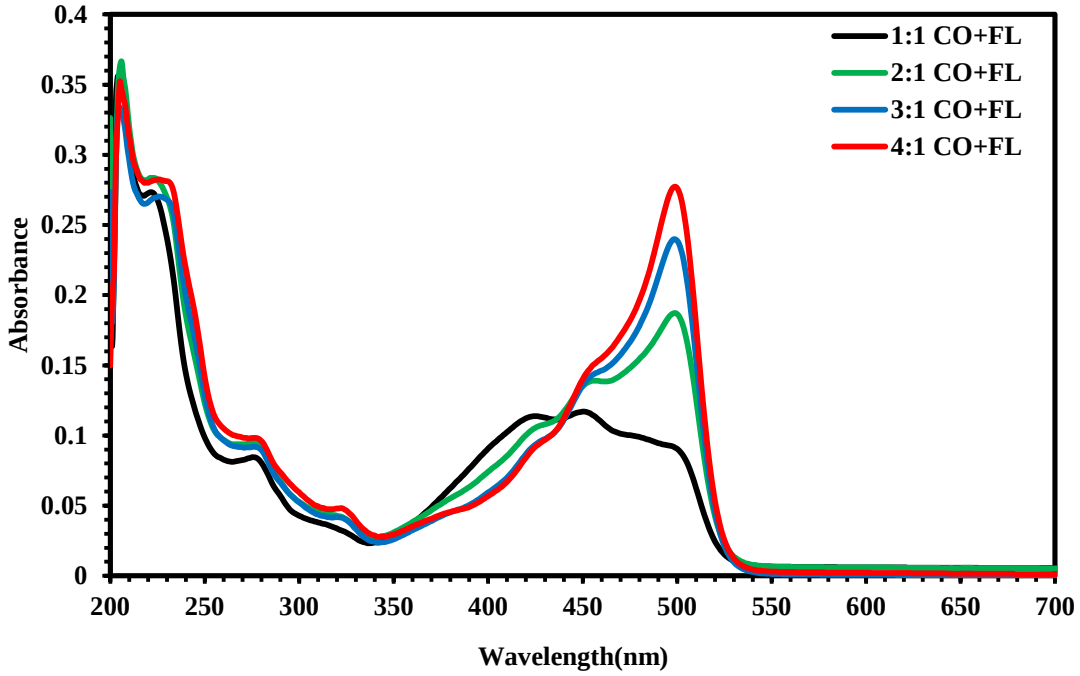

Figure (4.14):The absorbance spectra for mixing of (CO+FL) organic laser dyes at concentration (3×10^{-5}) M with different mixing ratios.

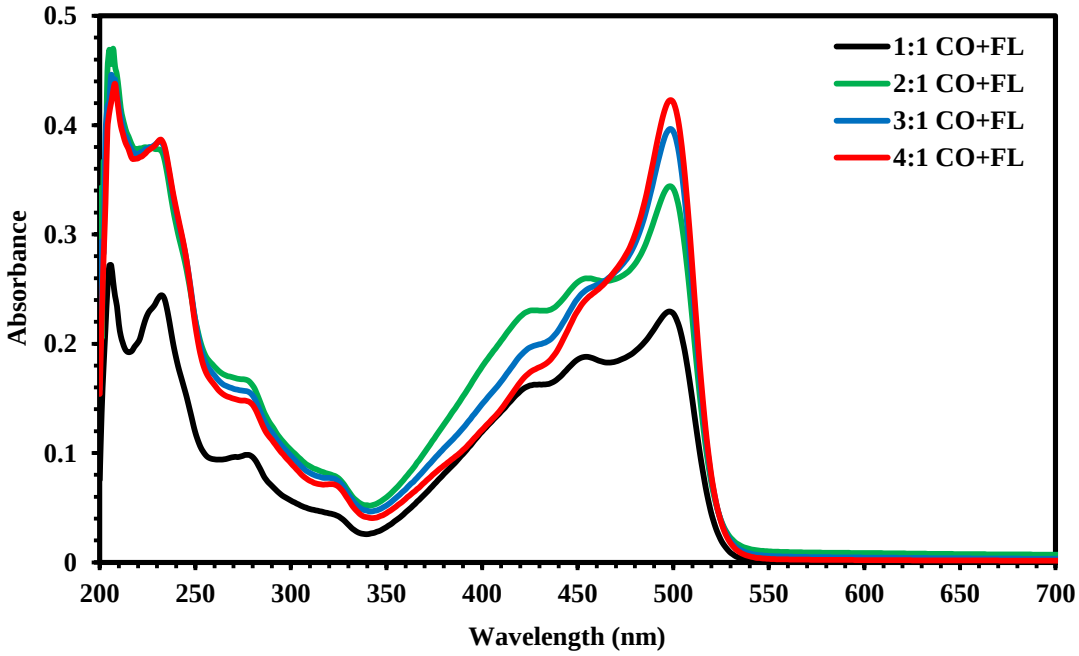

Figure (4.15):The absorbance spectra for mixing of (CO+FL) organic laser dyes at concentration (5×10^{-5}) M with different mixing ratios.

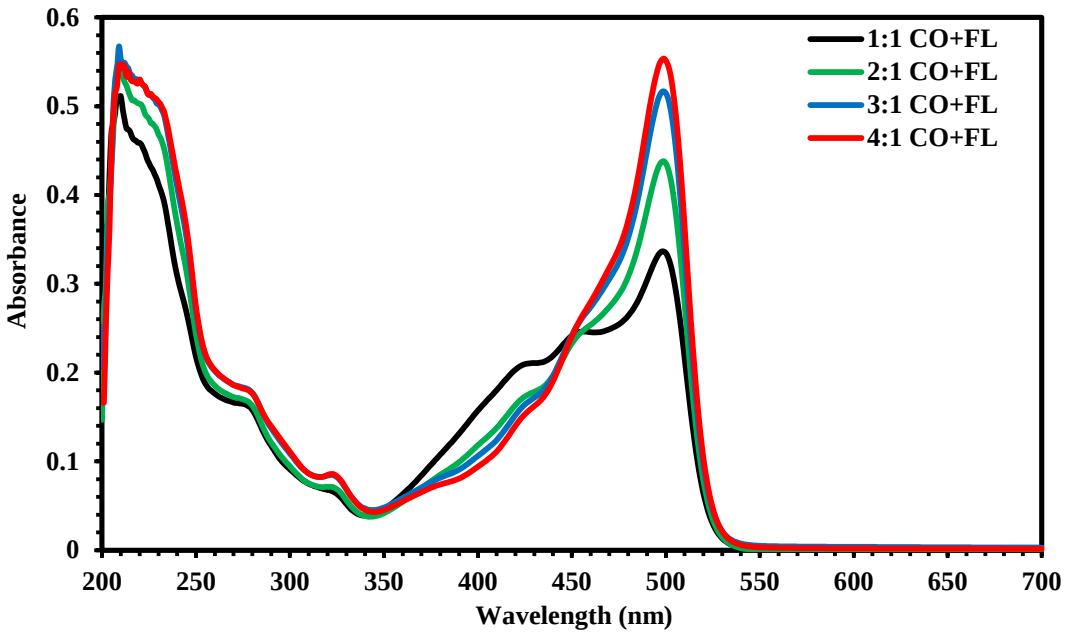

Figure (4.16):The absorbance spectra for mixing of (CO+FL) organic laser dyes at concentration (7×10^{-5}) M with different mixing ratios.

4.4.1.2 The Absorbance Spectra of Coumarin (334), Fluorescein Organic Laser Dyes and their mixture (as Thin Films)

The linear absorbance spectra of thin films of Coumarin (334), Fluorescein organic laser dyes and their mixture with (PVA) polymer doped (Ag , Al_2O_3 nanoparticles) at (10^{-3}) M at ratio (4:1) prepared by drop- casting method are shown in Figures (4.17- 4.19) respectively. (The present results show that the absorption peaks were shifted toward the longer wavelengths after addition (PVA) polymer with nanoparticles to pure dye).

This shift obtain due to electronic and vibrational states of interfacial molecules, which is lead to increasing absorption for all samples of nanocomposites at UV region, this is suggested to take place because of the excitations of high occupation molecular orbital (HOMO) electrons to the lowest inoccupation molecular orbital (LUMO). The high absorbance of samples for nanocomposites at UV region attributed to the energy of photon enough to interact with atoms, the electron excites from a lower to higher energy level by absorbing a photon of known energy. Fundamental absorption of absorption

spectra refers to band or excitation transition, at visible and near infrared regions, the absorption of all samples for nanocomposites has low values, this behavior attributed to the energy of incident photons doesn't enough to interact with atoms, thus the photons will be transmitted when the wavelength increases when the amount of energy required for transmission decreases [113].

Dyes doped mixture have large linear optical properties as compared with pure single dyes, it agree with the study in reference [30]. Tables (4.2-4.5) show the linear absorption coefficient (α_o) and linear refractive index (n_o) of Coumarin (334) Fluorescein organic laser dyes and mixture of them at concentrations (1×10^{-5}, 3×10^{-5}, 5×10^{-5}, and 7×10^{-5}) M as solutions at different ratios (1:1, 2:1, 3:1 and 4:1), and thin films with PVA polymer doped Ag and Al_2O_3 nanoparticles obtained from Equations (2.15) and (2.16) respectively. The values of (α_o) for mixing of two dyes are larger than values for pure dyes, as well as, the values of (α_o) and values (n_o) for thin films are larger than those values for same materials as solutions. This behavior agrees with references [17]. The results showed that the absorbance of the thin films doped with nanoparticles (Ag) is higher than that of the thin films doped with (Al_2O_3) nanoparticles and the absorbance of the thin films doped nanoparticles (Ag and Al_2O_3) is higher than that of thin films with PVA polymer.

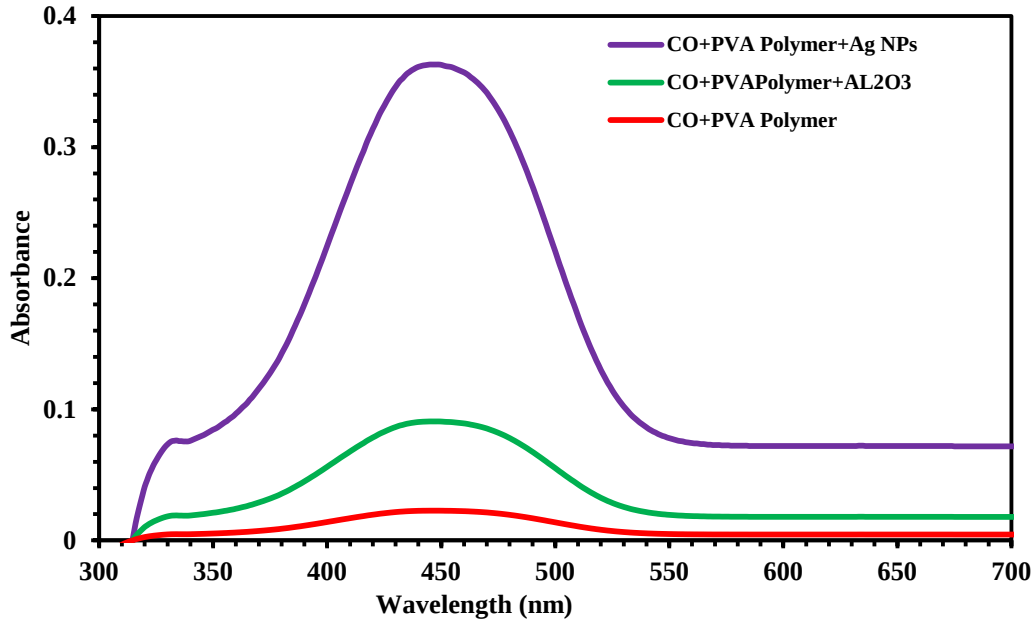

Figure (4.17): The absorbance spectra for thin films of Coumarin 334 organic laser dye with PVA polymer doped (Al_2O_3 , Ag) NPs.

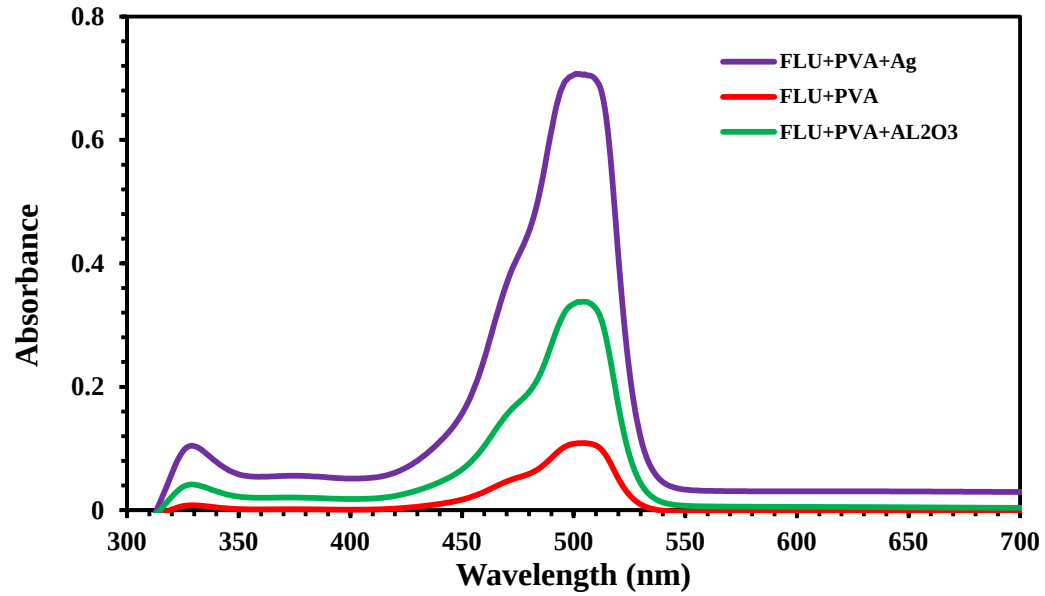

Figure (4.18): The absorbance spectra for thin films of Fluorescein organic laser dye with PVA polymer doped (Al_2O_3 , Ag) NPs.

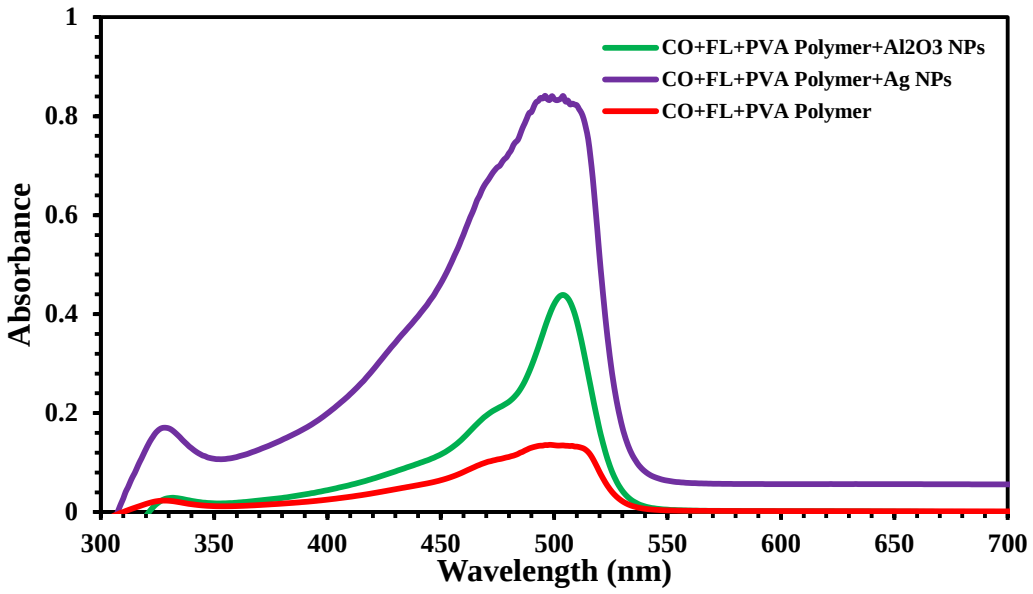

Figure (4.19): The absorbance spectra for thin films of mixing of two organic dyes with PVA polymer and (Al_2O_3 , Ag) NPs.

4.5.1The Transmittance Spectra of Coumarin (334) And Fluorescein Organic Laser Dyes and their mixture (as solutions)

Transmittance spectra of Coumarin (334) at different concentrations (1×10^{-5}, 3×10^{-5}, 5×10^{-5}, and 7×10^{-5}) M in Ethanol solvent prepared at room temperature (25-30) C°, are shown in Figure (4.20). The optical transmittance curve of all samples show a variable behavior of the transmission as a function of the incident wavelength, this behavior agrees with [15]. The transmittance decreases with increaseing ratios at the same wavelength. Figure (4.21) show transmittance spectra of Fluorescein at different concentrations (1×10^{-5}, 3×10^{-5}, 5×10^{-5}, and 7×10^{-5}) M in Ethanol solvent prepared at room temperature (25-30) C°.

The optical transmission curve of all samples showed a variable behavior of the transmittance as a function of the incident wavelength, this behavior agrees with [18].The transmittance decreases with increases ratios at the same wavelength. Transmittance spectra for mixing of Coumarin (334), Fluorescein organic laser dyes at concentrations (3×10^{-5}, 5×10^{-5}, and 7×10^{-5}) as solutions at different mixing ratios (1:1, 2:1, 3:1, and 4:1) M are shown in Figures (4.22-

4.24) respectively. The same behavior can be observed, the optical transmission curve of all samples showed a variable behavior of the transmittance as a function of the incident wavelength.The transmittance decreases with increases ratios at the same wavelength. This behavior agrees with [15].

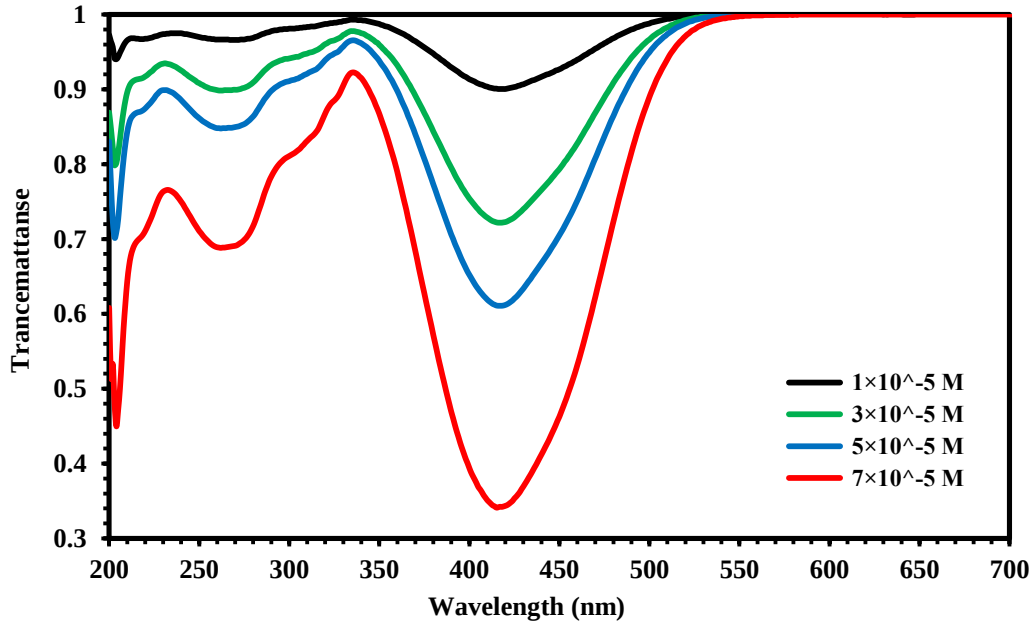

Figure(4.20):Transmittance spectra for (Coumarin 334) organic laser dye at different concentrations.

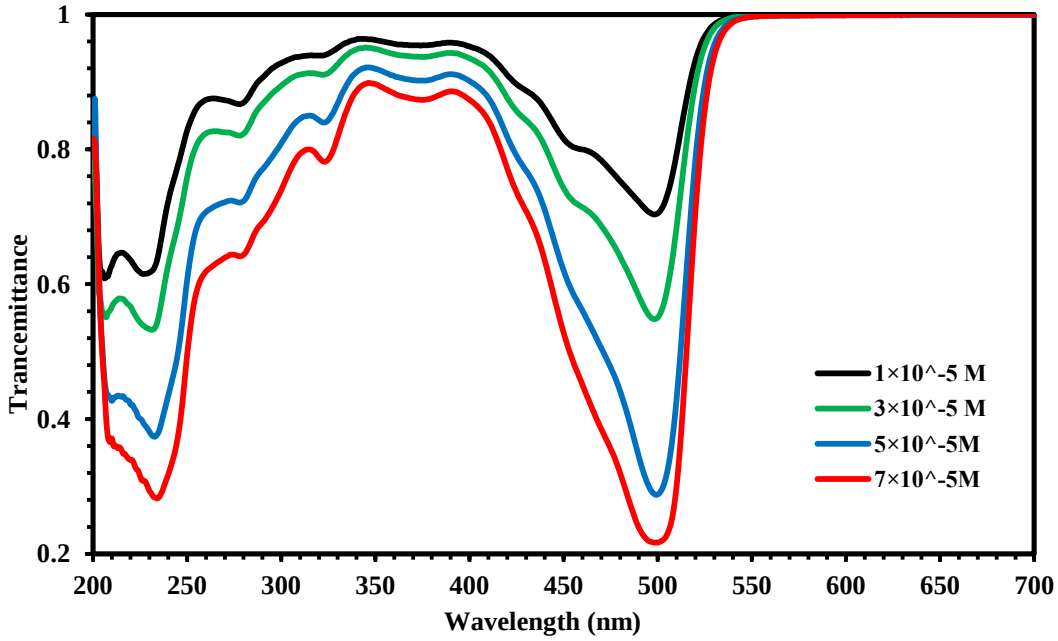

Figure (4.21): Transmittance spectra Fluorescein organic laser dye at different concentrations.

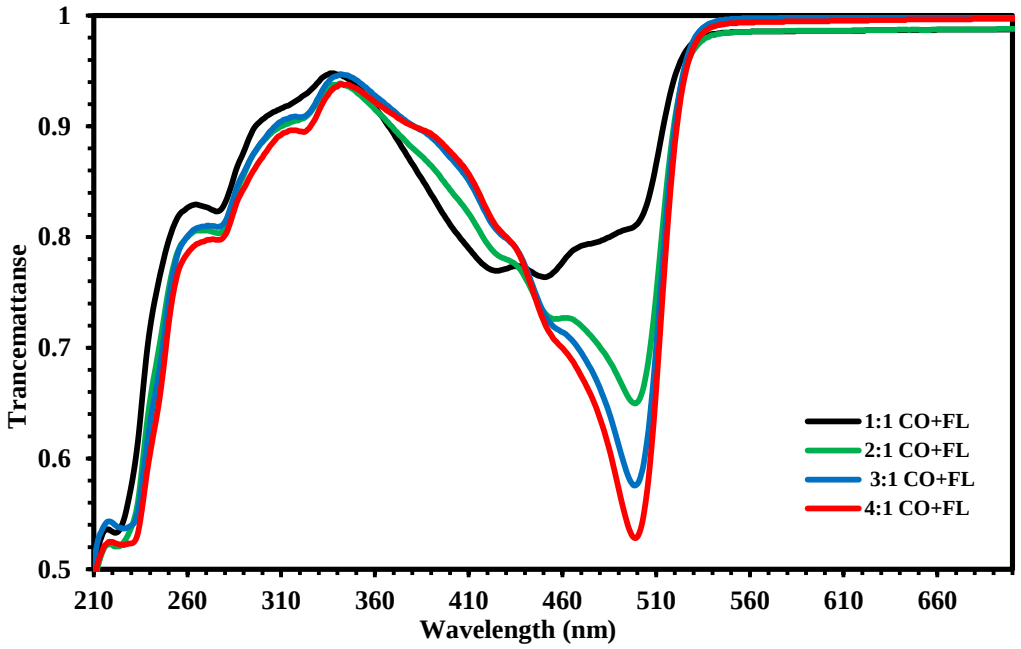

Figure (4.22): Transmittance spectra for Mixing of (CO+FL) organic laser dyes at concentration (3×10^{-5}) M with different mixing ratios.

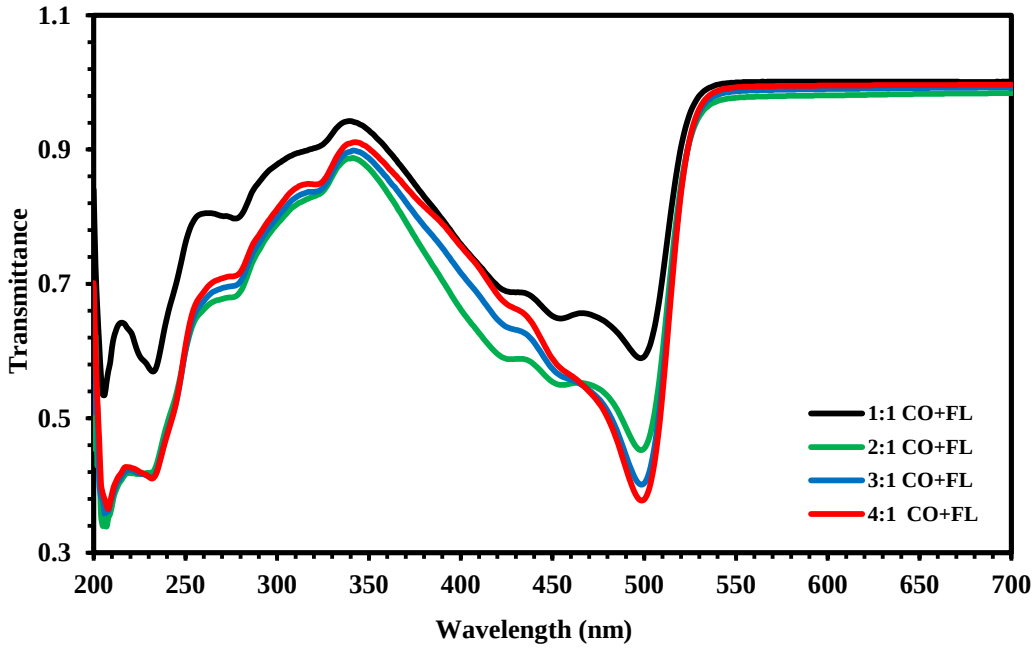

Figure (4.23): Transmittance spectra for mixing of (CO+FL) organic laser dyes at concentration (5×10^{-5}) M with different mixing ratios.

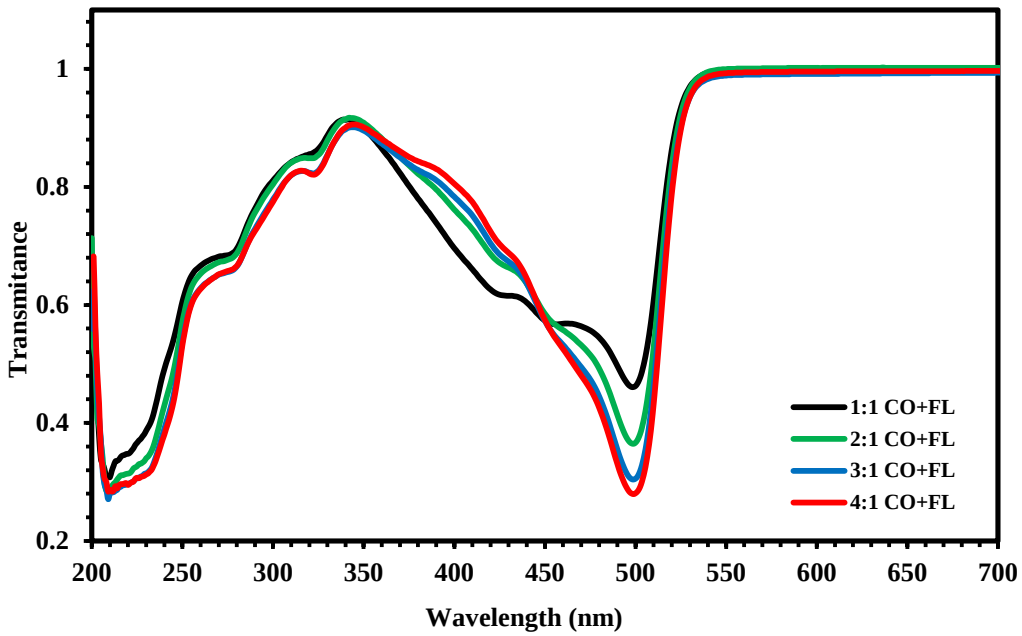

Figure (4.24):Transmittance spectra for Mixing of (CO+FL) organic laser dyes at concentration (7×10^{-5}) M with different mixing ratios.

4.5.2The Transmittance Spectra of Coumarin (334) ,Fluorescein Organic Laser Dyes and their mixture (as thin films)

The transmittance spectra of thin films of Coumarin (334) and Fluorescein organic laser dyes and their mixture doped with (PVA) polymer doped (Ag , Al_2O_3 nanoparticles) at concentration (10^{-3}) M with mixing ratio (4:1) prepared by drop- casting method, are shown in Figures (4.25-4.27) respectively. The optical transmission curve of all samples show a variable behavior of the transmittance as a function of the incident wavelength. The transmittance intensity of dye doped with PVA and nanoparticles was lower than intensity of dye doped with PVA.

Transmittance decreases, this is suggested to take place because of (Ag and Al_2O_3) nanoparticle contain electrons which can be the absorption of electromagnetic energy of the incident light and travel to higher energy levels.

This process is not accompanied by emission of radiation because the traveled electron to higher levels have occupied vacant positions of energy bands,

thus part of the incident light is absorbed by the substance and does not penetrate through it. This behavior agrees with [114].

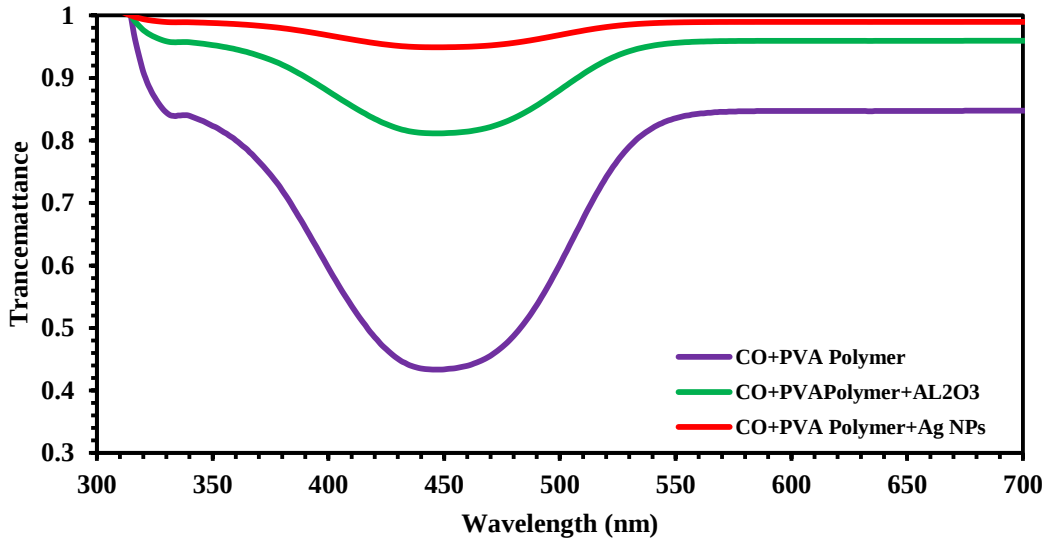

Figure (4.25): Transmittance spectra for thin films of Coumarin (334) organic laser dye with PVA polymer doped (Al_2O_3 , Ag) NPs.

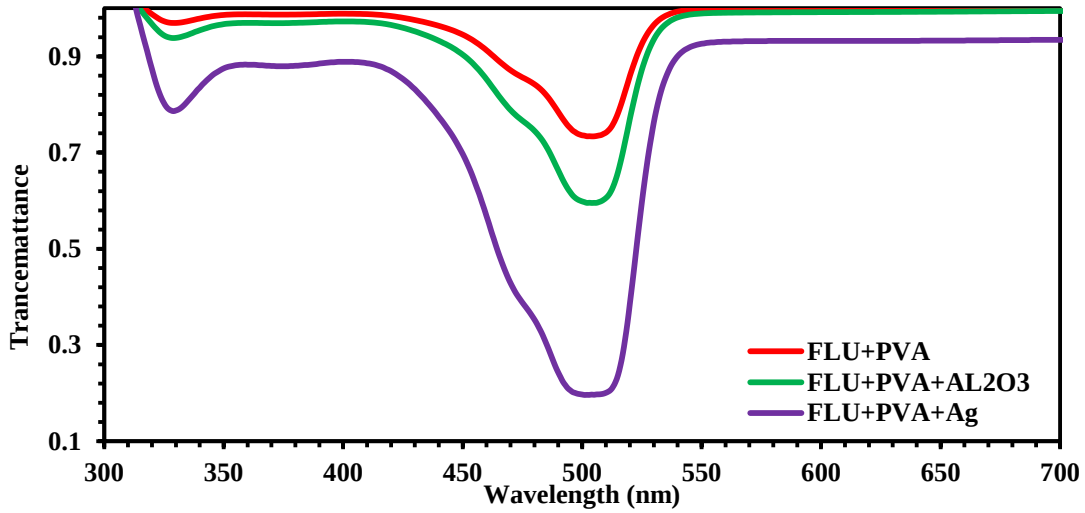

Figure (4.26): Transmittance spectra for thin films of Fluorescein organic laser dye with PVA polymer doped (Al_2O_3 , Ag) NPs.

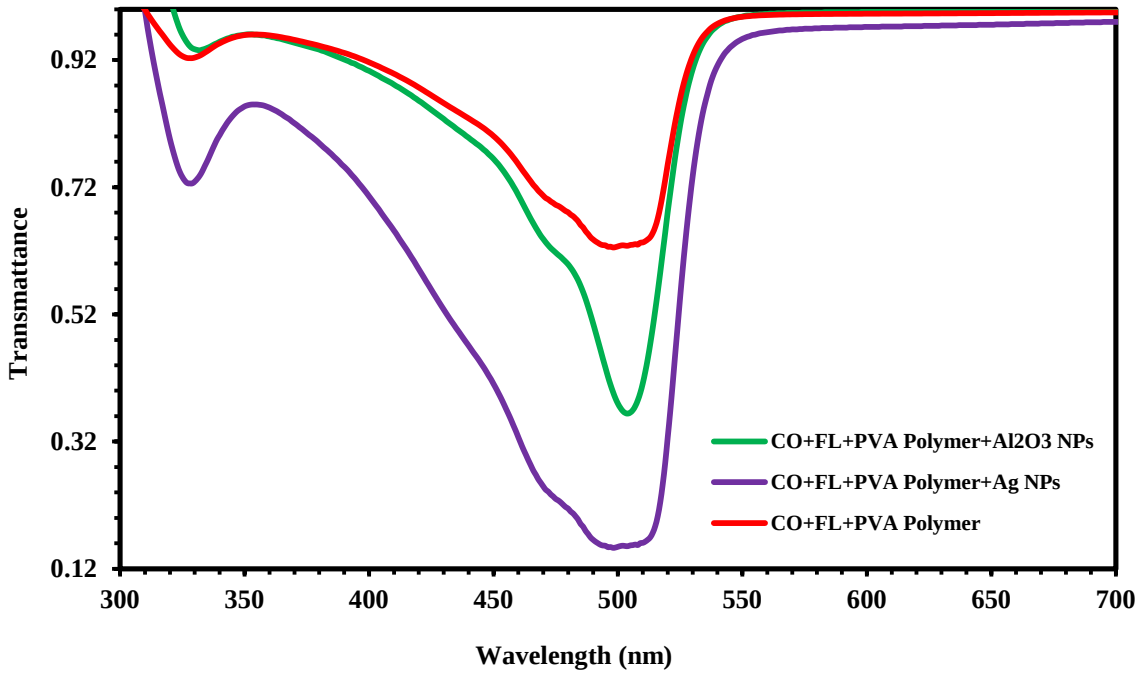

Figure (4.27): Transmittance spectra for thin films of mixing of two organic dyes (Coumarin 334 and Fluorescein) with PVA polymer doped (Al_2O_3 , Ag) NPs.

Table (4.2): Linear optical parameters for different concentrations of Coumarin (344) dye and its thin films at (λ=457nm).

Material	Concentration (Mol/L)	T	($\alpha_\circ$) cm^{-1}	$n_\circ$
Coumarin (344) (Solutions)	1×10^{-5}	0.9353	0.0667	1.1470
	3×10^{-5}	0.8170	0.20208	1.4296
	5×10^{-5}	0.7361	0.3062	1.6777
	7×10^{-5}	0.5086	0.6759	2.0583
CO+PVA polymer (Thin films)	1×10^{-3}	0.6018	5374.2	1.158
CO+PVA polymer + Al_2O_3 NPs (Thin films)	1×10^{-3}	0.5717	5971.44	1.1623
CO+PVA polymer + AgNPs (Thin films)	1×10^{-3}	0.4087	7113.42	1.1774

Table (4.3): Linear optical parameters for different concentrations of Fluorescein dye and its thin films at(λ=457nm).

Material	Concentration (Mol/L)	T	($\alpha_\circ$) cm^{-1}	$n_\circ$
Fluorescein (Solutions)	1×10^{-5}	0.8016	0.2210	1.2931
	3×10^{-5}	0.7194	0.3293	1.4955
	5×10^{-5}	0.5760	0.5515	1.7849
	7×10^{-5}	0.4714	0.7519	1.9216
FL+PVA polymer (Thin films)	1×10^{-3}	0.6748	6396.33	1.1652
FL+PVA polymer + Al_2O_3NPs (Thin films)	1×10^{-3}	0.6402	6806.97	1.1852
FL+PVA polymer + AgNPs (Thin films)	1×10^{-3}	0.6130	7589.42	1.1920

Table (4.4): Linear optical parameters for solutions of mixture of Coumarin 344, Fluorescein dyes at different mixing ratios and different concentrations at (λ=457nm).

Material	Mixing Ratios	T	($\alpha_\circ$) cm^{-1}	$n_\circ$
Mixture of (CO+FL) at (3×10^{-5}) M	1:1	0.7708	0.2602	1.3935
	2:1	0.7260	0.3201	1.4243
	3:1	0.7169	0.3327	1.7072
	4:1	0.7050	0.3494	1.7594
Mixture of (CO+FL) at (5×10^{-5}) M	1:1	0.6497	0.4312	1.496
	2:1	0.5497	0.5734	1.7675
	3:1	0.5603	0.6120	1.8627
	4:1	0.5694	0.6195	1.9996
Mixture of (CO+FL) at (7×10^{-5}) M	1:1	0.5671	0.5671	1.7853
	2:1	0.5635	0.6480	1.7901
	3:1	0.5422	0.7792	1.8273
	4:1	0.5382	0.8630	1.9843

Table (4.5): Linear optical parameters for thin films of Coumarin 344 and Fluorescein dyes at mixing ratio (4:1) at concentration (10^{-3} M) at (λ=457nm).

Material	Mixing Ratios	T	($\alpha_\circ$) cm^{-1}	$n_\circ$
Mixture doped with PVA polymer	**4:1**	**0.7281**	**7783. 03**	**1.3146**
Mixture doped with PVA polymer and AL_2O_3 NPs	**4:1**	**0.3547**	**8216.11**	**1.5964**
Mixture doped with PVA polymer and Ag NPs	**4:1**	**0.2159**	**8923.95**	**1.620**

4.6 Fluorescence Spectra

Fluorescence spectra for Coumarin (334) ,Fluorescein (CO and FL) organic laser dyes at concentrations (1×10^{-5},3×10^{-5}, 5×10^{-5}, and 7×10^{-5})M as solutions with different mixing ratios (1:1, 2:1, 3:1, and 4:1) M and thin films with PVA polymer doped (Ag and Al_2O_3) NPs at concentration (10^{-3}M).

4.6.1 Fluorescence Spectra for of Coumarin 334, Fluorescein Organic Laser Dyes and their mixture (as solutions)

Figure (4.28) show that fluorescence intensity for Coumarin (334) organic laser dye at different concentrations (1×10-5, 3×10-5, 5×10-5, and 7×10-5) M. Fluorescence intensity increases linearly with increasing of concentrations, it agree with references [15], as it happened in the absorption spectra. Fluorescence phenomenon occurs when a molecule absorbs photons causing a transition to a high energy electronic state afterward it returns back to the first excited state through heat or vibrations. Finally, it emits photon when it returns to its initial state, so that the radiative emitted energy is less than the exciting energy i.e., the emission wavelength is always longer than the excitation

wavelength. The fluorescence of a molecule depends on the structure and environment of the molecule [15].

Figure (4.29) shows fluorescence intensity for Fluorescein organic laser dye at different concentrations (1×10^{-5},3×10^{-5}, 5×10^{-5}, and 7×10^{-5}) M. At fluorescence intensity increases linearly with increasing of concentrations, it agree with references [13]. The largest number of molecules increases the transition rate of molecules from upper energy levels to the lower energy level (fluorescence emission rate). It is clear from the table (4.6-4.7) that the Coumarin 334 laser dye give more fluorescence intensity than Fluorescein laser dye which has highest fluorescence wavelength than first. The increasing of fluorescence maximum wavelength is resulted with increasing of scattering particles weights. It can be interpreted by that the scattering particles cause more losses in this medium, so few of molecules absorbed energy can contribute in fluorescence emission [15]. The fluorescence spectra of many organic dyes in liquid solution depend on the local electric field which is induced by the surrounding polar solvent molecules,

So this effect is a result of intermolecular solute-solvent interaction forces (such as dipole-dipole or dipole-induced dipole) that tend to stretch the molecular bonds and shift the charge distribution on molecules and thus altering the energy difference between the ground and excited states of the solute molecules. This shift is not special case for fluorescence spectra but in the same principles in absorption spectra where the fluorescence represents a mirror image for the absorption [115].

Figures (4.30-4.32) show the fluorescence intensity for mixing of (CO+FL) organic laser dyes at concentrations (3×10^{-5}, 5×10^{-5}, and 7×10^{-5}) as solutions with different ratios (1:1, 2:1, 3:1, and 4:1) M. At higher concentrations fluorescence examination of these spectra indicated that the emission peaks shift to longer wavelength with increasing concentration. This

shift was obtained due to increasing number of molecules per volume unit at high concentrations [20].

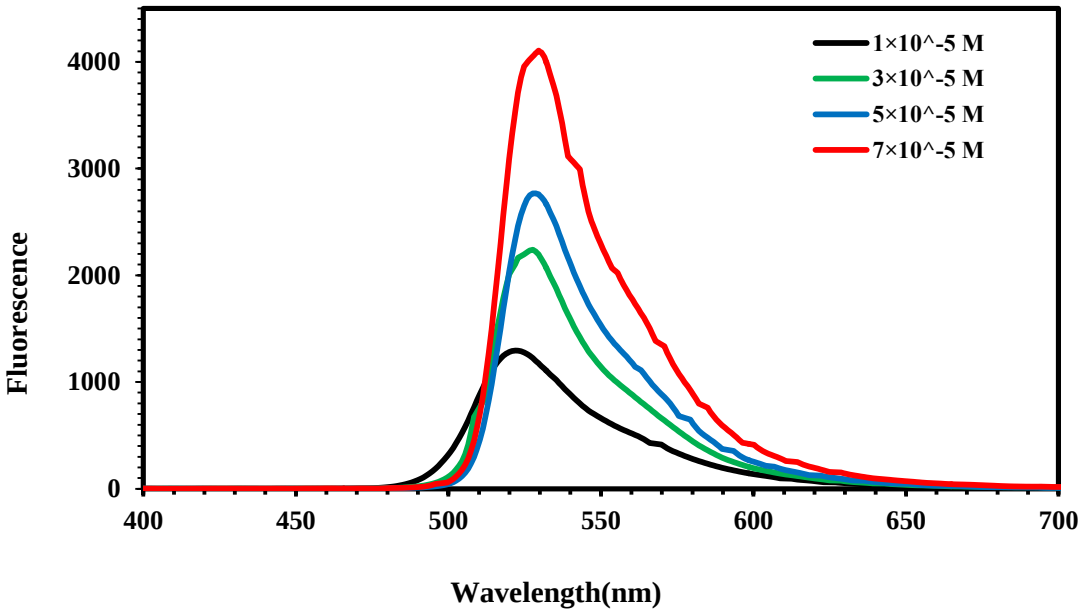

Figure (4:28): Fluorescence spectra for Coumarin 334 organic laser dye at different concentrations.

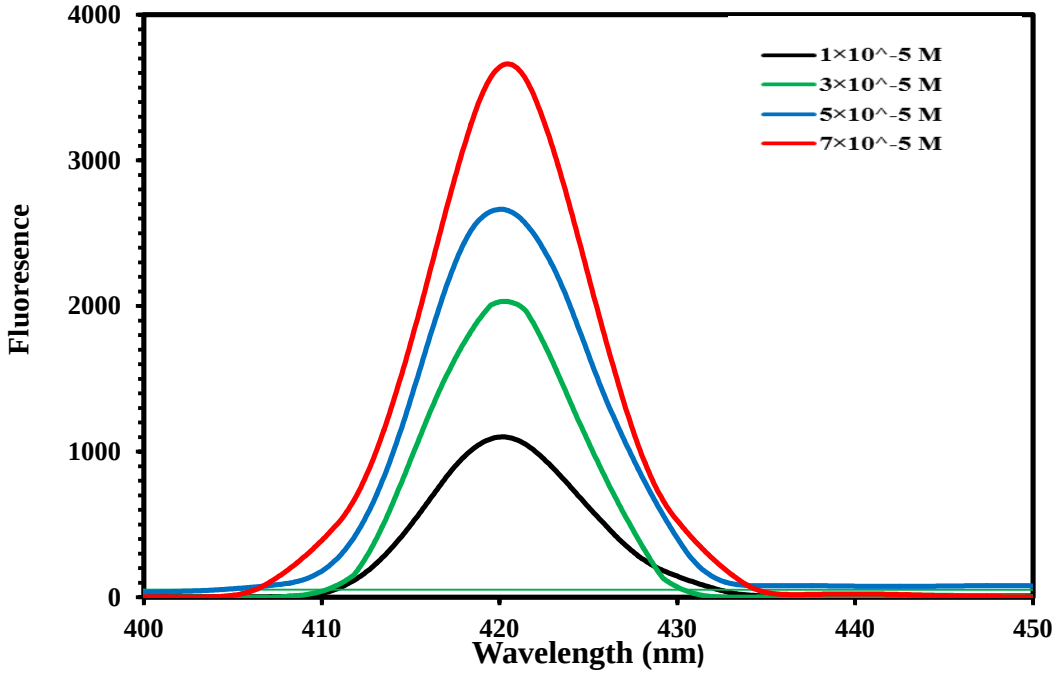

Figure (4:29): Fluorescence spectra for Fluorescein organic laser dye at different concentrations.

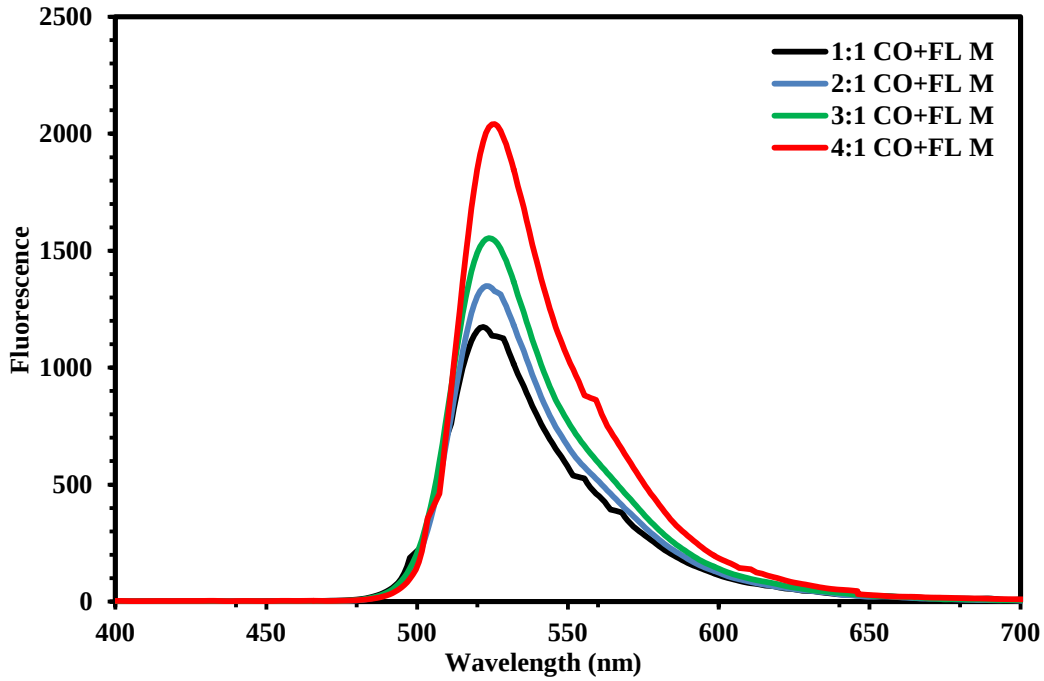

Figure (4:30): Fluorescence spectra for mixing of two organic dyes (CO+FL) concentration (3×10^{-5}) M at different mixing ratios.

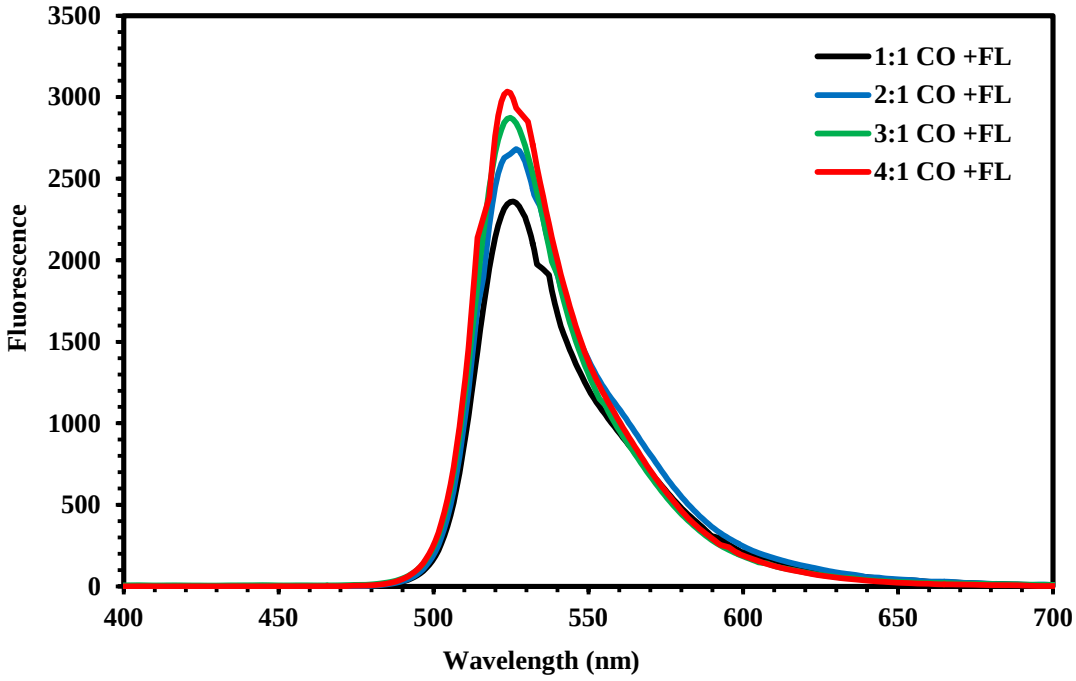

Figure (4:31): Fluorescence spectra for mixing of two organic dyes (CO+FL) organic laser dyes at concentration (5×10^{-5}) M different mixing ratios.

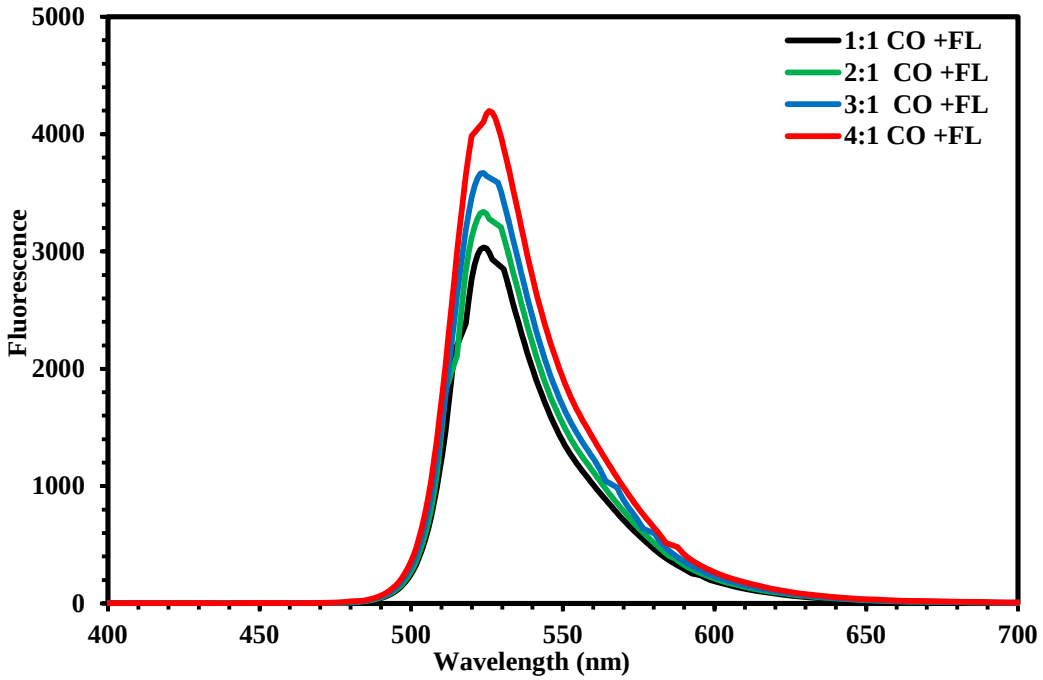

Figure (4:32): Fluorescence spectra for mixing of two organic dyes (CO+FL) at concentration (7×10^{-5}) M with different mixing ratios.

4.6.2 Fluorescence Spectra for Coumarin (334), Fluorescein Organic Laser Dyes and their mixture (as thin films)

Fluorescence spectra of thin films of Coumarin (334) , Fluorescein organic laser dyes and their mixture with PVA polymer doped Ag and Al_2O_3 nanoparticle at ratio (4:1) prepared by drop-casting method, are shown in Figures (4.33 and 4.35) . From these Figures, it is observed that they have narrower band width than dyes as solution also the emission peaks are higher intensity than as solution because the formation of dimers less and less aggregates increases the fluorescence emission.

There are many factors that have effect on fluorescence of dyes are concentration, impurities and self-absorption, that could affect directly the fluorescence quantum yield and consequently the energy yield of the fluorescence [116]. Furthermore, the observed peaks for the films with PVA was at longer wavelengths. One of the most important characteristics of the dye doped in solid matrix is the Stokes shift. In addition, the values of the Stokes

shift were increased by increasing the concentration. it agree with reference [19].

Fluorescence spectra of all samples of mixture of (CO+FL) doped with PVA polymer doped (Ag, Al_2O_3) NPs were shifted towards long wavelengths. Using polymer and nanoparticles with the dye reduces the reabsorption process and increases the fluorescence efficiency. Thin films of (dye +PVA polymer +Al_2O_3 NPs) high Fluorescence than (dye +PVA polymer +Ag NPs). Thin films showed narrow band width of the emission peaks, also increase intensity due to nanoparticles due to the increase in the surface area of the volume which agrees with references [20, 21]. (Increasing the fluorescence intensity of the films prepared for all mixture after adding nanoparticles (Ag and Al_2O_3).)

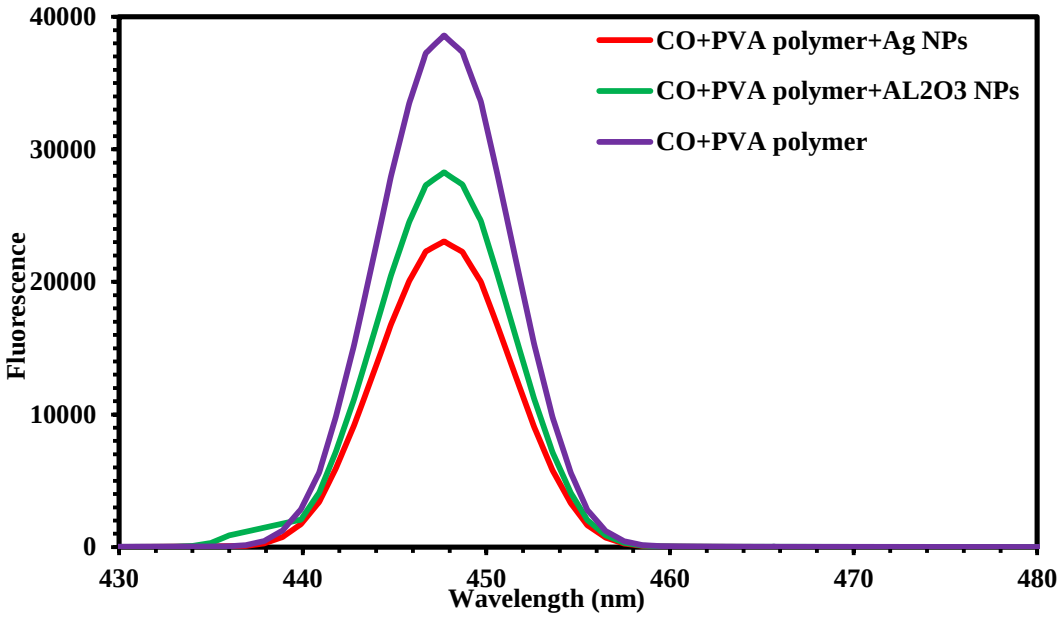

Figure (4.33): Fluorescence spectra for thin films of Coumarin (334) organic laser dye with PVA polymer doped (Al_2O_3 , Ag) NPs.

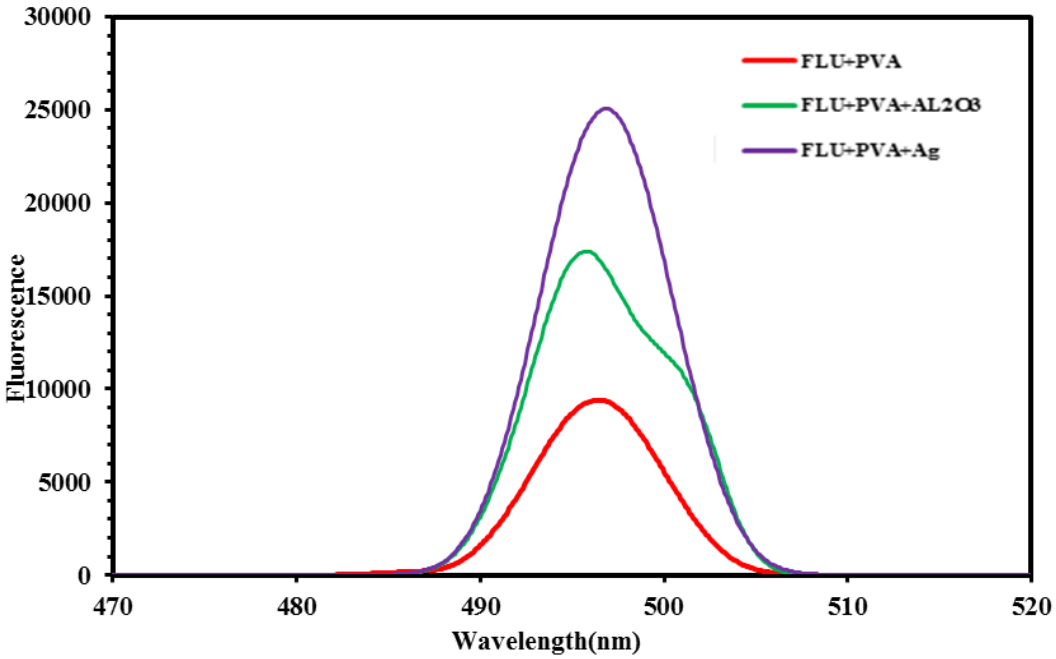

Figure (4.34): Fluorescence spectra for thin films of Fluorescein organic laser dye with PVA polymer doped (Al_2O_3 , Ag) NPs.

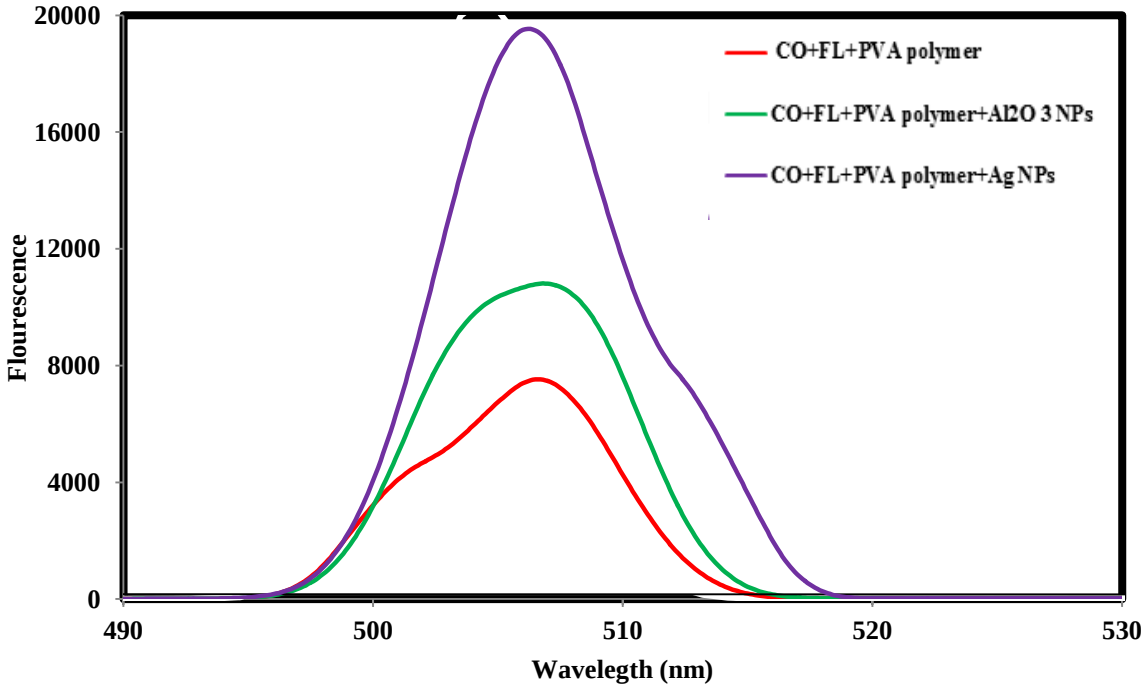

Figure (4.35): Fluorescence spectra for thin films of mixing of two organic dyes (CO+FL) with PVA polymer doped (Al_2O_3 , Ag) NPs.

4.7 Calculation of Quantum Efficiency and Life Time

Figure (4.36 - 4.40) shows the overlap between absorption and fluorescence spectra mixing of Coumarin (334), Fluorescein organic laser dyes

at concentrations (1×10^{-5},3×10^{-5}, 5×10^{-5}, and 7×10^{-5}) M as solutions and different mixing ratios (1:1, 2:1, 3:1, and 4:1). Calculation of life time and quantum efficiency according to Equations (2.5) and (2.8) respectively as tabulated in Tables (4.6 and 4.7) . Increasing the dye concentrations used in the preparation of solutions causes an increase in the interference between the absorption and fluorescence spectra, which results in greater absorption losses. In addition, increasing the concentration increases the chance for the dye molecules to form dimers that are pairs of dye molecules.

With the concentration of molecular spectra and laser output where toning is done, the concentration changes, although the fluorescence is shifted towards long wavelengths (low energies) more compared with absorption spectra due to irradiation processes, which include internal transformation and transit. By observing the fluorescence spectra, we found that fluorescence spectra have the characteristic of mismatch of fluorescence peak with absorption peak due to the loss of the molecule part of its energy (irradiation) before it returns to stable state.

Therefore, the fluorescence energy is less than absorption and increaseing dye concentration leads to the displacement of the fluorescence to long wavelengths with low energies.

Quantum efficiency is the ratio between the area of the emission spectrum and the area of the absorption spectrum, as the efficiency increases with decreasing concentration [15]. In the mixture, an energy transfer occurs from the donor to the acceptor, where a transfer of energy occurs from the highly absorbent dye, which is Fluorescein to the less absorbent dye, which is Coumarin 334.

The explanation is to increase the concentration of the dye solution, the local electric field in the solution will be enhanced and the charges will be rearranged due to the electron transfer of the molecule. It became dipole of ground state more stability the than excited level its due to increase of solvent

solution , its reduce energy level. The following displacement position peak of the fluorescence spectrum to the longer wavelength (red shift) agree with [16]. The results showed that the highest quantitative efficiency at ratio (4:1). When the concentration of organic laser dyes increases, the quantitative efficiency decreases. The reason is because the quantitative efficiency is the ratio between the area under the curve of the fluorescence to the area under the curve for absorption. When the concentration increases, the absorbance increases according to Beer-Lambert's law, and in case of increasing the absorbance, the quantitative efficiency decreases.

It has been observed that the absorption and fluorescence intensity at maximum wavelength was increase with increasing concentration for two types of dye laser (CO+FL). This is because of low concentration adopted the dye molecules became more relaxed and there are a large intermolecular distance. In addition to the wavelength displacement (red shifting) in peaks position which is attributed to the self - absorption which modifies the observed fluorescence spectrum by reducing the intensity of the short wavelength region of spectrum (due to overlap with the absorption spectrum) and enhancing the intensity of the long wavelength region.

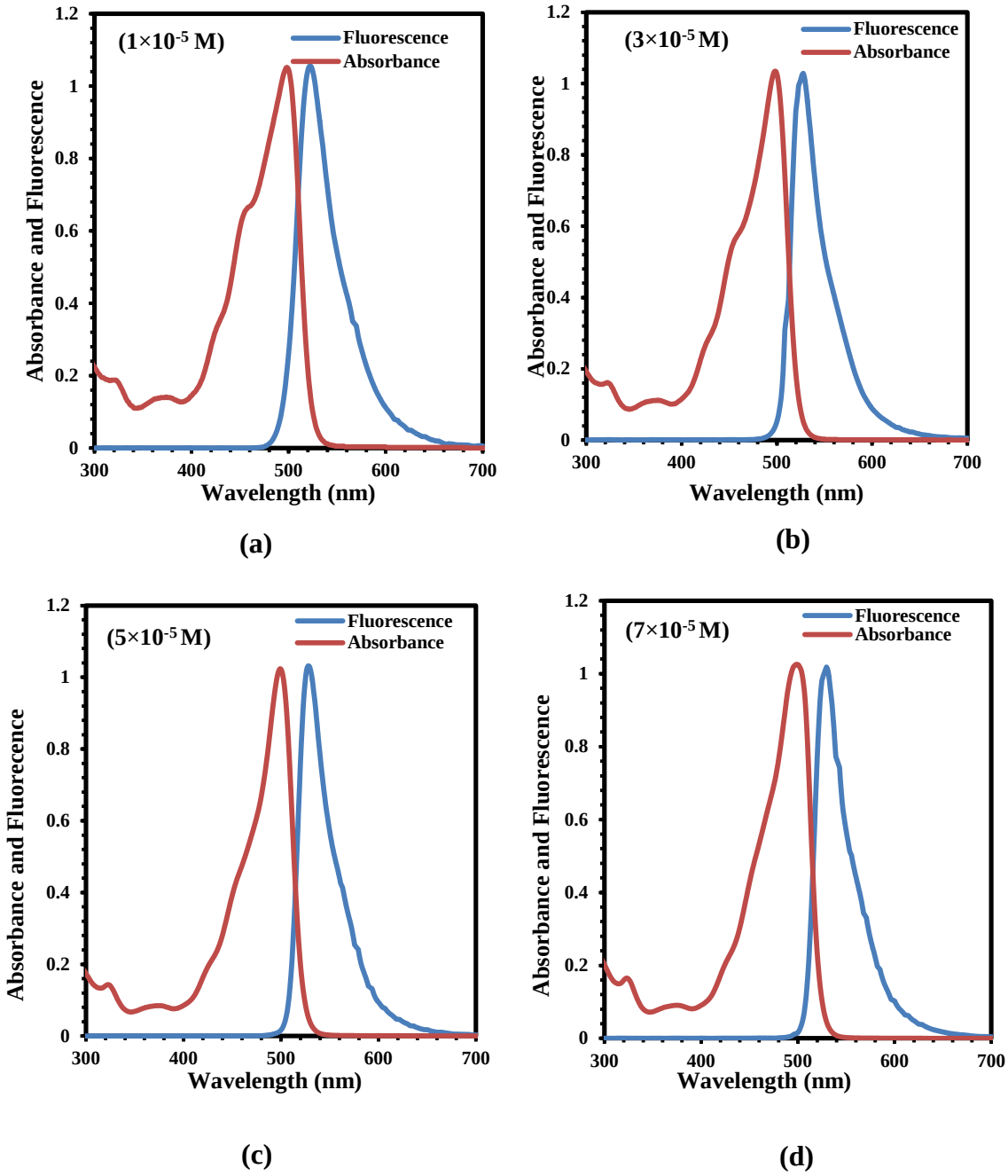

Figure (4.36: a, b, c, d): Interference between absorption and fluorescence spectra for Fluorescein organic laser dye at different concentrations.

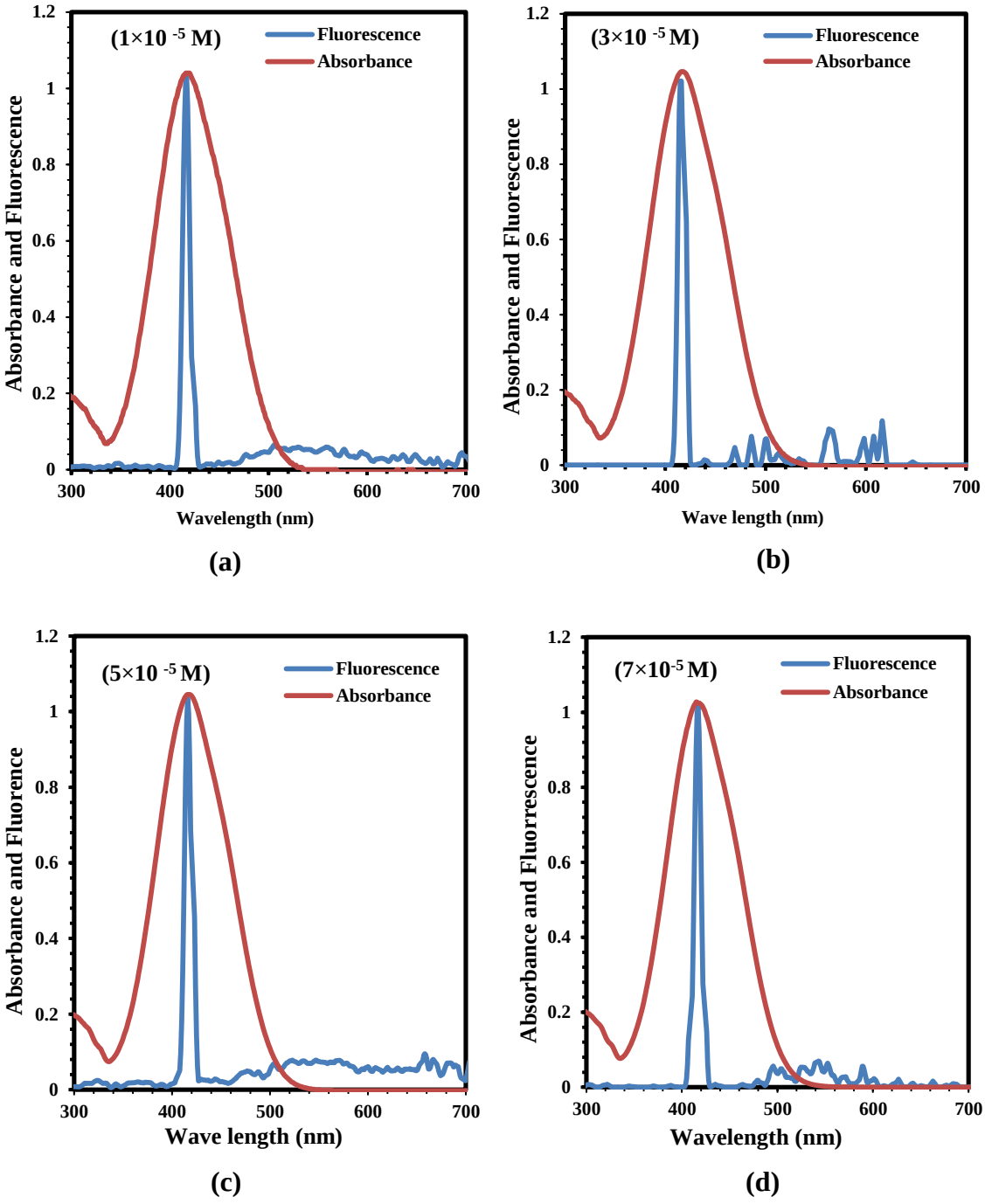

Figure (4.37: a, b, c, d): Interference between absorption and fluorescence spectra for Coumarin (334) organic laser dye at different concentrations.

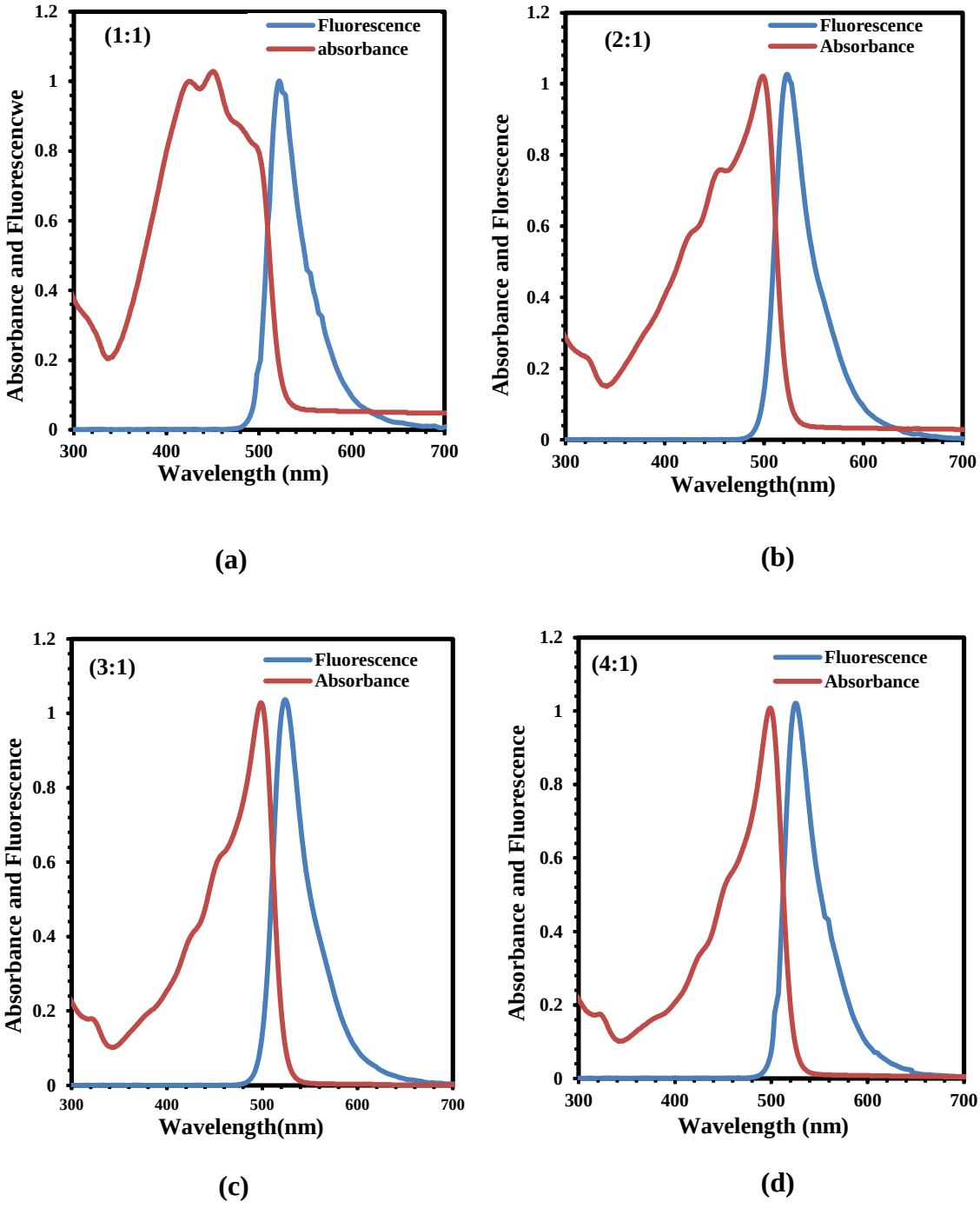

(4.38: a, b, c, d): Interference between absorption and fluorescence spectra for mixing of (CO+FL) organic laser dyes at concentration (3×10^{-5}) M different mixing ratios.

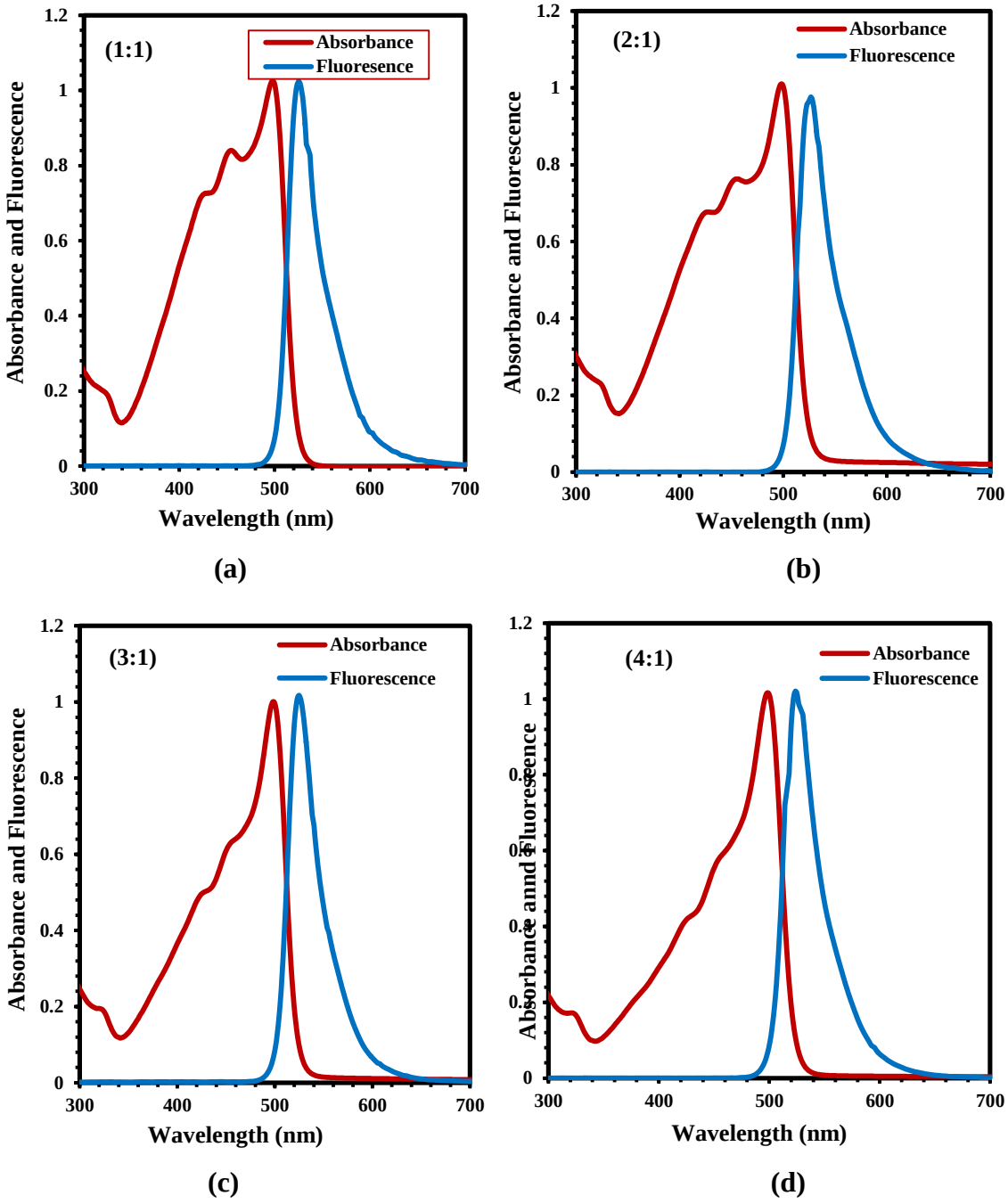

Figure (4.39: a, b, c, d): Interference between absorption and fluorescence spectra for mixing of (CO+FL) organic laser dyes at concentration (5×10^{-5}) M different mixing ratios.

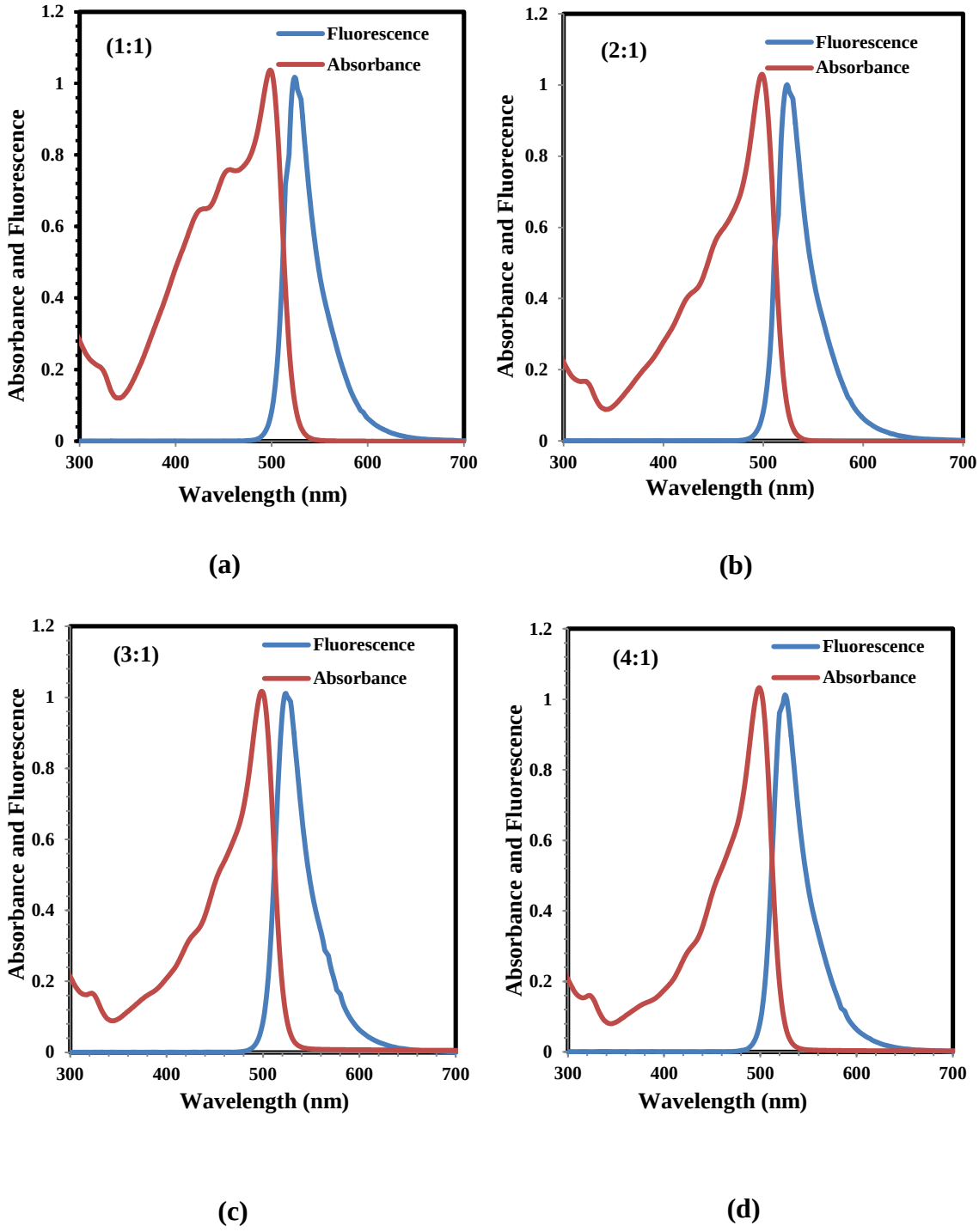

Figure (4.40: a, b, c, d): Interference between absorption and fluorescence spectra for mixing of (CO+FL) organic laser dyes at concentration (7×10^{-5}) M different mixing ratios.

Table (4.6): Absorbance intensity, fluorescence intensity at maximum wave lengths, quantum efficiency and life time parameters for Coumarin 334 and Fluorescein organic laser dyes at different concentrations.

Materials	Concentration (Mol/L)	λ max (Absorbance) nm	Absorbance Intensity	λ max (fluorescence) nm	Fluorescence intensity	τ_F (ns)	Φ_F
Coumarin 344	1×10^{-5}	408	0.043	415	1290	0.108	91%
	3×10^{-5}	410	0.137	415	2360	0.113	89 %
	5×10^{-5}	411	0.209	415	2735	0.118	83 %
	7×10^{-5}	412	0.463	416	4401	0.123	82%
Fluorescein	1×10^{-5}	491	0.143	526	1015	0.104	89%
	3×10^{-5}	493	0.248	526	2100	0.110	85%
	5×10^{-5}	495	0.520	526	2614	0.115	82%
	7×10^{-5}	496	0.658	527	3750	0.119	76%

Table (4.7): Absorbance intensity, fluorescence intensity at maximum wave lengths, quantum efficiency and life time parameters for mixture of Coumarin (334) and Fluorescein organic laser dyes with different ratios and different concentrations.

Concentration (M/L)	Mixing Ratios	λ max (Absorbance) nm	Absorbance intensity	λ max (fluorescence) nm	Fluorescence intensity	τ_F (ns)	Φ_F
(3×10^{-5})	(1:1)	492	0.092	522	1211	0.123	84%
	(2:1)	492	0.185	522	1289	0.138	85%
	(3:1)	492	0.236	522	1492	0.141	87%
	(4:1)	492	0.272	522	1998	0.149	94%
(5×10^{-5})	(1:1)	495	0.312	524	2292	0.125	85%
	(2:1)	495	0.401	524	2600	0.142	86%
	(3:1)	495	0.505	524	2788	0.145	89%
	(4:1)	495	0.521	524	2964	0.158	95%
(7×10^{-5})	(1:1)	496	0.324	525	3117	0.128	91%
	(2:1)	496	0.425	525	3260	0.154	93%
	(3:1)	496	0.527	525	3547	0.159	95%
	(4:1)	496	0.539	525	4051	0.164	96%

4.8 Nonlinear Optical Properties of Coumarin (334),Fluorescein Organic Laser Dyes and their mixture

The nonlinear optical properties were investigated of Fluorescein and Coumarin (334) (CO and FL) organic laser dyes and mixture of them with ratios (1:1, 2:1, 3:1 and 4:1) as solutions at different concentration's (1×10^{-5},3×10^{-5}, 5×10^{-5} and 7×10^{-5}) M and thin films with (PVA polymer doped (Ag, Al_2O_3) nanoparticles) at concentration (10^{-3}) M using continuous wave (CW) diode pumped solid state laser at wavelength 457 nm and power 84mW. There are two parts were used to measure the nonlinear properties of the material by Z-Scan technique. The first part is open-aperture Z-Scan and the second part is the closed-aperture Z-scan.

4.8.1 Nonlinear Refractive Index of Coumarin (334), Fluorescein Organic Laser Dyes and their mixture

The nonlinear refractive index is measured for (Fluorescein, Coumarin (334) organic laser dyes and mixture of them with ratios (1:1, 2:1, 3:1 and 4:1) as solutions at different concentration (1×10^{-5}, 3×10^{-5}, 5×10^{-5} and 7×10^{-5}) M and thin films with PVA polymer doped (Ag , Al_2O_3) nanoparticles at concentration (10^{-3}) M) were measured by closed-aperture Z-Scan technique.

The normalized transmittances of Z-Scan measurements as a function of distance in (Ethanol) solvent for Coumarin (334) is shown in Figures (4.41). the nonlinear effect region is extended from (-2) mm to (2) mm. The valley followed by peak a transmittance curve obtained from the closed aperture Z-Scan data indicates that the sign of the refraction nonlinearity is positive ($n_2 > 0$), leading to self-focusing lensing in these samples [88].

while Fluorescein organic laser dyes and mixture of them as shown in Figures (4.42-4.48). The peak followed by a valley transmittance curve obtained from the closed aperture Z-Scan data indicates that the sign of the refraction nonlinearity is negative ($n_2 < 0$), leading to self-defocusing lensing in these

samples The valley-peak configuration indicates the positive sign of n_2 The scan started from distance far away from the focus, the beam The scan started with a linear behavior at different distances from the far field of the sample position (-Z) with respect to the focal plane at Z=0 mm. The behavior of z-scan curves was in good agreement with [37]. In order to describe the Z-Scan behavior in the previous Figures (4.42- 4.48), when the sample moves far from the focus, the transmitted beam intensity is low and the transmittance remains relatively constant.

As the sample approaches the beam focus, intensity increases, leading to self-lensing in the sample tend to collimate the beam on the aperture in the far field, increasing the measured transmittance at the iris position. If the beam experiences any nonlinear phase shift due to the sample as it is translated through the focal region, then the fraction of light falling on the detector will vary due to the self-lensing generated in the material by the intense laser beam. In this case, the signal measured by detector will exhibit a peak and valley as the sample is translated [117]. The position of the peak and valley, relative to the z-axis, depends on the sign of the nonlinear phase shift .Where the change in the normalized transmittance from the peak of the curve to the valley (ΔT_{p-v}) is directly proportional to the nonlinear phase shift imparted on the beam. Moreover, if the beam is transmitted through the nonlinear medium the induced phase shift can also be either negative or positive accordingly when the medium is self- defocusing or self-focusing, respectively [14]. The magnitude of the phase shift can be determined from the change in transmittance between peak and valley. After the focal plane, the self-defocusing increases the beam divergence, leading to a widening of the beam at the focus and thus reducing the measured transmittance. Far from focus (Z > 0), again the nonlinear refraction is low resulting in a transmittance Z-independent . The nonlinearity of doped dyes is larger than those for pure dyes. As well as thin films possess very large nonlinearity as compared with dyes as solution. The relation between the

nonlinear refractive index and the nonlinear phase shift is a linear increasing relation. Z-Scan measurements indicated that pure and dye doped and their thin films exhibited negative nonlinear refractive index, it agrees with reference [118].

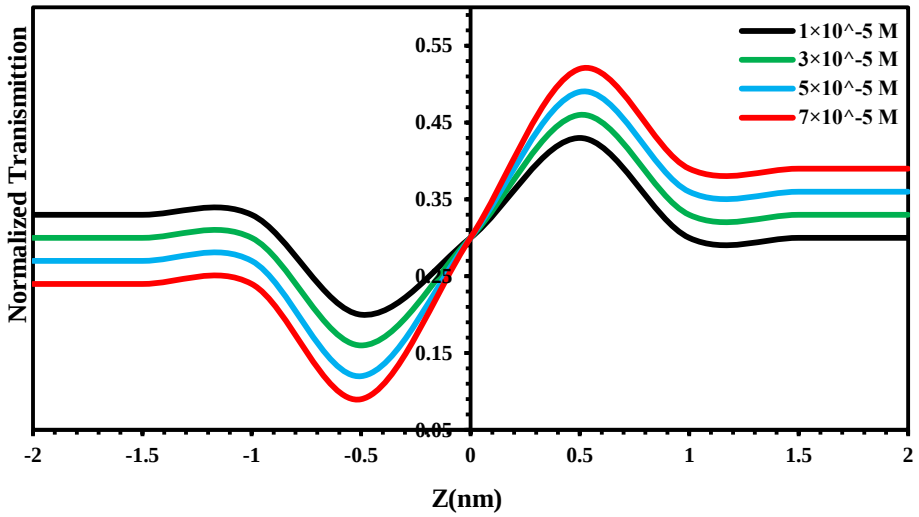

Figure (4.41): Closed-aperture Z-Scan data at different concentrations of Coumarin 334 organic laser dye in Ethanol solvent.

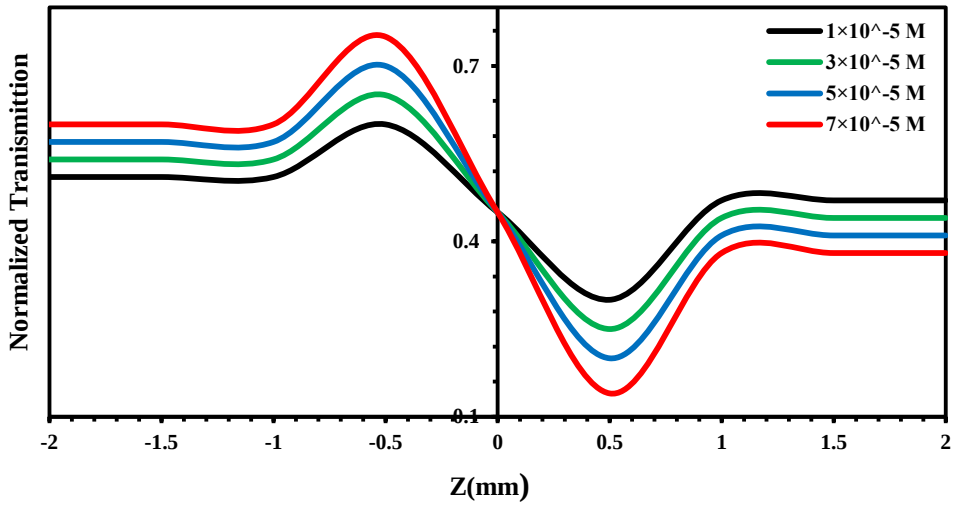

Figure (4.42): Closed-aperture Z-Scan data at different concentrations of Fluorescein organic laser dye in Ethanol solvent.

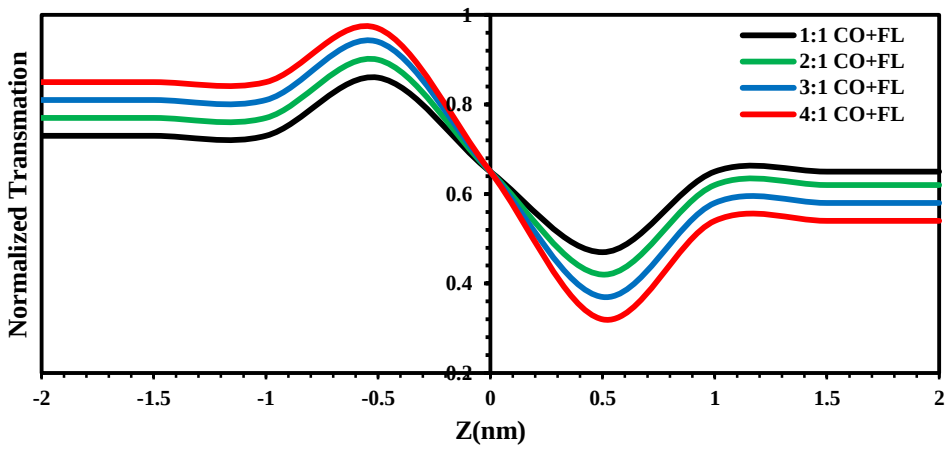

Figure (4.43): Closed-aperture Z-Scan data at different ratios of mixing of (CO+FL) organic laser dyes in Ethanol solvent at concentration (3×10^{-5}) M.

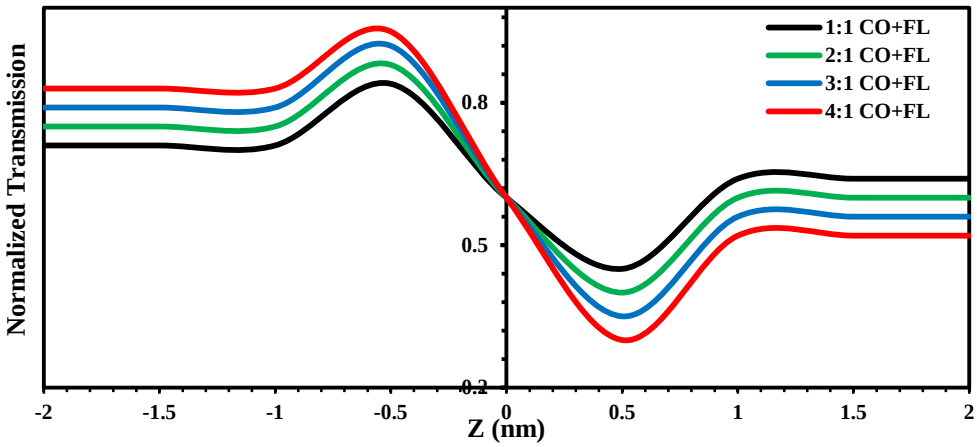

Figure (4.44): Closed-aperture Z-Scan data for different ratios of mixing of (CO+FL) organic laser dyes in (Ethanol) solvent at concentration (5×10^{-5}) M.

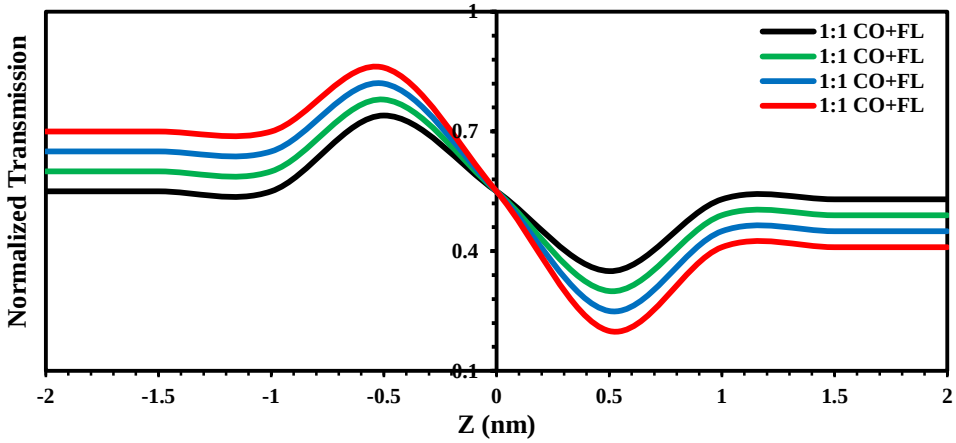

Figure (4.45): Closed-aperture Z-Scan data for different ratios of mixing of (CO+FL) organic laser dyes in Ethanol solvent at concentration (7×10^{-5}) M.

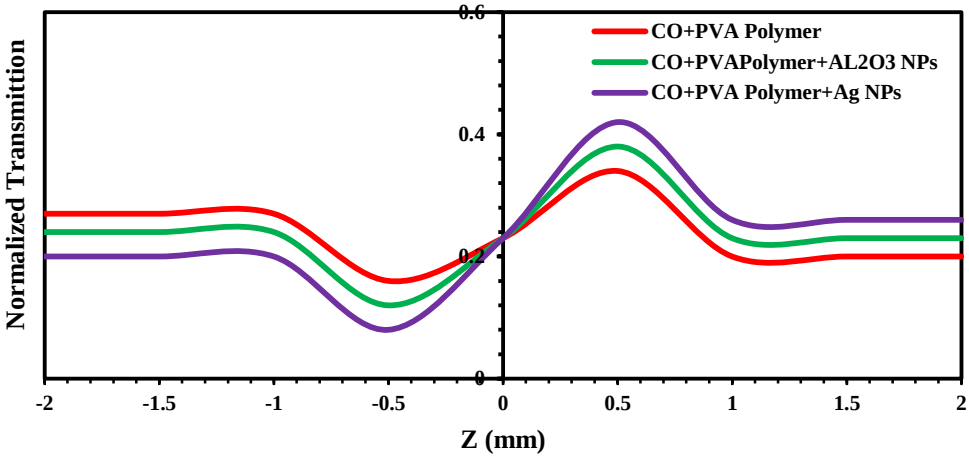

Figure (4.46): Closed-aperture Z-Scan data for thin films of Coumarin 334 organic laser dye with PVA polymer doped (Al_2O_3 , Ag) NPs.

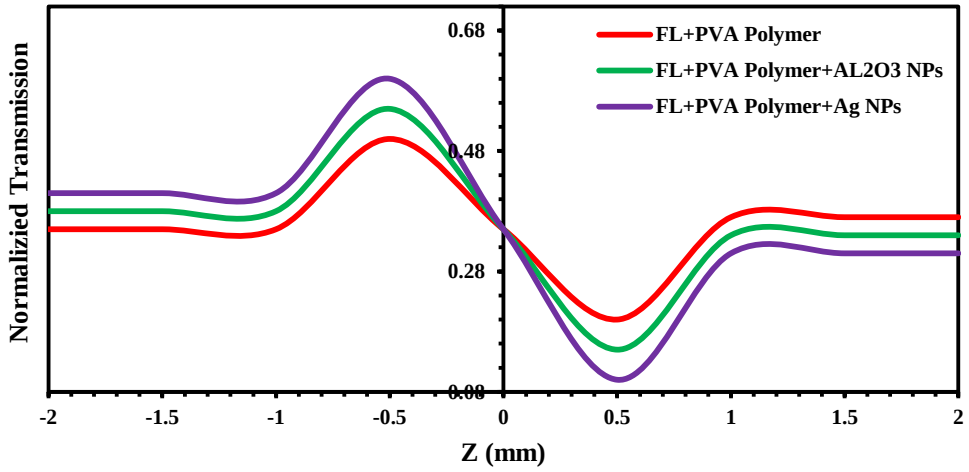

Figure (4.47): Closed-aperture Z-Scan data for thin films of Fluorescein organic laser dye with PVA polymer doped (Al_2O_3 , Ag) NPs.

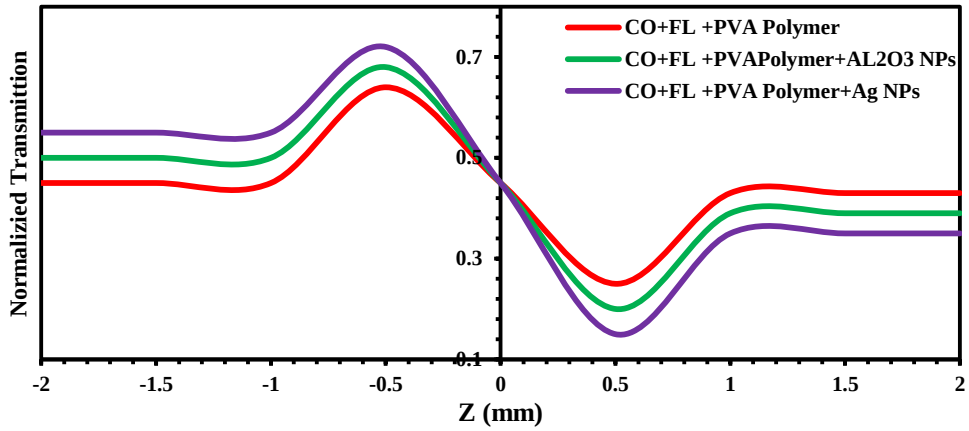

Figure (4.48): Closed-aperture Z-Scan data for thin films of mixing of (CO+FL) organic laser dyes with PVA polymer doped (Al_2O_3 , Ag) NPs.

4.8.2 Nonlinear Absorption Coefficient of Coumarin (334), Fluorescein Organic Laser Dyes and their mixture

The nonlinear absorption coefficient of Fluorescein and Coumarin (334) organic laser dyes and mixture of them with ratios (1:1, 2:1, 3:1 and 4:1) as solutions at different concentration's (3×10^{-5}, 5×10^{-5} and 7×10^{-5}) M and thin films with PVA polymer doped (Ag, Al_2O_3) nanoparticles at concentration (10^{-3}) M in Ethanol solvent, can be measured by performing the open aperture Z-Scan technique at wavelength 457nm and power 84 mW. The performed open aperture-Scan exhibits an increasing in the transmission about the focus of the lens.

Open-aperture Z-Scan of Fluorescein, Coumarin (334) and mixing of them as solutions are shown in Figures (4.49-4.56). Its noticed (two photon absorption) phenomenon. The behavior of transmittance starts linearly at different distances from the far field of the sample position (-Z). At the near field, the transmittance curve begins to decrease until it reaches the minimum value (T_{min}) at the focal point, where Z=0 mm. The transmittance begins to increase towards the linear behavior at the far field of the sample position (+Z). The change of intensity in this case is caused by two photon absorption when in the sample travels through beam waist. This behavior agrees with reference [88].The open-aperture Z-Scan of thin films of Fluorescein and Coumarin (334) organic laser dyes and mixture of them with ratio (4:1) as thin films doped with PVA polymer and Ag , Al_2O_3 nanoparticles at concentration (10^{-3}) M in ethanol solvent defines variable transmittance values, which was used to determine absorption coefficient. Saturable absorption phenomenon was observed for open-aperture Z-Scan technique as shown in Figures (4.54-4.56).

The behavior of transmittance curves starts linearly at different distance from the far field of the sample position (-Z). At the near field the transmittance curve begins to increase until it reaches the maximum value (T_{max}) at the focal

point, where Z=0 mm. Afterwards, the transmittance begins to decrease toward the linear behavior at the far field of the sample position (+Z). The transmittance is sensitive to the nonlinear absorption as a function of input power intensity. The change in intensity is caused by saturation absorption in the sample as it travels through the beam waist [88]. In the focal plane where the intensity is greatest, the largest nonlinear absorption is observed. At the far field of the Gaussian beam, where, the beam intensity is too weak to elicit nonlinear effects.

A symmetric peak value is contributed to the negative nonlinear absorption coefficient β, indicates that the sample shows a bleaching-like behavior (saturation of absorption) [88]. The nonlinear parameters are calculated , as tabulated in Tables (4.8- 4.11) these Tables show that the values of nonlinear parameters (n_2 and β) for Fluorescein, Coumarin (334) organic laser dyes and mixture of them with ratios (1:1, 2:1, 3:1 and 4:1) as solutions are increased but (β)decreased with increasing the concentrations, as increasing the values of linear parameters (α_o and n_o). This is due to decreasing number of molecules per volume unit at low concentrations [119]. The closed-aperture Z-Scan defines variable transmittance values, which used to determine the nonlinear phase shift $\Delta\Phi$ using equation (2.13) and the nonlinear refractive index (n_2) using equation (2.12), nonlinear absorption coefficient (β) using equation (2.18), as listed in Tables (4.4-4.7) respectively. Thin films of all samples were exhibited better nonlinearity than liquid samples.

This is suggested to be take place due to the $\pi-\pi^*$ stacking in supramolecular interactions between delocalized electrons in solid samples. In addition, in the case of thin films, the molecule orientation is crucial where molecules can be arranged either by homotopic alignment or columnar stacking on the substrate as almost organic dyes are self-organized materials. The nonlinearity of doped dyes are larger than those for pure dyes agree with [118]. As well as thin films of Fluorescein, Coumarin (334) organic laser dyes and mixture of them with ratios (4:1) possess very large nonlinearity as compared

with dyes as solution. This is due to increasing number of molecules per volume unit at high concentrations, as well as thin films have thickness larger than dyes as solutions, which is lead to increasing the nonlinear phase shift agree with [115]. The results showed that the nonlinear optical properties of the films with doped nanoparticles were higher than the films without nanoparticles.

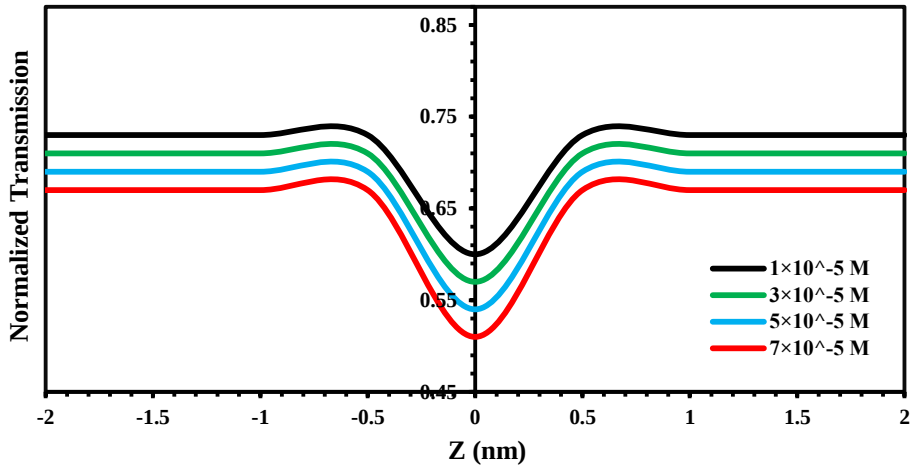

Figure (4.49): Open-aperture Z-Scan data for different concentrations of Coumarin (334) organic laser dye in Ethanol solvent.

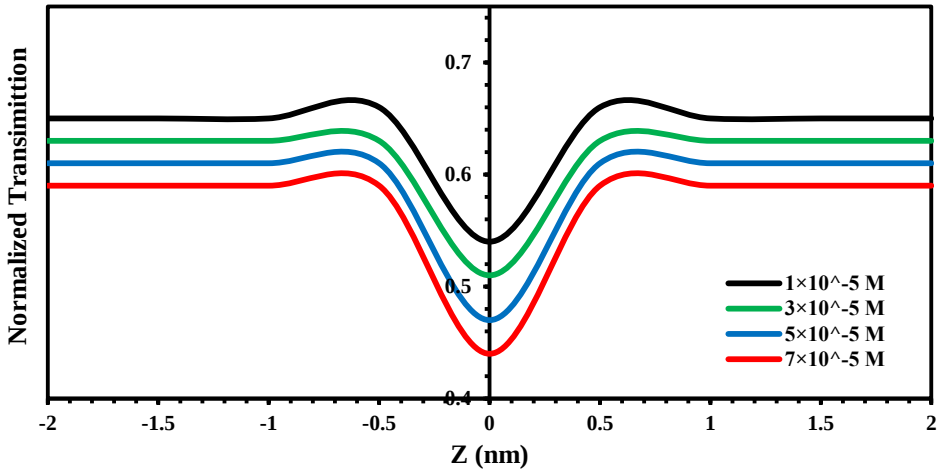

Figure (4.50): Open-aperture Z-Scan data for different concentrations of Fluorescein organic laser dye in Ethanol solvent.

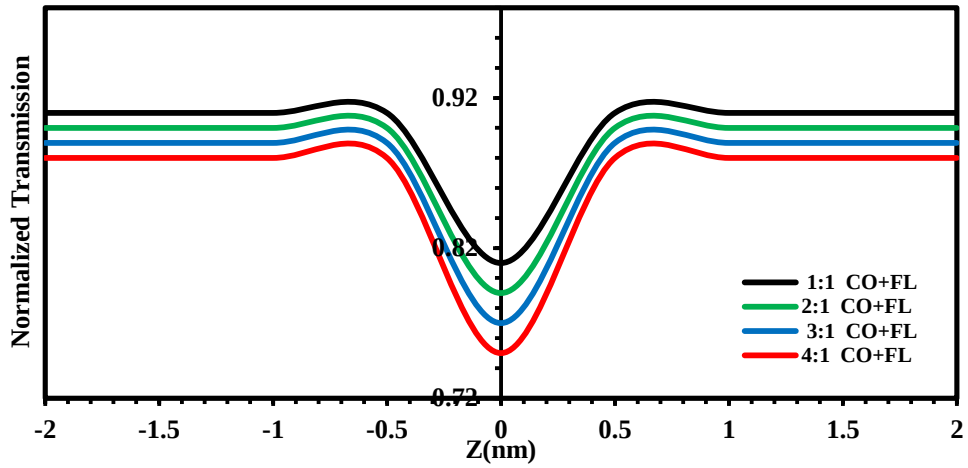

Figure (4.51): Open-aperture Z-Scan data for different ratios of mixing of (CO+FL) organic laser dyes in Ethanol solvent at concentration (3×10^{-5}) M.

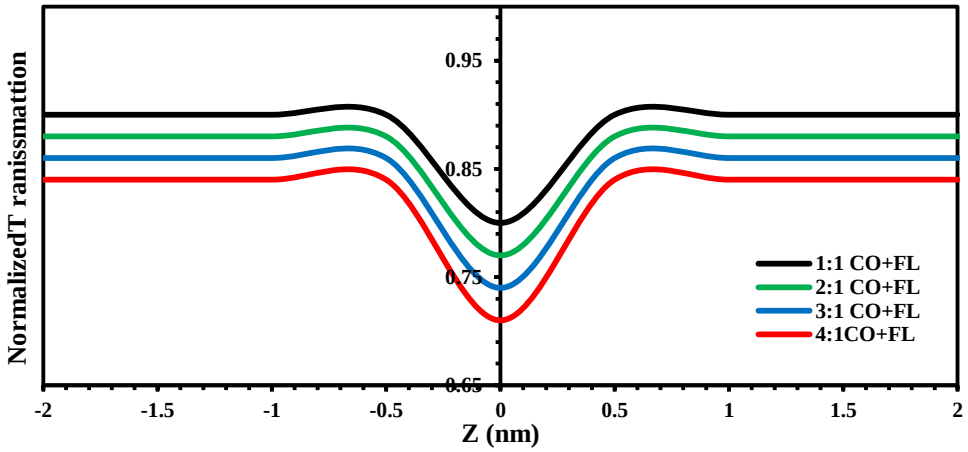

Figure (4.52): Open-aperture Z-Scan data for different ratios of mixing of (CO+FL) organic laser dyes in Ethanol solvent at concentration (5×10^{-5}) M.

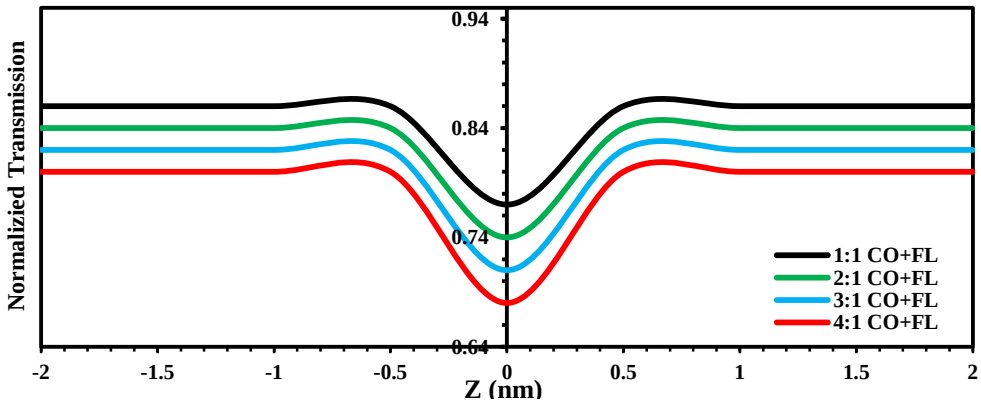

Figure (4.53): Open-aperture Z-Scan data for different ratios of mixing (CO+FL) organic laser dyes in (Ethanol) solvent at concentration (7×10^{-5}) M.

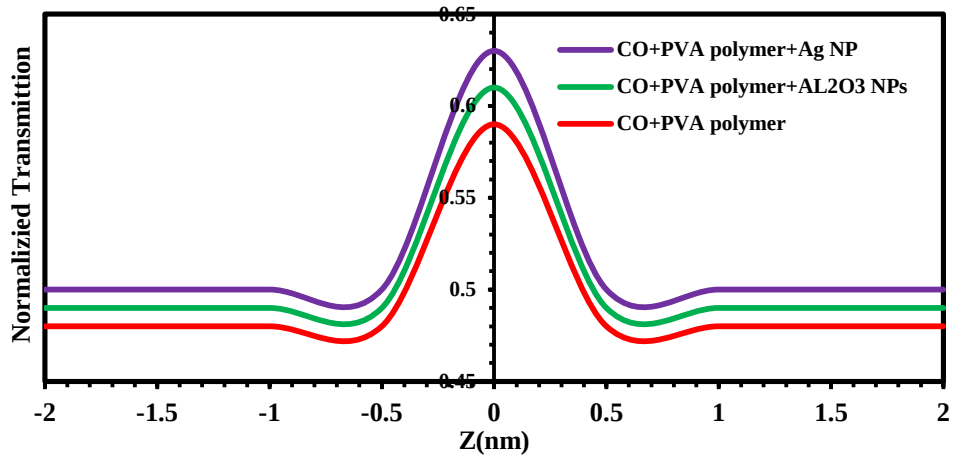

Figure (4.54): Open-aperture Z-Scan data for thin films of Coumarian (334) organic laser dye with PVA polymer doped (Al_2O_3 , Ag) NPs.

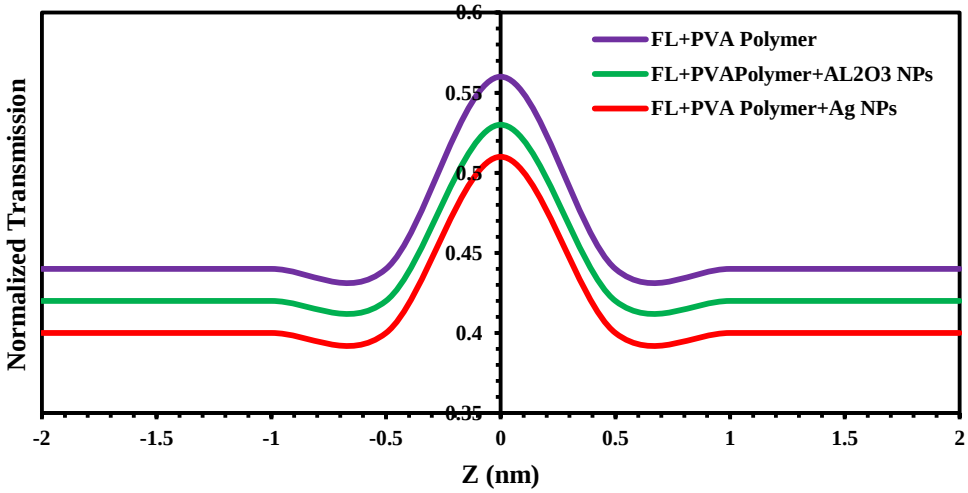

Figure (4.55): Open-aperture Z-Scan data for thin films of Fluorescein organic laser dye with PVA polymer doped (Al_2O_3 , Ag) NPs.

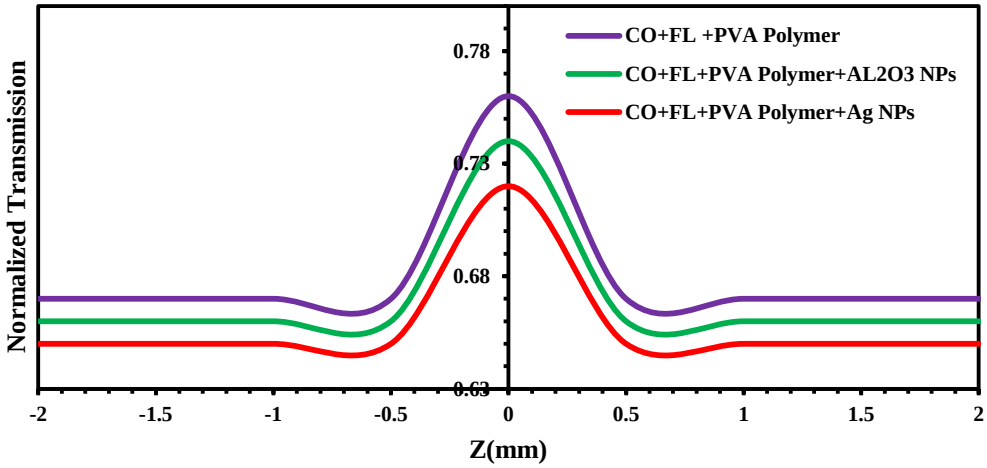

Figure (4.56): Open-aperture Z-Scan data for thin films for mixing of (CO+FL) organic laser dyes with PVA polymer doped (Al_2O_3 , Ag) NPs.

Table (4.8): Nonlinear optical parameters for different concentrations of Coumarin (334) dye and its thin films at (λ=457 nm).

Material	Concentration (Mol/L)	ΔT_{P-V}	n_2 (cm^2/mW)	T(z)	β (cm/mW)
Coumarin (344) (Solutions)	1×10^{-5}	0.011	2.1188×10^{-11}	0.61	1.4265×10^{-3}
	3×10^{-5}	0.024	4.2731×10^{-11}	0.75	1.3073×10^{-3}
	5×10^{-5}	0.031	6.3839×10^{-11}	0.54	1.0786×10^{-3}
	7×10^{-5}	0.043	6.9855×10^{-11}	0.51	0.8392×10^{-3}
CO+PVA polymer (Thin films)	1×10^{-3}	0.110	1.73×10^{-7}	0.59	1.245
CO+PVA polymer + Al_2O_3 NPs (Thin films)	1×10^{-3}	0.123	2.34×10^{-7}	0.61	2.673
CO+PVA polymer + AgNPs (Thin films)	1×10^{-3}	0.145	3.84×10^{-7}	0.63	3.53

Table (4.9): Nonlinear optical parameters for different concentrations of Fluorescein dye and its thin films at(λ=457nm).

Material	Concentration (Mol/L)	ΔT_{P-V}	n_2 (cm^2/mW)	T(z)	β (cm/mW)
Fluorescein (Solutions)	1×10^{-5}	0.0277	3.5016×10^{-11}	0.54	1.6264×10^{-3}
	3×10^{-5}	0.0361	5.5024×10^{-11}	0.51	1.5068×10^{-3}
	5×10^{-5}	0.0416	7.6834×10^{-11}	0.47	1.4198×10^{-3}
	7×10^{-5}	0.0527	8.5168×10^{-11}	0.44	1.2947×10^{-3}
FL+PVA polymer (Thin films)	1×10^{-3}	0.132	2.91×10^{-7}	0.51	2.023
FL+PVA polymer + Al_2O_3NPs (Thin films)	1×10^{-3}	0.154	3.89×10^{-7}	0.53	3.765
FL+PVA polymer + AgNPs (Thin films)	1×10^{-3}	0.162	4.59×10^{-7}	0.56	4.567

Table (4.10): Nonlinear optical parameters for solutions of mixture of Coumarin 334 , Fluorescein dyes at different mixing ratios and different concentrations at (λ=457nm).

Material	Mixing Ratios	ΔT_{P-V}	n_2 (cm^2/mW)	T(z)	β (cm/mW)
Mixture of (CO+FL) at (3×10^{-5}) M	1:1	0.022	6.7122×10^{-11}	0.81	2.76×10^{-3}
	2:1	0.024	8.2243×10^{-11}	0.77	2.70×10^{-3}
	3:1	0.040	10.8465×10^{-11}	0.74	2.69×10^{-3}
	4:1	0.060	13.2376×10^{-11}	0.71	2.64×10^{-3}
Mixture of (CO+FL) at (5×10^{-5}) M	1:1	0.038	8.5382×10^{-11}	0.8	2.89×10^{-3}
	2:1	0.043	10.0725×10^{-11}	0.77	2.85×10^{-3}
	3:1	0.055	13.8256×10^{-11}	0.74	2.80×10^{-3}
	4:1	0.065	17.6725×10^{-11}	0.71	2.78×10^{-3}
Mixture of (CO+FL) at (7×10^{-5}) M	1:1	0.046	10.6356×10^{-11}	0.77	3.21×10^{-3}
	2:1	0.054	13.8876×10^{-11}	0.74	3.15×10^{-3}
	3:1	0.065	17.7945×10^{-11}	0.71	3.02×10^{-3}
	4:1	0.0732	18.5352×10^{-11}	0.68	2.98×10^{-3}

Table (4.11): Nonlinear optical parameters for thin films of Coumarin 344 and Fluorescein dyes at mixing ratio (4:1) at concentration (10^{-3} M) at (λ=457 nm).

Material	Mixing Ratios	ΔT_{P-V}	n_2 (cm^2/mW)	T(z)	*B* (cm/mW)
Mixture doped with PVA polymer	4:1	0.203	11.41×10^{-7}	0.72	4.472
Mixture doped with PVA polymer and Al_2O_3 NPs	4:1	0.258	13.32×10^{-7}	0.74	5.738
Mixture doped with PVA polymer and Ag NPs	4:1	0.291	15.123×10^{-7}	0.76	7.52

4.9 Optical Limiting Behavior of Coumarin (334), Fluorescein Organic Laser Dyes and their mixture

The optical limiting behavior of Fluorescein, Coumarin (334) organic laser dyes and mixture of them with ratios (1:1, 2:1, 3:1 and 4:1) as solutions at different concentration's (3×10^{-5}, 5×10^{-5} and 7×10^{-5}) M and thin films with PVA polymer doped (Ag ,Al_2O_3) nanoparticles at concentration (10^{-3}) M were performed by closed-aperture Z-Scan with the same laser used in Z-Scan technique. Figures (4.57-4.64) give the optical limiting characteristics at room temperature (25-30) C° for all samples were dissolved in (Ethanol) solvent. The samples show very good optical limiting behavior arising from nonlinear refraction. The output power rises initially with the increasing input power, but after a certain threshold value, the sample starts defocusing the beam resulting in a greater part of the beam cross-section being cut off by the aperture. Thus, the transmittance recorded by the photodetector remained reasonably constant showing a plateau region agree with [12]. Thin films of Fluorescein , Coumarin and mixing of them with ratios (4:1) give optical power limiting threshold and limiting amplitude less as compared with the materials as solutions, therefore,

the optical limiting behavior was significantly optimized in the case of thin films in comparison to liquid samples and in the polymer and nanoparticles modified dyes in general, from the threshold intensity for optical limiting for each sample, the optical power limiting threshold is inversely proportional to the concentration, that's mean the properties of the optical limiting be better with increasing the concentrations, as listed in Tables (4.12 - 4.14) respectively.

Optical limiting protects the human eye by attenuating of the laser beam, this behavior agrees with the study in reference [120]. Fluorescein dissolved in (Ethanol) solvent give optical power limiting threshold and limiting amplitude less as compared with the Coumarin dye (CO).

while the mixing with Ag that dissolved in Ethanol solvent give optical power limiting threshold and limiting amplitude less as compared with the pure dyes, therefore, the properties of optical limiting at different concentrations for all samples of mixing (Ag and Al_2O_3) are better than the same samples of dyes (CO and FL) as pure dyes.

The threshold of the optical limiting on the axis of the out power and the amplitude of the limiting on the axis of the input power can be measure using the tangent of the beginning of the bending the curve in Figures (4.57-4.64), where the lower the threshold and amplitude of the optical limiting, the more suitable the sample is to do as optical limiting.

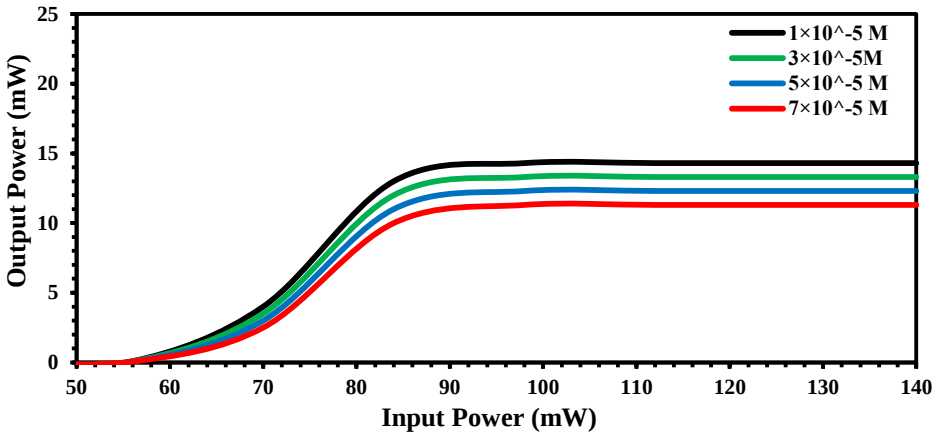

Figure (4.57): The optical limiting response of Coumarin 334

organic laser dye at different concentrations in Ethanol solvent.

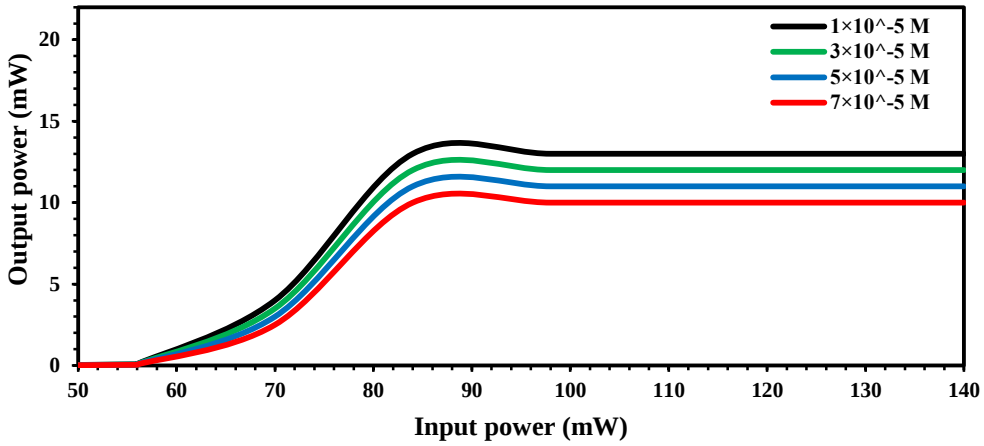

Figure (4.58): The optical limiting response of Fluorescein organic laser dye at different concentrations in Ethanol solvent.

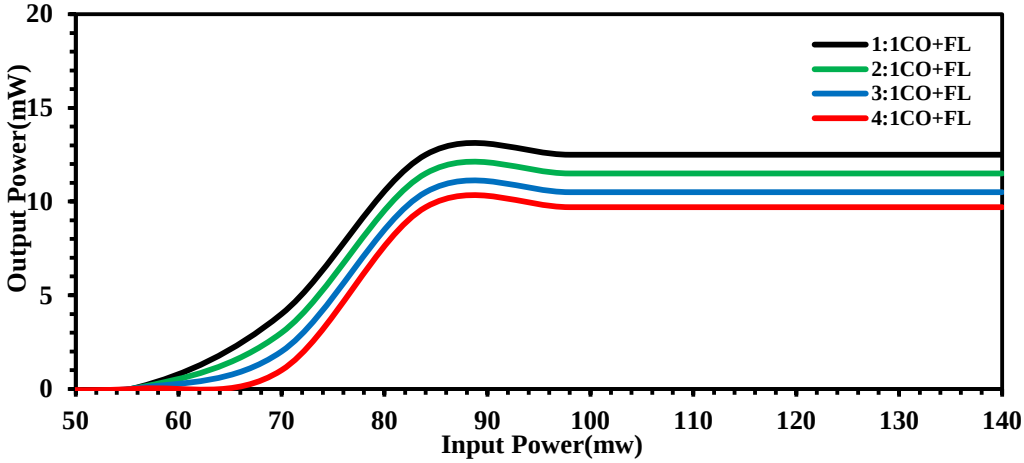

Figure (4.59): The optical limiting response for different ratios of (CO+FL) organic laser dyes in Ethanol solvent at concentration (3×10^{-5}) M.

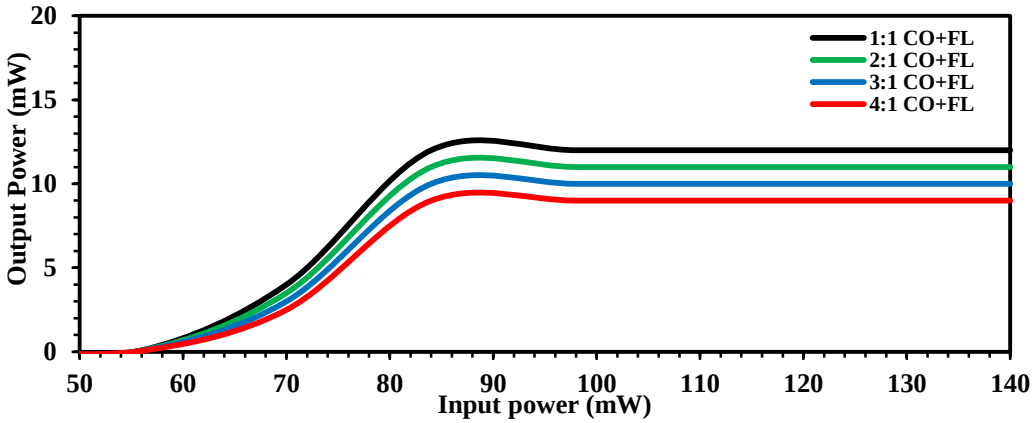

Figure (4.60): The optical limiting response for different ratios of (CO+FL) organic laser dyes in Ethanol solvent at concentration (5×10^{-5}) M.

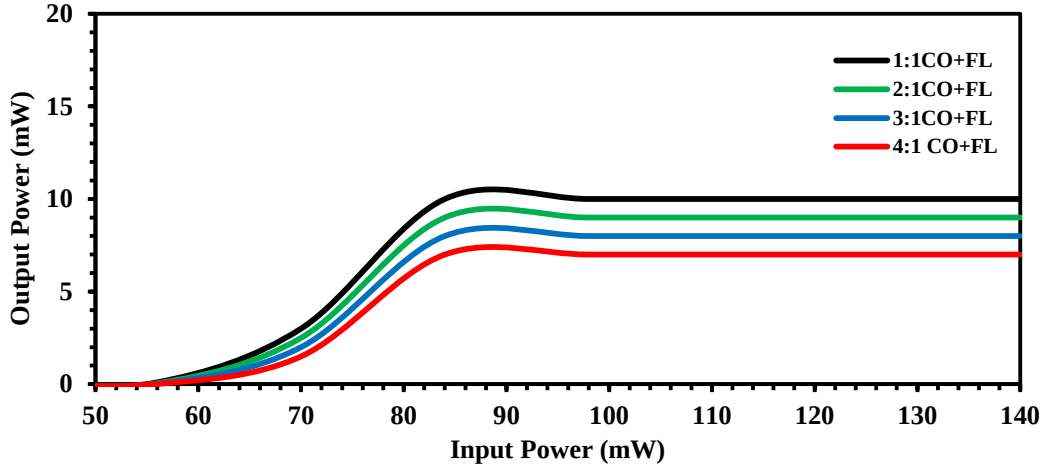

Figure (4.61): The optical limiting response for different ratios of mixing (CO+FL) organic laser dyes in Ethanol solvent at concentration (7×10^{-5}) M.

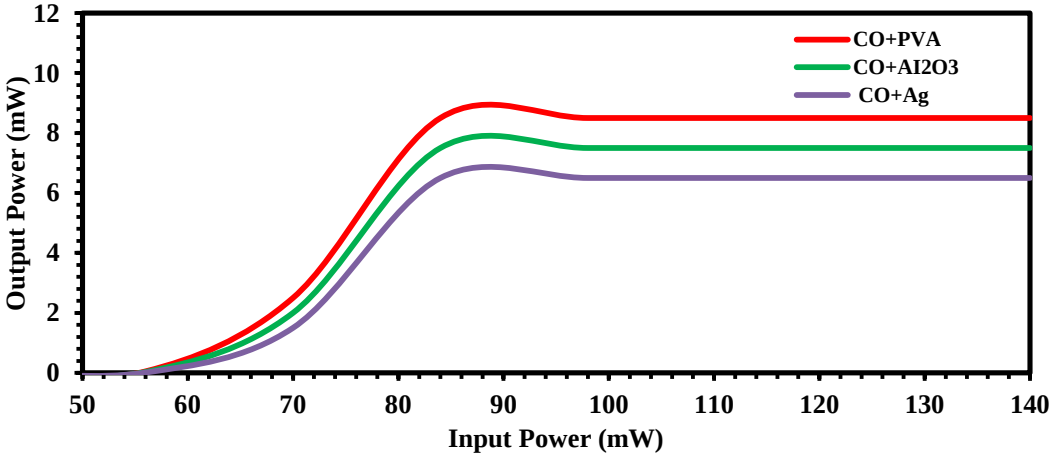

Figure (4.62): The optical limiting response of thin films of Coumarin 334 organic laser dye with PVA polymer doped (Al_2O_3 , Ag) NPs.

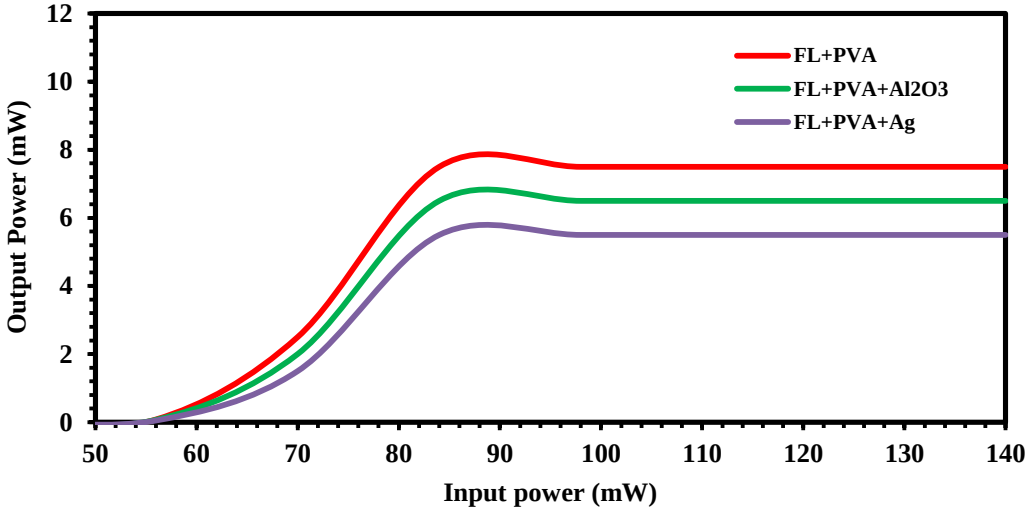

Figure (4.63): The optical limiting response of thin films of Fluorescein organic laser dye with PVA polymer doped (Al_2O_3 , Ag)NPs

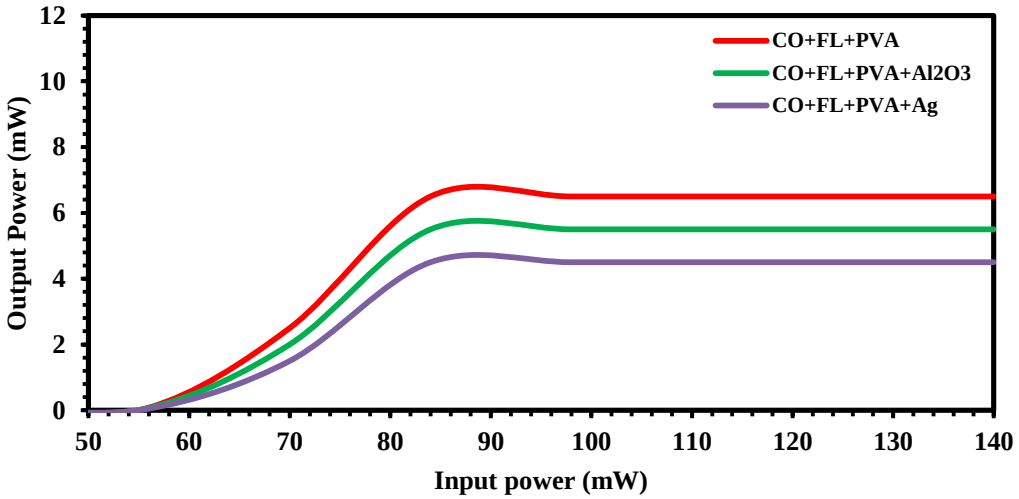

Figure (4.64): The optical limiting response of thin films of mixing of (CO+FL) organic laser dyes with PVA polymer doped (Al_2O_3 , Ag) NPs.

Table (4.12): The optical limiting response of Fluorescein and Coumarin 344 organic laser dyes at different concentrations.

Material	Concentration (M)	Limiting Threshold (mW)	Limiting Amplitude (mW)
Fluorescein	1×10^{-5}	13.8	85
	3×10^{-5}	12.7	84.5
	5×10^{-5}	11.4	84
	7×10^{-5}	10.2	83
Coumarin (344)	1×10^{-5}	14	89
	3×10^{-5}	13.2	88.4
	5×10^{-5}	12	88
	7×10^{-5}	11.4	87.5

Table (4.13): The optical limiting response of mixture of Coumarin 344 and Fluorescein organic laser dyes at different mixing ratios and different concentrations.

Material	Concentration (M)	Limiting Threshold (mW)	Limiting Amplitude (mW)
Mixture (CO+FL) at (3×10^{-5}) M	1:1	12	85
	2:1	11.3	84.4
	3:1	10	83
	4:1	9.7	80.5
Mixture (CO+FL) at (5×10^{-5}) M	1:1	12	80
	2:1	11	80.5
	3:1	10	79.5
	4:1	9	79
Mixture (CO+FL) at (7×10^{-5}) M	1:1	10	78.3
	2:1	9	77.3
	3:1	8	76
	4:1	7	75

Table (4.14): The optical limiting response of thin films mixture of Coumarin 344 and Fluorescein organic laser dyes at ratio (4:1) with PVA polymer doped (Ag, Al_2O_3) nanoparticles at (7×10^{-5}) M.

Material	Limiting Threshold (mW)	Limiting Amplitude (mW)
Thin Film of FL+PVA polymer	8	88
Thin Film of FL+PVA polymer +AL_2O_3 NPs	7.6	87
Thin Film of FL+PVA polymer +Ag NPs	6.5	86
Thin Film of CO+PVA polymer	7.5	84.8
Thin Film of CO+PVA polymer +Al_2O_3 NPs	6.4	84
Thin Film of CO+PVA polymer +Ag NPs	5.7	84.5
Thin Film of Mixture CO+FL + PVA polymer	6.8	84
Thin Film of Mixture CO+FL + PVA polymer +Al_2O_3NPs	5.5	83.2
Thin Film Mixture CO+FL + PVA polymer +Ag NPs	4.2	83

4.10 Conclusions

The main conclusions that we have obtained in our research:

1. The linear and nonlinear optical properties of Fluorescein dye are larger than those for Coumarin 334 dye.
2. The values of the linear and nonlinear optical properties of solution of mixture laser dyes with mixing ratio (4:1) and concentration (7×10^{-5}) M are show higher than the other mixing ratios and other concentrations.
3. The linear and nonlinear optical properties of all samples of laser dyes doped with PVA polymer and Ag nanoparticles are higher than samples doped with PVA polymer and Al_2O_3 nanoparticles.
4. All samples of mixture laser dyes possess large linear and nonlinear optical properties as compared with samples of pure laser dyes, as a result it can be used as optical and photonic devices.
5. The nonlinear refractive index for Coumarin (334) dye shows the behavior of self- focusing and self- defocusing for Fluorescein for dye all solution and mixture laser dye, and two photon absorption in nonlinear absorption coefficient. The nonlinear absorption coefficient for all thin films of laser dyes and their mixtures show saturable absorption phenomena.
6. Fluorescence intensity of all samples of Coumarin (344) dye, Fluorescein dye and mixture laser dye increasing linearly with increasing of concentrations. The Fluorescence spectra of thin films have narrower band width than dyes as solutions also the emission peaks are higher intensity than solutions.
7. The inecrease in the value of quantum efficiency with the increase in concentration for all prepared samples.

8. Fluorescence spectra of solution of mixture laser dyes with mixing ratio (4:1) and concentration (7×10^{-5}) M are higher than the other ratios and concentrations, as a result it can be used as active laser medium.
9. Optical limiting properties of all samples of Fluorescein dye are better than Coumarin (344) dye. The Optical limiting properties increase with decreasing concentrations for all samples.
10. Optical limiting properties of mixture dyes as solutions and thin films are better than those for pure dyes.The Optical limiting properties of laser dyes doped with polymer PVA and Ag nanoparticles are better than thin films doped with Al_2O_3nanoparticles, as a result it can be used as better optical limiting in electro-optical devices

4.11 The Suggestions and Future Works

In this context, a further investigation can be suggested as future works:

1. Studying spectral, linear and nonlinear optical properties of mixture dyes with another types of solvents at different concentrations.
2. Studying nonlinear optical properties of dyes using lasers with different wave lengths and different powers.
3. Studying effect for adding another types of polymer and nanoparticles on spectral, linear and non-linear of new mixture of other laser dyes.

4.8 Nonlinear Optical Properties

The nonlinear optical properties were investigated of Fluorescein and Coumarin (334) (CO and FL) organic laser dyes and mixture of them with ratios (1:1, 2:1, 3:1 and 4:1) as solutions at different concentration's (1×10^{-5}, 3×10^{-5}, 5×10^{-5} and 7×10^{-5}) M and thin films doped with (PVA polymer and (Ag and Al_2O_3) nanoparticles) at concentration (10^{-3}) using continuous wave (CW) diode pump solid state laser at wavelength (457 nm) and power (84mW). There are two parts were used to measure the nonlinear properties of the material by Z-Scan technique. The first part is open-aperture Z-Scan and the second part is the closed-aperture Z-Scan.

4.8.1 Nonlinear Refractive Index

The nonlinear refractive index of Fluorescein and Coumarin (334) organic laser dyes and mixture of them with ratios (1:1, 2:1, 3:1 and 4:1) as solutions at different concentration's (1×10^{-5}, 3×10^{-5}, 5×10^{-5} and 7×10^{-5}) M and thin films doped with (PVA polymer and (Ag ,Al_2O_3) nanoparticles) at concentration (10^{-3}) were measured by closed-aperture Z-Scan technique.

The normalized transmittances of Z-Scan measurements as a function of distance in (Ethanol) solvent for Coumarin (334) is shown in Figures (4.41). the nonlinear effect region is extended from (-2) mm to (2) mm. The valley followed by peak a transmittance curve obtained from the closed aperture Z-Scan data indicates that the sign of the refraction nonlinearity is positive ($n_2 > 0$), leading to self-focusing lensing in these samples [143].

The normalized transmittances of Z-Scan measurements as a function of distance in (Ethanol) solvent for Fluorescein organic laser dyes and mixture of them as shown in Figures (4.42- 4.48) the nonlinear effect region is extended from (-2) mm to (2) mm. The peak followed by a valley transmittance curve obtained from the closed aperture Z-Scan data indicates that the sign of the refraction nonlinearity is negative ($n_2 < 0$), leading to self-defocusing lensing in these samples it agree with references [143].The valley-peak configuration indicates the positive sign of n_2 .The scan started from distance far away from the focus, the beam The scan started with a linear behavior at different distances from the far field of the sample position (-Z) with respect to the focal plane at Z=0 mm. The behavior of z-scan curves was in good agreement with [144]. In order to describe the Z-Scan behavior in the previous Figures, when the sample moves far from the focus, the transmitted beam intensity is low and the transmittance remains relatively constant.

As the sample approaches the beam focus, intensity increases, leading to self-lensing in the sample tend to collimate the beam on the aperture in the far field, increasing the measured transmittance at the iris position. If the beam experiences any nonlinear phase shift due to the sample as it is translated through the focal region, then the fraction of light falling on the detector will vary due to the self-lensing generated in the material by the intense laser beam. In this case, the signal measured by detector will exhibit a peak and valley as the sample is translated [145].The position of the peak and valley, relative to the z-axis, depends on the sign of the nonlinear phase shift .Where the change in the normalized transmittance from the peak of the curve to the valley (ΔT_{p-v}) is directly proportional to the nonlinear phase shift imparted on the beam. Moreover, if the beam is transmitted through the nonlinear medium the

induced phase shift can also be either negative or positive accordingly when the medium is self- defocusing or self-focusing, respectively [51]. The magnitude of the phase shift can be determined from the change in transmittance between peak and valley. After the focal plane, the self-defocusing increases the beam divergence, leading to a widening of the beam at the focus and thus reducing the measured transmittance. Far from focus (Z > 0), again the nonlinear refraction is low resulting in a transmittance Z-independent . The nonlinearity of doped dyes is larger than those for pure dyes. As well as thin films possess very large nonlinearity as compared with dyes as solution. The relation between the nonlinear refractive index and the nonlinear phase shift is a linear increasing relation. Z-Scan measurements indicated that pure and dye doped and their thin films exhibited negative nonlinear refractive index , it agree with reference [144].

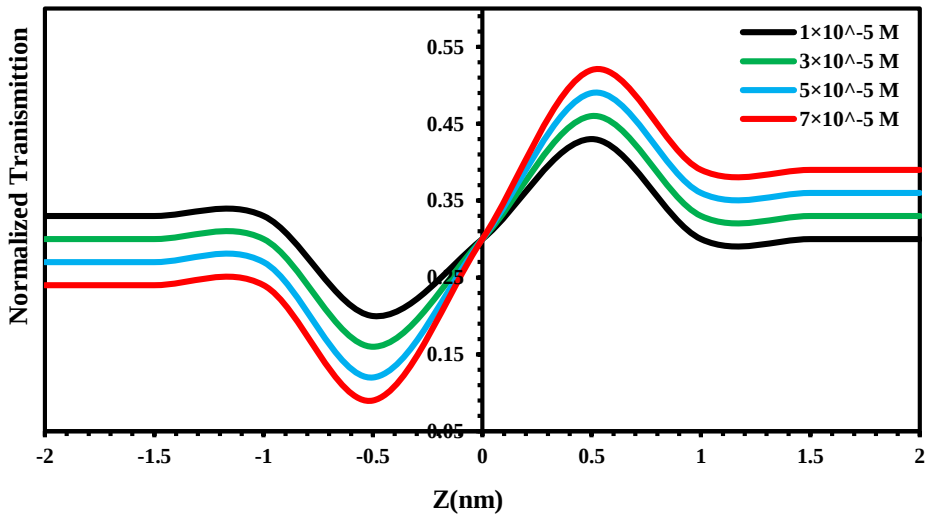

Figure (4.41):Closed-aperture Z-Scan data for different concentrations of Coumarin 334 organic laser dye in Ethanol solvent.

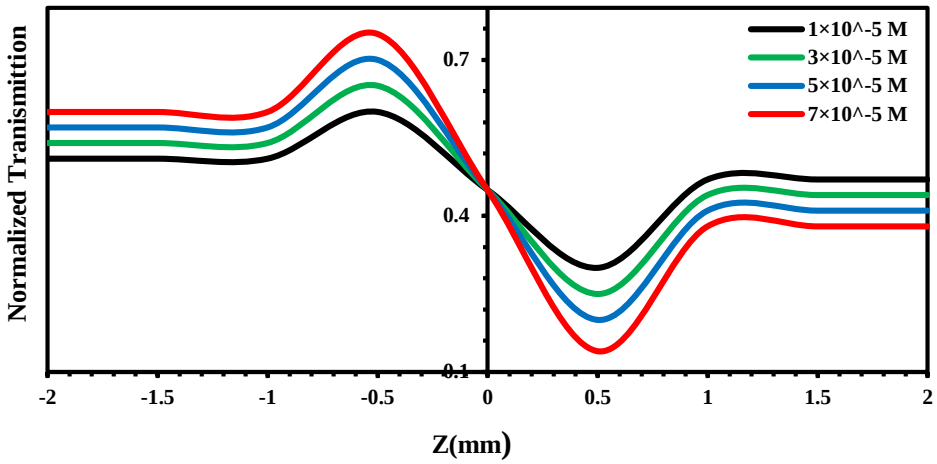

Figure (4.42): Closed-aperture Z-Scan data for different concentrations of Fluorescein organic laser dye in Ethanol solvent.

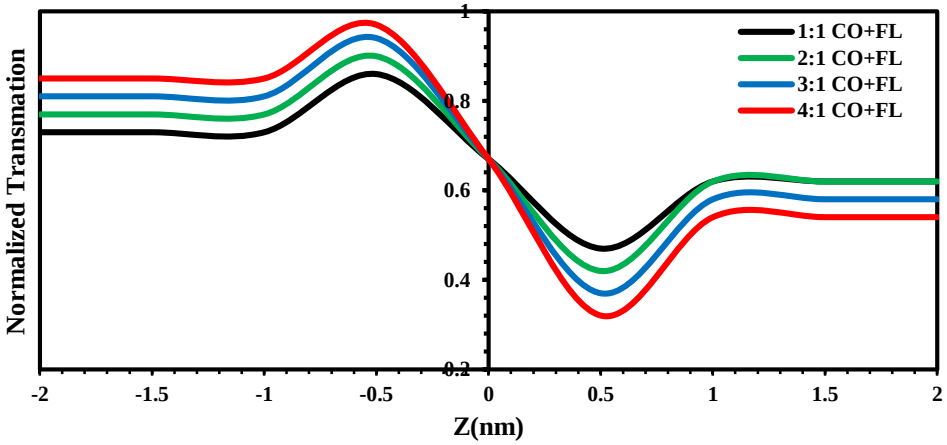

Figure (4.43): Closed-aperture Z-Scan data for different ratios of mixing (CO+FL) organic laser dyes in Ethanol solvent at concentration (3×10^{-5})M.

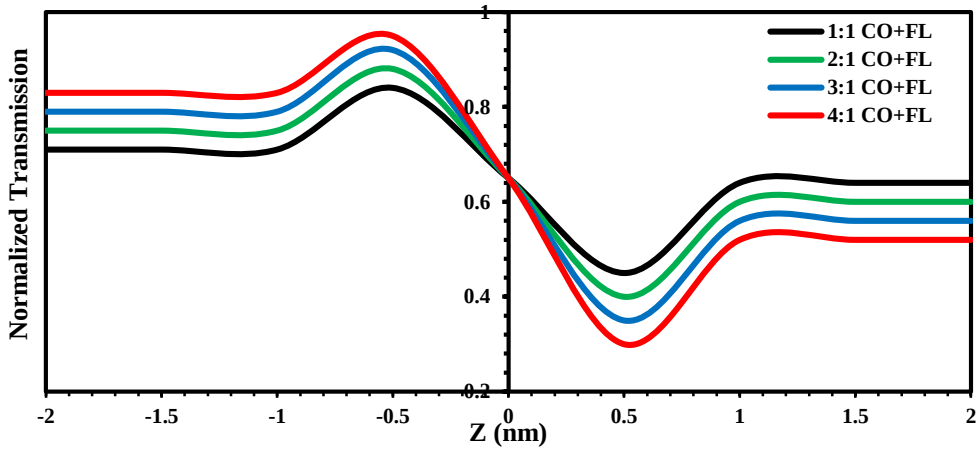

Figure (4.44): Closed-aperture Z-Scan data for different ratios of mixing (CO+FL) organic laser dyes in (Ethanol) solvent at concentration (5×10^{-5}) M.

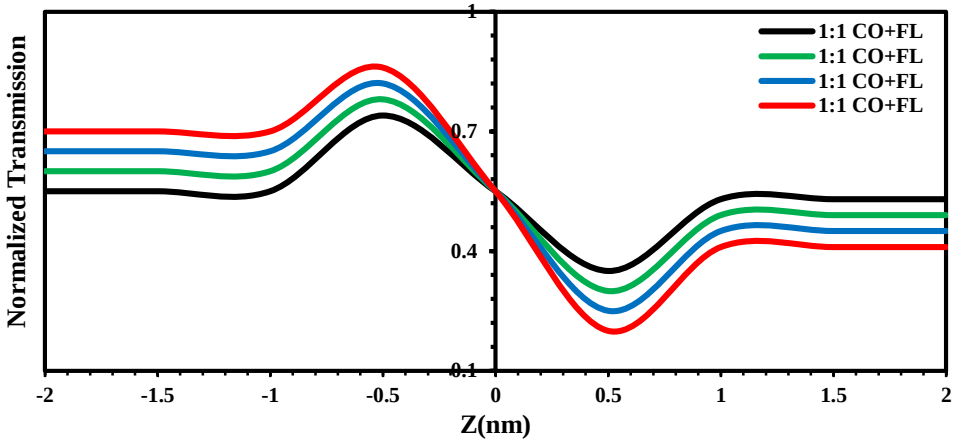

Figure (4.45): Closed-aperture Z-Scan data for different ratios of mixing of (CO+FL) organic laser dyes in Ethanol solvent at concentration (7×10^{-5}) M.

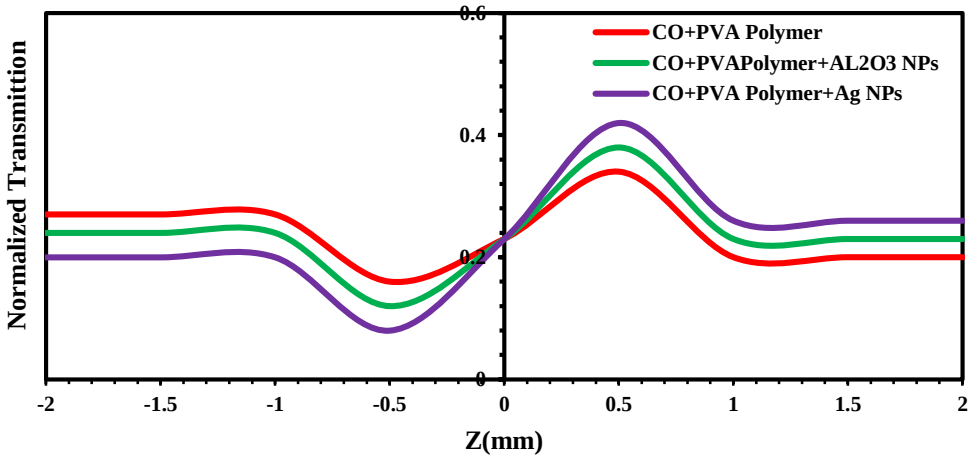

Figure (4.46): Closed-aperture Z-Scan data for thin films of Coumarin 334 organic laser dye doped with PVA polymer and (Al_2O_3 , Ag) NPs.

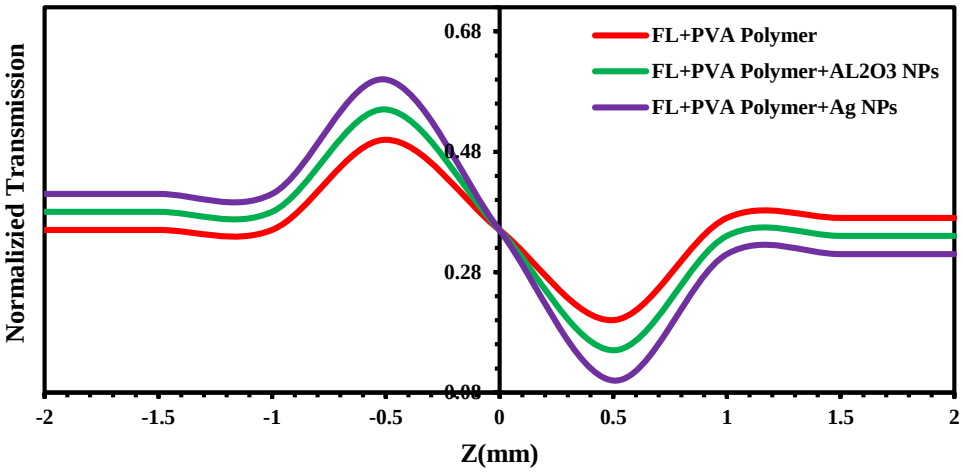

Figure (4.47): Closed-aperture Z-Scan data for thin films of Fluorescein organic laser dye doped with PVA polymer and (Al_2O_3 , Ag) NPs.

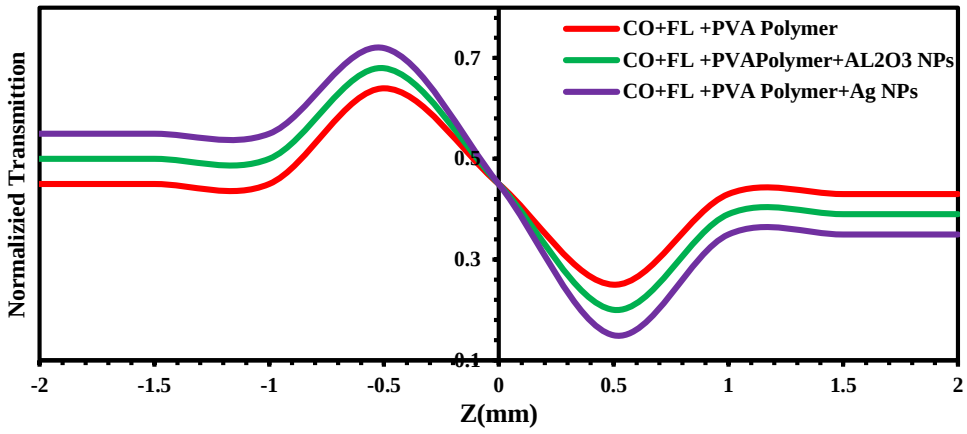

Figure (4.48): Closed-aperture Z-Scan data for thin films of mixing of (CO+FL) organic laser dyes doped with PVA polymer and (Al_2O_3 , Ag) NPs.

4.8.2 Nonlinear Absorption Coefficient

The nonlinear absorption coefficient of Fluorescein and Coumarin (334) organic laser dyes and mixture of them with ratios (1:1, 2:1, 3:1 and 4:1) as solutions at different concentration's (3×10^{-5}, 5×10^{-5} and 7×10^{-5}) M and thin films doped with PVA polymer and (Ag, Al_2O_3) nanoparticles at concentration (10^{-3}) M in ethanol solvent, can be measured by performing the open aperture Z-Scan technique at wavelength (457nm) and power (84 mW). The performed open aperture-Scan exhibits an increasing in the transmission about the focus of the lens.

Open-aperture Z-Scan of Fluorescein , Coumarin (334) and mixing of them as solutions are shown in Figures (4.75-4.80). Its noticed (two photon absorption) phenomenon. The behavior of transmittance starts linearly at different distances from the far field of the sample position (-Z). At the near field, the transmittance curve begins to decrease until it reaches the minimum value (T_{min}) at the focal point, where Z=0 mm. The transmittance begins to

increase towards the linear behavior at the far field of the sample position (+Z). The change of intensity, in this case, is caused by two photon absorption when in the sample travels through beam waist. This behavior agrees with reference [145].The open-aperture Z-Scan of thin films of Fluorescein and Coumarin (334) organic laser dyes and mixture of them with ratios (1:1, 2:1, 3:1 and 4:1) as thin films doped with PVA polymer and Ag , Al_2O_3 nanoparticles at concentration (10^{-3}) M in ethanol solvent are defines variable transmittance values, which was used to determine absorption coefficient. Saturable absorption phenomenon was observed for open-aperture Z-Scan technique as shown in Figures (4.49-4.56).

The behavior of transmittance curves starts linearly at different distance from the far field of the sample position (-Z). At the near field the transmittance curve begins to increase until it reaches the maximum value (T_{max}) at the focal point, where Z=0 mm. Afterwards, the transmittance begins to decrease toward the linear behavior at the far field of the sample position (+Z) [12].The transmittance is sensitive to the nonlinear absorption as a function of input power intensity. The change in intensity is caused by saturation absorption in the sample as it travels through the beam waist [148]. In the focal plane where the intensity is greatest, the largest nonlinear absorption is observed. At the far field of the Gaussian beam, where, the beam intensity is too weak to elicit nonlinear effects.

A symmetric peak value is contributed to the negative nonlinear absorption coefficient β, indicates that the sample shows a bleaching-like behavior (saturation of absorption) [148]. The nonlinear parameters are calculated , as tabulated in Tables (4.4- 4.9) these Tables show that the values of nonlinear parameters (n_2 and β) for Fluorescein , Coumarin (334) organic laser dyes and

mixture of them with ratios (1:1, 2:1, 3:1 and 4:1) as solutions are increased but β decreased with increasing the concentrations, as increasing the values of linear parameters (α_o and n_o). This is due to decreasing number of molecules per volume unit at low concentrations[149].The closed-aperture Z-Scan defines variable transmittance values, which used to determine the nonlinear phase shift $\Delta\Phi$ using equation (2.18) and the nonlinear refractive index (n_2) using equation (2.17), nonlinear absorption coefficient (β) using equation (2.18), as listed in Tables (4.4-4.7) respectively. Thin films of all samples were exhibited better nonlinearity than liquid samples.

This is suggested to be take place due to the π–π^* stacking in supramolecular interactions between delocalized electrons in solid samples. In addition, in the case of thin films, the molecule orientation is crucial where molecules can be arranged either by homotopic alignment or columnar stacking on the substrate as almost organic dyes are self-organized materials [51]. The nonlinearity of doped dyes are larger than those for pure dyes agree with [144]. As well as thin films of Fluorescein and Coumarin (334) organic laser dyes and mixture of them with ratios (4:1) possess very large nonlinearity as compared with dyes as solution. This is due to increasing number of molecules per volume unit at high concentrations, as well as thin films have thickness larger than dyes as solutions, which is lead to increasing the nonlinear phase shift agree with [150]. The results showed that the nonlinear optical properties of the films with doped nanoparticles were higher than the films without nanoparticles.

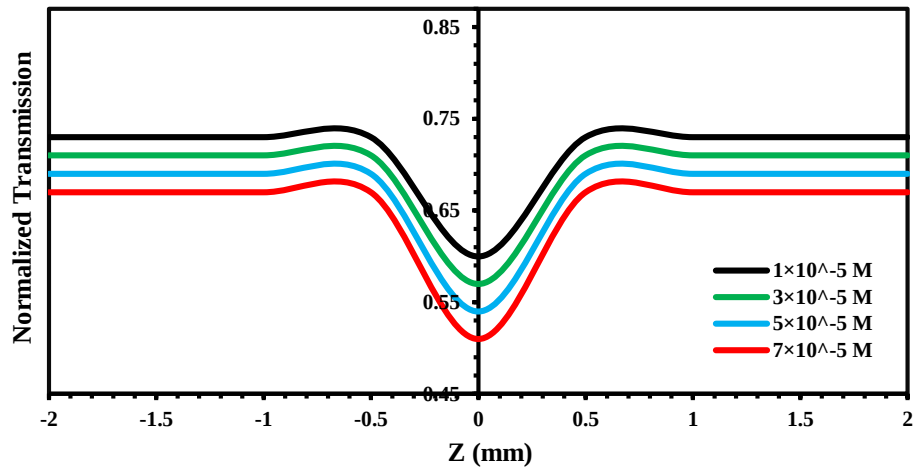

Figure (4.49): Open-aperture Z-Scan data for different concentrations of Coumarin (334) organic laser dye in ethanol solvent.

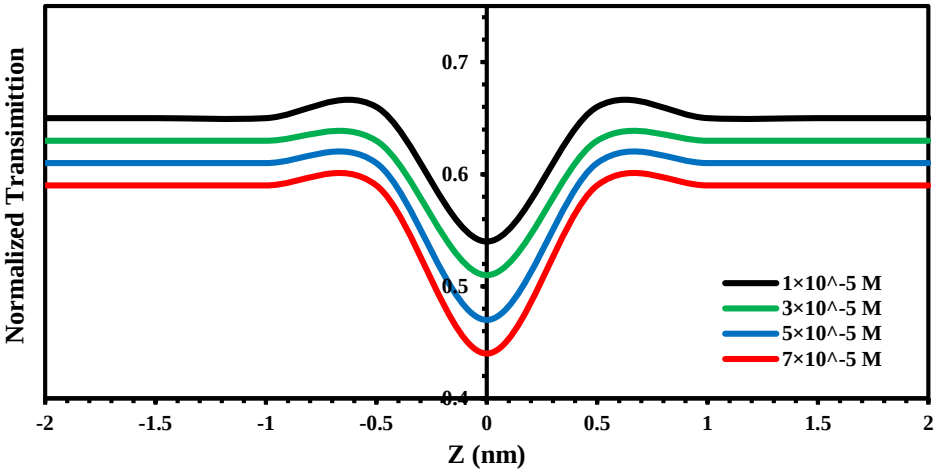

Figure (4.50): Open-aperture Z-Scan data for different concentrations of Fluorescein organic laser dye in ethanol solvent.

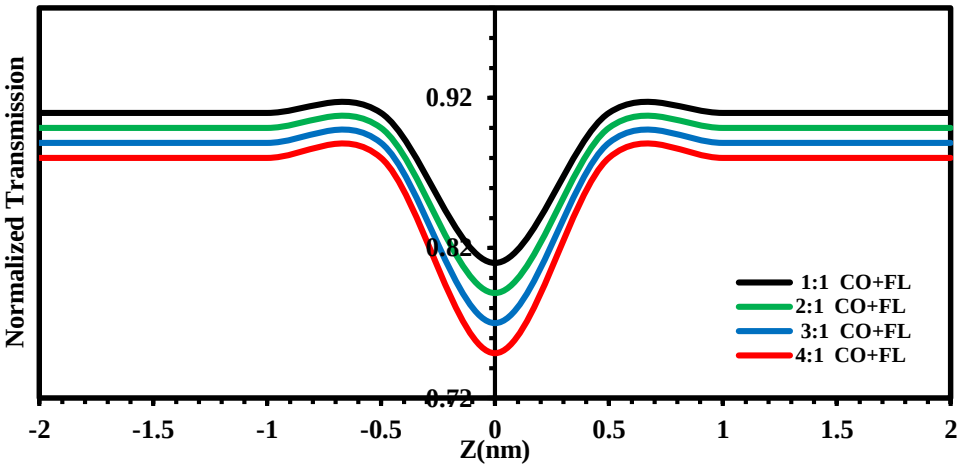

Figure (4.51): Open-aperture Z-Scan data for different ratios of mixing of (CO+FL) organic laser dyes in Ethanol solvent at concentration (3×10^{-5})M.

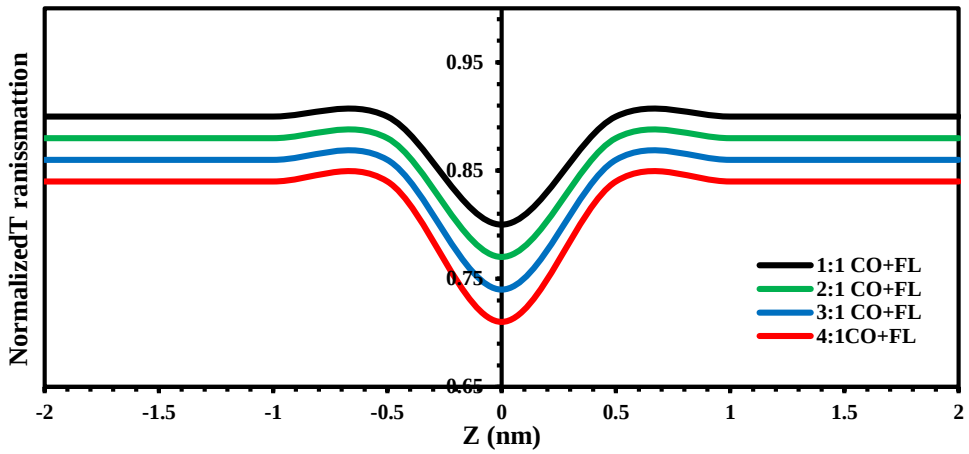

Figure (4.52): Open-aperture Z-Scan data for different ratios of mixing of (CO+FL) organic laser dyes in Ethanol solvent at concentration (5×10^{-5})M.

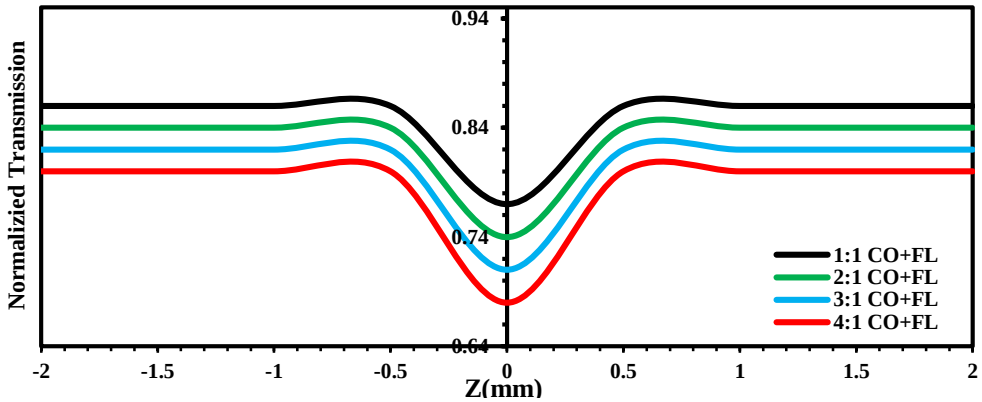

Figure (4.53): Open-aperture Z-Scan data for different ratios of mixing (CO+FL) organic laser dyes in (Ethanol) solvent at concentrations (7×10^{-5})M.

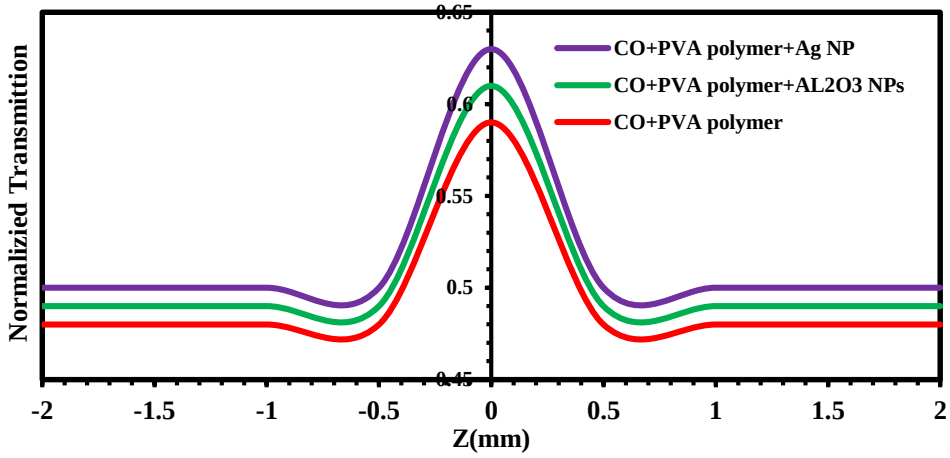

Figure (4.54): Open-aperture Z-Scan data for thin films of Coumarian (334) organic laser dye doped with PVA polymer and (Al_2O_3 , Ag) NPs.

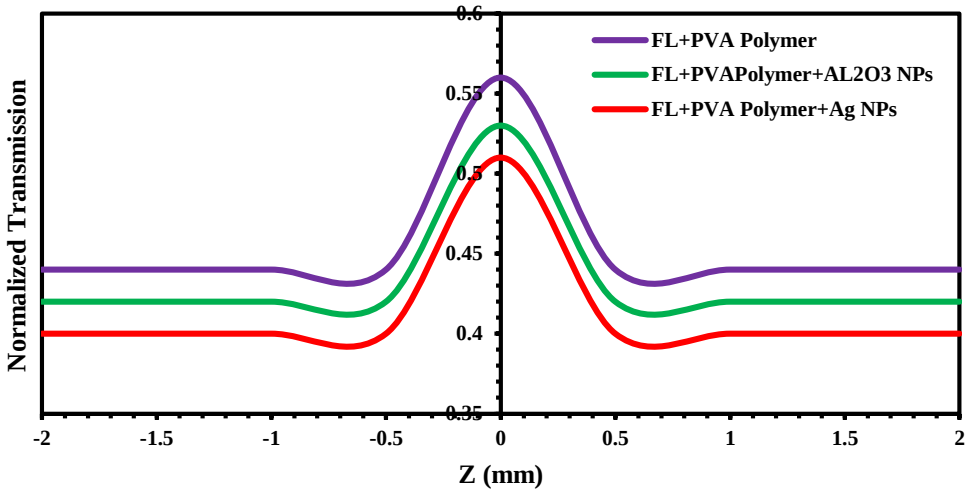

Figure (4.55): Open-aperture Z-Scan data for thin films of Fluorescein organic laser dye doped with PVA polymer and(Al_2O_3 , Ag) NPs.

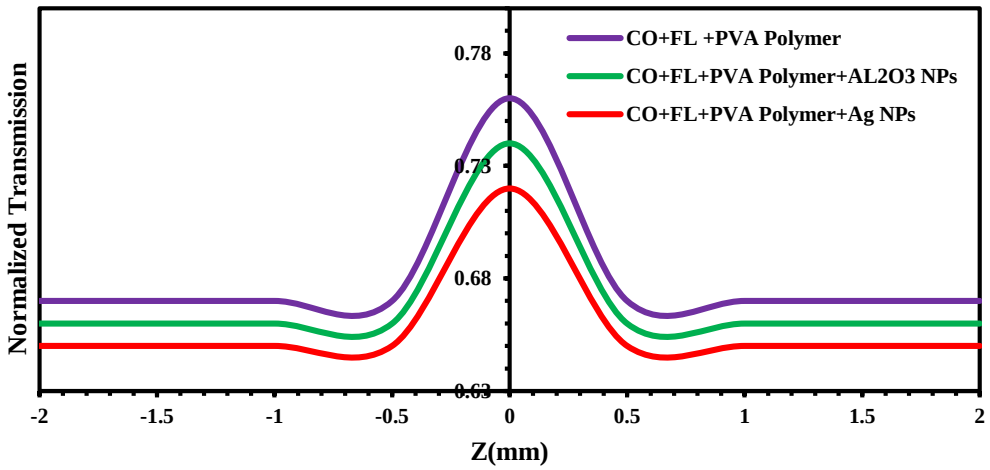

Figure (4.56): Open-aperture Z-Scan data for thin films for mixing of (CO+FL) organic laser dyes doped with PVA polymer and (Al_2O_3 , Ag) NPs.

Table (4.4): Linear and nonlinear optical parameters for different concentrations of Coumarin (344) and its thin films at (λ=457nm).

Material	Concentration (Mol/L)	T	($\alpha_\circ$) cm^{-1}	$n_\circ$	ΔT_{P-V}	n_2 (cm^2/mW)	T(z)	*B* (cm/mW)
Coumarin (344) (Solutions)	1×10^{-5}	0.9353	0.0667	1.1470	0.011	2.1188×10^{-11}	0.28	0.8392×10^{-3}
	3×10^{-5}	0.8170	0.20208	1.4296	0.024	4.2731×10^{-11}	0.25	1.0786×10^{-3}
	5×10^{-5}	0.7361	0.3062	1.6777	0.031	6.3839×10^{-11}	0.22	1.3073×10^{-3}
	7×10^{-5}	0.5086	0.6759	2.0583	0.043	6.9855×10^{-11}	0.26	1.4265×10^{-3}
CO+PVA polymer (Thin films)	1×10^{-3}	0.6018	5374.2	1.158	0.110	1.7310^{-7}	0.44	1.245
CO+PVA polymer + Al_2O_3 NPs (Thin films)	1×10^{-3}	0.5717	5971.44	1.1623	0.123	2.3410^{-7}	0.41	2.673

Table (4.5): Linear and nonlinear optical parameters for different concentrations of Fluorescein and its thin films at(λ=457nm).

Material	Concentration (Mol/L)	T	($\alpha_\circ$) cm^{-1}	$n_\circ$	ΔT_{P-V}	n_2 (cm^2/mW)	T(z)	*β* (cm/mW)
Fluorescein (Solutions)	1×10^{-5}	0.8016	0.2210	1.2931	0.0277	3.5016×10^{-11}	0.56	1.2947×10^{-3}
	3×10^{-5}	0.7194	0.3293	1.4955	0.0361	5.5024×10^{-11}	0.51	1.4198×10^{-3}
	5×10^{-5}	0.5760	0.5515	1.7849	0.0416	7.6834×10^{-11}	0.41	1.5068×10^{-3}
	7×10^{-5}	0.4714	0.7519	1.9216	0.0527	8.5168×10^{-11}	0.38	1.6264×10^{-3}
FL+PVA polymer (Thin films)	1×10^{-3}	0.6748	6396.33	1.1652	0.132	2.9110^{-7}	0.70	2.023
FL+PVA polymer + Al_2O_3NPs (Thin films)	1×10^{-3}	0.6402	6806.97	1.1852	0.154	3.8910^{-7}	0.67	3.765
FL+PVA polymer + AgNPs (Thin films)	1×10^{-3}	0.6130	7589.42	1.1920	0.162	4.5910^{-7}	0.65	4.567

Table (4.6): Linear and nonlinear optical parameters for solutions of mixture of Coumarin 344 and Fluorescein dyes at different mixing ratios at concentrations (3×10^{-5} , 5×10^{-5} and 7×10^{-5})M at (λ=457nm).

Material	Mixing Ratios	T	($\alpha_\circ$) cm^{-1}	$n_\circ$	ΔT_{P-V}	n_2 (cm^2/mW)	T(z)	*B* (cm/mW)
Mixture of (CO+FL) at (3×10^{-5}) M	1:1	0.7708	0.2602	1.3935	0.022	6.7122×10^{-11}	0.88	2.76×10^{-3}
	2:1	0.7260	0.3201	1.4243	0.024	8.2243×10^{-11}	0.86	2.70×10^{-3}
	3:1	0.7169	0.3327	1.7072	0.040	10.8465×10^{-11}	0.83	2.69×10^{-3}
	4:1	0.7050	0.3494	1.7594	0.060	13.2376×10^{-11}	0.81	2.64×10^{-3}
Mixture of (CO+FL) at (5×10^{-5}) M	1:1	0.6497	0.4312	1.496	0.038	8.5382×10^{-11}	0.86	2.89×10^{-3}
	2:1	0.5497	0.5734	1.7675	0.043	10.0725×10^{-11}	0.85	2.85×10^{-3}
	3:1	0.5603	0.6120	1.8627	0.055	13.8256×10^{-11}	0.83	2.80×10^{-3}
	4:1	0.5694	0.6195	1.9996	0.065	17.6725×10^{-11}	0.82	2.78×10^{-3}
Mixture of (CO+FL) at (7×10^{-5}) M	1:1	0.5671	0.5671	1.7853	0.046	10.6356×10^{-11}	80	3.21×10^{-3}
	2:1	0.5635	0.6480	1.7901	0.054	13.8876×10^{-11}	81	3.15×10^{-3}
	3:1	0.5422	0.7792	1.8273	0.065	17.7945×10^{-11}	79	3.02×10^{-3}
	4:1	0.5382	0.8630	1.9843	0.732	18.5352×10^{-11}	76	2.98×10^{-3}

Table (4.7): Linear and nonlinear optical parameters for thin films of Coumarin 344 and Fluorescein dyes at different mixing ratios at concentration (10^{-3} M) at (λ=457nm).

Material	Mixing Ratios	T	($\alpha_\circ$) cm^{-1}	$n_\circ$	ΔT_{P-V}	n_2 (cm^2/mW)	T(z)	*B* (cm/mW)
Mixture doped with PVA polymer	4:1	0.7281	7783. 03	1.3146	0.203	11.4110^{-7}	0.34	4.472
Mixture doped with PVA polymer and AL_2O_3 NPs	4:1	0.3547	8216.11	1.5964	0.258	13.3210^{-7}	0.32	5.738
Mixture doped with PVA polymer and Ag NPs	4:1	0.2159	8923.95	1.620	0.291	15.12310^{-7}	0.30	7.52

4.9 Optical Limiting Behavior of organic Dyes

The optical limiting behavior of Fluorescein and Coumarin (334) organic laser dyes and mixture of them with ratios (1:1, 2:1, 3:1 and 4:1) as solutions at different concentration's (3×10^{-5}, 5×10^{-5} and 7×10^{-5}) M and thin films doped with (PVA polymer and (Ag ,Al_2O_3) nanoparticles) at concentration (10^{-3}) M were performed by closed-aperture Z-Scan with the same laser used in Z-Scan technique. Figures (4.57-4.64) give the optical limiting characteristics at room temperature (25-30)C° for all samples were dissolved in (Ethanol) solvent respectively. The samples show very good optical limiting behavior arising from nonlinear refraction. The output power rises initially with the increasing in input power, but after a certain threshold value, the sample starts defocusing the beam resulting in a greater part of the beam cross-section being cut off by the aperture. Thus, the transmittance recorded by the photodetector remained

reasonably constant showing a plateau region agree with [151]. Thin films of Fluorescein , Coumarin and mixing of them with ratios (4:1) give optical power limiting threshold and limiting amplitude less as compared with the materials as solutions, therefore, the optical limiting behavior was significantly optimized in the case of thin films in comparison to liquid specimens and in the polymer and nanoparticles modified dyes in general, as shown in Figures (4.93-4.98). From the threshold intensity for optical limiting for each sample, the optical power limiting threshold is inversely proportional to the concentration, that's mean the properties of the optical limiting be better with increasing the concentrations, as listed in Tables (4.8-4.10) respectively.

Optical limiting protects the human eye by attenuating of the laser beam, this behavior agrees with the study in reference [152]. Fluorescein dissolved in (Ethanol) solvent give optical power limiting threshold and limiting amplitude less as compared with the Coumarin dye (CO), while the mixing with Ag that dissolved in Ethanol solvent give optical power limiting threshold and limiting amplitude less as compared with the pure dyes, therefore, the properties of optical limiting at different concentrations for all samples of mixing (Ag and Al_2O_3) are better than the same samples of dyes (CO and FL) as pure dyes. The threshold of the optical limiting on the axis of the out power and the amplitude of the limiting on the axis of the input power can be measure using the tangent of the beginning of the bending the curve in figures (4.87-4.98), where the lower the threshold and amplitude of the optical limiting, the more suitable the sample is to do as optical limiting.

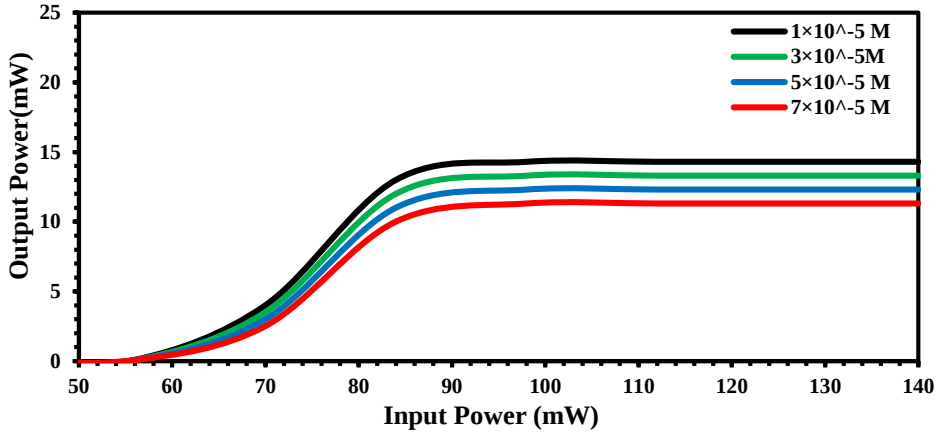

Figure (4.57): The optical limiting response of Coumarin 334 organic laser dye at different concentrations in Ethanol solvent.

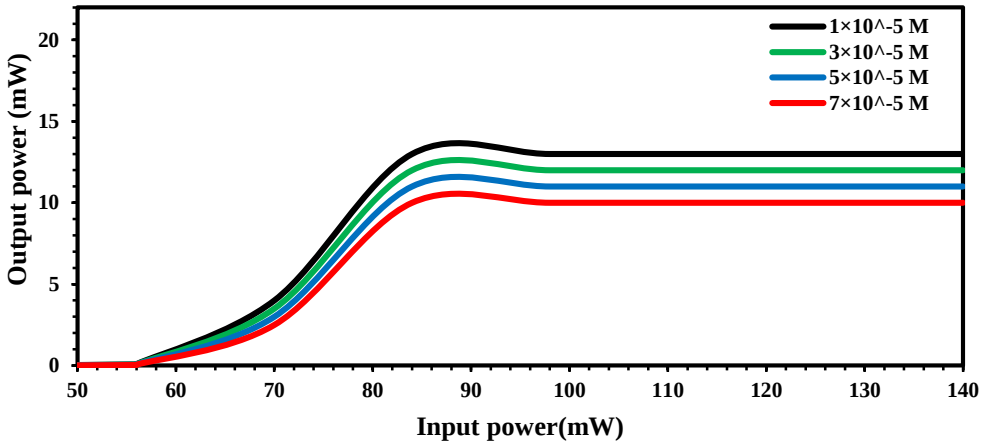

Figure (4.58): The optical limiting response of Fluorescein organic laser dye at different concentrations in Ethanol solvent.

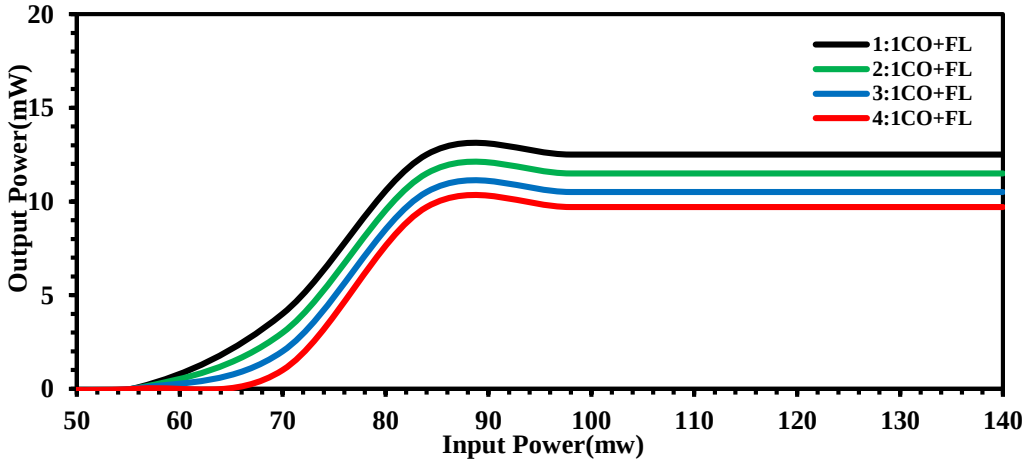

Figure (4.59): The optical limiting response for different ratios of mixing (CO+FL) organic laser dyes in Ethanol solvent at concentration (3×10^{-5})M.

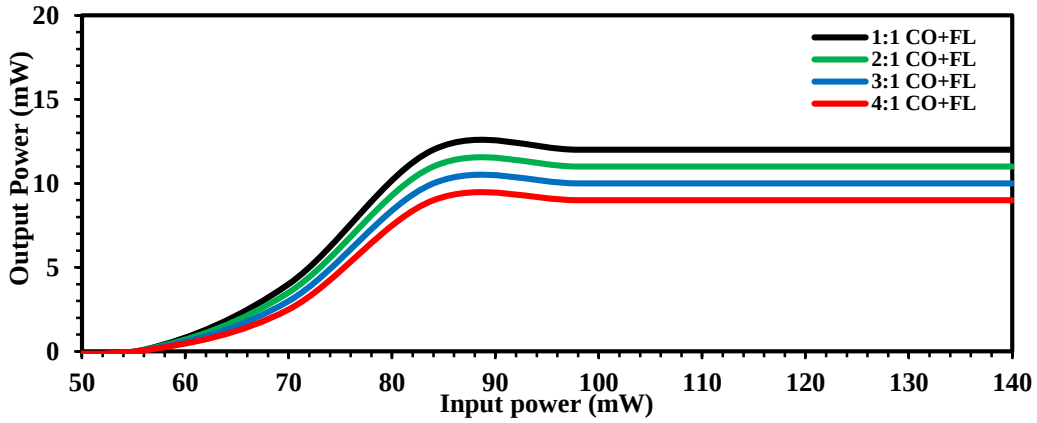

Figure (4.60): The optical limiting response for different ratios of mixing (CO+FL) organic laser dyes in Ethanol solvent at concentration (5×10^{-5}) M.

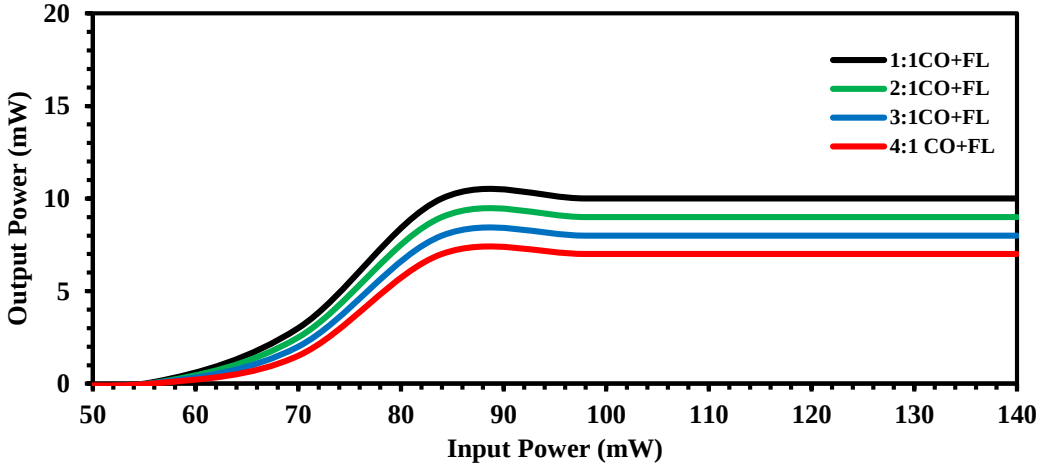

Figure (4.61): The optical limiting response for different ratios of mixing (CO+FL) organic laser dyes in Ethanol solvent at concentration (7×10^{-5}) M.

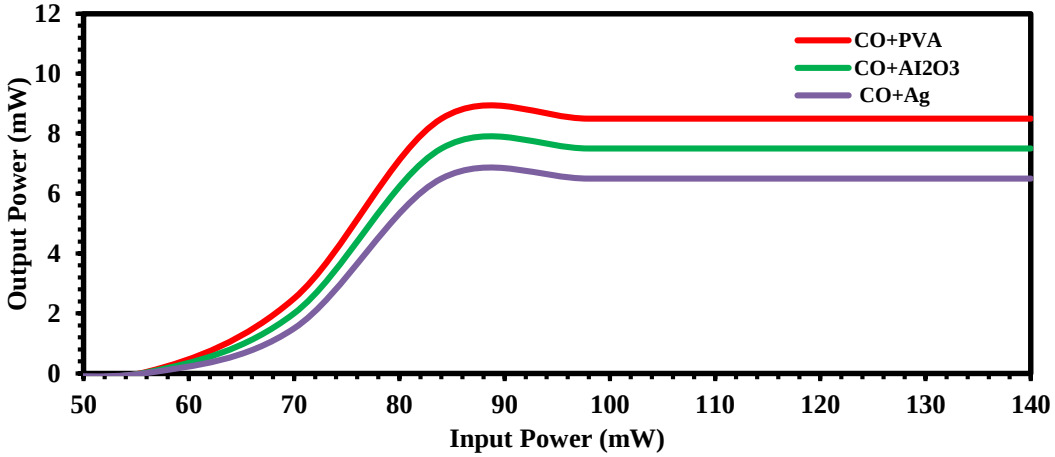

Figure (4.62): The optical limiting response of thin films of Coumarin 334

organic laser dye doped with PVA polymer and(Al_2O_3 , Ag) NPs.

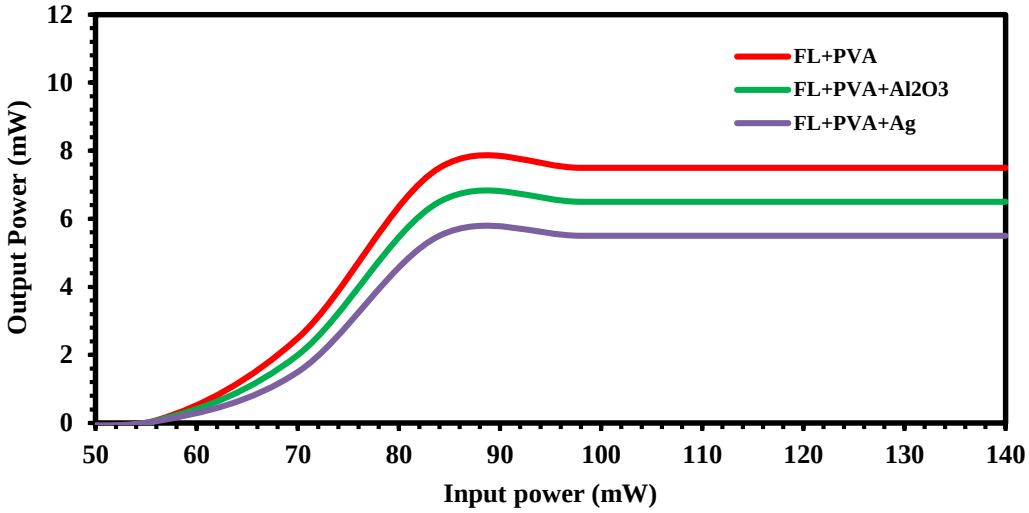

Figure (4.63): The optical limiting response of thin films of Fluorescein organic laser dye doped with PVA polymer and (Al_2O_3 , Ag)NPs

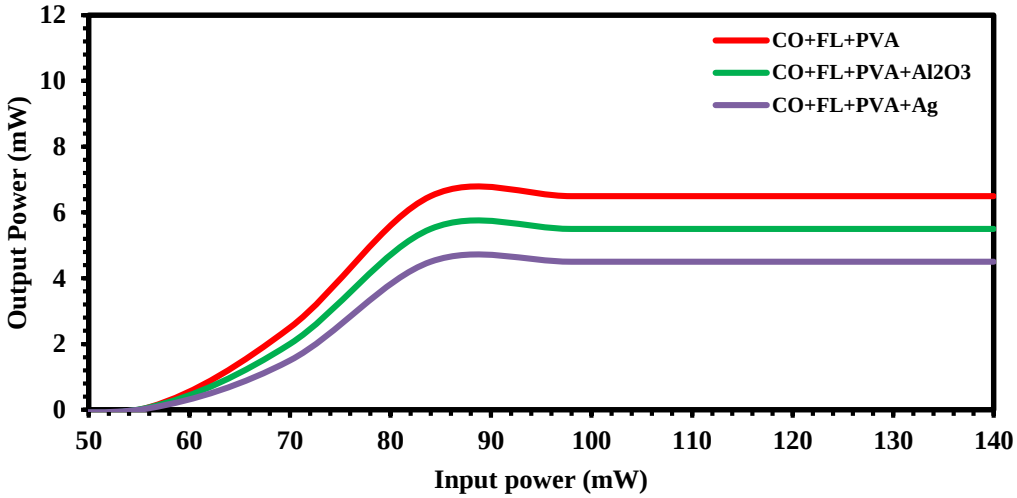

Figure (4.64): The optical limiting response of thin films of mixing of (CO+FL) organic laser dyes doped with PVA polymer and (Al_2O_3 , Ag)NPs.

Table (4.8): The optical limiting response of Fluorescein and Coumarin 344 organic laser dyes at different concentrations.

Material	Concentration (M)	Limiting Threshold (mw)	Limiting Amplitude (mw)
Fluorescein	1×10^{-5}	13.8	85
	3×10^{-5}	12.7	84.5
	5×10^{-5}	11.4	84
	7×10^{-5}	10.2	83
Coumarin (344)	1×10^{-5}	14	89
	3×10^{-5}	13.2	88.4
	5×10^{-5}	12	88
	7×10^{-5}	11.4	87.5

Table (4.9): The optical limiting response of mixture of Coumarin 344 and Fluorescein organic laser dyes at different mixing ratios as solutions and different concentrations.

Material	Concentration (M)	Limiting Threshold (mw)	Limiting Amplitude (mw)
Mixture (CO+FL) at (3×10^{-5}) M	1:1	12	85
	2:1	11.3	84.4
	3:1	10	83
	4:1	9.7	80.5
Mixture (CO+FL) at (5×10^{-5}) M	1:1	12	80
	2:1	11	80.5
	3:1	10	79.5
	4:1	9	79
Mixture (CO+FL) at (7×10^{-5}) M	1:1	10	78.3
	2:1	9	77.3
	3:1	8	76
	4:1	7	75

Table (4.10): The optical limiting response of mixture of Coumarin 344 and Fluorescein organic laser dyes at different ratios as thin films doped with PVA polymer and (Ag,Al_2O_3) nanoparticles at (7×10^{-5} M).

Material	Limiting Threshold (mw)	Limiting Amplitude (mw)
Thin Film of FL+PVA polymer	7.5	84.8
Thin Film of FL+PVA polymer +AL_2O_3 NPs	6.4	84
Thin Film of FL+PVA polymer +Ag NPs	5	83
Thin Film of CO+PVA polymer	8	88
Thin Film of CO+PVA polymer +Al_2O_3 NPs	7.6	87
Thin Film of CO+PVA polymer +Ag NPs	6.5	86
Thin Film of Mixture CO+FL + PVA polymer	6	85
Thin Film of Mixture CO+FL + PVA polymer +Al_2 O_3NPs	5.5	84
Thin Film Mixture CO+FL + PVA polymer +Ag NPs	4.2	83

4.10. Conclusions

The main conclusions that we have obtained in our research:

1. Preparation of new mixture of two laser organic dyes Fluorescein dye and Coumarin 344 dye in different mixing ratios as solutions and thin films have been successfully by drop-coating method on glass substrate.
2. The grain size of the thin films, calculated from atomic force microscope (AFM) in the range of (18 - 69) nm.
3. The linear and nonlinear optical properties of Fluorescein dye are larger than those for Coumarin 344 dye.
4. The linear and nonlinear optical properties of solution of mixture laser dyes with mixing ratio (4:1) and concentration (7×10^{-5}) M are higher than the other mixing ratios and other concentrations.
5. The linear and nonlinear optical properties of thin films of mixture laser dyes with mixing ratio (4:1) are higher than the other ratios.
6. The linear and nonlinear optical properties of laser dyes doped with polymer PVA and nanoparticles are higher than thin films without doping with nanoparticles .
7. The linear and nonlinear optical properties of all samples of laser dyes doped with PVA polymer and Ag nanoparticles are higher than samples doped with PVA polymer and Al_2O_3 nanoparticles.
8. All samples of mixture laser dyes possess large linear and nonlinear optical properties as compared with samples of pure laser dyes, as a result it can be used as optical and photonic devices.
9. The nonlinear optical properties of all samples of Fluorescein dye are larger than those for Coumarin (344) dye.

10.The nonlinear refractive index for Coumarin (344) shows the behavior of self- focusing and self- defocusing for Fluorescein and mixture laser dye, and two photon absorption in nonlinear absorption coefficient .

11.The nonlinear absorption coefficient for all thin films of laser dyes and their mixtures show saturable absorption phenomena.

12. Fluorescence intensity of all samples of Coumarin (344), Fluorescein and mixture laser dye increasing linearly with increasing of concentrations.

13.Fluorescence spectra of thin films have narrower band width than dyes as solutions also the emission peaks are higher intensity than solutions.

14.The decrease in the value of quantum efficiency with the increase in concentration for all prepared samples.

15. Fluorescence spectra of solution of mixture laser dyes with mixing ratio (4:1)and concentration (7×10^{-5})M are higher than the other ratios and concentrations, as a result it can be used as active laser medium.

16. Optical limiting properties of all samples of Fluorescein dye are better than Coumarin (344) dye.

17. Optical limiting properties increase with decreasing concentrations for all samples.

18. Optical limiting properties of mixture dyes as solutions and thin films are better than those for pure dyes.

19. Optical limiting properties of laser dyes doped with polymer PVA and nanoparticles Ag are better than thin films doped with Al_2O_3nanoparticles, as a result it can be used as better optical limiting in electro-optical devices.

4.11 The Suggestions and Future Works

In this context, a further investigation can be suggested as future works:

1. Studying spectral linear and nonlinear optical properties of mixture dyes solution with another types of solvents at different concentrations.
2. Studying nonlinear optical properties of dyes using lasers with different wave lengths and different laser powers.
3. Studying effect for adding another types of polymer and nanoparticles on spectral, linear and non-linear of new mixture of other laser dyes.

4.8 Nonlinear Optical Properties of Coumarin (334) , Fluorescein Organic Laser Dyes and their mixture (as Thin Films)

The nonlinear optical properties were investigated of Fluorescein ,Coumarin (334) (CO and FL) organic laser dyes and mixture of them with ratios (1:1, 2:1, 3:1 and 4:1) as solutions at different concentration's (1×10^{-5}, 3×10^{-5}, 5×10^{-5} and 7×10^{-5}) M and thin films with (PVA polymer doped (Ag and Al_2O_3) nanoparticles) at concentration (10^{-3})M using continuous wave (CW) diode pump solid state laser at wavelength (457 nm) and power (84mW). There are two parts were used to measure the nonlinear properties of the material by Z-Scan technique. The first part is open-aperture Z-Scan and the second part is the closed-aperture Z-Scan.

4.8.1 Nonlinear Refractive Index of Coumarin (334) , Fluorescein Organic Laser Dyes and their mixture (as Thin Films)

The nonlinear refractive index of Fluorescein and Coumarin (334) organic laser dyes and mixture of them with ratios (1:1, 2:1, 3:1 and 4:1) as solutions at different concentration's (1×10^{-5}, 3×10^{-5}, 5×10^{-5} and 7×10^{-5}) M and thin films doped with (PVA polymer and (Ag ,Al_2O_3) nanoparticles) at concentration (10^{-3}) were measured by closed-aperture Z-Scan technique.

The normalized transmittances of Z-Scan measurements as a function of distance in (Ethanol) solvent for Coumarin (334) is shown in Figures (4.41). the nonlinear effect region is extended from (-2) mm to (2) mm. The valley followed by peak a transmittance curve obtained from the closed aperture Z-Scan data indicates that the sign of the refraction nonlinearity is positive ($n_2 > 0$), leading to self-focusing lensing in these samples.

The normalized transmittances of Z-Scan measurements as a function of distance in (Ethanol) solvent for Fluorescein organic laser dyes and mixture of

them as shown in Figures (4.42- 4.48) the nonlinear effect region is extended from (-2) mm to (2) mm. The peak followed by a valley transmittance curve obtained from the closed aperture Z-Scan data indicates that the sign of the refraction nonlinearity is negative ($n_2 < 0$), leading to self-defocusing lensing in these samples it.The valley-peak configuration indicates the positive sign of n_2 .The scan started from distance far away from the focus, the beam The scan started with a linear behavior at different distances from the far field of the sample position (-Z) with respect to the focal plane at Z=0 mm. The behavior of z-scan curves was in good agreement with [37]. In order to describe the Z-Scan behavior in the previous Figures, when the sample moves far from the focus, the transmitted beam intensity is low and the transmittance remains relatively constant.

As the sample approaches the beam focus, intensity increases, leading to self-lensing in the sample tend to collimate the beam on the aperture in the far field, increasing the measured transmittance at the iris position. If the beam experiences any nonlinear phase shift due to the sample as it is translated through the focal region, then the fraction of light falling on the detector will vary due to the self-lensing generated in the material by the intense laser beam. In this case, the signal measured by detector will exhibit a peak and valley as the sample is translated [132].The position of the peak and valley, relative to the z-axis, depends on the sign of the nonlinear phase shift .Where the change in the normalized transmittance from the peak of the curve to the valley (ΔT_{p-v}) is directly proportional to the nonlinear phase shift imparted on the beam. Moreover, if the beam is transmitted through the nonlinear medium the induced phase shift can also be either negative or positive accordingly when the medium is self- defocusing or self-focusing, respectively [51]. The

magnitude of the phase shift can be determined from the change in transmittance between peak and valley. After the focal plane, the self-defocusing increases the beam divergence, leading to a widening of the beam at the focus and thus reducing the measured transmittance. Far from focus (Z > 0), again the nonlinear refraction is low resulting in a transmittance Z-independent . The nonlinearity of doped dyes is larger than those for pure dyes. As well as thin films possess very large nonlinearity as compared with dyes as solution. The relation between the nonlinear refractive index and the nonlinear phase shift is a linear increasing relation. Z-Scan measurements indicated that pure and dye doped and their thin films exhibited negative nonlinear refractive index , it agree with reference [131].

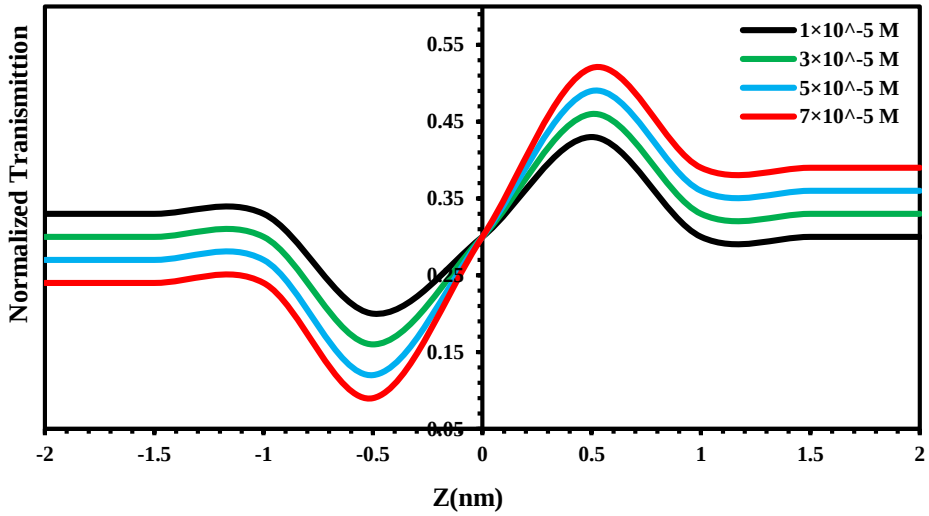

Figure (4.41):Closed-aperture Z-Scan data at different concentrations of Coumarin 334 organic laser dye in Ethanol solvent.

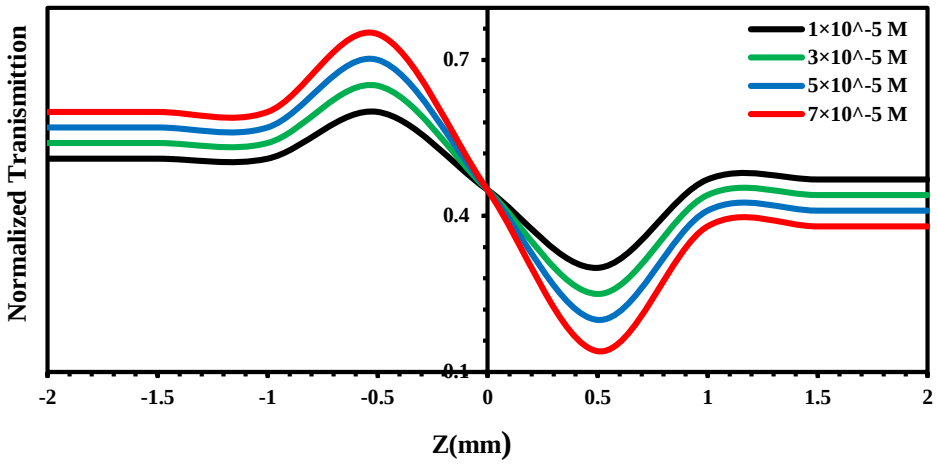

Figure (4.42): Closed-aperture Z-Scan data at different concentrations of Fluorescein organic laser dye in Ethanol solvent.

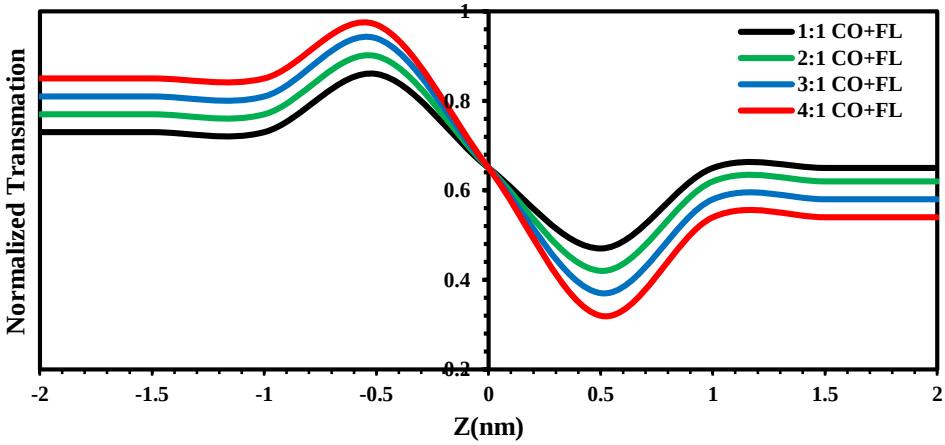

Figure (4.43): Closed-aperture Z-Scan data for different ratios of mixing of (CO+FL) organic laser dyes in Ethanol solvent at concentration (3×10^{-5})M.

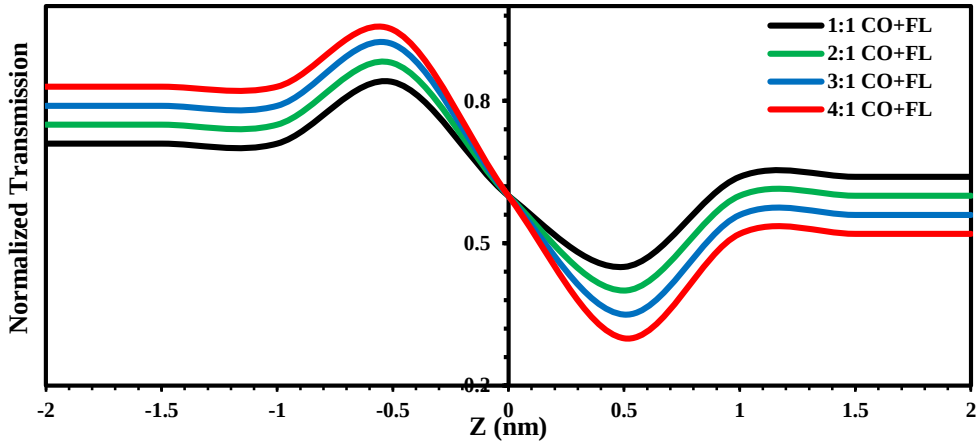

Figure (4.44): Closed-aperture Z-Scan data for different ratios of mixing of (CO+FL) organic laser dyes in (Ethanol) solvent at concentration (5×10^{-5}) M.

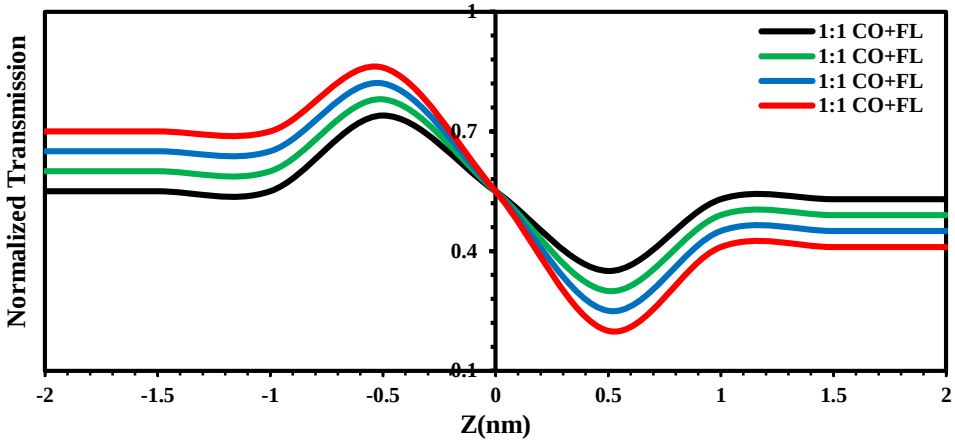

Figure (4.45): Closed-aperture Z-Scan data for different ratios of mixing of (CO+FL) organic laser dyes in Ethanol solvent at concentration (7×10^{-5}) M.

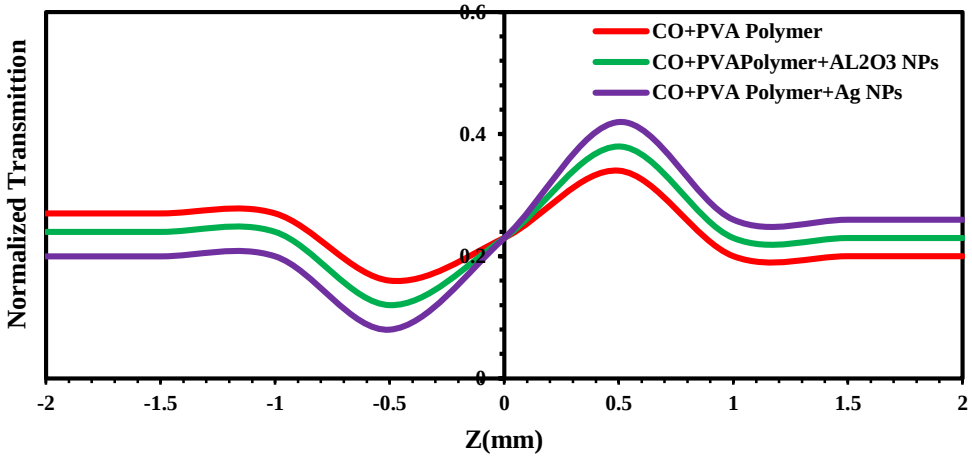

Figure (4.46): Closed-aperture Z-Scan data for thin films of Coumarin 334 organic laser dye with PVA polymer doped (Al_2O_3 , Ag) NPs.

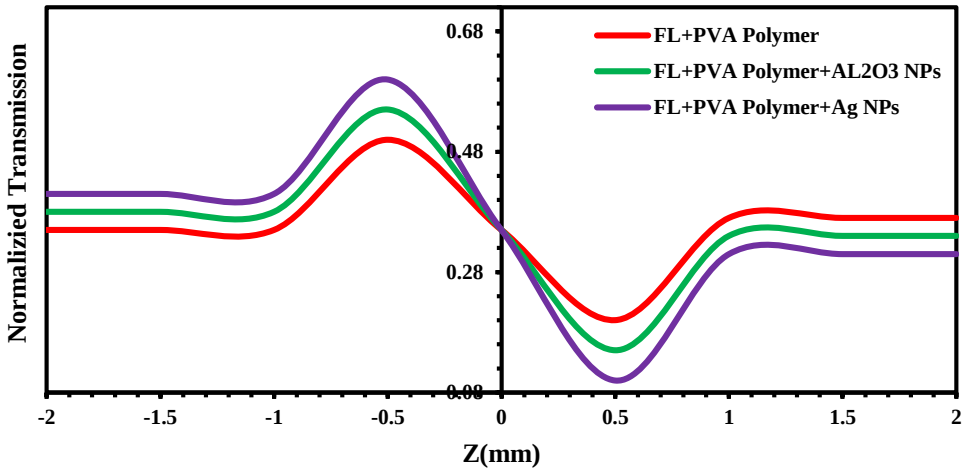

Figure (4.47): Closed-aperture Z-Scan data for thin films of Fluorescein organic laser dye with PVA polymer doped (Al_2O_3 , Ag) NPs.

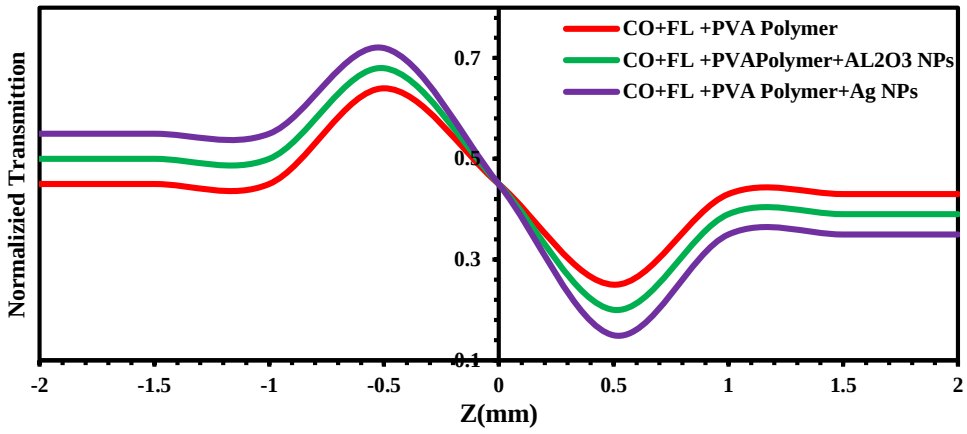

Figure (4.48): Closed-aperture Z-Scan data for thin films of mixing of (CO+FL) organic laser dyes with PVA polymer doped (Al_2O_3 , Ag) NPs.

4.8.2 Nonlinear Absorption Coefficient

The nonlinear absorption coefficient of Fluorescein and Coumarin (334) organic laser dyes and mixture of them with ratios (1:1, 2:1, 3:1 and 4:1) as solutions at different concentration's (3×10^{-5}, 5×10^{-5} and 7×10^{-5}) M and thin films doped with PVA polymer and (Ag, Al_2O_3) nanoparticles at concentration (10^{-3}) M in ethanol solvent, can be measured by performing the open aperture Z-Scan technique at wavelength (457nm) and power (84 mW). The performed open aperture-Scan exhibits an increasing in the transmission about the focus of the lens.

Open-aperture Z-Scan of Fluorescein , Coumarin (334) and mixing of them as solutions are shown in Figures (4.75-4.80). Its noticed (two photon absorption) phenomenon. The behavior of transmittance starts linearly at different distances from the far field of the sample position (-Z). At the near field, the transmittance curve begins to decrease until it reaches the minimum value (T_{min}) at the focal point, where Z=0 mm. The transmittance begins to

increase towards the linear behavior at the far field of the sample position (+Z). The change of intensity, in this case, is caused by two photon absorption when in the sample travels through beam waist. This behavior agrees with reference [145].The open-aperture Z-Scan of thin films of Fluorescein and Coumarin (334) organic laser dyes and mixture of them with ratios (1:1, 2:1, 3:1 and 4:1) as thin films doped with PVA polymer and Ag , Al_2O_3 nanoparticles at concentration (10^{-3}) M in ethanol solvent are defines variable transmittance values, which was used to determine absorption coefficient. Saturable absorption phenomenon was observed for open-aperture Z-Scan technique as shown in Figures (4.49-4.56).

The behavior of transmittance curves starts linearly at different distance from the far field of the sample position (-Z). At the near field the transmittance curve begins to increase until it reaches the maximum value (T_{max}) at the focal point, where Z=0 mm. Afterwards, the transmittance begins to decrease toward the linear behavior at the far field of the sample position (+Z) [12].The transmittance is sensitive to the nonlinear absorption as a function of input power intensity. The change in intensity is caused by saturation absorption in the sample as it travels through the beam waist [148]. In the focal plane where the intensity is greatest, the largest nonlinear absorption is observed. At the far field of the Gaussian beam, where, the beam intensity is too weak to elicit nonlinear effects.

A symmetric peak value is contributed to the negative nonlinear absorption coefficient β, indicates that the sample shows a bleaching-like behavior (saturation of absorption) [148]. The nonlinear parameters are calculated , as tabulated in Tables (4.4- 4.9) these Tables show that the values of nonlinear parameters (n_2 and β) for Fluorescein , Coumarin (334) organic laser dyes and

mixture of them with ratios (1:1, 2:1, 3:1 and 4:1) as solutions are increased but β decreased with increasing the concentrations, as increasing the values of linear parameters (α_o and n_o). This is due to decreasing number of molecules per volume unit at low concentrations[149].The closed-aperture Z-Scan defines variable transmittance values, which used to determine the nonlinear phase shift $\Delta\Phi$ using equation (2.18) and the nonlinear refractive index (n_2) using equation (2.17), nonlinear absorption coefficient (β) using equation (2.18), as listed in Tables (4.4-4.7) respectively. Thin films of all samples were exhibited better nonlinearity than liquid samples.

This is suggested to be take place due to the $\pi-\pi^*$ stacking in supramolecular interactions between delocalized electrons in solid samples. In addition, in the case of thin films, the molecule orientation is crucial where molecules can be arranged either by homotopic alignment or columnar stacking on the substrate as almost organic dyes are self-organized materials [51]. The nonlinearity of doped dyes are larger than those for pure dyes agree with [144]. As well as thin films of Fluorescein and Coumarin (334) organic laser dyes and mixture of them with ratios (4:1) possess very large nonlinearity as compared with dyes as solution. This is due to increasing number of molecules per volume unit at high concentrations, as well as thin films have thickness larger than dyes as solutions, which is lead to increasing the nonlinear phase shift agree with [150]. The results showed that the nonlinear optical properties of the films with doped nanoparticles were higher than the films without nanoparticles.

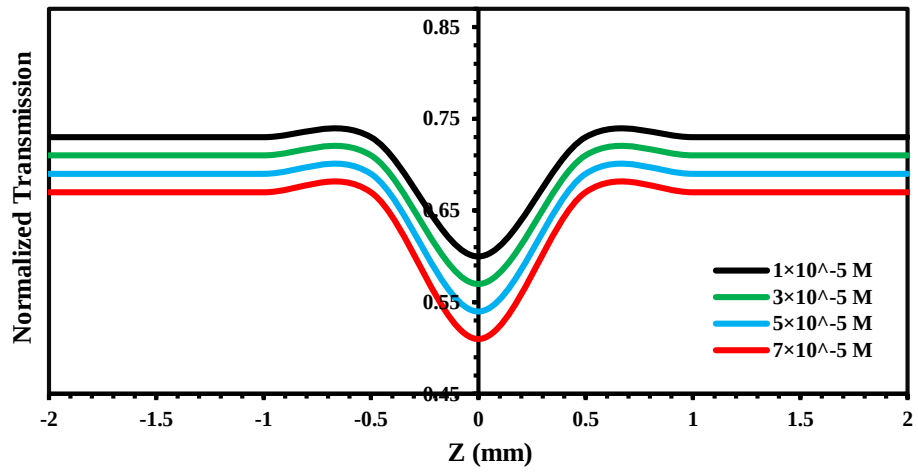

Figure (4.49): Open-aperture Z-Scan data for different concentrations of Coumarin (334) organic laser dye in ethanol solvent.

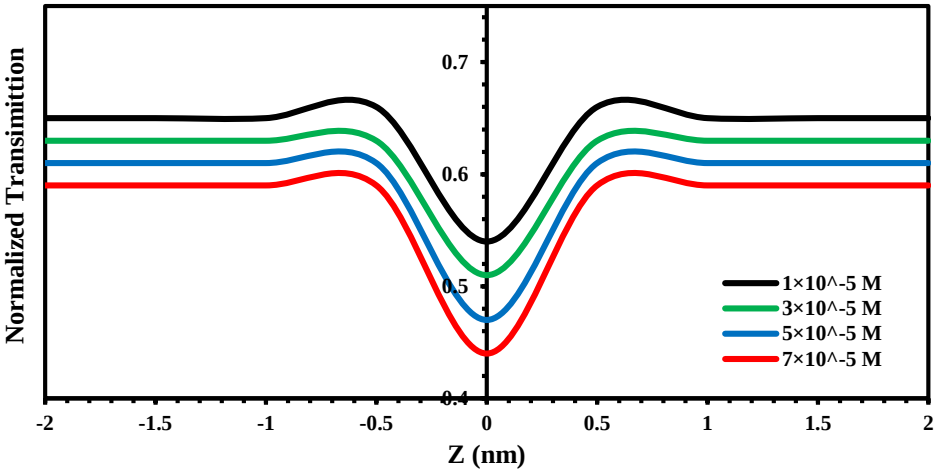

Figure (4.50): Open-aperture Z-Scan data for different concentrations of Fluorescein organic laser dye in ethanol solvent.

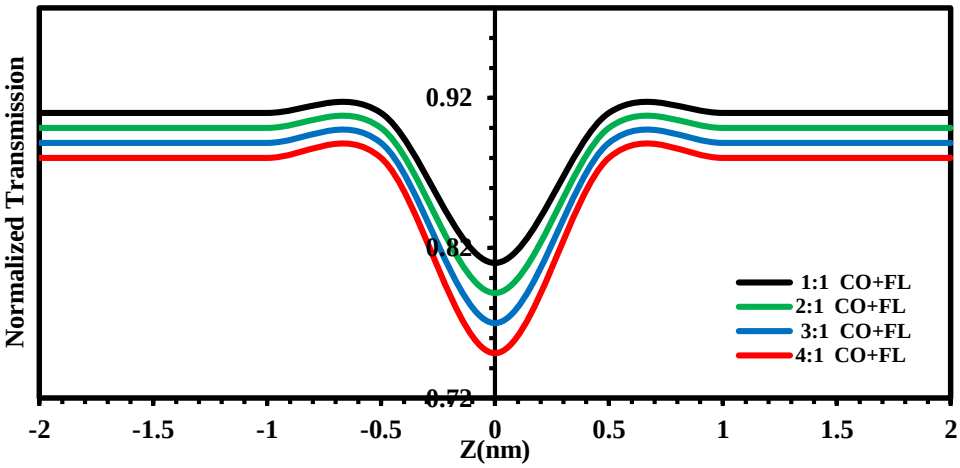

Figure (4.51): Open-aperture Z-Scan data for different ratios of mixing of (CO+FL) organic laser dyes in Ethanol solvent at concentration (3×10^{-5})M.

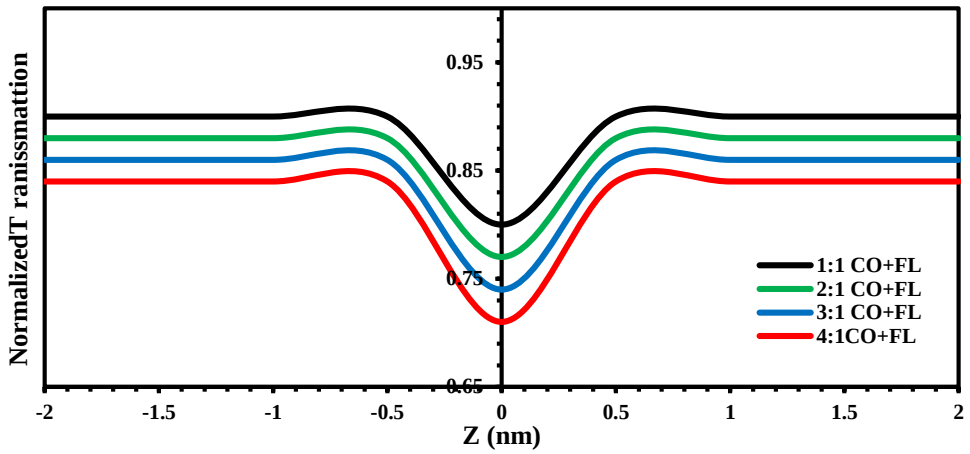

Figure (4.52): Open-aperture Z-Scan data for different ratios of mixing of (CO+FL) organic laser dyes in Ethanol solvent at concentration (5×10^{-5})M.

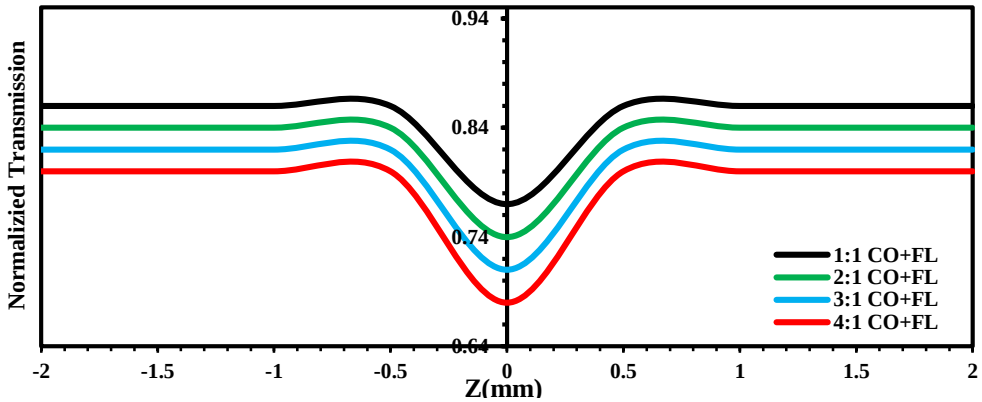

Figure (4.53): Open-aperture Z-Scan data for different ratios of mixing (CO+FL) organic laser dyes in (Ethanol) solvent at concentrations (7×10^{-5})M.

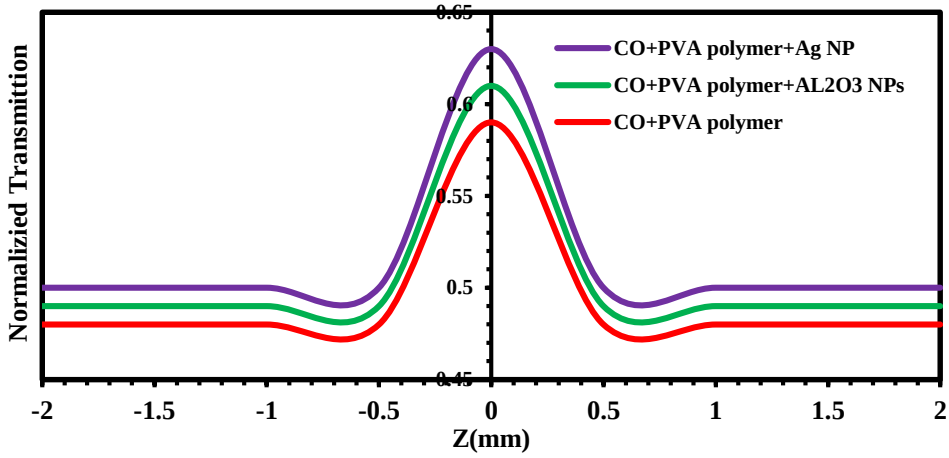

Figure (4.54): Open-aperture Z-Scan data for thin films of Coumarian (334) organic laser dye doped with PVA polymer and (Al_2O_3 , Ag) NPs.

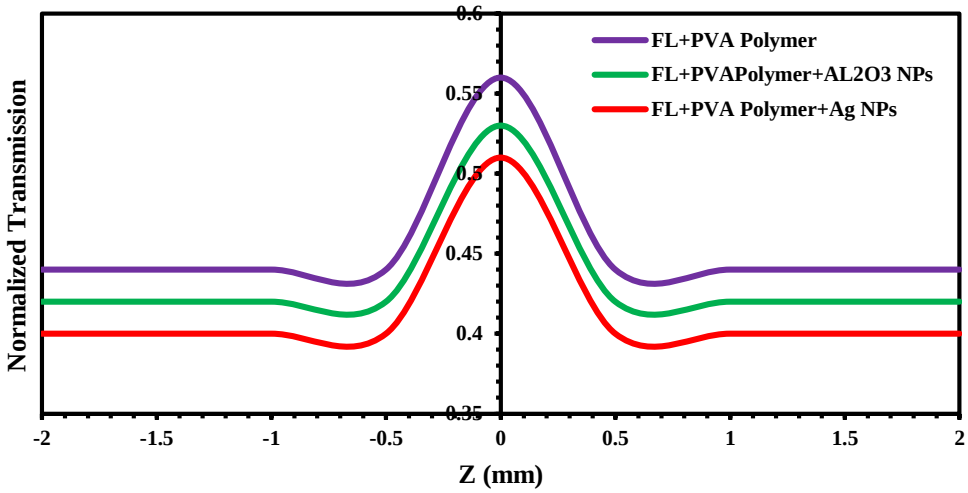

Figure (4.55): Open-aperture Z-Scan data for thin films of Fluorescein organic laser dye doped with PVA polymer and(Al_2O_3 , Ag) NPs.

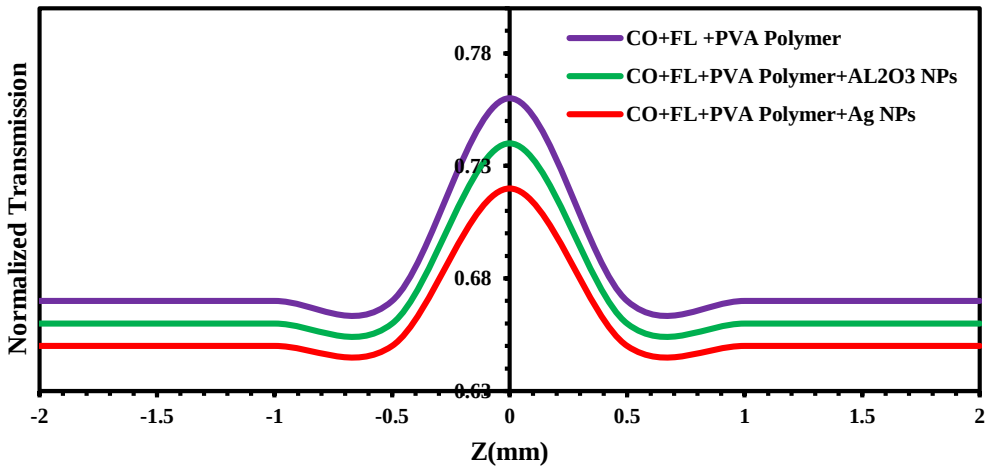

Figure (4.56): Open-aperture Z-Scan data for thin films for mixing of (CO+FL) organic laser dyes doped with PVA polymer and (Al_2O_3 , Ag) NPs.

Table (4.4): Linear and nonlinear optical parameters for different concentrations of Coumarin (344) and its thin films at (λ=457nm).

Material	Concentration (Mol/L)	T	($\alpha_\circ$) cm^{-1}	$n_\circ$	ΔT_{P-V}	n_2 (cm^2/mW)	T(z)	*B* (cm/mW)
Coumarin (344) (Solutions)	1×10^{-5}	0.9353	0.0667	1.1470	0.011	2.1188×10^{-11}	0.28	0.8392×10^{-3}
	3×10^{-5}	0.8170	0.20208	1.4296	0.024	4.2731×10^{-11}	0.25	1.0786×10^{-3}
	5×10^{-5}	0.7361	0.3062	1.6777	0.031	6.3839×10^{-11}	0.22	1.3073×10^{-3}
	7×10^{-5}	0.5086	0.6759	2.0583	0.043	6.9855×10^{-11}	0.26	1.4265×10^{-3}
CO+PVA polymer (Thin films)	1×10^{-3}	0.6018	5374.2	1.158	0.110	1.7310^{-7}	0.44	1.245
CO+PVA polymer + Al_2O_3 NPs (Thin films)	1×10^{-3}	0.5717	5971.44	1.1623	0.123	2.3410^{-7}	0.41	2.673

Table (4.5): Linear and nonlinear optical parameters for different concentrations of Fluorescein and its thin films at(λ=457nm).

Material	Concentration (Mol/L)	T	($\alpha_\circ$) cm^{-1}	$n_\circ$	ΔT_{P-V}	n_2 (cm^2/mW)	T(z)	*β* (cm/mW)
Fluorescein (Solutions)	1×10^{-5}	0.8016	0.2210	1.2931	0.0277	3.5016×10^{-11}	0.56	1.2947×10^{-3}
	3×10^{-5}	0.7194	0.3293	1.4955	0.0361	5.5024×10^{-11}	0.51	1.4198×10^{-3}
	5×10^{-5}	0.5760	0.5515	1.7849	0.0416	7.6834×10^{-11}	0.41	1.5068×10^{-3}
	7×10^{-5}	0.4714	0.7519	1.9216	0.0527	8.5168×10^{-11}	0.38	1.6264×10^{-3}
FL+PVA polymer (Thin films)	1×10^{-3}	0.6748	6396.33	1.1652	0.132	2.9110^{-7}	0.70	2.023
FL+PVA polymer + Al_2O_3NPs (Thin films)	1×10^{-3}	0.6402	6806.97	1.1852	0.154	3.8910^{-7}	0.67	3.765
FL+PVA polymer + AgNPs (Thin films)	1×10^{-3}	0.6130	7589.42	1.1920	0.162	4.5910^{-7}	0.65	4.567

Table (4.6): Linear and nonlinear optical parameters for solutions of mixture of Coumarin 344 and Fluorescein dyes at different mixing ratios at concentrations (3×10^{-5} , 5×10^{-5} and 7×10^{-5})M at (λ=457nm).

Material	Mixing Ratios	T	($\alpha_\circ$) cm^{-1}	$n_\circ$	ΔT_{P-V}	n_2 (cm^2/mW)	T(z)	*B* (cm/mW)
Mixture of (CO+FL) at (3×10^{-5}) M	1:1	0.7708	0.2602	1.3935	0.022	6.7122×10^{-11}	0.88	2.76×10^{-3}
	2:1	0.7260	0.3201	1.4243	0.024	8.2243×10^{-11}	0.86	2.70×10^{-3}
	3:1	0.7169	0.3327	1.7072	0.040	10.8465×10^{-11}	0.83	2.69×10^{-3}
	4:1	0.7050	0.3494	1.7594	0.060	13.2376×10^{-11}	0.81	2.64×10^{-3}
Mixture of (CO+FL) at (5×10^{-5}) M	1:1	0.6497	0.4312	1.496	0.038	8.5382×10^{-11}	0.86	2.89×10^{-3}
	2:1	0.5497	0.5734	1.7675	0.043	10.0725×10^{-11}	0.85	2.85×10^{-3}
	3:1	0.5603	0.6120	1.8627	0.055	13.8256×10^{-11}	0.83	2.80×10^{-3}
	4:1	0.5694	0.6195	1.9996	0.065	17.6725×10^{-11}	0.82	2.78×10^{-3}
Mixture of (CO+FL) at (7×10^{-5}) M	1:1	0.5671	0.5671	1.7853	0.046	10.6356×10^{-11}	80	3.21×10^{-3}
	2:1	0.5635	0.6480	1.7901	0.054	13.8876×10^{-11}	81	3.15×10^{-3}
	3:1	0.5422	0.7792	1.8273	0.065	17.7945×10^{-11}	79	3.02×10^{-3}
	4:1	0.5382	0.8630	1.9843	0.732	18.5352×10^{-11}	76	2.98×10^{-3}

Table (4.7): Linear and nonlinear optical parameters for thin films of Coumarin 344 and Fluorescein dyes at different mixing ratios at concentration (10^{-3} M) at (λ=457nm).

Material	Mixing Ratios	T	($\alpha_\circ$) cm^{-1}	$n_\circ$	ΔT_{P-V}	n_2 (cm^2/mW)	T(z)	*B* (cm/mW)
Mixture doped with PVA polymer	4:1	0.7281	7783. 03	1.3146	0.203	11.4110^{-7}	0.34	4.472
Mixture doped with PVA polymer and AL_2O_3 NPs	4:1	0.3547	8216.11	1.5964	0.258	13.3210^{-7}	0.32	5.738
Mixture doped with PVA polymer and Ag NPs	4:1	0.2159	8923.95	1.620	0.291	15.12310^{-7}	0.30	7.52

4.9 Optical Limiting Behavior of organic Dyes

The optical limiting behavior of Fluorescein and Coumarin (334) organic laser dyes and mixture of them with ratios (1:1, 2:1, 3:1 and 4:1) as solutions at different concentration's (3×10^{-5}, 5×10^{-5} and 7×10^{-5}) M and thin films doped with (PVA polymer and (Ag ,Al_2O_3) nanoparticles) at concentration (10^{-3}) M were performed by closed-aperture Z-Scan with the same laser used in Z-Scan technique. Figures (4.57-4.64) give the optical limiting characteristics at room temperature (25-30)C° for all samples were dissolved in (Ethanol) solvent respectively. The samples show very good optical limiting behavior arising from nonlinear refraction. The output power rises initially with the increasing in input power, but after a certain threshold value, the sample starts defocusing the beam resulting in a greater part of the beam cross-section being cut off by the aperture. Thus, the transmittance recorded by the photodetector remained

reasonably constant showing a plateau region agree with [151]. Thin films of Fluorescein , Coumarin and mixing of them with ratios (4:1) give optical power limiting threshold and limiting amplitude less as compared with the materials as solutions, therefore, the optical limiting behavior was significantly optimized in the case of thin films in comparison to liquid specimens and in the polymer and nanoparticles modified dyes in general, as shown in Figures (4.93-4.98). From the threshold intensity for optical limiting for each sample, the optical power limiting threshold is inversely proportional to the concentration, that's mean the properties of the optical limiting be better with increasing the concentrations, as listed in Tables (4.8-4.10) respectively.

Optical limiting protects the human eye by attenuating of the laser beam, this behavior agrees with the study in reference [152]. Fluorescein dissolved in (Ethanol) solvent give optical power limiting threshold and limiting amplitude less as compared with the Coumarin dye (CO), while the mixing with Ag that dissolved in Ethanol solvent give optical power limiting threshold and limiting amplitude less as compared with the pure dyes, therefore, the properties of optical limiting at different concentrations for all samples of mixing (Ag and Al_2O_3) are better than the same samples of dyes (CO and FL) as pure dyes. The threshold of the optical limiting on the axis of the out power and the amplitude of the limiting on the axis of the input power can be measure using the tangent of the beginning of the bending the curve in figures (4.87-4.98), where the lower the threshold and amplitude of the optical limiting, the more suitable the sample is to do as optical limiting.

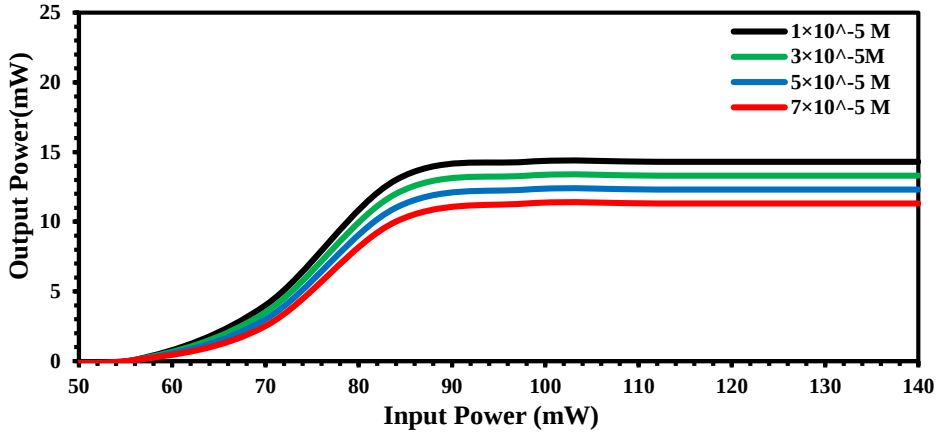

Figure (4.57): The optical limiting response of Coumarin 334 organic laser dye at different concentrations in Ethanol solvent.

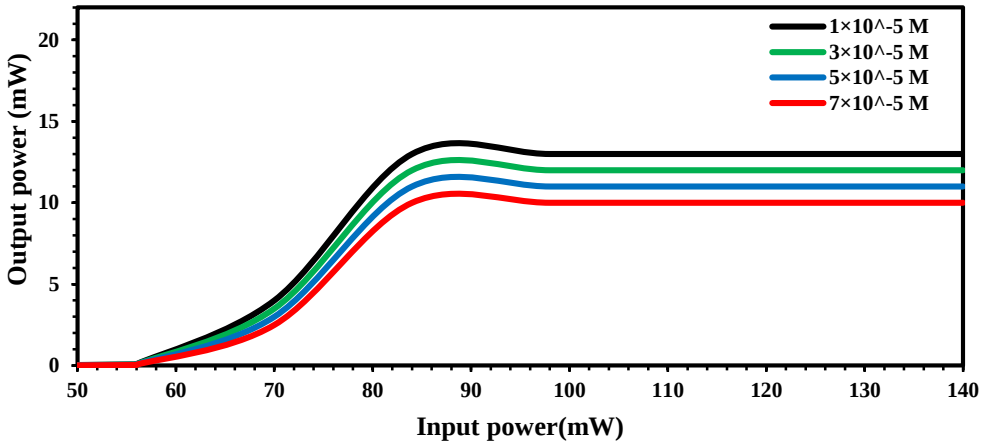

Figure (4.58): The optical limiting response of Fluorescein organic laser dye at different concentrations in Ethanol solvent.

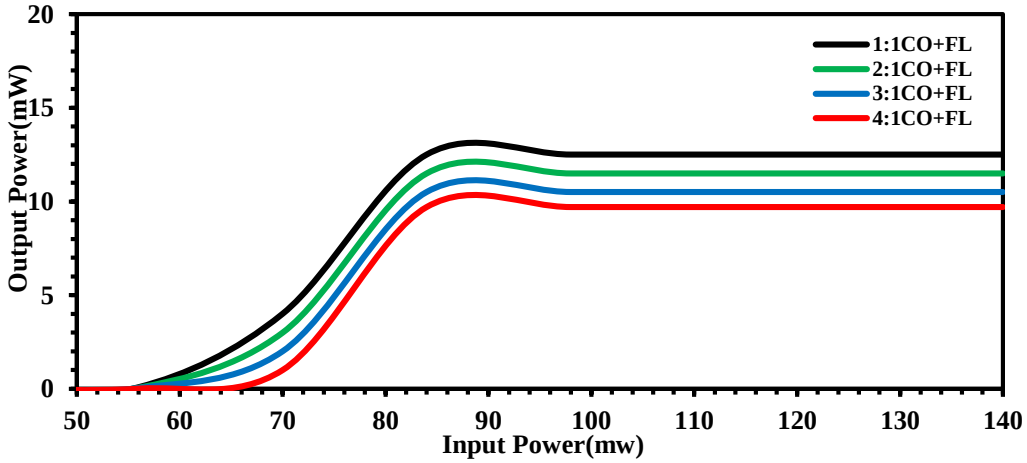

Figure (4.59): The optical limiting response for different ratios of mixing (CO+FL) organic laser dyes in Ethanol solvent at concentration (3×10^{-5})M.

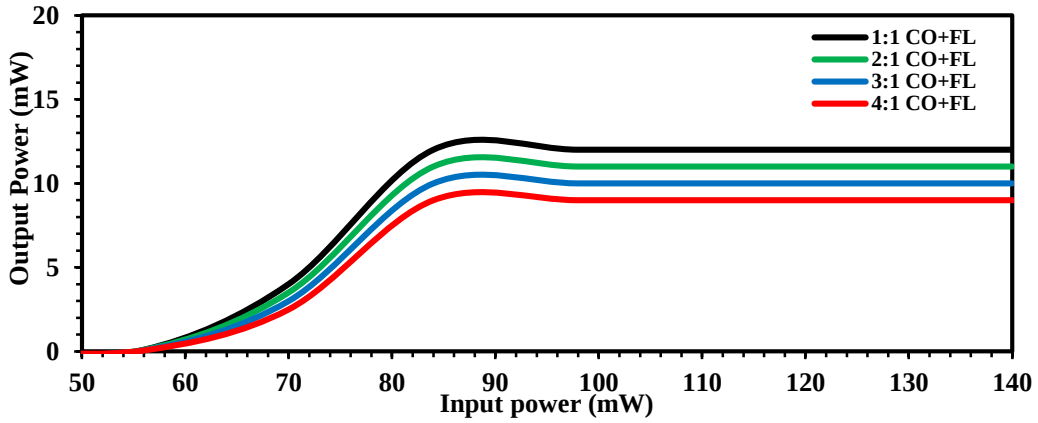

Figure (4.60): The optical limiting response for different ratios of mixing (CO+FL) organic laser dyes in Ethanol solvent at concentration (5×10^{-5}) M.

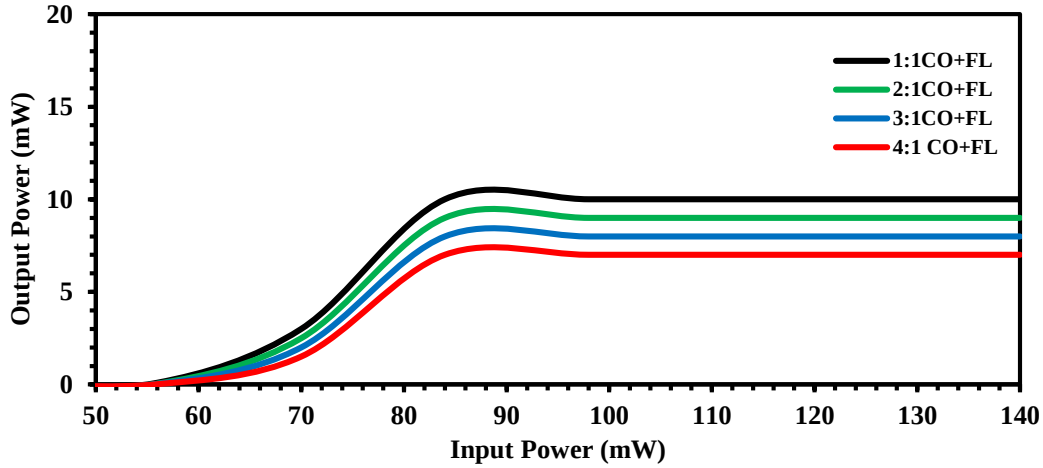

Figure (4.61): The optical limiting response for different ratios of mixing (CO+FL) organic laser dyes in Ethanol solvent at concentration (7×10^{-5}) M.

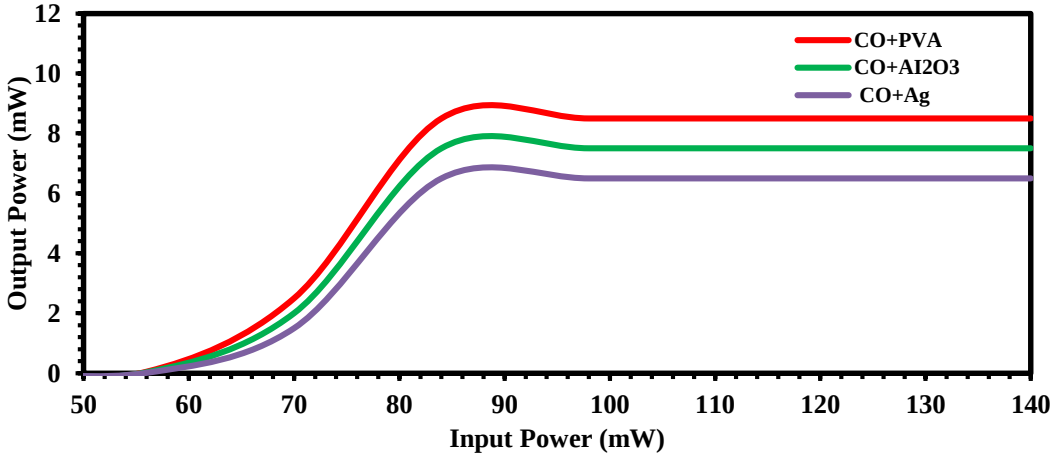

Figure (4.62): The optical limiting response of thin films of Coumarin 334 organic laser dye doped with PVA polymer and(Al_2O_3 , Ag) NPs.

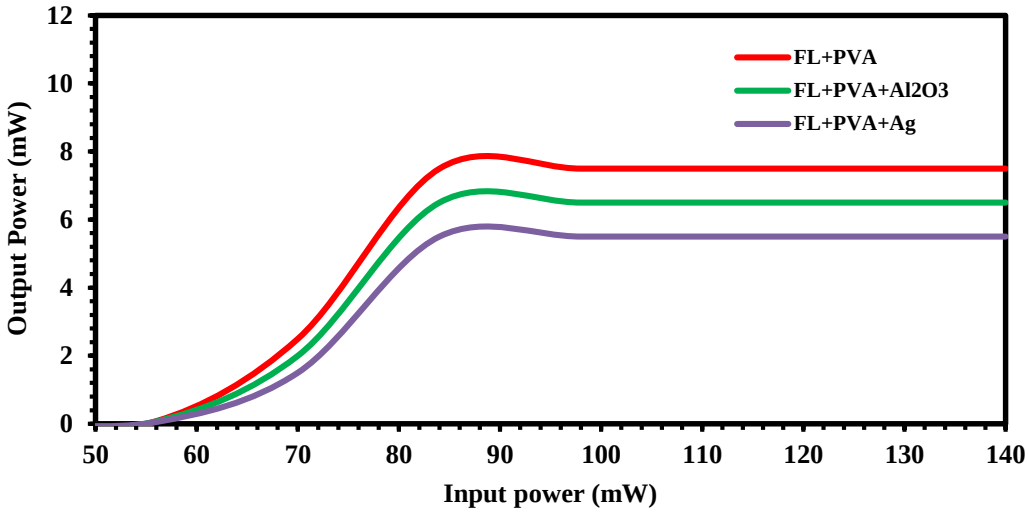

Figure (4.63): The optical limiting response of thin films of Fluorescein organic laser dye doped with PVA polymer and (Al_2O_3 , Ag)NPs

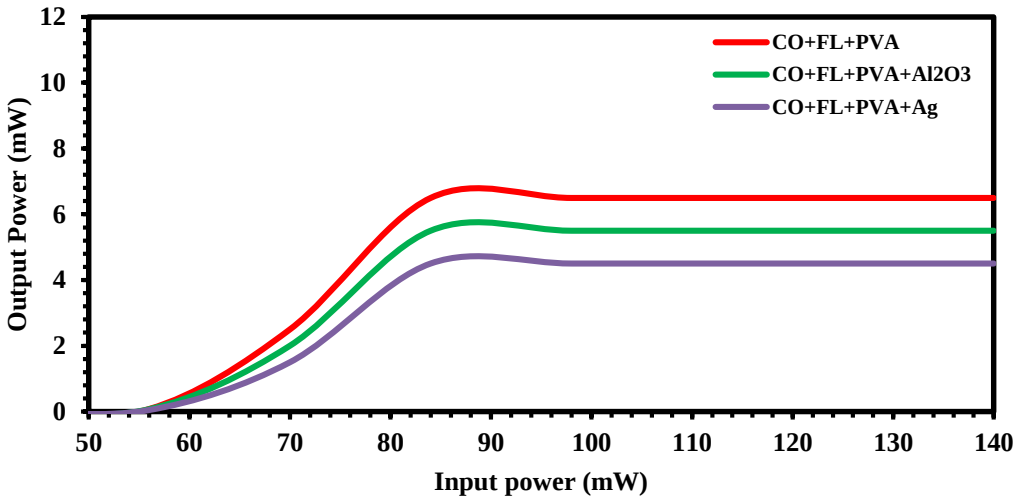

Figure (4.64): The optical limiting response of thin films of mixing of (CO+FL) organic laser dyes doped with PVA polymer and (Al_2O_3 , Ag)NPs.

Table (4.8): The optical limiting response of Fluorescein and Coumarin 344 organic laser dyes at different concentrations.

Material	Concentration (M)	Limiting Threshold (mw)	Limiting Amplitude (mw)
Fluorescein	1×10^{-5}	14.8	100
	3×10^{-5}	13.7	98
	5×10^{-5}	12.4	97
	7×10^{-5}	11.2	96
Coumarin (344)	1×10^{-5}	18	105
	3×10^{-5}	16.2	104
	5×10^{-5}	14	103
	7×10^{-5}	11.4	101

Table (4.9): The optical limiting response of mixture of Coumarin 344 and Fluorescein organic laser dyes at different mixing ratios as solutions and different concentrations.

Material	Concentration (M)	Limiting Threshold (mw)	Limiting Amplitude (mw)
Mixture (CO+FL) at (3×10^{-5}) M	1:1	14.9	89
	2:1	13.5	88.4
	3:1	12.4	88
	4:1	11.2	87.5
Mixture (CO+FL) at (5×10^{-5}) M	1:1	13.5	87
	2:1	12.4	87
	3:1	11.6	86.4
	4:1	9.8	86
Mixture (CO+FL) at (7×10^{-5}) M	1:1	10.8	85
	2:1	9.7	84.3
	3:1	8.5	84
	4:1	7.2	83

Table (4.10): The optical limiting response of mixture of Coumarin 344 and Fluorescein organic laser dyes at different ratios as thin films doped with PVA polymer and (Ag,Al_2O_3) nanoparticles at (7×10^{-5} M).

Material	Limiting Threshold (mw)	Limiting Amplitude (mw)
Thin Film of FL+PVA polymer	11	87.8
Thin Film of FL+PVA polymer +AL_2O_3 NPs	9.4	87
Thin Film of FL+PVA polymer +Ag NPs	8.5	86
Thin Film of CO+PVA polymer	11.4	89
Thin Film of CO+PVA polymer +Al_2O_3 NPs	9.6	87
Thin Film of CO+PVA polymer +Ag NPs	8.5	86
Thin Film of Mixture CO+FL + PVA polymer	8.2	86
Thin Film of Mixture CO+FL + PVA polymer +Al_2 O_3NPs	7	85
Thin Film Mixture CO+FL + PVA polymer +Ag NPs	6.2	84

4.10. Conclusions

The main conclusions that we have obtained in our research:

1. Preparation of new mixture of two laser organic dyes Fluorescein dye and Coumarin 344 dye in different mixing ratios as solutions and thin films have been successfully by drop-coating method on glass substrate.
2. The grain size of the thin films, calculated from atomic force microscope (AFM) in the range of (18 - 69) nm.
3. The linear and nonlinear optical properties of Fluorescein dye are larger than those for Coumarin 344 dye.
4. The linear and nonlinear optical properties of solution of mixture laser dyes with mixing ratio (4:1) and concentration (7×10^{-5}) M are higher than the other mixing ratios and other concentrations.
5. The linear and nonlinear optical properties of thin films of mixture laser dyes with mixing ratio (4:1) are higher than the other ratios.
6. The linear and nonlinear optical properties of laser dyes doped with polymer PVA and nanoparticles are higher than thin films without doping with nanoparticles .
7. The linear and nonlinear optical properties of all samples of laser dyes doped with PVA polymer and Ag nanoparticles are higher than samples doped with PVA polymer and Al_2O_3 nanoparticles.
8. All samples of mixture laser dyes possess large linear and nonlinear optical properties as compared with samples of pure laser dyes, as a result it can be used as optical and photonic devices.
9. The nonlinear optical properties of all samples of Fluorescein dye are larger than those for Coumarin (344) dye.

10.The nonlinear refractive index for Coumarin (344) shows the behavior of self- focusing and self- defocusing for Fluorescein and mixture laser dye, and two photon absorption in nonlinear absorption coefficient .

11.The nonlinear absorption coefficient for all thin films of laser dyes and their mixtures show saturable absorption phenomena.

12. Fluorescence intensity of all samples of Coumarin (344), Fluorescein and mixture laser dye increasing linearly with increasing of concentrations.

13.Fluorescence spectra of thin films have narrower band width than dyes as solutions also the emission peaks are higher intensity than solutions.

14.The decrease in the value of quantum efficiency with the increase in concentration for all prepared samples.

15. Fluorescence spectra of solution of mixture laser dyes with mixing ratio (4:1)and concentration (7×10^{-5})M are higher than the other ratios and concentrations, as a result it can be used as active laser medium.

16. Optical limiting properties of all samples of Fluorescein dye are better than Coumarin (344) dye.

17. Optical limiting properties increase with decreasing concentrations for all samples.

18. Optical limiting properties of mixture dyes as solutions and thin films are better than those for pure dyes.

19. Optical limiting properties of laser dyes doped with polymer PVA and nanoparticles Ag are better than thin films doped with Al_2O_3nanoparticles, as a result it can be used as better optical limiting in electro-optical devices.

4.11 The Suggestions and Future Works

In this context, a further investigation can be suggested as future works:

1. Studying spectral linear and nonlinear optical properties of mixture dyes solution with another types of solvents at different concentrations.
2. Studying nonlinear optical properties of dyes using lasers with different wave lengths and different laser powers.
3. Studying effect for adding another types of polymer and nanoparticles on spectral, linear and non-linear of new mixture of other laser dyes.

4.8 Nonlinear Optical Properties of Coumarin (334) , Fluorescein Organic Laser Dyes and their mixture (as Thin Films)

The nonlinear optical properties were investigated of Fluorescein and Coumarin (334) (CO and FL) organic laser dyes and mixture of them with ratios (1:1, 2:1, 3:1 and 4:1) as solutions at different concentration's (1×10^{-5},3×10^{-5}, 5×10^{-5} and 7×10^{-5}) M and thin films with (PVA polymer doped (Ag , Al_2O_3) nanoparticles) at concentration (10^{-3}) M using continuous wave (CW) diode pump solid state laser at wavelength (457 nm) and power (84mW). There are two parts were used to measure the nonlinear properties of the material by Z-Scan technique. The first part is open-aperture Z-Scan and the second part is the closed-aperture Z-scan.

4.8.1 Nonlinear Refractive Index of Coumarin (334) , Fluorescein Organic Laser Dyes and their mixture (as Thin Films)

The nonlinear refractive index of Fluorescein , Coumarin (334) organic laser dyes and mixture of them with ratios (1:1, 2:1, 3:1 and 4:1) as solutions at different concentration's (1×10^{-5}, 3×10^{-5}, 5×10^{-5} and 7×10^{-5}) M and thin films with PVA polymer doped (Ag ,Al_2O_3) nanoparticles at concentration (10^{-3}) were measured by closed-aperture Z-Scan technique.

The normalized transmittances of Z-Scan measurements as a function of distance in (Ethanol) solvent for Coumarin (334) is shown in Figures (4.41). the nonlinear effect region is extended from (-2) mm to (2) mm. The valley followed by peak a transmittance curve obtained from the closed aperture Z-Scan data indicates that the sign of the refraction nonlinearity is positive ($n_2 > 0$), leading to self-focusing lensing in these samples [88].

The normalized transmittances of Z-Scan measurements as a function of distance in (Ethanol) solvent for Fluorescein organic laser dyes and mixture of them as shown in Figures (4.42- 4.48) the nonlinear effect region is extended from (-2) mm to (2) mm. The peak followed by a valley transmittance curve obtained from the closed aperture Z-Scan data indicates that the sign of the

refraction nonlinearity is negative ($n_2 < 0$), leading to self-defocusing lensing in these samples The valley-peak configuration indicates the positive sign of n_2 .The scan started from distance far away from the focus, the beam The scan started with a linear behavior at different distances from the far field of the sample position (-Z) with respect to the focal plane at Z=0 mm. The behavior of z-scan curves was in good agreement with [37]. In order to describe the Z-Scan behavior in the previous Figures, when the sample moves far from the focus, the transmitted beam intensity is low and the transmittance remains relatively constant.

As the sample approaches the beam focus, intensity increases, leading to self-lensing in the sample tend to collimate the beam on the aperture in the far field, increasing the measured transmittance at the iris position. If the beam experiences any nonlinear phase shift due to the sample as it is translated through the focal region, then the fraction of light falling on the detector will vary due to the self-lensing generated in the material by the intense laser beam. In this case, the signal measured by detector will exhibit a peak and valley as the sample is translated [117].The position of the peak and valley, relative to the z-axis, depends on the sign of the nonlinear phase shift .Where the change in the normalized transmittance from the peak of the curve to the valley (ΔT_{p-v}) is directly proportional to the nonlinear phase shift imparted on the beam. Moreover, if the beam is transmitted through the nonlinear medium the induced phase shift can also be either negative or positive accordingly when the medium is self- defocusing or self-focusing, respectively [14]. The magnitude of the phase shift can be determined from the change in transmittance between peak and valley. After the focal plane, the self-defocusing increases the beam divergence, leading to a widening of the beam at the focus and thus reducing the measured transmittance. Far from focus ($Z > 0$), again the nonlinear refraction is low resulting in a transmittance Z-independent . The nonlinearity of doped dyes is larger than those for pure dyes. As well as thin films possess very large

nonlinearity as compared with dyes as solution. The relation between the nonlinear refractive index and the nonlinear phase shift is a linear increasing relation. Z-Scan measurements indicated that pure and dye doped and their thin films exhibited negative nonlinear refractive index , it agree with reference [118].

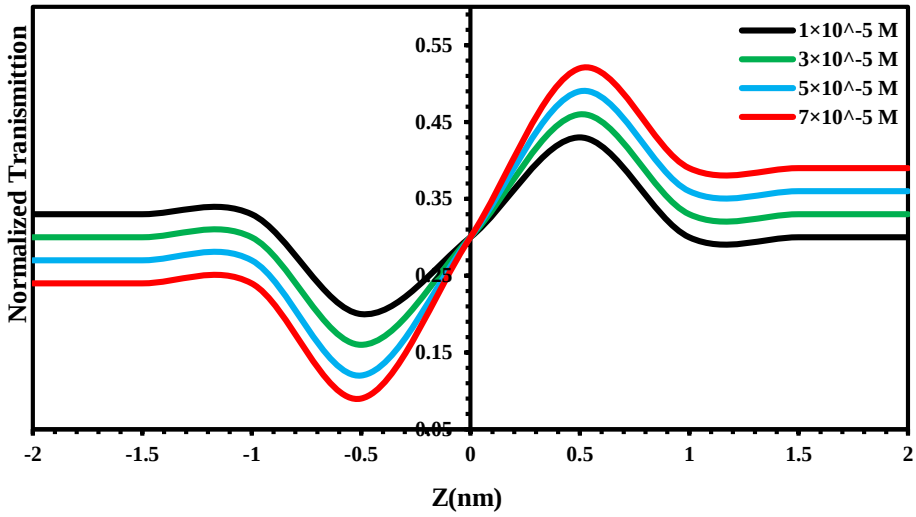

Figure (4.41):Closed-aperture Z-Scan data at different concentrations of Coumarin 334 organic laser dye in Ethanol solvent.

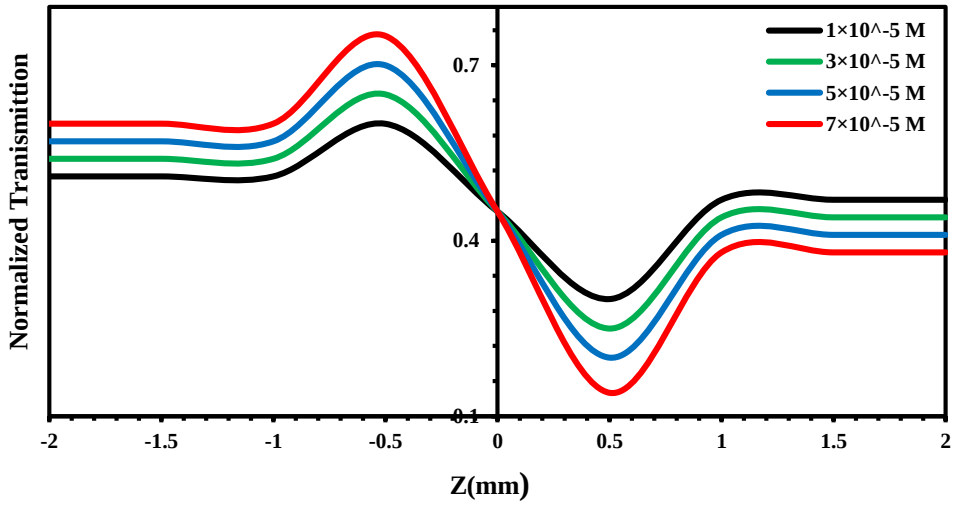

Figure (4.42): Closed-aperture Z-Scan data at different concentrations of Fluorescein organic laser dye in Ethanol solvent.

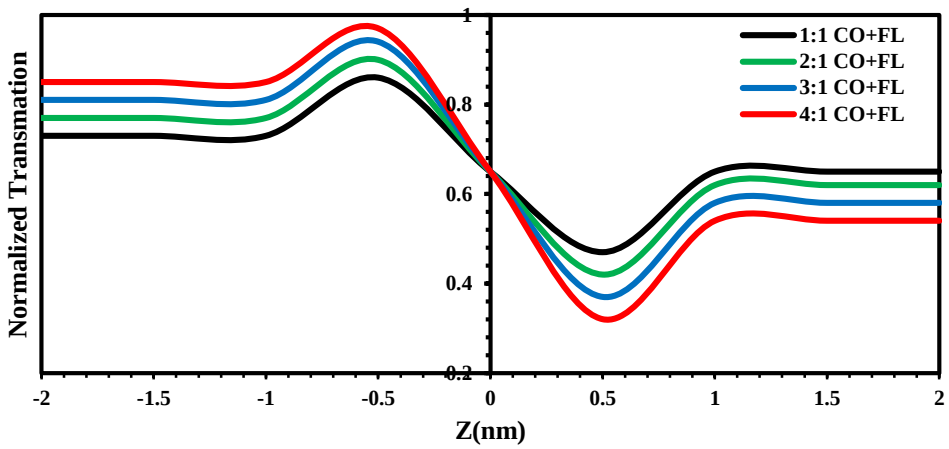

Figure (4.43): Closed-aperture Z-Scan data at different ratios of mixing of (CO+FL) organic laser dyes in Ethanol solvent at concentration (3×10^{-5})M.

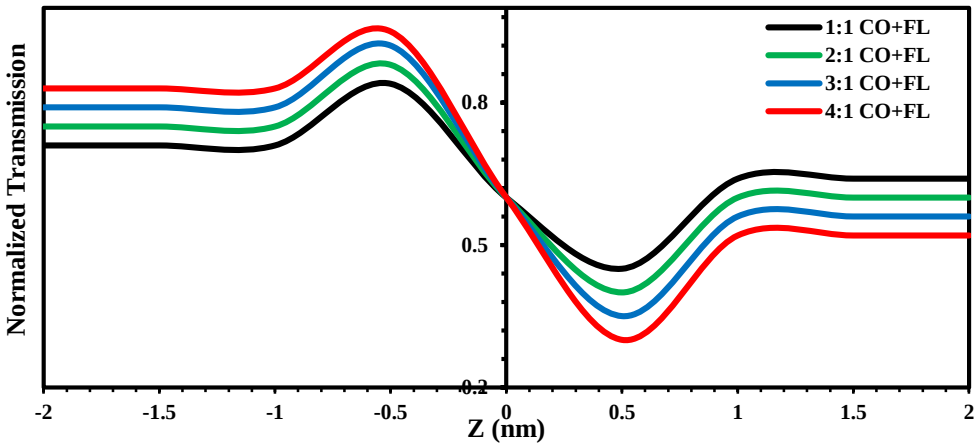

Figure (4.44): Closed-aperture Z-Scan data for different ratios of mixing of (CO+FL) organic laser dyes in (Ethanol) solvent at concentration (5×10^{-5}) M.

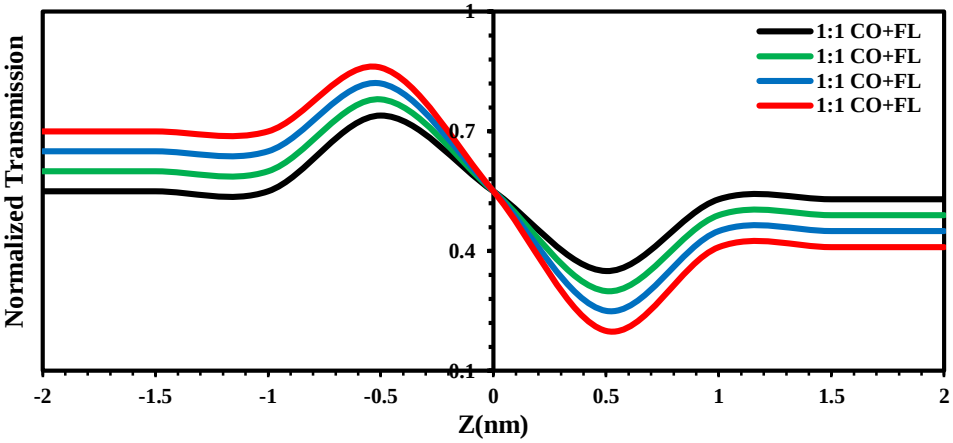

Figure (4.45): Closed-aperture Z-Scan data for different ratios of mixing of (CO+FL) organic laser dyes in Ethanol solvent at concentration (7×10^{-5}) M.

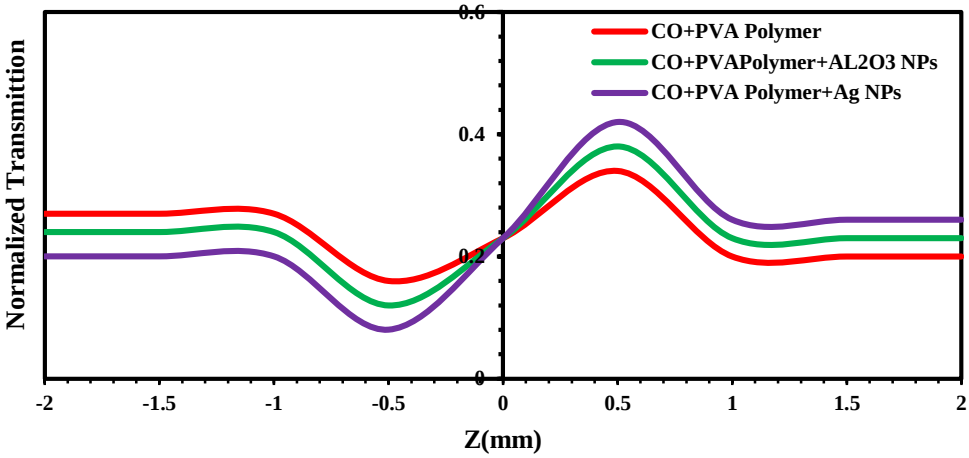

Figure (4.46): Closed-aperture Z-Scan data for thin films of Coumarin 334 organic laser dye with PVA polymer doped (Al_2O_3 , Ag) NPs.

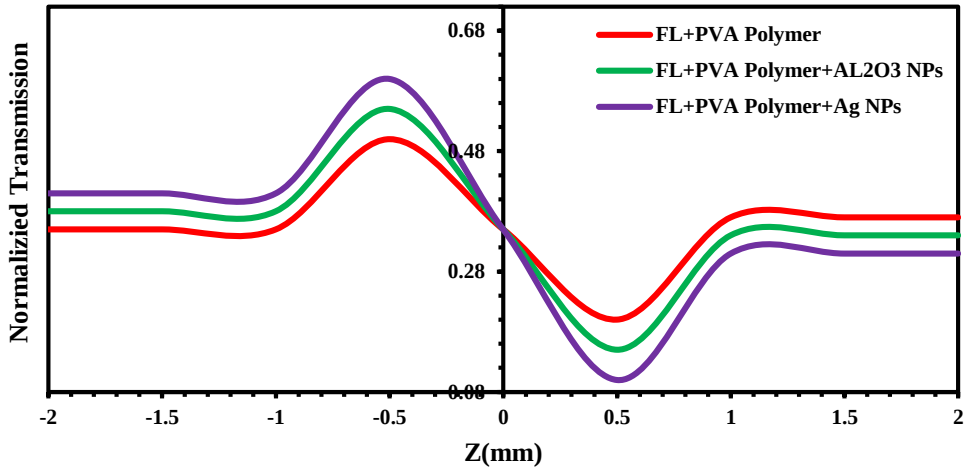

Figure (4.47): Closed-aperture Z-Scan data for thin films of Fluorescein organic laser dye with PVA polymer doped (Al_2O_3 , Ag) NPs.

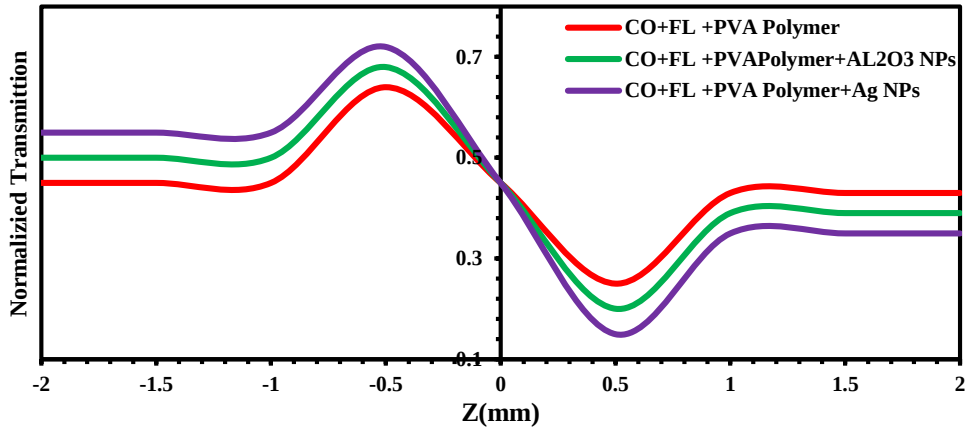

Figure (4.48): Closed-aperture Z-Scan data for thin films of mixing of (CO+FL)organic laser dyes with PVA polymer doped (Al_2O_3 , Ag) NPs.

4.8.2 Nonlinear Absorption Coefficient of Coumarin (334) ,Fluorescein Organic Laser Dyes and their mixture (as Thin Films)

The nonlinear absorption coefficient of Fluorescein and Coumarin (334) organic laser dyes and mixture of them with ratios (1:1, 2:1, 3:1 and 4:1) as solutions at different concentration's (3×10^{-5}, 5×10^{-5} and 7×10^{-5}) M and thin films with PVA polymer doped (Ag, Al_2O_3) nanoparticles at concentration (10^{-3}) M in Ethanol solvent, can be measured by performing the open aperture Z-Scan technique at wavelength (457nm) and power (84 mW). The performed open aperture-Scan exhibits an increasing in the transmission about the focus of the lens.

Open-aperture Z-Scan of Fluorescein , Coumarin (334) and mixing of them as solutions are shown in Figures (4.49-4.56). Its noticed (two photon absorption) phenomenon. The behavior of transmittance starts linearly at different distances from the far field of the sample position (-Z). At the near field, the transmittance curve begins to decrease until it reaches the minimum value (T_{min}) at the focal point, where Z=0 mm. The transmittance begins to increase towards the linear behavior at the far field of the sample position (+Z). The change of intensity, in this case, is caused by two photon absorption when in the sample travels through beam waist. This behavior agrees with reference [88].The open-aperture Z-Scan of thin films of Fluorescein and Coumarin (334) organic laser dyes and mixture of them with ratios (1:1, 2:1, 3:1 and 4:1) as thin films doped with PVA polymer and Ag , Al_2O_3 nanoparticles at concentration (10^{-3}) M in ethanol solvent are defines variable transmittance values, which was used to determine absorption coefficient. Saturable absorption phenomenon was observed for open-aperture Z-Scan technique as shown in Figures (4.54-4.56).

The behavior of transmittance curves starts linearly at different distance from the far field of the sample position (-Z). At the near field the transmittance curve begins to increase until it reaches the maximum value (T_{max}) at the focal point, where Z=0 mm. Afterwards, the transmittance begins to decrease toward

the linear behavior at the far field of the sample position (+Z) .The transmittance is sensitive to the nonlinear absorption as a function of input power intensity. The change in intensity is caused by saturation absorption in the sample as it travels through the beam waist [88]. In the focal plane where the intensity is greatest, the largest nonlinear absorption is observed. At the far field of the Gaussian beam, where, the beam intensity is too weak to elicit nonlinear effects.

A symmetric peak value is contributed to the negative nonlinear absorption coefficient β, indicates that the sample shows a bleaching-like behavior (saturation of absorption) [88]. The nonlinear parameters are calculated , as tabulated in Tables (4.4- 4.7) these Tables show that the values of nonlinear parameters (n_2 and β) for Fluorescein , Coumarin (334) organic laser dyes and mixture of them with ratios (1:1, 2:1, 3:1 and 4:1) as solutions are increased but (β)decreased with increasing the concentrations, as increasing the values of linear parameters (α_o and n_o). This is due to decreasing number of molecules per volume unit at low concentrations[119].The closed-aperture Z-Scan defines variable transmittance values, which used to determine the nonlinear phase shift $\Delta\Phi$ using equation (2.18) and the nonlinear refractive index (n_2) using equation (2.17), nonlinear absorption coefficient (β) using equation (2.18), as listed in Tables (4.4-4.7) respectively. Thin films of all samples were exhibited better nonlinearity than liquid samples.

This is suggested to be take place due to the $\pi-\pi^*$ stacking in supramolecular interactions between delocalized electrons in solid samples. In addition, in the case of thin films, the molecule orientation is crucial where molecules can be arranged either by homotopic alignment or columnar stacking on the substrate as almost organic dyes are self-organized materials. The nonlinearity of doped dyes are larger than those for pure dyes agree with [118]. As well as thin films of Fluorescein , Coumarin (334) organic laser dyes and mixture of them with ratios (4:1) possess very large nonlinearity as compared

with dyes as solution. This is due to increasing number of molecules per volume unit at high concentrations, as well as thin films have thickness larger than dyes as solutions, which is lead to increasing the nonlinear phase shift agree with [115]. The results showed that the nonlinear optical properties of the films with doped nanoparticles were higher than the films without nanoparticles.

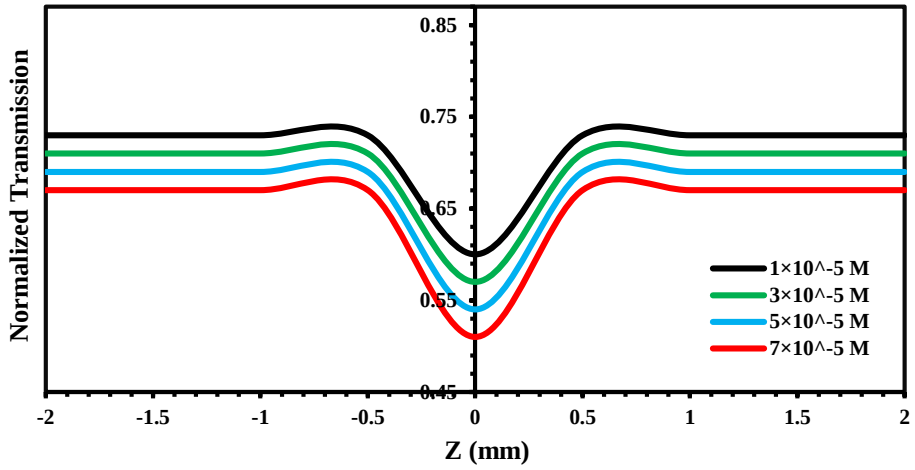

Figure (4.49): Open-aperture Z-Scan data for different concentrations of Coumarin (334) organic laser dye in Ethanol solvent.

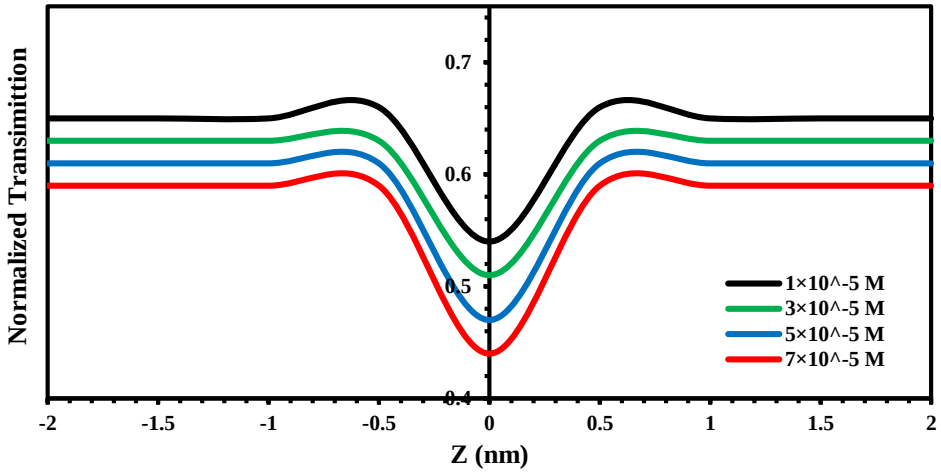

Figure (4.50): Open-aperture Z-Scan data for different concentrations of Fluorescein organic laser dye in Ethanol solvent.

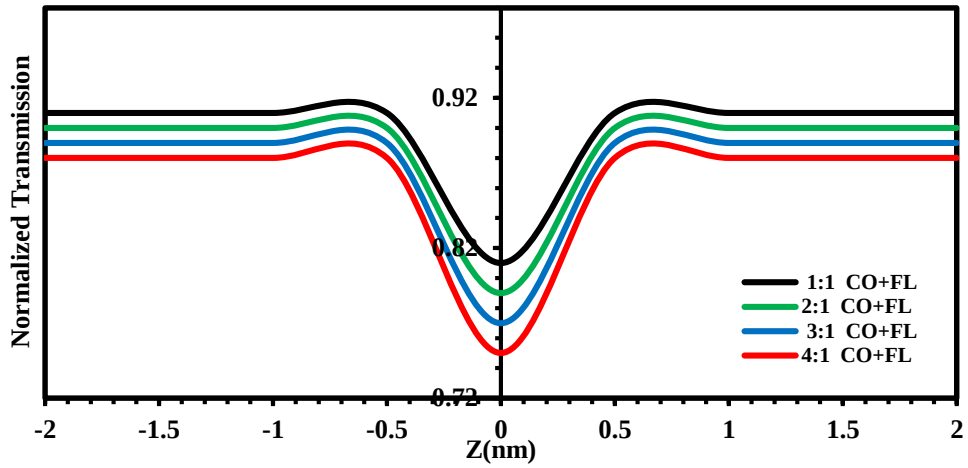

Figure (4.51): Open-aperture Z-Scan data for different ratios of mixing of (CO+FL) organic laser dyes in Ethanol solvent at concentration (3×10^{-5})M.

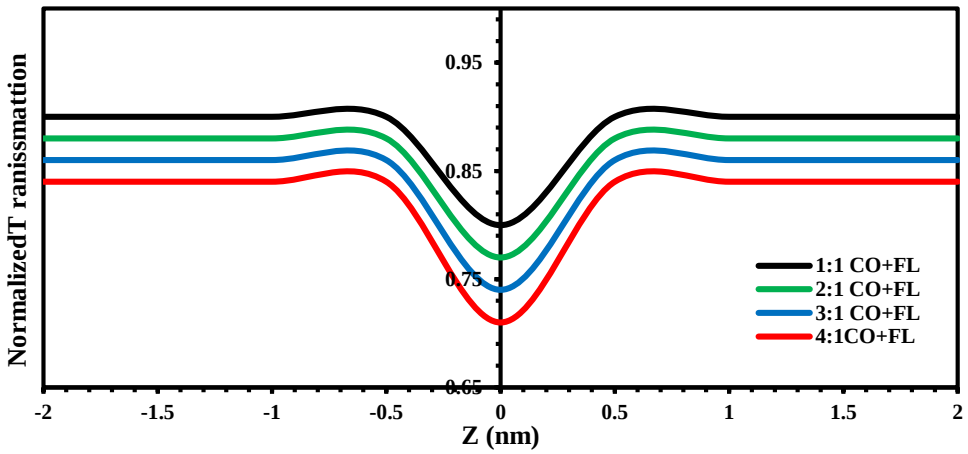

Figure (4.52): Open-aperture Z-Scan data for different ratios of mixing of (CO+FL) organic laser dyes in Ethanol solvent at concentration (5×10^{-5})M.

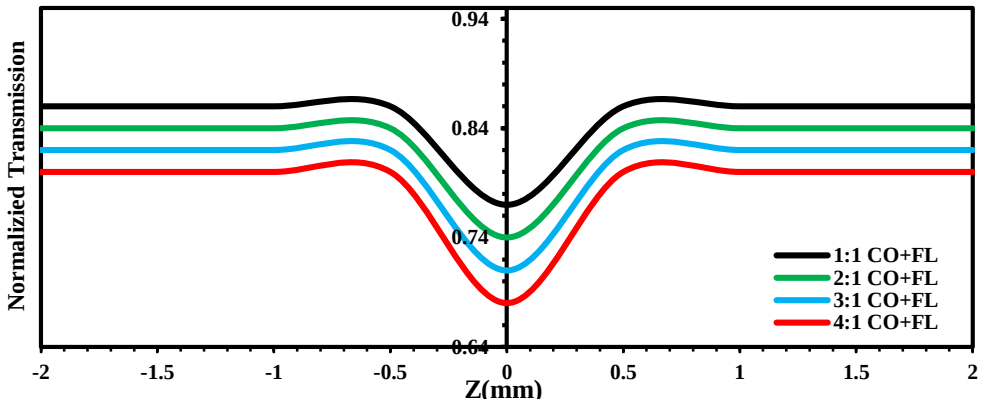

Figure (4.53): Open-aperture Z-Scan data for different ratios of mixing (CO+FL) organic laser dyes in (Ethanol) solvent at concentration (7×10^{-5})M.

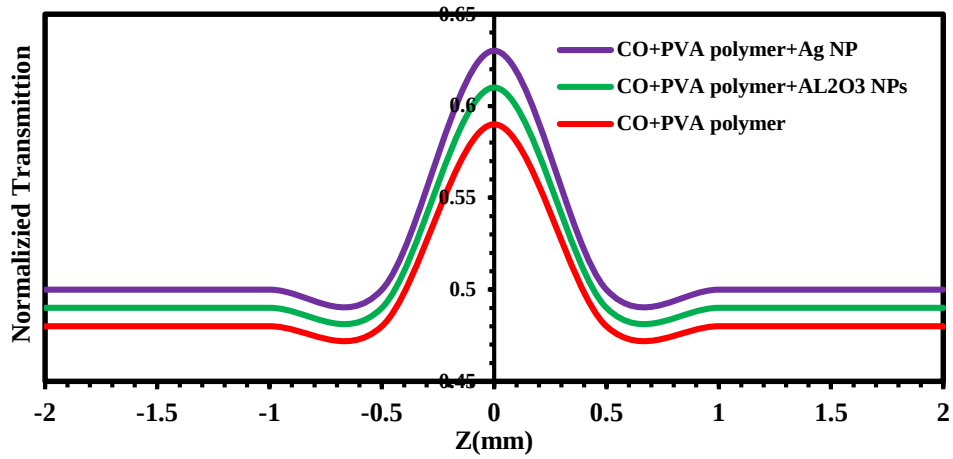

Figure (4.54): Open-aperture Z-Scan data for thin films of Coumarian (334) organic laser dye with PVA polymer doped (Al_2O_3 , Ag) NPs.

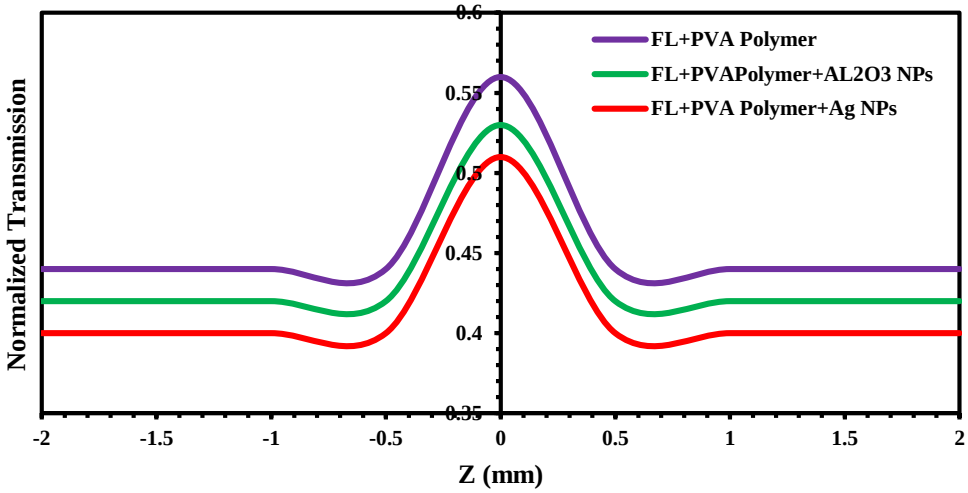

Figure (4.55): Open-aperture Z-Scan data for thin films of Fluorescein organic laser dye with PVA polymer doped (Al_2O_3 , Ag) NPs.

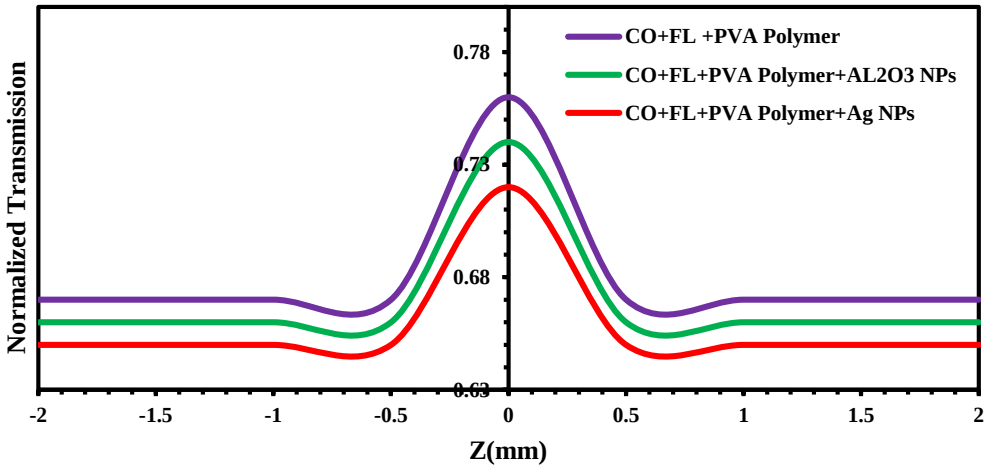

Figure (4.56): Open-aperture Z-Scan data for thin films for mixing of (CO+FL) organic laser dyes with PVA polymer doped (Al_2O_3 , Ag) NPs.

Table (4.4): Linear and nonlinear optical parameters for different concentrations of Coumarin (344) dye and its thin films at (λ=457nm).

Material	Concentration (Mol/L)	T	($\alpha_\circ$) cm^{-1}	$n_\circ$	ΔT_{P-V}	n_2 (cm^2/mW)	T(z)	B (cm/mW)
Coumarin (344) (Solutions)	1×10^{-5}	0.9353	0.0667	1.1470	0.011	2.1188×10^{-11}	0.28	1.4265×10^{-3}
	3×10^{-5}	0.8170	0.20208	1.4296	0.024	4.2731×10^{-11}	0.25	1.3073×10^{-3}
	5×10^{-5}	0.7361	0.3062	1.6777	0.031	6.3839×10^{-11}	0.22	1.0786×10^{-3}
	7×10^{-5}	0.5086	0.6759	2.0583	0.043	6.9855×10^{-11}	0.26	0.8392×10^{-3}
CO+PVA polymer (Thin films)	1×10^{-3}	0.6018	5374.2	1.158	0.110	1.73×10^{-7}	0.44	1.245
CO+PVA polymer + Al_2O_3 NPs (Thin films)	1×10^{-3}	0.5717	5971.44	1.1623	0.123	2.34×10^{-7}	0.41	2.673
CO+PVA polymer + AgNPs (Thin films)	1×10^{-3}	0.4087	7113.42	1.1774	0.145	3.84×10^{-7}	0.38	3.53

Table (4.5): Linear and nonlinear optical parameters for different concentrations of Fluorescein dye and its thin films at(λ=457nm).

Material	Concentration (Mol/L)	T	($\alpha_\circ$) cm^{-1}	$n_\circ$	ΔT_{P-V}	n_2 (cm^2/mW)	T(z)	β (cm/mW)
Fluorescein (Solutions)	1×10^{-5}	0.8016	0.2210	1.2931	0.0277	3.5016×10^{-11}	0.56	1.6264×10^{-3}
	3×10^{-5}	0.7194	0.3293	1.4955	0.0361	5.5024×10^{-11}	0.51	1.5068×10^{-3}
	5×10^{-5}	0.5760	0.5515	1.7849	0.0416	7.6834×10^{-11}	0.41	1.4198×10^{-3}
	7×10^{-5}	0.4714	0.7519	1.9216	0.0527	8.5168×10^{-11}	0.38	1.2947×10^{-3}
FL+PVA polymer (Thin films)	1×10^{-3}	0.6748	6396.33	1.1652	0.132	2.91×10^{-7}	0.70	2.023
FL+PVA polymer + Al_2O_3NPs (Thin films)	1×10^{-3}	0.6402	6806.97	1.1852	0.154	3.89×10^{-7}	0.67	3.765
FL+PVA polymer + AgNPs (Thin films)	1×10^{-3}	0.6130	7589.42	1.1920	0.162	4.59×10^{-7}	0.65	4.567

Table (4.6): Linear and nonlinear optical parameters for solutions of mixture of Coumarin 344 , Fluorescein dyes at different mixing ratios and different concentrations at (λ=457nm).

Material	Mixing Ratios	T	($\alpha_\circ$) cm^{-1}	$n_\circ$	ΔT_{P-V}	n_2 (cm^2/mW)	T(z)	*B* (cm/mW)
Mixture of (CO+FL) at (3×10^{-5}) M	1:1	0.7708	0.2602	1.3935	0.022	6.7122×10^{-11}	0.88	2.76×10^{-3}
	2:1	0.7260	0.3201	1.4243	0.024	8.2243×10^{-11}	0.86	2.70×10^{-3}
	3:1	0.7169	0.3327	1.7072	0.040	10.8465×10^{-11}	0.83	2.69×10^{-3}
	4:1	0.7050	0.3494	1.7594	0.060	13.2376×10^{-11}	0.81	2.64×10^{-3}
Mixture of (CO+FL) at (5×10^{-5}) M	1:1	0.6497	0.4312	1.496	0.038	8.5382×10^{-11}	0.86	2.89×10^{-3}
	2:1	0.5497	0.5734	1.7675	0.043	10.0725×10^{-11}	0.85	2.85×10^{-3}
	3:1	0.5603	0.6120	1.8627	0.055	13.8256×10^{-11}	0.83	2.80×10^{-3}
	4:1	0.5694	0.6195	1.9996	0.065	17.6725×10^{-11}	0.82	2.78×10^{-3}
Mixture of (CO+FL) at (7×10^{-5}) M	1:1	0.5671	0.5671	1.7853	0.046	10.6356×10^{-11}	80	3.21×10^{-3}
	2:1	0.5635	0.6480	1.7901	0.054	13.8876×10^{-11}	0.81	3.15×10^{-3}
	3:1	0.5422	0.7792	1.8273	0.065	17.7945×10^{-11}	0.79	3.02×10^{-3}
	4:1	0.5382	0.8630	1.9843	0.0732	18.5352×10^{-11}	0.76	2.98×10^{-3}

Table (4.7): Linear and nonlinear optical parameters for thin films of Coumarin 344 and Fluorescein dyes at mixing ratio (4:1) at concentration (10^{-3} M) at (λ=457nm).

Material	Mixing Ratios	T	($\alpha_\circ$) cm^{-1}	$n_\circ$	ΔT_{P-V}	n_2 (cm^2/mW)	T(z)	*B* (cm/mW)
Mixture doped with PVA polymer	4:1	0.7281	7783. 03	1.3146	0.203	11.41×10^{-7}	0.34	4.472
Mixture doped with PVA polymer and AL_2O_3 NPs	4:1	0.3547	8216.11	1.5964	0.258	13.32×10^{-7}	0.32	5.738
Mixture doped with PVA polymer and Ag NPs	4:1	0.2159	8923.95	1.620	0.291	15.123×10^{-7}	0.30	7.52

4.9 Optical Limiting Behavior of Coumarin (334) , Fluorescein Organic Laser Dyes and their mixture (as Thin Films) .

The optical limiting behavior of Fluorescein , Coumarin (334) organic laser dyes and mixture of them with ratios (1:1, 2:1, 3:1 and 4:1) as solutions at different concentration's (3×10^{-5}, 5×10^{-5} and 7×10^{-5}) M and thin films with PVA polymer doped (Ag ,Al_2O_3) nanoparticles at concentration (10^{-3}) M were performed by closed-aperture Z-Scan with the same laser used in Z-Scan technique. Figures (4.57-4.64) give the optical limiting characteristics at room temperature (25-30)C° for all samples were dissolved in (Ethanol) solvent respectively. The samples show very good optical limiting behavior arising from nonlinear refraction. The output power rises initially with the increasing in input power, but after a certain threshold value, the sample starts defocusing the beam resulting in a greater part of the beam cross-section being cut off by the aperture. Thus, the transmittance recorded by the photodetector remained reasonably constant showing a plateau region agree with [12]. Thin films of Fluorescein , Coumarin and mixing of them with ratios (4:1) give optical power limiting threshold and limiting amplitude less as compared with the materials as solutions, therefore, the optical limiting behavior was significantly optimized in

the case of thin films in comparison to liquid samples and in the polymer and nanoparticles modified dyes in general, From the threshold intensity for optical limiting for each sample, the optical power limiting threshold is inversely proportional to the concentration, that's mean the properties of the optical limiting be better with increasing the concentrations, as listed in Tables (4.8-4.10) respectively.

Optical limiting protects the human eye by attenuating of the laser beam, this behavior agrees with the study in reference [120]. Fluorescein dissolved in (Ethanol) solvent give optical power limiting threshold and limiting amplitude less as compared with the Coumarin dye (CO), while the mixing with Ag that dissolved in Ethanol solvent give optical power limiting threshold and limiting amplitude less as compared with the pure dyes, therefore, the properties of optical limiting at different concentrations for all samples of mixing (Ag and Al_2O_3) are better than the same samples of dyes (CO and FL) as pure dyes. The threshold of the optical limiting on the axis of the out power and the amplitude of the limiting on the axis of the input power can be measure using the tangent of the beginning of the bending the curve in Figures (4.57-4.64), where the lower the threshold and amplitude of the optical limiting, the more suitable the sample is to do as optical limiting.

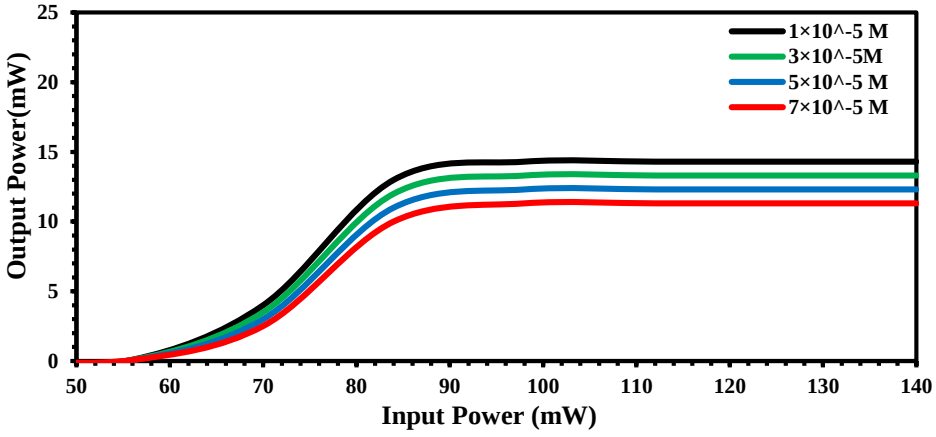

Figure (4.57): The optical limiting response of Coumarin 334 organic laser dye at different concentrations in Ethanol solvent.

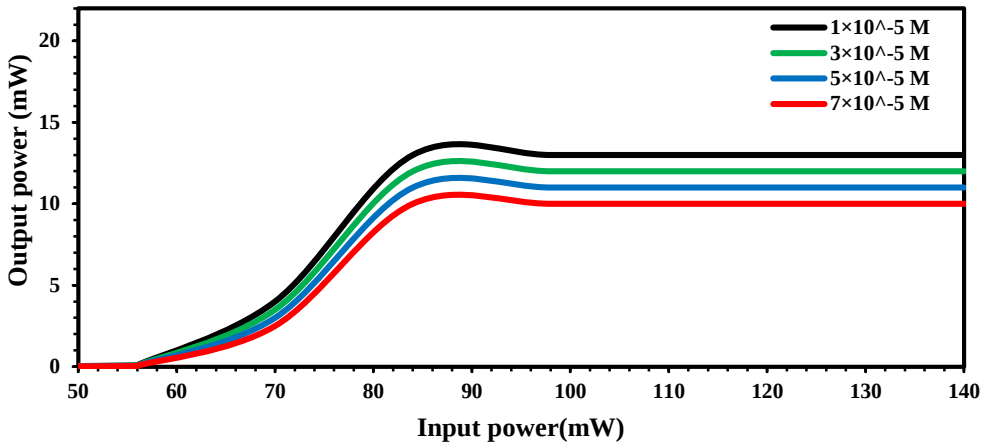

Figure (4.58): The optical limiting response of Fluorescein organic laser dye at different concentrations in Ethanol solvent.

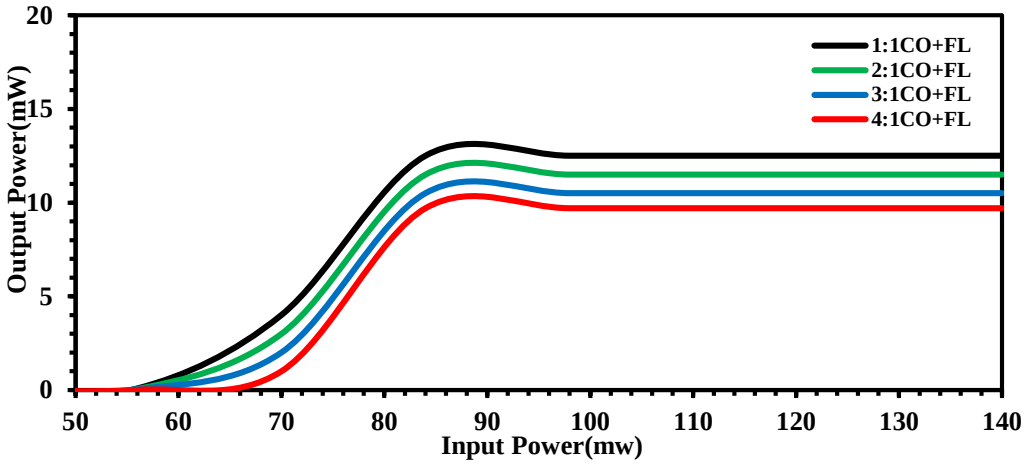

Figure (4.59): The optical limiting response for different ratios of (CO+FL) organic laser dyes in Ethanol solvent at concentration (3×10^{-5})M.

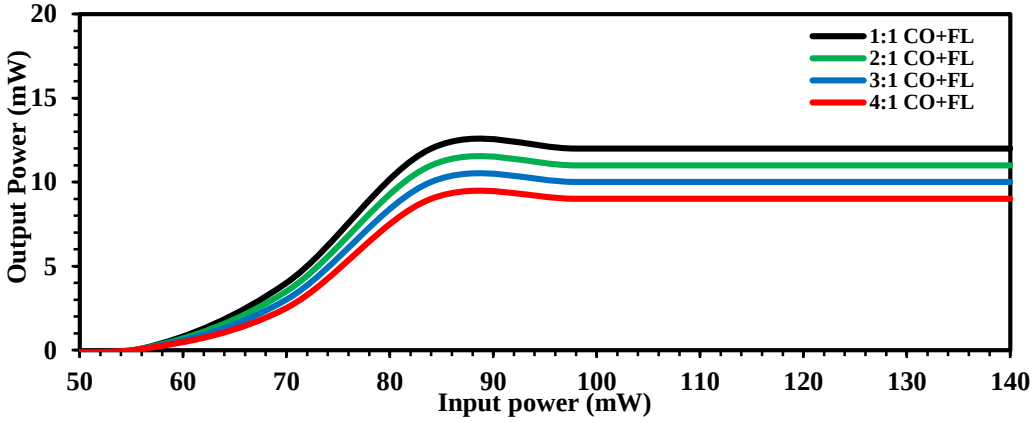

Figure (4.60): The optical limiting response for different ratios of (CO+FL) organic laser dyes in Ethanol solvent at concentration (5×10^{-5}) M.

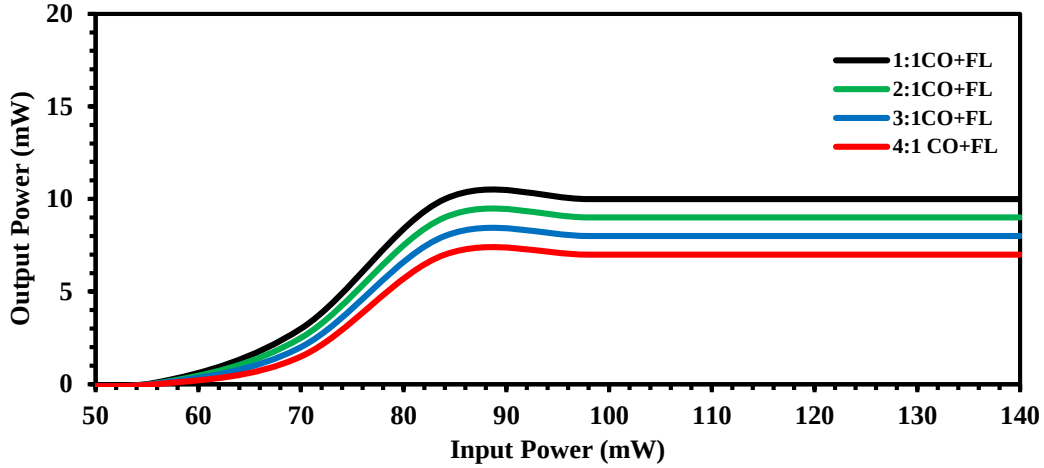

Figure (4.61): The optical limiting response for different ratios of mixing (CO+FL) organic laser dyes in Ethanol solvent at concentration (7×10^{-5}) M.

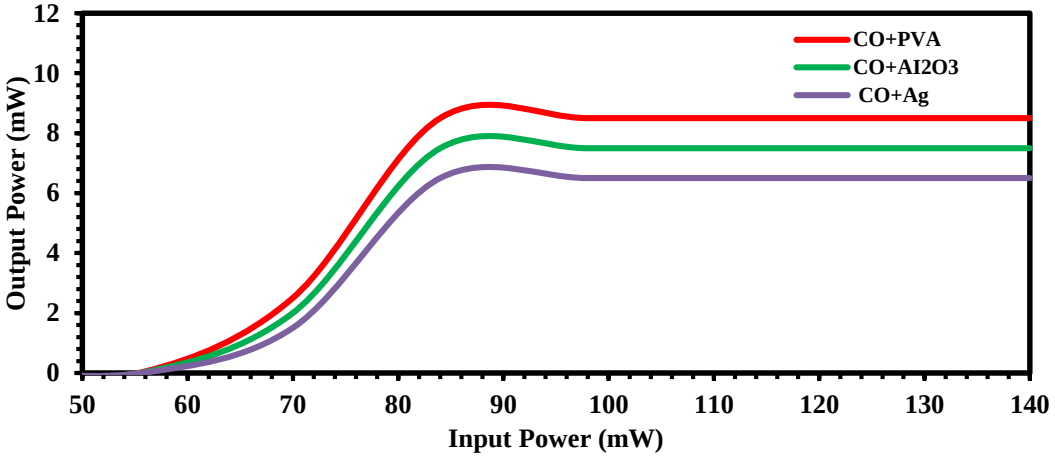

Figure (4.62): The optical limiting response of thin films of Coumarin 334 organic laser dye with PVA polymer doped (Al_2O_3 , Ag) NPs.

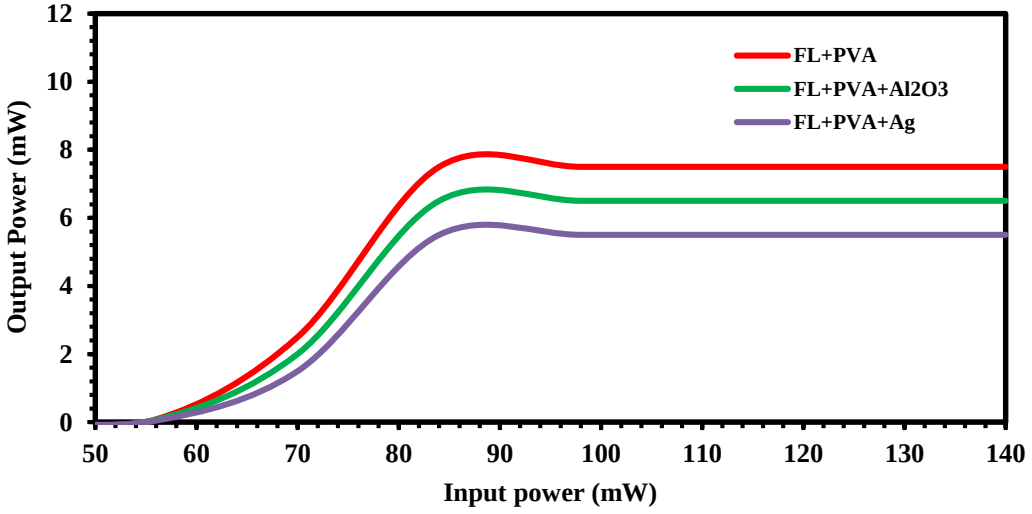

Figure (4.63): The optical limiting response of thin films of Fluorescein organic laser dye with PVA polymer doped (Al_2O_3 , Ag)NPs

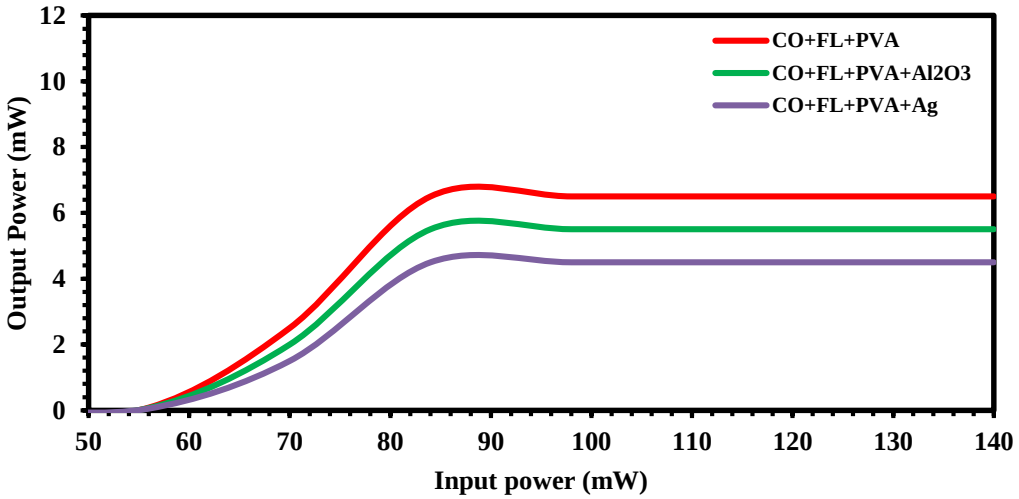

Figure (4.64): The optical limiting response of thin films of mixing of (CO+FL) organic laser dyes with PVA polymer doped (Al_2O_3 , Ag) NPs.

Table (4.8): The optical limiting response of Fluorescein and Coumarin 344 organic laser dyes at different concentrations.

Material	Concentration (M)	Limiting Threshold (mw)	Limiting Amplitude (mw)
Fluorescein	1×10^{-5}	13.8	85
	3×10^{-5}	12.7	84.5
	5×10^{-5}	11.4	84
	7×10^{-5}	10.2	83
Coumarin (344)	1×10^{-5}	14	89
	3×10^{-5}	13.2	88.4
	5×10^{-5}	12	88
	7×10^{-5}	11.4	87.5

Table (4.9): The optical limiting response of mixture of Coumarin 344 and Fluorescein organic laser dyes at different mixing ratios and different concentrations.

Material	Concentration (M)	Limiting Threshold (mw)	Limiting Amplitude (mw)
Mixture (CO+FL) at (3×10^{-5}) M	1:1	12	85
	2:1	11.3	84.4
	3:1	10	83
	4:1	9.7	80.5
Mixture (CO+FL) at (5×10^{-5}) M	1:1	12	80
	2:1	11	80.5
	3:1	10	79.5
	4:1	9	79
Mixture (CO+FL) at (7×10^{-5}) M	1:1	10	78.3
	2:1	9	77.3
	3:1	8	76
	4:1	7	75

Table (4.10): The optical limiting response of thin films mixture of Coumarin 344 and Fluorescein organic laser dyes at ratio (4:1) with PVA polymer doped (Ag,Al_2O_3) nanoparticles at (7×10^{-5} M).

Material	Limiting Threshold (mw)	Limiting Amplitude (mw)
Thin Film of FL+PVA polymer	8	88
Thin Film of FL+PVA polymer +AL_2O_3 NPs	7.6	87
Thin Film of FL+PVA polymer +Ag NPs	6.5	86
Thin Film of CO+PVA polymer	7.5	84.8
Thin Film of CO+PVA polymer +Al_2O_3 NPs	6.4	84
Thin Film of CO+PVA polymer +Ag NPs	5.7	84.5
Thin Film of Mixture CO+FL + PVA polymer	6.8	84
Thin Film of Mixture CO+FL + PVA polymer +Al_2 O_3NPs	5.5	83.2
Thin Film Mixture CO+FL + PVA polymer +Ag NPs	4.2	83

4.10 Conclusions

The main conclusions that we have obtained in our research:

1. Preparation of new mixture of two laser organic dyes Fluorescein dye and Coumarin 344 dye in different mixing ratios as solutions and thin films have been successfully by drop-coating method on glass substrate.
2. The grain size of the thin films, calculated from atomic force microscope (AFM) in the range of (69 - 89) nm.
3. The linear and nonlinear optical properties of Fluorescein dye are larger than those for Coumarin 334 dye.
4. The linear and nonlinear optical properties of solution of mixture laser dyes with mixing ratio (4:1) and concentration (7×10^{-5}) M are higher than the other mixing ratios and other concentrations.
5. The linear and nonlinear optical properties of thin films of mixture laser dyes with mixing ratio (4:1) are higher than the other ratios.
6. The linear and nonlinear optical properties of laser dyes with polymer PVA and nanoparticles are higher than thin films without doping with nanoparticles.
7. The linear and nonlinear optical properties of all samples of laser dyes doped with PVA polymer and Ag nanoparticles are higher than samples doped with PVA polymer and Al_2O_3 nanoparticles.
8. All samples of mixture laser dyes possess large linear and nonlinear optical properties as compared with samples of pure laser dyes, as a result it can be used as optical and photonic devices.
9. The nonlinear refractive index for Coumarin (344) dye shows the behavior of self- focusing and self- defocusing for Fluorescein for dye all solution and mixture laser dye, and two photon absorption in nonlinear absorption coefficient.

10. The nonlinear absorption coefficient for all thin films of laser dyes and their mixtures show saturable absorption phenomena.
11. Fluorescence intensity of all samples of Coumarin (344) dye, Fluorescein dye and mixture laser dye increasing linearly with increasing of concentrations.
12. Fluorescence spectra of thin films have narrower band width than dyes as solutions also the emission peaks are higher intensity than solutions.
13. The decrease in the value of quantum efficiency with the increase in concentration for all prepared samples.
14. Fluorescence spectra of solution of mixture laser dyes with mixing ratio (4:1) and concentration (7×10^{-5})M are higher than the other ratios and concentrations, as a result it can be used as active laser medium.
15. Optical limiting properties of all samples of Fluorescein dye are better than Coumarin (344) dye.
16. Optical limiting properties increase with decreasing concentrations for all samples.
17. Optical limiting properties of mixture dyes as solutions and thin films are better than those for pure dyes.
18. Optical limiting properties of laser dyes doped with polymer PVA and Ag nanoparticles are better than thin films doped with Al_2O_3nanoparticles, as a result it can be used as better optical limiting in electro-optical devices.

4.11 The Suggestions and Future Works

In this context, a further investigation can be suggested as future works:

1. Studying spectral, linear and nonlinear optical properties of mixture dyes with another types of solvents at different concentrations.
2. Studying nonlinear optical properties of dyes using lasers with different wave lengths and different powers.
3. Studying effect for adding another types of polymer and nanoparticles on spectral, linear and non-linear of new mixture of other laser dyes.

References

[1] W. Jaber, ***"A Study of Optical Properties of Acridine Dye and Alumina Nanoparticles Doped in PMMA Polymer''***, M.Sc. Thesis, University of Babylon, (2015).

[2] R. Menzel, ***"Photonics: Linear and Nonlinear Interactions of Laser Light and Matter"***, 2nd .Edition, Springer, Berlin, ISBN: 978-3-662-04521-3 ,(2001).

[3] R. Mohamed, ***"Nonlinear Optical Properties of PMMA Composite Using Z-Scan Technique"***, University of Baghdad, Institute of Laser for Postgraduate Studies, Journal Iraqi of Laser,12, 27-35 (2013).

[4] U.Brackmann, "***Laser Dyes***", 3rd Edition, Lambda Physik, Gottingen, (2000).

[5] S. Singh, V.Kanetkar ,G.Sridhar, V. Muthuswamy and K. Raja, ***" Solid-State Polymeric Dye Lasers"***, Journal of Luminescence, 1, 285–291, (2003).

[6] D. Paul and L.Robeson, "***Polymer Nanotechnology:Nanocomposites"***, Journal of polymer, 49, 3187–3204, (2008).

[7] F. Mauro, ***"Thermo-Optical Effects in Z-Scan Measurements Using High-Repetition-RateLasers"***, Journal Optics, Pure Applied, Optics, 1, 6, 662- 667, (1999).

[8] D. Petrov, ***" Reflection Z-scan technique for the study of nonlinear refraction and absorption of a single interface and thin film"***, Journal of the Optical Society of America,13, 7, (1996).

[9] Y. Wenhui, W. Hongcai, O. Masanori and Y. Katsumi , ***"Enhancement of Third- Order Optical Nonlinearities By Conjugate Polymer-Bonded Carbon Nanotubes"***, Journal of Applied Physics, 98, 3, 034301- 034307, (2005).

[10] F. Amal , N. Israa and M. Ansam, ***" Nonlinear Properties of Olive Oil Films Doped with Poly (Methyl Methacrylate), Polystyrene and their Blend by***

Using Z-Scan Technique", International Journal of Advanced Technology in Engineering and Science, 3, 43-59, (2020).

[11] F. Radhi, ***" Nonlinear Responses and Optical Limiting Behavior of 2-Chloro-5-Nitroanisole Dye Under CW Laser Illumination"***, Journal of Kerbala University ,10,4 ,181 – 186, (2012).

[12] B. Anand, N.Roy, S. Siva and R. Philip,"***Spectral dispersion of ultrafast optical limiting in Coumarin-120 by white-light continuum Z-scan"*** , Applied Physics Letters ,20 (5) ,102, (2013).

[13] A. Hassan, A. Al-Hamdani and F. Abbas," ***Study the Effect of Concentration on Spectroscopic Properties of Fluorescein Sodium dye in Ethanol"*** *Journal of* Kufa - Physics , 6 (1) (2014).

[14] R. Nader ***"The study of non-linear properties for fluorescein sodium dye in water",*** International Journal of science and research, 6,1, 2279- 2281, (2015).

[15] N. Habeeb and N. Ali, ***'Energy transfer process between two laser compounds coumarin 334& rhodamine 590",*** Iraqi Journal of Physics, 14, 31, 61-70, (2016)

[16] T. Ali Naser, ***'Effect of Solvent Polarity on the Fluorescence Energy Transfer in Laser Dye Solutions",*** M.Sc.Thesis,College of Science for Women, University of Babylon, (2017).

[17] M. Jassim, H. Yassin, and M.Mithaq , ***"The Study of A Linear and Non-Linear Optical Property for PMMA Thin Films Doped with the Rhodamine B Laser Dye and Ag Nano Particles are Used in Medicine"***, Journal of Global Pharma Technology, (9), 207-2013, (2017).

[18] A. Lafta , H. Badran and H. Hussain, ***"Optical limiting studies and saturated output of continuous wave laser in Fluorescein solution"*** ,International Journal of Engineering and Applied Sciences (IJEAS) 2394-3661, V-5, 8 (2018).

[19] K. Jamel and F. Tawil**" *Study the optical properties of Fluorescein sodium dye doped in polymer Poly Polyvinyl alcohol for different thickness* "** , Journal University of Kerbala , 16 (1) (2018).

[20] N.Al-huda Talib, ***"Spectroscopic Study of Some New Prepared Organic Dyes as Optical Limiting"***,Ph.D. Thesis,College of Science, University of Babylon, (2019).

[21] S. Haider, ***"Effect of Energy Transfer on Spectral Properties of a Mixture of Laser Organic Dyes"***, M.Sc.Thesis, College of Education for Pure Sciences University of Babylon, (2020).

[22] A.Afrah and A. Ban, "***Non-Linear Optical Properties of Organic Laser Dye*" ,** Annals of the Romanian Society for Cell Biology ,25,6, 11556-11567, (2021).

[23] H . Fadhel and A. Ban, "***Optical Nonlinearities and Optical Limiting Behaviors forMixture of Organic Laser Dyes***", 1st Samarra International Conference for Pure and Applied Sciences , 1,8, 2524, (2022).

[24] A. Afrah, A. Ban , R.Tuama , and M.Talib " ***Non-Linear Optical Properties of Azure A Organic Laser Dye***", 1st Samarra International Conference for Pure and Applied Sciences ,24, 10, 2394, (2022).

[25] M .Sarah, M. Afrah, A. Alhak , A. Ban and J. Menaa **"*Optical limiting characteristics of organic laser dye*"** , 1st International Conference on Achieving the Sustainable Development Goals,12, 4, 4-1 (2023).

[26] S. Hemalatha , B. Rajagobalan and T. Geethakrishnan, **"*Fabrication, Characterization of Basic Blue 7 Dye-Doped PVA Films and Their Third-Order Nonlinear Optical Properties"*,** Journal of Fluorescence 57- 10 (4) (2023).

[27] F. Duarte, ***"Tunable Laser Optics"***, Elsevier Academic, New York, Appendix of Laser Dyes, (2003).

[28] K. Shanshal, *" Study of The Effect of Concentration on The Quantum Efficiency of Copper Phthalocyanine Dye (CuPc)"*, M.S.c Thesis, University of Al-Mustansiriya, (2005).

[29] Z.Sadik and A. Jaffar, *"Third Order Optical Nonlinearities of C450 Doped Polymer Thin Film Investigated by The Z-Scan "*, Advances in Materials Physics and Chemistry, 2,43-49, (2012).

[30] M. Abdul, **"*Study Spectroscopic for Dyes R101 and CV670 in Liquid and Solid Media*"**, M.Sc.Thesis, University of Baghdad,(2005).

[31] G. Vinitha and A. Ramalingam, *"Spectral Characteristics and Nonlinear Studies of Methyl Violet 2B Dye in Liquid and Solid Media"*, Nonlinear and quantum optics ,18,1, 37-42, (2007).

[32] F. Duarte, *"Tunable Laser Optics"* Elsevier Academic, New York, Appendix of Laser Dyes, (2003).

[33] Y. Yang, G. Qian, S. Deliang, Z. Wang and M. Wang, *"Energy Transfer Mechanism Between Laser Dyes Doped in Ormosils"*, Chemical Physics Letters, 402, 38, 389–394, (2005).

[34] G. Svetlana, *"Nonlinear Optical Response of Cyanobiphenyl Liquid Crystals to High-Power, Nanosecond Laser Radiation",* Journal of Nonlinear Optical Physics and Materials, 9, 3, 365-411, (2000).

[35] T. Umakanta, R. Justin, B. Prem, and A. Subrahamanyam, "*Optical Nonlinearity of Organic Dyes As Studied By Z-Scan and Transient Grating Techniques",* Indian Acad , 114, 6, 557-564, (2002).

[36] L. Gómez, S. Cuppo, and A. Neto,"*Nonlinear Optical Properties of Liquid Crystals Probed by Z-Scan Technique",* Braz. Journal Physics, 33 , 4, 813- 820, (2003).

[37] A. Ali and Z . Mahdi , *"Investigation of Nonlinear Optical Properties for laser dyes-doped polymer thin film",* Iraqi Journal of Physics, 10, 19, 54-69 , (2012).

[38] S. Kelly and and O. Neill, ***"Handbook of Advanced Electronic andPhotonic Materials and Devices***", Edited by Nalwa.H.S, Vol.7: Ch1, Academic Press, ISBN012-513757-5, (2000).

[39] D.Hercules, ***"Fluorescence & Phosphorescence Analysis",*** Inter Science Publisher adivision of John Wiley & Sons. New York. London. Sydney, (1960).

[40] M. Fox, ***''Optical Properties of Solids''***, 2nd Edition, Oxford University Press, (2006).

[41] P. Marek,"***Biomimetic Dye Aggregate Solar Cells***", Ph.D. Thesis, Technische University Darmstadt, (2012).

[42] C. Dudley,***"Absorption, Fluorescence and Amplified Spontaneous Emission of Blue-Emitting Dyes"***,M.Sc.Thesis, Washington State University, (2004).

[43] J. Lakowicz, ***"Principles of Fluorescence Spectroscopy"***, Plenum Press, New York, (1983).

[44] D.Elson, J.Siegel, K. Lauritsen, M. Wahl, and R. Erdmann, ***"Fluorescence Lifetime System for Microscopy and Multiwell Plate Imaging with a Blue Picosecond Diode Laser"***, Optics Letters , 27, 16,(2002).

[45] D. Avnir , D. Levy and R. Reisfeld, ***"The Nature of the Silica Cage As Reflected by Spectral Changes and Enhanced Photostability of Trapped Rhodamine 6G"***, Journal of Physics and Chemistry ,88, 5956-5959, (1984).

[46] H. Joakim***," Atomic Force and Scanning Tunneling Microscopy Studies of Single Walled Carbon Nanotubes",*** Ph.D , Thesis, Karlstad's university, (2006).

[47] Y .Ahmad, M. Palanichant, and P.Palanisamy***,"Influence of Solvents Polarity on NLO Properties of Fluorone Dye"*** International Journal of Nonlinear Science, 7, 3, 290-300, (2009).

[48] Z. Xiaoqiang, W. Changshun and L. Zenga, *"**Nonlinear Optical Properties of A Series of Azobenzene Liquid-Crystalline Materials**"*, Optik, 123, 26–29, (2012).

[49] V. Lenart, G. Cruz, and S. Gomez,"***Nonlinear Optical Refraction of The Dye-Doped E7 Thermotropic Liquid Crystal at the Nematic-Isotropic Phase Transition***", cond. mat. soft , arxiv:1304.4537, 1-5, (2013).

[50] H. Lazem, A. Sami, and D. Noor,*"**Spectroscopic Study of (E) benzylideneamino) Hydroxy Phenol Crystal and Study Nonlinear Optical Properties of It**"*, Academic Research International, 5,5, 65- 72, (2014).

[51] H. Ali, I. Slafa and A. Ruqaya, *"**Non-linear Properties for Membranes of Rhodamine Tincture by Using Z-Scan Technique**"*, International Journal of Application or Innovation in Engineering and Management, 4, 9, 2319 – 4847, (2015).

[52] K. Wasan, *"**A Study of Linear and Nonlinear Optical Properties of Composite Poly Vinyl Cloride – B by Using Z-Scan Technique**"*, Journal of Babylon of pure and applied science, 23, 1, 368-377,(2015).

[53] I. Al-Deen and A. Al-Saidi *''**Third - Order Nonlinear Optical Properties and Optical Limiting Behavior of Celestin Blue B Dye Doped Polymer Films**''*, Journal of Photonic Materials and Technology, 4,1-7, (2019).

[54] E . Bahaa, *"**Fundamentals of Photonics**"*, Ch.19,Wiley and Sons, 471-8396 5-5, (1991).

[55] M. Bahae, A. Said, T. Wei, D. Hagan and E. Stryland, "***Sensitive Measurement of Optical Nonlinearities Using a Single Beam**"*, IEEE Journal of Quantum Electronics, 26, 4, 760-769 (1990).

[56] R. Philip, G. Kumar, N. Sandhyarani , and T. Pradeep , "***Nonlinear Optical Absorption and Induced Thermal Scattering Studies in Organic and Inorganic Nanostructures***", Journal of Physics Review 62, 13160, (2000).

[57] A. Ban ***"Preparation and Study Non-linear Optical Properties of Nematic Liquid Crystal Materials Doped by Nanoparticles",*** Ph.D. Thesis, University of Babylon, College of science, (2016).

[58] A. Jawad and A. Lateef, "***Study of the Nonlinear Optical and Optical Limiting Properties of New Structures of Organic - Inorganic Materials for Photoinc Applications",*** M.Sc. University of Basrah, (2012).

[59] C. Vijila and A Ramalingam***"Photophysical characteristics of coumarin 485 dye doped poly(methyl methacrylate) modified with various additives***" Journal Mater. Chem, 11, 749-755, (2001).

[60] Z . Sadik, D. Al-Amiedy and A. Jaffar,"***Third Order Optical Nonlinearities of C450 Doped Polymer Thin Film Investigated by the Z-Scan***", Advances in Materials Physics and Chemistry, 243-49, (2012).

[61] K. Schebesch . A. Brawanski, C. Hohenberger and J. Hohne ,***"Fluorescein Soduim guided surgery of malignant brain tumors history, current concepts and future projects",*** Turk neurosurg, 26(2) 185-194, (2016).

[62] S .Shavakandi, and S.Sharifi, ***"Linear and nonlinear optical properties of fluorescein sodium salt doped droplet***", Journal of Optical and quantum electronics,.49, 1, 26, (2017).

[63] R. Kubin,***"Fluorescence Quantum Yields of Some Rhodamine Dyes"***, Journal of Luminescence , 27 (4), 455–462 , (1983).

[64] M. Stevens, "***Polymer Chemistry"***, 3rd Edition by Oxford University Press, New York, (1999).

[65] F. Billmeyer, ***"Textbook of Polymer Science"***, 2nd Edition Wiley-Interscience, New York, (1971).

[66] A. Tanger, ***"Physical Chemistry of Polymers"***, Mir Publishers Moscow, (1973).

[67] J. Mark, "***Physical properties of polymers handbook***", New York: Springer, 1076, (2007).

[68] B. Bhushan ***''Nanotechnology"***, Hand Book, Springer Heidelberg Dordrecht London New York, Nanoprobe Laboratory for Bio- and Nanotechnology and Biomimetics (NLB2) Ohio State University, ISBN: 978-3-642-02524-2, (2010).

[69] R. Boyd, ***''Nonlinear Optics''***, 3rd .Edition, New York,USA, ISBN: 978-0-12-369470-6, (2008).

[70] B. Snavely, ***''Organic Molecular Photo Physics''***, Birk, John Wiley and Sons, (1973).

[71] I. Alarcon, M. Griffith, and I. Klas , ***"Silver Nanoparticle Applications"*** ,Springer International Publishing,10,978-3, (2015) .

[72] E.Manias, G.Polizes, H.Nakajima, and M. Heiedecker, ***"Flame Retardant PolymerNanocomposites***", 1st JohnWiley&Sons-Inc, New Jersey (2007).

[73] C.Chen , J. Jian and F.Yen ***," Preparation and Characterization of epoxy/γ-aluminum oxide nanocomposites",*** Composites: Part A, 40, 463–468, (2009).

[74] A.Omrania, C. Simonb and A. Rostamia***," The effects of alumina nanoparticle on the properties of an epoxy resin system"***, Journal of Materials Chemistry and Physics 114, 145–150 (2009).

[75] G. Natu, ***"Design and Synthesis of Metal Oxide Nanomaterials and Study of Their Electronic Properties for Energy Conversion via Dye-sensitized Solar Cells",*** Thesis, The Ohio State University, (2012).

[76] V. Millar***,"New Extended Methine Dyes for Application in Laser Technology"***, Ph.D. Thesis, Leeds University, (1993).

[77] A. Ban, A. Asim, A.Alhak, and O. Abdulazeez,*" **Study of the Nonlinear Optical Properties of New Diarylethene Perfluorocyclopentene Derivative by Using Z-Scan Technique",***Journal of Engineering and Applied Sciences,18, 1816-949, (2018).

[78] J. Alda, ***"Laser and Gaussian Beam Propagation and Transformation*** ", Marcel Dekker .Inc , Encyclopedia of Optical Engineering, 270, 999-1013, (2003).

[79] C. Ostela, ***" Spectral-luminescent and lasing properties of laser active media based on distyrylbenzene derivatives in various media"***, Journal of Appl Phys ,80, 6, 3167-3173, (1996).

[80] N. Jawad***, " Non-linear Optical Studies of Liquid Crystal Materials Using Z-Scan Technique"***, M.Sc. Thesis, University of Babylon, (2018).

[81] R. Khalaf, ***"Studing Of Nonlinear Optical Properties for Organic Dye",*** thesis, University of Basrah, (2013).

[82] C. Annamalai, "***Current Trends in X-Ray Crystallography***", In Tech, Ch.7,161-190, (2011).

[83] T. Theivasanthi, and M. Alagar, "***X-Ray Diffraction Studies of Coppe Nanopowder"***, Archives of physics research, 1, 2, 112-117,(2010).

[84] W. Silfvast, ***"Laser Fundamentals***", 2nd Edition , Cambridg University Press, (2004).

[85] P. Biswas and Y.Chang, " ***Nanopartical and the Environment***", Journal of Air and Waste Management Association, Taylor and Francis Group, 55,6,708-746, (2005).

[86] V. Roman, V. Mykola, Z. Serhiy, and S. Oleksandr, ***" Spatial C2oherency of Light and Nonlinear Optical Properties of Colloidal Gold Studied by CW Z-ScanTechnique"***, Journal of Nano World , 2,1,5-9, (2016).

[87] G.Saini, "***Spectroscopic studies of rhodamine 6G dispersed in polymethyl cyanoacrylate",*** Spectro chimica Acta Part A .61, 653–658, (2005).

[88] Z. Fryad and S. Patil ,*" Nonlinear Optical Properties and Optical Limiting Measurements of (1Z) (Dimethylamino) Phenyl]Methylene}4-Nitrobenzocarboxy Hydrazone Monohydrate under CW Laser Regime"*, Journal of Photonics,4, 182-188, (2014).

[89] A. Ketamm and A. Hussain, "***The Study of the Nonlinear Optical Properties of Solutions under CW Laser Illumination***", Journal of Basrah Researches Sciences, 38,4 ,73-79, (2012).

[90] I .Kareem,*" **Optical Properties of Prepared Nanostructure Palladium",*** thesis, M.Sc University of Baghdad Institute of Laser for Postgraduate Studies, (2014).

[91] S. Patil, R. Shivaraj, S. Venugopal, and M. Dharmaprakash, ***"Crystalline Perfection, Third-Order Nonlinear Optical Properties and Optical Limiting Studies Of 3,4-Dimethoxy-4-Methoxy Chalcone Single Crystal"***, Journal of Optics and Laser technology, 81, 70-76, (2016).

[92] F. Amal, ***"Optical Nonlinearity of Oxazine Dye Doped PMMA Films by Z-ScanTechniques"***, Journal of Al-Nahrain University,15,2 ,106- 112, (2012).

[93] A. Hussain, Y. Alaa, and F. Mohammad, ***"Study of The Linear and Nonlinear Optical Properties of Neutral Red Doped Polyvinylpyrrolidone Film"***, Journal of Basrah Researches (Sciences), 37, 2 , 57-63, (2011).

[94] I. Dancus, "***Low Power Laser Induced Optical Nonlinearities in Organic Molecules"***, Romanian Reports in Physics, 62, 3,567–580,(2010).

[95] P. Biswas and Y.Chang, " ***Nanopartical and the Environment***", Journal of Air and Waste Management Association, Taylor and Francis Group, 55, 6, 708-746, (2005).

[96] B. Bhushan," ***Hand Book of Nanotechnology***",3rd. Editio, ISBN:978- 3-642-02524-2, Springer-Verlag Berlin Heidelberg, (2010).

[97] C.Winter, R.Manning, S.Oliver, and C.Hill ***"Measurment of the Large Optical Nonlinearity of Nickel Dithioene Doped Polymers"***, Journal of Elsevier Science,90, 139-143, (1992).

[98] H. Roger, ***"Chemistry of Dyes and Pigments***", Heriot-Watt University, (2017).

[99] N. Hamdi, M. Chebli, H. Grib, M. Brahimi, A. Silva, "***Synthesis DFT/TD-DFT theoretical studies and experimental solvatochromic shift methods on determination of ground and excited state dipole moments of 3-(2-hydroxybenzoyl) coumarins***", Journal of Molecular Structure 1175, 811–820, (2019)

[100] N. Khanapurmath, M. Kulkarni, L. Pallavi, J. Yenagi, J. Tonannavar, "***Solvatochromic studies on 4-bromomethyl-7-methyl coumarins***", Journal of Molecular Structure ,1160, 50–56, (2018)

[101] S. Samundeeswari, M. Kulkarni, J. Yenagi, J. Tonannavar, Dual "***fluorescence and solvatochromic study on 3-acyl coumarins***", Journal Fluoresc, 27, 1247–1255, (2017).

[102] P. Carthy and G. Blancbard' "***AM1 Study of the Electronic Structure of Coumarins*** ", Journal of Physical Chemistry, 97, 47, (1993).

[103] A. Song, J. Zhang, M. Zhang, T .Shen and J. Tang "***Spectral properties and structure of fluorescein and its alkyl derivatives in micelles***", Physicochemical and Engineering Aspects, 253–262 , (2000).

[104] N. Barbero, E.Barni, C.Barolo, P.Quagliotto, G.Viscardi, L.Napione, S.Pavan and F.Bussolino***,"Astudy of the Interaction between Fluorescein Sodium Salt and Bovine Serum Albumin by Steady-State Fluorescence, Dyes and Pigments"***, Indian Acad , 80,3,307-313, (2009).

[105] N.Limpan, T.Prodpran, S.Benjakul, S.Prasarpran, ***''Influences of Degree of Hdrolysis and Molecular Weight of Poly Vinyl Aclohol(PVA) on Properties of Fish Myofibrillar Protein/PVA Blend Films''***, Food Hydrocoll, 29,226-233, (2012).

[106] R. Tripathi, R. Pudake, B. Shrivastav and A. Shrivastav,***"Antibacterial activity of poly (vinyl alcohol)-biogenic silver nanocomposite film for food packaging material"***, Advances in Natural Sciences Nanoscience and Nanotechnology, 9, 1-5, (2018).

[107]Y. Donga*," Fabrication and mechanical properties of nano-/micro-sized Al_2O_3/SiC Composites*", Materials Science and Engineering A, 504, 49–54, (2009).

[108] Y. Saito, M. Kato, A .Nomura, and T. Kana, ***"Simultaneous Three Primary Color Laser Emissions From Dye Mixtures"***, Journal of Applied Physics. Lett. 56 ,9, (1990).

[109] M. Bahae, J. Zeller, and W. Rudolph, ***"Anomalous Nonlinear Photo Response In An In Gan/Gan Heterostructure",*** Journal of Applied Physics 95, 11, 6152-6158,(2004).

[110] F. Mahasin and S. Zahraa **" effect** ***of Doping Ratio on FTIR Spectrum of Coumarin Doped Polystyrene films*"** Chemistry and Materials Research, 3 ,12, (2013).

[111] F.Mahasin and E. Mohi ***, "FTIR spectrum of laser dye fluorescein doped polymer PMMA films*" ,** Research and Reviews in Polymer 3(3), 102-106, (2012).

[112] S. Sreeja, S. Sreedhanya, N. Smijesh, R. Philipc and C.Muneera ***"Organic Dye Impregnated Poly (Vinyl Alcohol) Nanocomposite as an Efficient Optical Limiter: Structure, Morphology and Photophysical Properties"***, Journal of Materials Chemistry C, 1.24, 3851-3861, (2013).

[113] D. Seth, D. Chakrabarty, and N. Sarkar, ***"Study of Energy Transfer from 7-Amino Coumarin Donors to Rhodamine 6G Acceptor in Non-Aqueous Reverse Micelles"***, Chemical Physics Letters, 401, (2005).

[114] *T. Elrasasi, M. Attallah, N. Shash, M. El-Shaarawy,* ***" Linear and non-linear optical properties of PVA-Ag/Coumarin Nanocomposites"*** , Egypt Solids, 44, (2022).

[115] Q.Ali ," ***Photobleaching Spectroscopic Studies and lifetime Measurements of Fluorescent Organic Dyes ",***ph.D. Thesis, University of Baghdad, College of Science, (2013).

[116] I. Slafa and H. Majid ***,"Optical Spectral Study of Rhodamin Mixture Solution in Chloroform"***, Journal of Engineering and Technology, 31,4, (2013).

[117] S.Sinha, R.Alok and K. Dasgupta, ***"Solvent Dependent Nonlinear Refraction in Organic Dye Solution"***, Journal of Applied Physics 87.7, 3222-3226, (2000).

[118] A.Ahmed and F.Zainab " ***Investigation of nonlinear optical properties for lasser dyes- dpped polymer thin film***", Iraqi Journal of Physics, 10, 19, 54-69 (2012) .

[119] A. Ketamm and A. Hussain, "***The Study of the Nonlinear Optical Properties of Solutions under CW Laser Illumination***", Journal of Basrah Researches Sciences, 38,4 ,73-79, (2012).

[120] R. Faris, Z. Mahdi , H. Jawad and D. Altaify***,"The Optical Limiting Behaviour of Prepared Silver Nanoparticles Embedded in Polymer Film"***, Iraqi Journal of Laser, 10, 23-29, (2011).